Exploring the role of glycosylation in vascular biology, immunology, and stem cell biology

A thesis submitted to the National University of Ireland, Galway for the degree of Doctor of Philosophy (Ph.D)

By

Satbir Kaur Gill, BSc, MSc

Glycoscience Group, and
Regenerative Medicine Institute
National Centre for Biomedical Engineering Science,
School of Natural Science,
College of Science,
National University of Ireland Galway

September 2016

Supervisors: Professor Lokesh Joshi and Professor Timothy O' Brien

Declaration

I certify that this thesis has not been previously submitted as an exercise for a degree at National University of Ireland, or at any other university, and I further declare that the work embodied in it is my own.

Satbir Kaur Gill

Acknowledgements

I would like to acknowledge first and foremost Prof. Lokesh Joshi and Prof. Timothy O'Brien, my PhD advisors. I am one such lucky PhD student with two supervisors, who had complete trust in me. Their guidance and support towards my research is invaluable. I would like to express my gratitude towards Prof. Rhodri Ceredig, who helped not only with my research but taught me much more beyond science. All their scientific contributions towards my work have always helped me to improve my output.

I would like to thanks Dr. Michelle Kilcoyne for her immense patience and support during my final year and then with tough job of writing. She is one of the best persons to work with, as she knows how to bring the best out of the other person. I also extend my thanks to Dr. Jared Q Gerlach, who was the first person in whom I found a mentor and friend. Even on his busy days, he accommodated my stupid questions and provided a supporting shoulder. I would also like to thank Dr. Iain Shaw and Dr. Nahidul Islam for the support for the whole blood culture work.

I spent most of my time with Glycoscience group doing my lab work and indulging in cake parties but I was a regular face in lab meeting in both Prof. Joshi's and Prof. O'Brien's lab meetings. I would like to thanks all the members of both Glycoscience group and REMEDI, who contributed to valuable memories of my PhD life. Outside lab, I had a huge circle of friends who made some of the dull days bright. All my Indian friends never let me feel homesick or miss the Indian food, festivals and movies. At NUIG, organizing the first event Diwali event at campus will always stay fresh in my mind.

I would again thank Prof. Joshi for not being supportive as my supervisor but being an idol for my life beyond PhD. Your kind words and strong critiques only made stronger, humble and patient. I would also thank Tamaru and the kids for being a part of my Galway life. I would also like the opportunity to thank my papa (the strongest), my family and my in-laws who have contributed in all my aspects of life. Finally, I would like to thank my best friend and husband, Dr. Shashank Sharma, who means world to me. Without your strong belief, love, support, I would not even thought being here in my life. You are the centre of my Universe and will always remain so.

I would like to thanks Simulation Sciences program for supporting my PhD financially.

ABSTRACT

Carbohydrates are important modulators in various biological and physiological processes. They are present ubiquitously and coat all cells, forming the glycocalyx of the cell. Glycosylation, a type of post-translational modification (PTM), is an enzymatic process of addition of carbohydrates to lipids and proteins leading to the formation of an abundant and diverse repertoire of glycoconjugates. These glycoconjugates participate in many key biological processes including cell adhesion, molecular trafficking and clearance, receptor activation, signal transduction, and immunomodulation.

Carbohydrate-based or -modified therapeutics are becoming increasingly attractive due to their potential roles in angiogenesis and immunomodulation. However, their mechanisms of action in different biological models are not fully explored. In this thesis, three different studies were undertaken to investigate the influence of glycosylation and its importance in different biological cell systems. These studies were aimed at understanding the influence of glycosylation of osteopontin (OPN) in vascular biology, investigating a panel of poly- and oligo-saccharides as potential immunomodulators, and exploring the alteration of extracellular matrix (ECM) components produced in response to variable oxygen concentration in stem cell culture.

In Chapter 2, OPN was investigated for its influence on angiogenic functions. OPN is a glycoprotein that upon pre- incubation with endothelial progenitor cells (EPCs) enhances the therapeutic benefit of EPCs after transplantation in a mouse model of hind limb ischemia. It is a pleiotropic molecule with diverse PTMs, including glycosylation and phosphorylation. It binds to a subset of integrin receptors activating intracellular pathways but the roles of PTMs in OPN towards its biological activities are not known. This study investigated the effect of PTMs on OPN for its functional activity using human umbilical vein endothelial cells (HUVECs) as a cell model system. OPN produced in various expression systems, including murine NS0 (rhOPN), bovine milk (bOPN), human breast milk (hOPN) and bacteria (eOPN), were digested with *endo*- and *exo*-glycosidases and characterised for their differential PTMs. The digestion studies confirmed the absence of *N*-linked oligosaccharides on

OPN molecules, presence of varied degrees of *O*-linked oligosaccharides and absence of phosphorylation on all molecules, except bOPN and the absence of PTMs on eOPN. The functional activities of bOPN, rhOPN and their glycoforms along with eOPN were compared to a control, i.e HUVECs incubated without OPN. OPN prolonged the lifetime of tubules, secretion of angioenic factors and increased cell proliferation. It also led to increased activity of p-PI3K- AKT signaling pathway. However, no significant differences were reported between the glycoforms and phosphoforms of OPN, which suggested no significant roles for OPN glycosylation and phosphorylation in these biological functions.

In Chapter 3, natural poly- and oligo-saccharides were assessed as potential immunomodulators. Natural polysaccharides offer relatively low toxicity, negligible side effects and ease of accessibility over conventional drugs for immunodulation. These test compounds were characterised for their molecular and physical properties. Upon incubation of human whole blood culture (HWBC) and a monocytic cell line, THP-1, with lipopolysaccharide (LPS) and six oligo- and poly-saccharides (inulin, galacturonan, heteroglycan and fucoidan, mannan and xyloglucan), the supernatant was screened for secreted cytokines and chemokines. TNF-α was measured by flow cytometry in HWBC cell sub-populations. Of the six oligo- and poly-saccharides, inulin, galacturonan, heteroglycan and fucoidan demonstrated pro-inflammatory properties in addition to LPS, while mannan and xyloglucan did not elicit any significant responses. Intracellular TNF-α expression was also increased in the monocytes of HWBC in response to inulin, galacturonan, heteroglycan and fucoidan. This study highlighted inulin and heteroglycan as potential immunomodulatory therapeutics and demonstrated HWBC to have a greater and more varied response in comparison to THP-1 cell, suggesting that HWBC may be a better model than single monocytic cell line to screen test compounds.

In Chapter 4, the glycomic and proteomic constituents of mouse stromal cell MS-5 secreted ECM under normoxic and hypoxic conditions were analysed. MS-5 is a feeder cell line that produces ECM that acts as sticky basement for the survival and maintenance of undifferentiated state of hematopoietic stem cells grown above it. When cultured under hypoxic conditions, MS-5 cells improve transcription of pluripotency genes and certain genes involved in mesenchymal cell lineage

commitment and their differentiation potential. However, the roles of ECM components in this beneficial effect are not known. To investigate differentially expressed ECM components produced under normoxia and hypoxia, ECM was prepared under normoxic (21% O_2) and hypoxic (2% O_2) conditions by feeder cells. *In silico* analyses led to the identification of proteins enriched in each condition and their associated biological functions. Of the identified proteins, 50% of the proteins were found to be ECM-related where they participate in ECM-receptor interactions, focal adhesion and leucocyte transendothelial migration pathway. Based on the abundance of glycosylation related proteins and glycosyltransferases from *in silico* analysis, a panel of lectins with appropriate specificities were selected for histochemistry of intact ECM *in situ.* Lectin blotting for the total proteome indicated increased sialylation, fucosylation and mannosylation in hypoxic proteins compared to normoxic. The identified proteins and glycosylation related proteins could be exploited in the development of biomaterials and bioactive scaffolds in the field of tissue engineering.

In addition to the above studies, small projects are presented in appendices. In Appendix 1, human OPN was cloned, expressed and purified in bacterial system to obtain OPN devoid of any PTMs. In Appendix 2, the natural oligo- and polysaccharides presented in Chapter 3 were also tested for their angiogenic and anti-angiogenic properties using HUVECs and angiogenesis related functional assays were performed. In Appendix 3, a statistical analysis for the lectin microarray profiling data of bovine milk fat globule membrane is presented.

With an interdisciplinary approach, diverse roles of carbohydrates were explored using different biological cell models. The studies described in this thesis helped to clarify the roles of PTMs, natural polysaccharides and environmental conditions towards the vascular biology, immunology and stem cell biology. These studies also provided the future directions for further elucidation or study of these molecules towards exploring their therapeutic properties. This thesis hence, provided an opportunity to integrate the field of glycobiology, that was once studied on its own, into the field of therapeutics, immunology and stem biology and utilising the available tools in each field.

LIST OF ABBREVIATIONS

AA:	Amino acid
AB:	Alcian blue
ATCC:	American Type Culture Collection
BFA:	Brefeldin
CBB:	Coomassie Brilliant Blue R-250
CFG:	Consortium for Functional Glycomics
DF:	Dilution Factor
DNA:	Deoxyribonucleic Acid
ECM:	Extracellular matrix
ELISA:	Enzyme Linked Immunosorbent Assay
EPC:	Endothelial Progenitor cells
ER:	Endoplasmic Reticulum
FASTA:	Fast Alignment
FBS:	Fetal calf serum
FITC:	Fluorescein isothiocyanate
Fuc:	Fucose
FUC:	Fucoidon
Gal:	Galactose
GAL:	Galacturonan
GalNAc:	*N*-acetylgalactosamine
Glc:	Glucose
GlcNAc:	*N*-acetlyglucosamine
GO:	Gene ontology
GT:	Glycosyltransferases
HGL:	Heteroglycan
HPLC:	High Performance Liquid Chromatography
hPSCs:	Human pluripotent stem cells
HRP:	Horseradish Peroxidase
HWBC:	Human whole blood culture
INL:	Inulin
Lac:	Lactose
LPS:	Lipopolysaccharide
Man:	Mannose
MAN:	Mannan
mEF:	mouse embryonic fibroblasts
MES:	2-(N-morpholino)ethanesulfonic acid buffer
mM:	Milli Molar
Mr.	Molecular weight
MS:	Mass Spectrometry
N	Neuraminidase
Neu:	Sialic acid
O	O-glycanase
OPN:	Osteopontin
PBS:	Phosphate Buffer Saline

PCR:	Polymerase Chain Reaction
pM	Pico Molar
PTM:	Post Translational Modification
RNA:	Ribonucleic Acid
RT:	Room Temperature
s:	Second
TRITC:	tetramethylrhodamine isothiocyanate
xGLU:	Xyloglucan
Xyl:	Xylose
µM:	Micro Molar

LIST OF FIGURES

CHAPTER 1- INTRODUCTION

CHAPTER 2- EFFECT OF POST TRANSLATIONAL MODIFICATIONS ON OSTEOPONTIN IN VASCULAR BIOLOGY

CHAPTER 3- IMMUNOMODULATORY PROPERTIES OF NATURAL OLIGO- AND POLY-SACCHARDIES

CHAPTER 3- PROTEOMIC AND GLYCOMIC ANALYSES OF EXTRACELLULAR MATRIX SECRETED BY MS-5 CELLS

APPENDIX 1- RECOMBINANT EXPRESSION OF OSTEOPONTIN IN *E. coli*

APPENDIX 2- ANTI-ANGIOGENIC PROPERTIES OF NATURAL OLIGO- AND POLY-SACCHRIDES

LIST OF TABLES

CHAPTER 1- INTRODUCTION

CHAPTER 2- EFFECT OF POST TRANSLATIONAL MODIFICATIONS ON OSTEOPONTIN IN VASCULAR BIOLOGY

CHAPTER 3- IMMUNOMODULATORY PROPERTIES OF NATURAL OLIGO- and POLY-SACCHARDIES

CHAPTER 4- PROTEOMIC AND GLYCOMIC ANALYSES OF EXTRACELLULAR MATRIX SECRETD BY MS-5 CELLS

APPENDIX 1- RECOMBINANT EXPRESSION OF OSTEOPONTIN IN *E. coli*

APPENDIX 2- ANTI-ANGIOGENIC PROPERTIES OF NATURAL OLIGO- AND POLY-SACCHRIDES

TABLE OF CONTENTS

CHAPTER 1- INTRODUCTION

CHAPTER 2- EFFECT OF POST TRANSLATIONAL MODIFICATIONS ON OSTEOPONTIN IN VASCULAR BIOLOGY

APPENDIX 1- RECOMBINANT EXPRESSION OF OSTEOPONTIN IN *E. coli*

APPENDIX 2- ANTI-ANGIOGENIC PROPERTIES OF NATURAL OLIGO- AND POLY-SACCHRIDES

CHAPTER 1

INTRODUCTION

1.1. Carbohydrates in biological function

Glycobiology is the study of structure, biosynthesis and biology of carbohydrates (glycans) found in nature. This discipline lies at the intersection of biochemistry, molecular biology and carbohydrate chemistry and deals with the understanding roles of carbohydrates in biological events. Glycomics is the analysis and understanding of the entire glycome and its functions in a given cell, tissue or organism. It complements other –omics, such as proteomics and genomics, to generate a deeper understanding of biology.

Carbohydrates are one of the most abundant and diverse classes of organic molecules on the planet. They are integral to formation of life and are essential constituents of all living beings. They are one of the four major groups of biologically important macromolecules, the others being nucleic acids, proteins and lipids. Carbohydrates attached to lipids or proteins result in various glycoconjugates such as glycoproteins, proteoglycans and glycolipids. The dense presentation of carbohydrates and other glycoconjugates on the cell surface form the glycocalyx, or sugar coat, of the cell (Brandley and Schnaar, 1986). The interactions between carbohydrates and their biological receptors, lectins, which are carbohydrate-binding proteins, play important roles in cell-cell and cell-extracellular matrix (ECM) communication and adhesion, protein and membrane structural stability, cellular signalling and immune and molecular recognition in diseases (Figure 1.1) (Boscher et al., 2011, Rabinovich et al., 2012, Svarovsky and Joshi, 2008)**.** The composition of the ECM provides various configurations to adapt for the tissue specific functions.

Glycosylation is a term used to define the addition of an oligosaccharide to a protein or a lipid via a covalent glycosidic linkage. Glycosylation is one of the most common among over 200 known post-translational modifications (PTMs). Carbohydrates not only can add a significant amount of mass to glycoconjugates but also influence their functions.

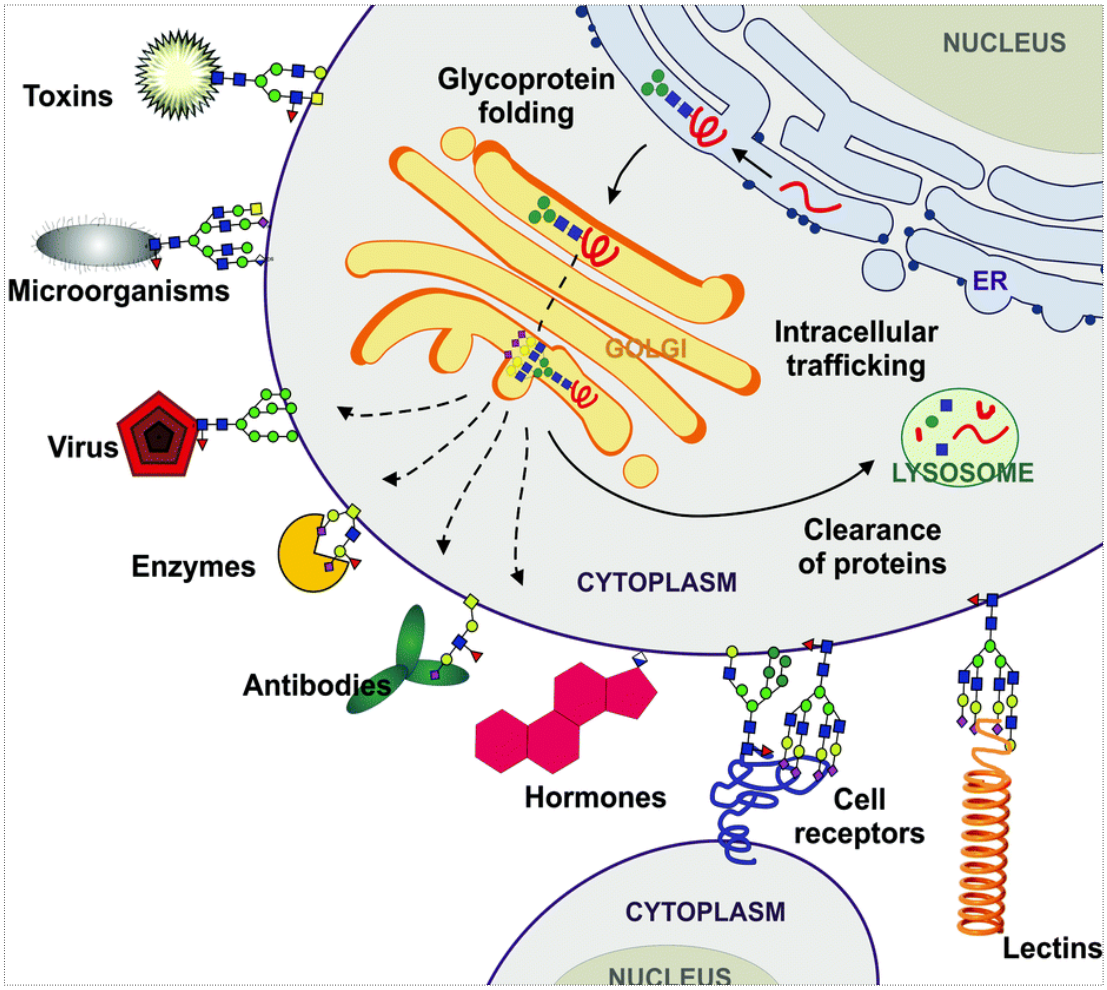

Figure 1.1. A cartoon of the roles of carbohydrates in multiple processes such as cellular regulation, nascent protein folding, intracellular trafficking, cell-cell communication and protection against pathogens.

Carbohydrates have a wide range of extracellular and intracellular roles. Intracellularly, they carry the molecular signalling and molecular recognition roles, while extracellularly, they carry out structural roles and aid in receptor-ligand interactions. They form the first line of contact with foreign bodies and thus function in human immunity. ECM embedded with glycoconjugates surrounds the cells, and provides an interface for the interactions between the cell surface and nearby cells. Glycoconjugates participate in the modulation of protein functions and binding events mediated by protein targeting, cell-matrix interactions or cell-cell interactions.

In the present thesis, carbohydrates were studied for their roles in vascular biology, stem cell biology, and as therapeutics to affect the immune system. In vascular biology, factors such as selectins, galectins and integrins mediate endothelial cell

migration and new blood vessel formation. Carbohydrate-based or -modified therapeutics have been widely used in cardiovascular and hematological treatments for inflammatory and anti-thrombolytic treatments in wound healing. In immunology and stem cell biology, carbohydrates play critical roles in immune recognition, homing of cells and leucocytes to regions of injury and inflammation (Gang et al., 2007, Dimitroff et al., 2000, Muramatsu and Muramatsu, 2004, Lasky, 1992).

In this thesis, I will present an examination of the roles and effects of glycosylation in different biological cell models. I have investigated the roles of glycosylation in three biological processes in particular;
i) PTMs on a glycoprotein, osteopontin, for their contribution to angiogenic properties,
ii) testing poly- and oligo-saccharides as potential immunomodulatory therapeutics, and,
iii) the effect of oxygen concentration on the glycome of ECM produced by feeder cells, that support the growth and expansion of hematopoietic stem cells.

1.1.1. PTMs of proteins

The central dogma of molecular biology states that the flow of genetic information starts with DNA that undergoes a tightly regulated process of transcription to RNA and then translation to form the protein. This linear, template-driven process of protein synthesis produces polypeptides. These proteins can then be further modified by the introduction of PTMs, which can modulate the biological activities of most eukaryotic proteins by increasing proteome diversity and complexity many-fold. PTMs affect the functionality of proteins directly or indirectly by influencing the three dimensional structures of proteins and their respective active sites, enzymes function and assembly (Ryšlavá et al., 2013). Around 5% of the human genome encodes for the enzymes that participate in PTMs (Walsh, 2006)**.** PTM types include phosphorylation, ubiquitination, methylation, nitrosylation and glycosylation. Up to 70% of eukaryotic proteins are glycosylated (Dell et al., 2011) and, in contrast to proteins and polynucleotides, carbohydrates are not direct genetic products. They are synthesised by pathways that are regulated by multiple factors such as metabolic levels of sugar nucleotides, expression and localisation of glycosylation enzymes,

and protein-trafficking mechanisms. Protein glycosylation is broadly studied as *N*-linked and *O*-linked, where *N*-linked glycosylation is more prevalent and conserved (Apweiler et al., 1999).

Due to a high number of structural permutations and combinations, carbohydrates are ideal for generating compact units with explicit informational properties (Winterburn, 1972). The following factors contribute to carbohydrate stereochemistry;

- Identity of the residue
- Anomericity
- Linkage positions
- Ring size
- Branching
- Introduction of site specific substitutions

For example, the possible number of theoretical combinations of three monosaccharides to form a trisaccharide is 38,016 compared to just 64 permutations of four possible nucleotides in a three base codon (Laine, 1997). However, out of all the potential monosaccharide permutations and combinations, a relatively smaller number of oligo- and poly-saccharides exist in nature. Approximately 7,000 different mammalian oligosaccharides can be generated from only ten monosaccharides; fucose (Fuc), galactose (Gal), glucose (Glc), *N*-acetylgalactosamine (GalNAc), *N*-acetylglucosamine (GlcNAc), glucuronic acid (GlcA), iduronic acid (IdoA), mannose (Man), sialic acid (Neu) and xylose (Xyl) (Figure 1.2) (Cummings, 2009, Moremen et al., 2012).

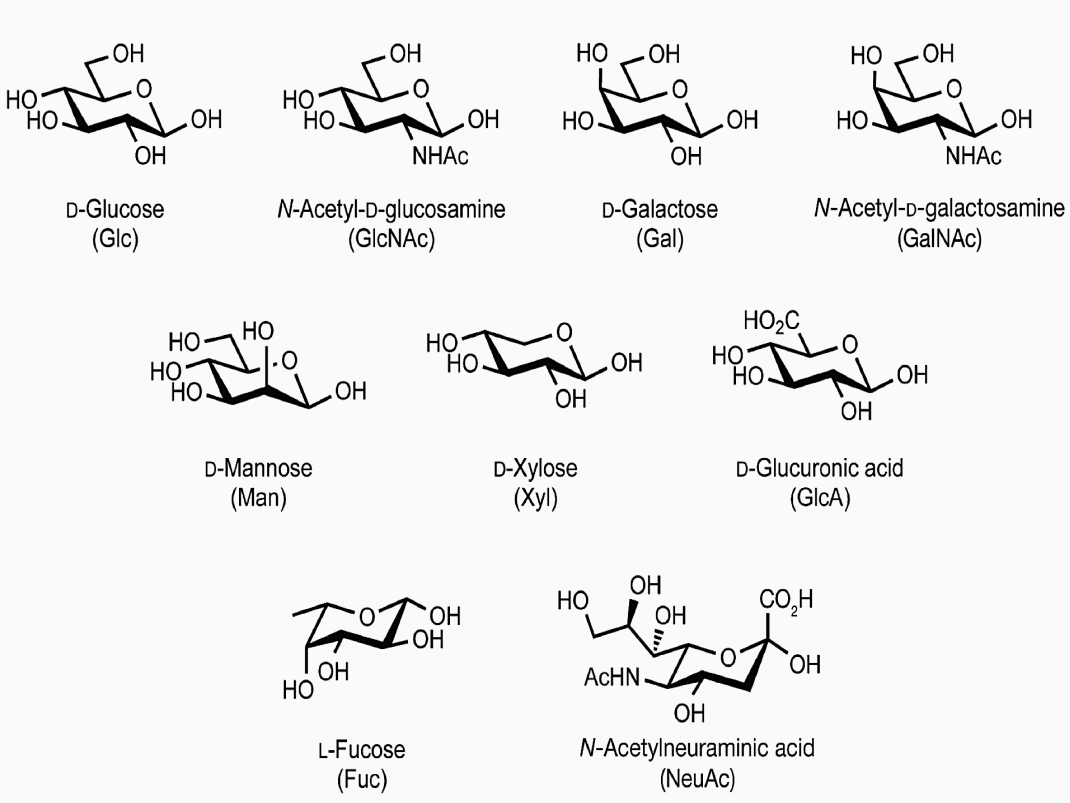

Figure 1.2. Common monosaccharides found in vertebrates.

1.1.2. *N*-linked glycosylation

N-linked glycosylation is both a co- and post-translational modification where oligosaccharides are covalently attached to asparagine in the consensus sequence of Asn-X-Ser/Thr, where X can be any amino acid except proline, or Asn-X-Cys to lesser extent, by an *N*-glycosidic bond, GlcNAc-β-Asn. The presence of this sequon is a requirement for the protein to be *N*-glycosylated but the sequon does not guarantee glycosylation (Jenkins et al., 1996) (Figure 1.3). Oligosaccharide biosynthesis is initiated in the endoplasmic reticulum (ER) and continues in the Golgi apparatus of the cell by enzymatic conversions carried out by ER- and Golgi-resident glycosyltransferases (GTs) and glycosidases (Taylor and Drickamer, 2011). The assembly and attachment of the glycan is carried by the action of GTs while the cleavage of glycosidic linkages is carried by glycosidases. Glycosidases are further categorised into endo-glycosidases that hydrolyse the internal bond to cleave more than one sugar while exo-glycosidases hydrolyse non-reducing glycosidic bond to cleave a single terminal sugar. Glycosidases comprise more than 100 different families containing a diverse range of structural folds. The GTs in the Golgi

apparatus are type II transmembrane proteins with a short cytosolic tail and a large luminal catalytic domain, whereas GTs in the ER are multi-transmembrane spanning proteins (Davies et al., 2005). GTs (Enzyme Commission (E.C.) number 2.4) transfer a monosaccharide from a sugar nucleotide donor to a specific hydroxyl group of a sugar acceptor such as an oligosaccharide, monosaccharide, polypeptide, lipid, small organic molecule, or even DNA. The acceptor specificity of GTs limits the number of possible structures produced. The expression and the localisation of GTs are tightly controlled to produce the correct oligosaccharide structures.

The biosynthesis of *N*-linked oligosaccharides is initiated by isoprenoid lipid dolichol phosphate (Dol-P) that carries the oligosaccharide and transfers it to nascent polypeptide chain during translation. In humans, the synthesis of dolichol lipid occurs *via* the mevalonate pathway and is made up of 19 isoprene units (Jones et al., 2009). The details of the co-translational modifications were known for decades (Kornfeld and Kornfeld, 1985) but knowledge about the mechanism of the oligosaccharide transfer is relatively recent (Lizak et al., 2011). The initial steps of *N*-linked glycosylation are common to all eukaryotes. The oligosaccharyltransferase (OST) catalyses oligosaccharide transfer to Asn-X-(Ser/Thr).

The biosynthesis process is initiated by a family of transferases encoded by asparagine-linked glycosylation (ALG) gene family. GlcNAc-P is transferred from UDP-GlcNAc by the enzyme GlcNAc-1-phosphotransferase, encoded by ALG7, to Dol-P to generate dolichol pyrophosphate GlcNAc (GlcNAc-P-P-Dol). This is followed by the stepwise addition of a second GlcNAc residue to the GlcNAc-P-P-Dol by the action of ALG14. A structure with $Man_5GlcNAc_2$-P-P-Dol is generated, on the cytoplasmic side of the ER by addition of five Man residues from GDP-Man. The first Man residue is added to $GlcNAc_2$-P-P-Dol by ALG1, a β-(1,4)-mannosyltransferase, whereas the subsequent addition of the two branching mannose residues is catalysed by a single enzyme, Alg2p (Aebi, 2013) (Figure 1.3).

The $Man_5GlcNAc_2$-P-P-Dol precursor is translocated (flipped) across the ER membrane layer by a not yet completely understood process. This precursor is extended further by the addition of four Man residues and three Glc residues transferred by Dol-P-Man and Dol-O-Glc respectively (Figure 1.3). This forms

$Glc_3Man_9GlcNAc_2$, referred as Dol-P-P-oligosaccharide and is transferred *en bloc* to a target asparagine residue of the nascent polypeptide by OST, a multi subunit complex. The final terminal α-(1,2)-linked Glc is required for the efficient recognition by OST before it adds *N*-linked oligosaccharides to the side chain nitrogen of the Asn residue by an *N*-glycosidic bond.

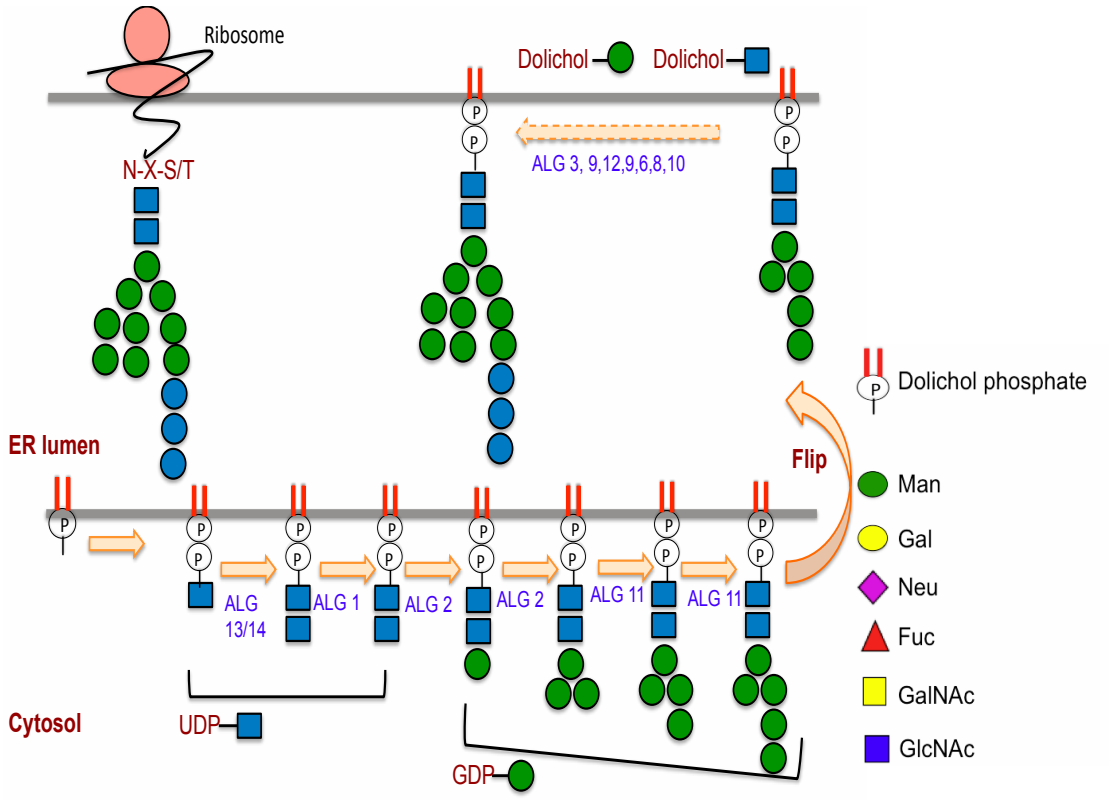

Figure 1.3. Schematic representation for the synthesis of *N*-linked oligosaccharide core structure and transfer to the polypeptide.

After the transfer, a series of trimming processes take place with the sequential removal of Glc residues by two α-glucosidases, I and II, and leads to the formation of a heavily mannosylated monoglucosylated structure, $Glc_1Man_9GlcNAc_2$, that allows the glycopolypeptide to interact with calnexin (CNX) and calreticulin (CRT) in a protein quality control process. CRT and CNX are homologous carbohydrate binding proteins that interact with glycoproteins only when they have monoglucosylated *N*-linked oligosaccharides and assist in proper protein folding (Hammond et al., 1994). CNX is a type I membrane protein while CRT is its soluble paralogue possessing

39% sequence homology (Wada et al., 1991) and they have similar but not identical oligosaccharide binding sites (Thomson and Williams, 2005).

After the oligosaccharide is released from the molecular chaperons CNX and CRT, glucosidase II removes the third Glc residue and waits for the glycoprotein to attain its native form before transporting it to the Golgi apparatus (Figure 1.4). If the glycoprotein still fails to attain its native form, a Glc residue is added by UDP-glucose:glycoprotein glucosyltransferase (UGGT) that acts as a folding sensor by interacting with both the oligosaccharide and the backbone of the protein being folded. This combinatorial regulation by CRT and CNX together with glucosidase II and UGGT increases the folding efficiency, prevents premature oligomeric assembly and prevents the export of misfolded glycoproteins from the ER (Ellgaard and Helenius, 2001). If the protein is still misfolded or unfolded, it is exported from ER lumen to the cytosol for deglycosylation, ubiquitation and degradation by 26S proteome by ER- associated protein degradations (ERAD) (Vembar and Brodsky, 2008). Cleavage of α-(1, 2)-linked Man is carried out by ER resident α-mannosidase I that regulates the signals for degradation after several rounds of folding during transport to the Golgi apparatus. Golgi resident GTs elongate the oligosaccharide structure further with Gal, GlcNAc, Neu and Fuc residues (Takahashi et al., 2009, Kornfeld and Kornfeld, 1985).

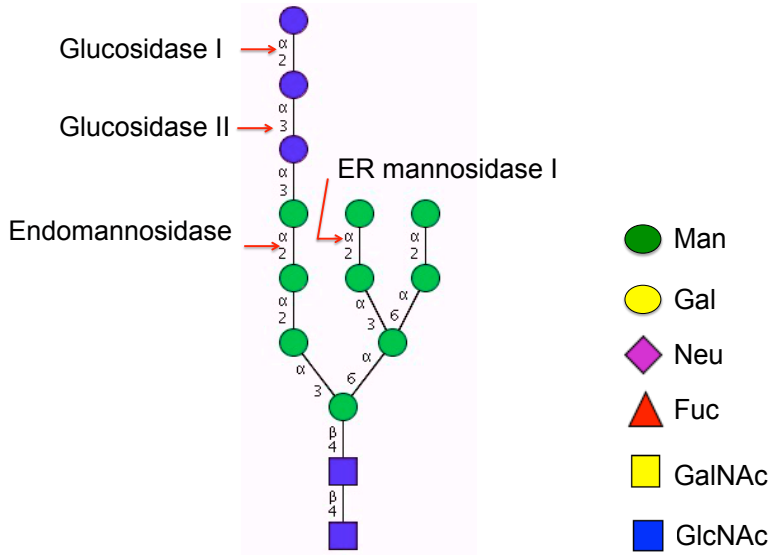

Figure 1.4. Enzymes that participate in the trimming of the core oligosaccharide structure before the exit from ER.

The resultant structures of *N*-linked oligosaccharides in the Golgi apparatus are classified as high mannose, hybrid or complex type (Figure 1.5). Biosynthesis of *N*-linked oligosaccharides forms the core structures of $Man_3GlcNAc_2$-Asn-X-Ser/Thr and the core is further modified to form three main types of *N*-linked oligosaccharides.

- High Man type oligosaccharides typically contain between five and nine Man residues and the terminal Man is unsubstituted (Figure 1.5 A).
- Complex *N*-linked oligosaccharides have two branches with alternating GlcNAc and Gal residues that can terminate with Neu or a core Fuc residue and can attach to the innermost GlcNAc residue (Figure 1.5, B).
- Hybrid type oligosaccharide has attributes of both high mannose and complex type *N*-linked oligosaccharides where unsubstituted Man is attached to Man-α-(1, 6) arm of the core and Man are substituted residues with GlcNAc (Figure 1.5, C).

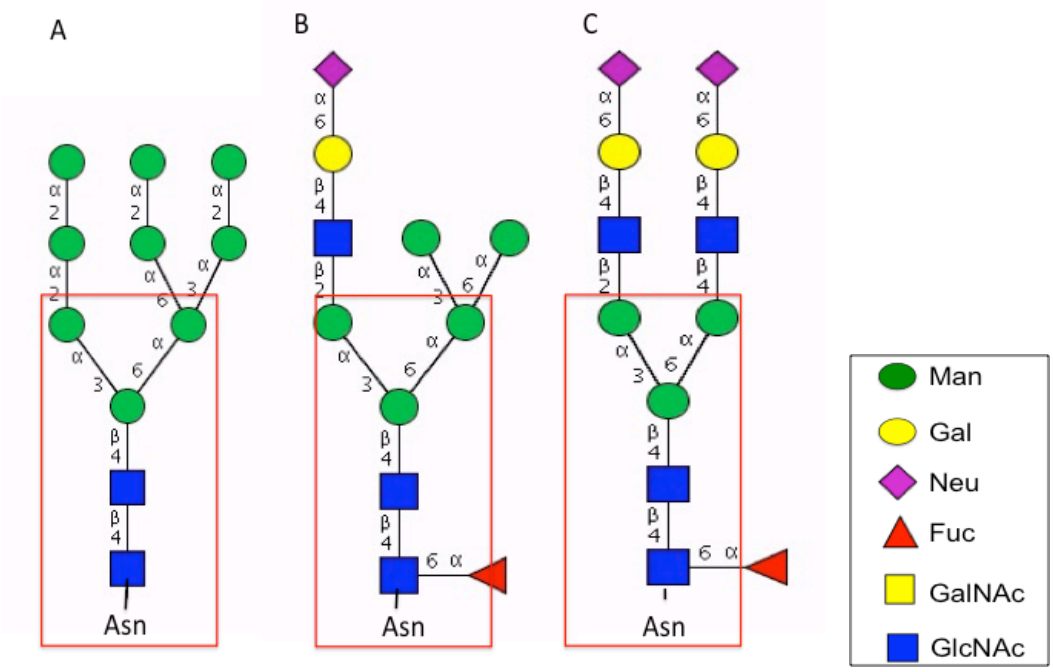

Figure 1.5. Types of *N*-linked oligosaccharide structures. (A) High mannose, (B) hybrid, and (C) complex. The conserved core structure is boxed in red for all structures.

1.1.3. *O*-linked glycosylation

The covalent addition of oligosaccharides to the hydroxyl group of Ser/Thr in a protein is termed as *O*-linked glycosylation (Brockhausen, 1995, Brockhausen and Kuhns, 1997). In contrast to *N*-linked glycosylation, there is no definite sequon identified for *O*-linked glycosylation but there are some computational programs that recognise putative *O*-glycosylation sites. *O*-linked glycosylation takes place exclusively in Golgi apparatus. There are several other *O*-linked glycosylation types that have been identified in various cell types in mammals such as *O*-linked GlcNAc, *O*-linked Man, *O*-linked Fuc, *O*-linked Glc and *O*-linked Gal. Mucin type *O*-linked glycosylation is perhaps the best understood.

Mucins are heavily *O*-glycosylated glycoproteins, where glycosylation occurs in clusters known as 'mucin domains' found on membrane-bound or secreted mucins (Perez-Vilar and Hill, 1999), and are encoded by the MUC family of genes. Mucin-type oligosaccharides can be divided into a core unit, an elongated chain and terminating residues. The first step in the biosynthesis of mucin-type *O*-linked oligosaccharide is carried out by a GalNAc transferase (UDP-GalNAc::polypeptide *N*-acetyl-galactosaminyltransferase, GalNAc-T) (Steen et al., 1998). Stepwise

enzymatic elongation on GalNAc by downstream GTs results in the formation of eight mucin-type core structures (Figure 1.6), which can be further elongated or modified by sialylation, sulfation, acetylation, fucosylation, and polylactosamine-extension (Steen et al., 1998, Harris and Spellman, 1993). Core 1 is formed by the addition of a Gal residue β-(1,3)-linked to the GalNAc. However, the formation of core 3 by addition of a GlcNAc residue β-(1,3)-linked to GalNAc seems to be specific to mucins (Steen et al., 1998). The trisaccharides core 2 and core 4 are formed by the addition of a β-(1,6)-GlcNAc to the core 1 and core 3 structures, respectively, by various different GlcNAc transferases. Extension of the core structures occurs by the addition of either a type 1 (Gal-β-(1,3)-GlcNAc) or type 2 (Gal-β-(1,4)-GlcNAc) *N*-acetyllactosamine unit (Bennett et al., 2012) . Around 20 GalNAc-T genes that code for these enzymes have been identified with >90% sequence homology across species (Bennett et al., 2012).

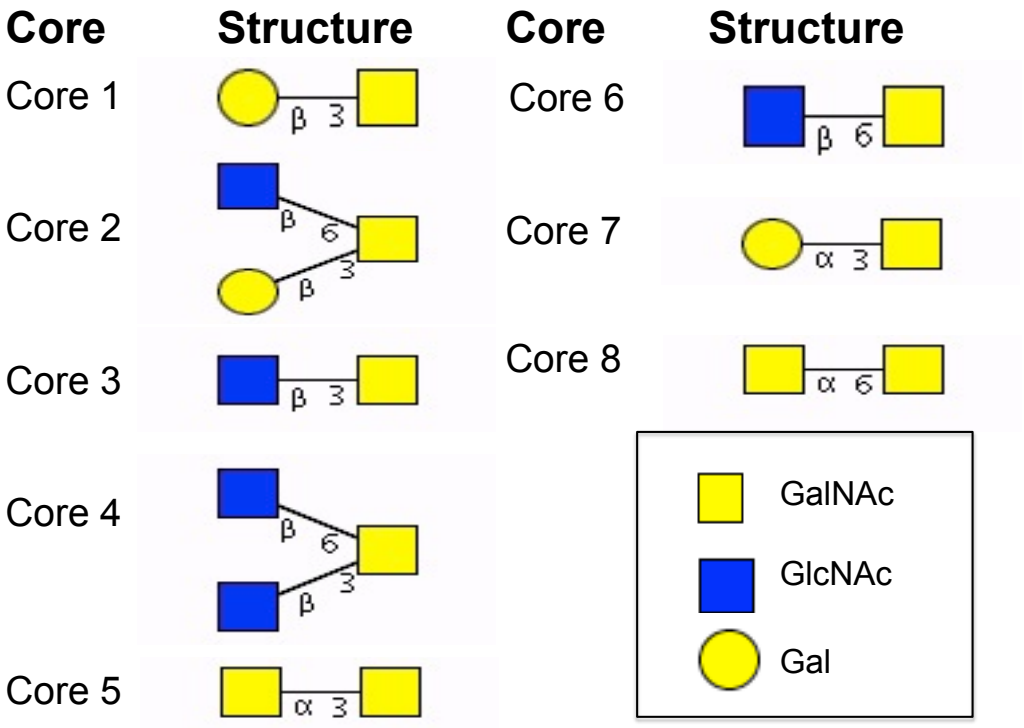

Figure 1.6. Mucin type core structures found in *O*-linked oligosaccharides.

1.1.4. Glycosylation in various expression systems

Recombinant protein-based therapeutics have been immensely successful in clinical studies to regulate biological functions and have revolutionised the treatment of many diseases. The production of recombinant proteins in different expression

systems leads to differences in their PTMs. These different PTMs span over complete repertoire of PTMs in higher mammals while there are very few PTMs in bacterial systems.

Mammalian cells have been used for expression of protein-based therapeutics, leading to improvements in human healthcare. The most widely used mammalian cells to produce biotherapeutics are Chinese hamster ovary (CHO) cells and mouse myeloma cells, including NS0 and Sp2/0 cells (Sethuraman and Stadheim, 2006). Stable mammalian cell lines can be exploited as tools for the expression of secreted and membrane-bound glycoproteins (Wilke et al., 2010). With the introduction of mutations in cell lines, it is possible to express glycoproteins yielding homogenous protein structures i.e. the same protein exhibiting similar structural and functional properties, thus mitigating batch-to-batch differences. The success of CHO cells in glycoprotein therapeutic production can be attributed to the extensive characterisation, history of regulatory approval, fast growth rate, and adaptability to growth in serum-free medium (SFM) formulations of CHO cells.

Other expression systems such as bacterial, insect cell lines, transgenic plants and yeast are also in use (Sethuraman and Stadheim, 2006). These expression systems are preferred for their high growth rate and inexpensive medium requirements. However, they cannot be used for the expression of every protein due to a lack of or dissimilar glycosylation compared to mammals (Figure 1.7). The *E. coli* expression system is widely used for the expression of proteins that do not require glycosylation because *E. coli* lacks the endomembrane system required for mammalian-like glycosylation. Yeast is a eukaryotic organism and therefore possesses cellular components and the requisite enzymes required for glycosylation. In fact, the first steps of the *N*-linked glycan assembly in the ER of yeast produces $Man_8GlcNAc_2$-containing glycoproteins, which is similar to the product from the ER of mammalian cells (Wildt and Gerngross, 2005). However, these oligosaccharides are further elongated in the Golgi apparatus through stepwise addition of Man, resulting in extended high-Man structures that often contain more than 100 Man residues. Yeast can be also be used for the production of human proteins that do not require glycosylation. Nevertheless, the production of glycoproteins with mammalian glycosylation profile

has become possible due to humanising the glycosylation machinery in yeast (Hamilton and Gerngross, 2007).

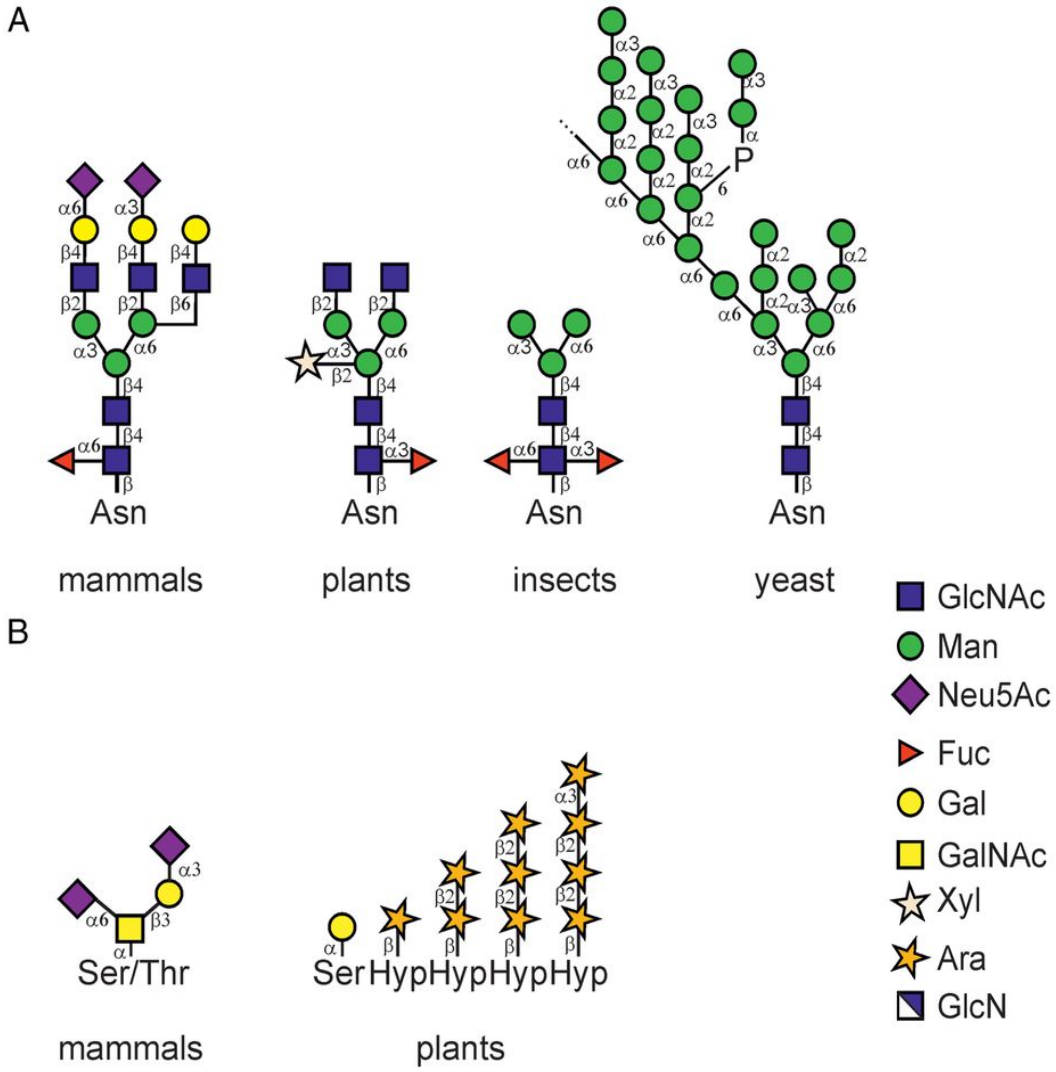

Figure 1.7. Different types of protein linked oligosaccharides. (A) Comparison of *N*-linked oligosaccharide structures among mammals, plants, insects and yeast. (B) Comparison of *O*-linked oligosaccharides between mammals and plants (modified from (Strasser, 2016)).

1.1.5. Altered glycosylation in various physiological conditions

The glycome of a cell is very sensitive and dynamic and it changes during differentiation and development. Also, alterations in the glycosylation patterns lead to many pathological conditions resulting in the formation and developments of various diseases. These alteration in structures arise due to several factors such as

overexpression of GTs, changes in the protein tertiary structures and variability of various acceptor substrates (Stowell et al., 2015). The changes in glycosylation affect cell-cell interaction and signalling, adhesion properties and interaction in immune system (Ohtsubo and Marth, 2006).

Alerted glycosylation is widely studied in various types of cancers. Altered glycosylation on *N*-linked oligosaccharides in cancers is associated with increased β-(1, 6) branching. Up regulation of GTs further lead to the expression of common tumour cell epitopes such as sialyl-Lewis^{x} and sialyl-Lewis^{a}, Tn and sTn antigens (Fuster and Esko, 2005). Differential expression of sialic acids and increased branching of *N*-linked oligosaccharides and fucosylation has been associated with hepatitis and hepatocellular carcinoma (Mondal et al., 2011). For *O*-linked oligosaccharides related malignancies, sole addition of α-linked GalNAc to the protein leads to Tn antigen (Brockhausen, 2006)

1.1.6. Deciphering glycosylation using lectins

Lectins are proteins that bind mono- and oligo-saccharides reversibly with high specificity, independent of catalytic activities. They exist in most organisms, ranging from viruses and bacteria to plants and animals. The first lectin was discovered in 1888 from castor beans *(Ricinus communis L.*) and found to have proteinaceous hemagglutinating properties. This hemagglutinin, which was also highly toxic, was named 'ricin' to denote the source of lectin. Later, more lectins were identified from multiple origins ranging from bacterial, fungal, lichens, plants and humans (Lis and Sharon, 1998).

Lectins usually have two or more carbohydrate recognitions domains (CRD). They act as recognition molecules inside cells, on cell surfaces and in physiological fluids (Sharon and Lis, 2004) and are responsible for protein modulation, cell growth and homeostasis (Ghazarian et al., 2011). Carbohydrate and lectin interactions play crucial roles in many biological processes by facilitating cell-cell communication. Lectins are involved in both symbiotic and pathogenic interactions between microorganisms and hosts, where lectins mediate adhesion to the surface and colonissation by microorganisms (Nachbar et al., 1980). In all organisms, lectins play several biological roles that range from their involvement in tumour biology, immune recognition, inflammatory pathways and infection process (Sharon, 1996).

Lectins in seeds and fruits defend plants against predators and pests. Lectins occurring in animals are sub grouped into the S-type lectins, the C-type lectins, the P-type lectins, and I-type lectins (Lis and Sharon, 1998).
Lectin with different binding specificities were used in chapter 2 and chapter 4 for lectin microarray, lectin blotting and lectin histochemistry.

1.2. Glycosylation in angiogenesis

Angiogenesis is a process for the formation of new blood vessels from pre-existing vasculature. It is a tightly regulated process that primarily occurs through sprouting, initiated by the activation of the endothelial cells of a mature blood vessel wall. Angiogenesis supplies oxygen, nutrients, and transport of factors required for the maintenance of tissue. Glycosylation has an impact on the activation, proliferation, and migration of endothelial cells, as well as the interaction of angiogenic endothelial cells with other cell types necessary to form blood vessels.

N-linked glycosylation was shown to be critical for angiogenesis, as inhibition of enzymes early in the glycosylation pathway blocks vessel growth. The inhibition of GlcNAc-1-phosphotransferase, which catalyses the first step of glycoprotein biosynthesis, blocks endothelial cell proliferation and alters endothelial cell–ECM interactions (Tiganis et al., 1992). Similarly, inhibition of glucosidase I and glucosidase II leads to significant reduction in endothelial cell migration *in vitro* and FGF-induced angiogenesis *in vivo* (Allan et al., 2013). Likewise, inhibition of the Golgi apparatus-resident α-mannosidase, which acts on the glucosidase I/II product, blocks angiogenesis *in vitro* (Nguyen et al. 1992).

O-linked glycosylation may be equally critical in angiogenesis. A mutation in *C1galt1* (or *T-syn*), the gene encoding the enzyme responsible for synthesis of core 1 in mice, has been demonstrated to be a leading cause of the death of mice by embryonic day 14. The missing core 1 structure in mice also has been reported to direct defective angiogenesis and fatal hemorrhage in mice (Xia et al., 2004).

A phosphoglycoprotein called osteopontin (OPN), identified as the most downregulated transcript in diabetic patients versus healthy controls, was also demonstrated to affect the angiogenesis process in mice (Vaughan et al., 2012b).

However, the structure of OPN and its mode of action on endothelial cells are not fully understood in the context of angiogenesis. The PTMs of OPN differ depending on the source of expression and may contribute to the differing roles of OPN in vascular biology.

1.2.1. Osteopontin (OPN)

OPN is a multifunctional, heavily-phosphorylated glycoprotein synthesised by several tissues and cells (Denhardt and Guo, 1993, Sodek et al., 2000). It exits both as a soluble cytokine secreted into body fluids and a component of the ECM. OPN can be very diverse structurally because of the various isoforms created by splice variants and the addition of considerable PTMs. Interactions between OPN binding sites and their receptors are linked to numerous physiological events such as cytokine production, bone remodelling and pathological processes such as infection, inflammation, wound healing, cancer-metastasis and tissue calcification (Wang and Denhardt, 2008, Singh et al., 2007). OPN has been known to play an important role in the process of angiogenesis (Vaughan et al., 2012b). The OPN gene is reported to exist as single copy gene in humans and mouse, but it also exists in various isoforms as a result of alternative splicing, alternative translation, alternative cleavage and different PTMs (Craig et al., 1989). OPN has a polypeptide backbone of up to 300 amino acid residues (Sgadari et al., 1996). The molecular weight (Mr) of OPN differs among species and expression systems due to differences in PTMs such as glycosylation and phosphorylation.

OPN has been identified as a plasma biomarker in chronic heart failure (Kleinman and Martin, 2005) and ovarian cancer and it has been recognised as an angiogenic factor in the progression of tumours (Taub et al., 1993). OPN is widely studied in vascular biology for its effects and it is differentailly regulated following a vascular injury repair (Vaughan et al., 2012a). It induces angiogenesis and controls endothelial cell migration. In contrast to reports of the up-regulated expression of OPN in different tumour models, the OPN transcript was found to be the down-regulated in type 1 diabetic patients (Vaughan et al., 2012a). An important role of OPN was established in postnatal vascularisation when OPN deficient mice were unable to recover from limb ischemia. OPN also plays a protective role by inhibiting endothelial cell apoptosis (Khan et al., 2002).

1.2.1.1. PTMs of OPN

The PTMs on OPN differ based on the originating species, tissues, cell and the pathological condition of the organism. Different PTMs that have been found on OPN are summarised in Table 1.1.

Table 1.1. OPN and its PTMs.

OPN source	*N*-linked glycosylation sites	*O*-linked glycosylation sites	Phosphorylation sites	References
Human milk	0	5	34 P-Ser and 2 P-Thr	(Christensen et al., 2005)
Rat bone	0	4	29 sites (1 sulfation site)	(Keykhosravani et al., 2005)
Rat kidney cells	-	-	Both phosphorylated and non-phosphorylated form.	(Nemir et al., 1989)
Bovine milk	0	3	27 P-Ser and 1 P-Thr	(Sørensen et al., 1995)
Bovine bone	-	-	7 P-Ser and 1 P-Thr	(Salih et al., 1996)
Chicken osteoclasts	-	-	5	(Salih et al., 1997)

1.2.1.2. Importance of OPN PTMs in physiological processes

Alterations in phosphorylation and glycosylation can lead to different binding affinities to cell receptors. Phosphorylation of OPN has been reported as necessary for various physiological activities such as migration of cancer cells (Al-Shami et al., 2005), cell adhesion and bone resorption by osteoclasts (Razzouk et al., 2002). Native OPN purified from rat neonatal smooth muscle cell cultures inhibits smooth muscle cell calcification but neither the dephosphorylated OPN or OPN expressed in *E. coli* (and therefore devoid of eukaryotic PTMs) can perform similarly (Jono et al., 2000). Also, native OPN, but not the dephosphorylated forms of OPN, affect the *de novo* formation or regulation of mineralisation by hydroxyapatite deposition (Gericke et al., 2005). With respect to glycosylation, decreased sialylation has been reported to reduce the binding of OPN to its receptor in the case of ras-transformed

cells. Concomitantly, mutations at the mucin type *O*-linked glycosylation sites inhibited downstream signalling in non-small cell lung cancer models *in vitro* and *in vivo* (Minai,Tehrani et al., 2013).

The role of OPN PTMs in vascular biology is currently unknown. There are no studies where comparative analyses of panels of OPN from different sources have been carried out together in order to distinguish the importance of individual OPNs. Also, there is a lack of studies where either isoforms or glycoforms are compared for their functional activities on a common biological bioassay. In chapter 2, characterisation of OPN molecules from different sources was carried out. These OPN molecules and their respective glycoforms were studied for their functional roles in angiogenesis using HUVECs. OPN can improve the vascular capabilities of EPCs in diabetic conditions. This work will improve our understanding about PTMs on OPN and further exploring its potential therapeutic properties in angiogenesis in diabetes or targeting angiogenesis in various tumours.

1.3. Glycosylation in immunomodulation

1.3.1. Immunosuppressive conditions and immunomodulatory drugs

Infections and physical trauma affect the immune status of the organism, inducing an initial inflammatory cascade followed by a transient anti-inflammatory response. Activated monocytes, macrophages and other immune cells participate towards maintaining the tissue homeostasis and immunity leading to the production of inflammatory mediators to overcome the trauma or biological insult. Inflammatory mediators, including cytokines and chemokines, have been well studied. Modulation of immune responses, either by suppression or enhancement, is a useful strategy for the treatment of infections and the suppression of autoimmune and inflammatory responses.

Post-traumatic immunosuppression (PTI) is the condition of suppressed immune status that follows major surgery or injury, and increases patient's susceptibility to acquire infections (Islam et al., 2014, Hälleberg Nyman et al., 2011). PTI ranges from mild to severe, where mild is exemplified by strenuous exercise and severe by

immunosuppression induced by multiple extensive poly-trauma, major injury or open surgery. PTI in hospital patients may also arise due to haemorrhage (Villarroel et al., 2013, Abraham and Chang, 1992), blood transfusions (Gharehbaghian et al., 2004, Silverboard et al., 2005, Shorr and Jackson, 2005) and use of immunosuppressive drugs (Ali et al., 2013, Gea-Banacloche et al., 2004). Immunosenescence, the weakening of the immune system in elderly persons, also aggravates PTI (Aw et al., 2007, Ginaldi et al., 2001). Boosting patients' immunity may therefore be beneficial to prevent PTI.

Sepsis was initially thought to induce systemic inflammatory responses (Bone et al., 1992). However, treatment of sepsis patients with immunosuppressive drugs in more than 30 clinical trials to date has mostly failed and even aggravated the clinical outcomes. Recent studies suggest the individual assessment of patients' immunity prior to administrating immunomodulatory treatments (Fry, 2012, Boomer et al., 2014, Hotchkiss et al., 2013). Furthermore, following the immunosuppressive phase of sepsis or trauma, patients may develop persistent immunosuppression (Gentile et al., 2012). Immunostimulatory therapy would therefore have a clinical benefit in these situations (Boomer et al., 2014).

However, there is a lack of immunomodulatory drugs available to enhance post-traumatic immunity and the mechanisms of the few drugs that are available, such as thalidomide, lenalidomide, and pomalidomide, are poorly understood. Pomalidomide is known to improve survival in multiple myeloma patients and shows adverse side-effects. Hence, there is a need to identify novel therapeutic molecules to enhance immunity. Carbohydrates (including polysaccharides) are key regulatory molecules in immune modulation. Understanding the structures and functions and exploiting naturally derived polysaccharides could help to prevent the immunosuppressed clinical state (Ghosh et al., 2009, Fattom et al., 2004).

1.3.2. Carbohydrates as immune modulators: polysaccharides

Compounds that are capable of interacting with the immune system have been classified as immunomodulators or biologic response modifiers (Tzianabos, 2000). These compounds can either up-regulate or down-regulate specific aspects of the host response. Polysaccharides fall under the category of natural immunomodulators,

which can enhance or reduce the immune response thus proving a regulatory mechanism for modulating immunity. The primary reason postulated for immunomodulation by polysaccharides is non-specific induction of innate immunity (Schepetkin and Quinn, 2006).

Polysaccharides derived from various natural sources have been studied for their immunomodulatory properties. For example, β-glucan from fungi, yeast and seaweed are well known to function as immuostimulating agents against infectious diseases and used as immunoadjuvants in cancers (Novak and Vetvicka, 2008). β-glucans have been demonstrated to have protective roles against infections of bacteria and protozoa. They stimulate a wide range of immune reactions such as release of cytokines, generation of nitric oxide and reactive oxygen species.

1.3.3. Role of polysaccharides in therapeutics

Carbohydrates have been employed in drug discovery and developments as glycoprotein-based therapeutics for the stability and modulation of protein activity or alone as saccharide-based therapeutics. For example, heparin and its derivatives particularly low Mr are used as anticoagulants since 1940s and a mix of low Mr heparin and dermatan sulfate are used in various cardiovascular dieseases. The advancement in understanding of structure–activity relationships of polysaccharides has paved the way for the development of new classes of therapeutics. There has been progress made in the field of tissue engineering and biomaterials based on both mammalian and non-mammalian polysaccharides such as alginates and hyaluronan (Baldwin and Kiick, 2010).

Polysaccharides have a large number of reactive groups, a wide range of Mr and varying chemical composition. All these features contribute to their diversity in structure and in property and make them ideal in tissue engineering and drug delivery systems. By virtue of their wide range of biological activities, relatively low toxicity, negligible side effects and ease of accessibility, naturally occurring carbohydrates, including polysaccharides, are an attractive potential therapeutic to modulate immune systems and enhance the host defence responses (Schepetkin and Quinn, 2006).

In Chapter 3 of this thesis, six different natural compounds were tested for their immunomodulatory properties using two model systems. These compounds were characterised for the structural properties and assessed for their ability to secrete pro- and anti-inflammatory cytokines and chemokines upon incubation with cells to assess their immunomodulatory properties.

1.4. Glycosylation in stem cell biology

1.4.1. Stem cells

Stem cells are present in the body throughout life, from embryo to the adult. These cells are different from other cell types in the body in that upon division, they have the unique ability to both self-renew and differentiate. They are not committed to any specific function until they receive external signals for the generation of specialised cells.

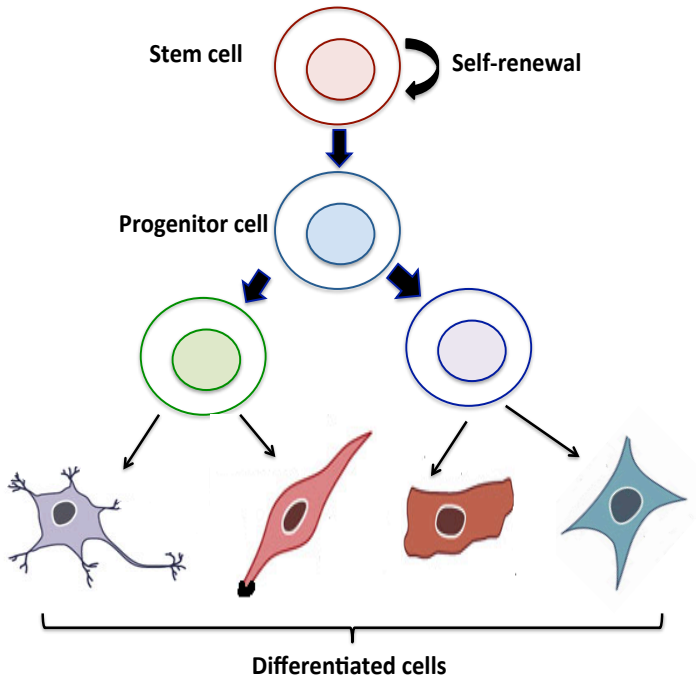

Figure 1.8. Stem cells and their characteristics.

The process by which unspecialised stem cells give rise to specialised cells is called differentiation. Hence, tissue stem cells maintain the homeostasis of that tissue by continually generating specialised end cells yet maintaining the stem cell pool. Stem cells can be broadly classified into foetal, adult or induced pluripotent stem cells

(iPSCs). Foetal and adult stem cells are called multipotent stem cells and are committed to specific developmental programs giving rise to only specific cell types with limited self-renewal and differentiation capacity. Stem cells in the foetus are required for growth, repair and maturation in the development of different organs and tissues. The primary roles of adult stem cells in humans are to repopulate the tissues by generating new mature cell types and regenerating damaged tissue in response to injury or disease (Choumerianou et al., 2008, Pappa and Anagnou, 2009).

In adults, the bone marrow (BM) is the home of hematopoietic stem cells (HSC). Non-hematopoietic (stromal) cells provide a niche for the maintenance of HSCs and their differentiation to mature cell progeny. Thus, stromal cells play an essential role in the regulation, growth and differentiation of HSCs. The bone marrow stroma consists of fibroblasts (reticular connective tissue), macrophages, adipocytes, osteoblasts, osteoclasts and endothelial cells, which form the sinusoids (Wasnik et al., 2012). Stromal cells either secrete the soluble factors or produce ECM that supports HSCs to stay in an undifferentiated state.

1.4.2. Markers of cell types

Cell surface antigens are used for the identification and purification of specific cell types from blood or immune system (Boyse and Old, 1969). Many cell surface antigens are either glycoprotein or glycolipids (Civin and Gore, 1993, Kannagi et al., 1983). During embryogenesis, the expression of carbohydrates is tightly regulated and restricted to specific stages. Stage-specific embryonic antigen (SSEA)-I was the first antigen discovered as an important marker in mouse development (Solter and Knowles, 1978). The structure of SSEA-1 corresponds to that of Lewis antigen (Le^X, Gal-β-(1,4)-[Fuc-α-(1,3)-]-GlcNAc). SSEA-1 first appears in late eight-cell embryos, and is expressed in the embryonic ectoderm, the visceral endoderm and trophoblasts in early post-implantation embryos (Muramatsu and Muramatsu, 2004). In the inner cell mass (ICM), SSEA-1 expression is weak in early stage and increases in later stages (Figure 1.9).

The other two biomarkers discovered were SSEA-3 and SSEA-4, which appear before SSEA-1. SSEA-3 and SSEA-4 are globo-series glycolipids and are not

observed on poly-*N*-acetyllactosamines. The glycolipids SSEA-3 and SSEA-4 are the most commonly used cell markers to identify embryonic stem cells (Muramatsu and Muramatsu, 2004). However, they are not important for maintaining human embryonic stem cells (Brimble et al., 2007). Two antigens, TRA-1–60 and TRA-1–81, have been shown to recognize a keratin sulfate proteoglycan in a neuraminidase-sensitive and insensitive fashion, respectively. These markers are mostly absent in pre-implantation mouse embryos, but appear in the ICM of human embryos (Henderson et al., 2002).

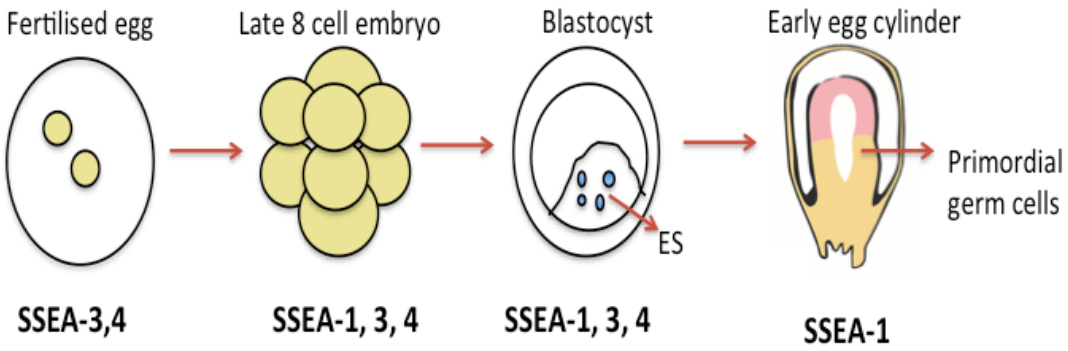

Figure 1.9. Expression of different SSEA markers associated with early embryo stages. SSEA-3 and 4 markers appear at earlier stages and are lost at early egg cylinder stage while SSEA appears at later 8-embryo stage and is expressed over later stages.

1.4.3. Role in signalling and homing

The "lymph node homing receptor" (now known as "L-selectin") known to direct lymphocyte migration to lymph nodes is expressed on lymphocytes and early hematopoietic progenitor cells and the novel selectin ligand present on early hematopoietic progenitor cells is called Hematopoietic Cell E-/L-selectin Ligand (HCELL) (Sackstein, 2004). HCELL is a unique glycoform of the glycoprotein CD44, and it is natively expressed on human hematopoietic stem cells. By mediating binding to marrow sinusoidal endothelium that constitutively expresses E-selectin, HCELL functions as the "bone marrow homing receptor" and directs stem cell migration into bone. The principal leukocyte counter-receptor for the vascular selectins (E-, P- and L-selectins) is the P-selectin glycoprotein ligand-1 (PSGL-1).

PSGL-1 is a cell surface mucin-like glycoprotein which can serve as a ligand for all three selectins (Sackstein, 2004).

Lymphocytes migrate to the parenchyma of lymph nodes through a multi-step process that mediates sequential adhesive interactions with high endothelial venules (HEV). In these interactions, chemokines are important for the activation of the lymphocytes, resulting in integrin activation and the subsequent firm attachment of lymphocytes to HEV. Chondroitin sulfate proteoglycan are reported to interact with chemokines (Kawashima, 2006). For example, basic fibroblast growth factor (bFGF), a low affinity receptor FGF-2, sends intercellular signals upon binding to high-affinity FGF receptors and lower-affinity HSPGs (Gospodarowicz, 1974). FGF-2 is a widely used mitogen for culturing stem cells and is involved in proliferation, differentiation, cell migration, tissue repair, wound healing, and tumour angiogenesis (Lanctot et al., 2007).

1.4.5. ECM

The interaction of cells with the microenvironment is mediated via glycoconjugates in the ECM. Together with cells, ECM defines the structure and properties of various tissues in the body. Broadly, ECM is composed of fibrous and heavily glycosylated proteoglycans (PGs) and proteins such as laminins, fibronectin, vitronectin, elastin, integrin and collagens.

Of all the macromolecules, collagens are the most abundant in ECM. Elastin provides the mechanical properties to ECM. Fibronectin is the second most abundant protein in the ECM and participates in various binding events through its binding domains. Laminin builds a separation barrier between the epithelium and the underlying connective tissues and muscles (Schwarzbauer, 1999). Aggrecan is a large proteoglycan found in cartilage while decorin, biglycan and fibromodulin are low Mr leucine rich family PGs distributed throughout the connective tissue. Decorin and fibromodulin participate in the organisation of ECM by binding to collagen I and collagen II (Svensson et al., 1999). Syndecans are cell surface PGs that play a role in developing and adult tissues and are expressed on different cell types (Fears and Woods, 2006). Syndecans expressed on endothelial cells and fibroblasts promote cell adhesion, angiogenesis and matrix assembly (Woods, 2001). CD44 is a broadly

distributed family of cell surface glycoprotein that can bind to hyaluronan, laminans and fibronectin and promote matrix dependent migration and provide structural organisation (Ponta et al., 2003).

Heparan sulfate and keratin sulfate are also present on cell membranes and ECMs. They serve as receptors for various ligands. The binding between GAGs and proteins affect processes such as haemostasis, lipid transport and absorption, cell growth and migration and development. For example, HSPGs are reported to be endogenous receptors for circulating growth factors and chemokines that regulate cell growth and migration (Linhardt and Toida, 1997).

1.4.5. Applications of stem cells

Stem cells have been used in clinical therapy since 1957 with the first bone marrow transplantation of hematopoietic stem cells (Thomas et al., 1957). They have the potential to treat congenital, developmental or degenerative diseases. The adult bone marrow remains the main source for HSCs today, although following so-called stem cell mobilisation, they can be more easily obtained from peripheral blood, providing a less invasive and more efficacious transplant procedure (Singhal et al., 2000). In newborns, HSCs can also be isolated from umbilical cord blood. HSC provide a unique model to study human embryonic developmental events that cannot be studied directly in intact human embryos (Wobus and Boheler, 2005).

Mesenchymal stem, or stromal, cells (MSCs) have been identified in a wide range of tissues (including adipose tissue, bone marrow, amniotic fluid, umbilical cord, placenta, menstrual blood and dental pulp) and have generated a great deal of clinical interest because they can be differentiated *in vitro* into adipocytes, chondrocytes, osteoblasts, and myocytes (Ma et al., 2014). Due to their immunomodulatory properties, MSCs have also been used in the treatment of different inflammatory disorders, such as graft versus host disease and rheumatoid arthritis and for tissue repair (Nauta and Fibbe, 2007).

MSCs also act as feeder cells that secrete ECM and help human pluripotent stem cells (hPSCs) to survive, proliferate, migrate and differentiate upon attachment to ECM. Culturing hPSCs on top of feeder cells thus helps the hPSCs to stay in an undifferentiated state. Feeder cells are hence beneficial in many ways in clinical

biology. Mesenchymal stromal cells (MS-5) are a known murine feeder cell line that have pro-angiogenic properties, and support the expansion of hPSCs by secreting a supportive ECM (Tiwari et al., 2013, Berthier et al., 1997). It is known that the oxygen concentration affects the differentiation capacities of MS-5 cells (Prado-Lopez et al., 2014, Sugrue et al., 2014). In hypoxia MSCs showed increased proliferation, increased expression of pluripotent genes and changed secreotome. ECM prepared under different oxygen concentrations supported expansion of two different cell types (Tiwari et al., 2013) However, the details of the ECM composition with respect to its constituents, the potential changes in the ECM composition when prepared in different environments such as different oxygen concentrations and their associated effects on the hPSCs are not known. .

In Chapter 4, MS-5 cells were cultured under hypoxia (2% O_2) and normoxia (21% O_2) to produce ECM. The compositions of the two ECM preparations were studied for ECM related proteins by mass spectrometry, lectin histochemistry and lectin blotting to understand the overall proteomic and glycomic changes in ECM.

1.5. Exploration of existing opportunities in glycobiology

For the identification and characterisation of carbohydrates on different molecules, a combination of approaches can be used. The first method that can be utilised for analysis of glycoproteins is gel electrophoresis which can be followed by preliminary characterisation with differential staining, chromatography, high-performance liquid chromatography (HPLC) with exoglycosidase digestion, western and lectin blotting, nuclear magnetic resonance (NMR) spectroscopy and mass spectrometry (MS). Within the scope of the thesis work, some of the following methods were employed.

1.5.1. Glycomics and glyco-informatics

Advancement in high throughput techniques has multiplied the generation of oligosaccharide data. This has been followed by increase in the methods of analysis where the details of oligosaccharides are maintained by different databases facilitated by search engines. In order to make this data readily assessable to researchers, bioinformatics has been utilised in glycobiology leading to a new field of glycoinformatics (Pérez and Mulloy, 2005). Progress has been made in technology and methodology to address the various attributes of carbohydrates and challenges in

glycomics. Glycome is never constant and it is always evolving and changing due to numerous factors such as underlying changes in genome and proteome, environmental nutrients, etc. Even the subtle changes in any of these factors can lead to drastic changes in the glycome. This feature makes glycomics research both exciting and also daunting (Varki et al., 2009).

The immediate need for glycoinformatics to progress is the development of algorithms to reliably support the characterisation of oligosaccharide structures for high-throughput applications. With this aim, several international collaborative efforts, including the Consortium for Functional Glycomics (CFG), EuroCarb and the Japanese Consortium for Glycomics, have been established (Table 1.2) to accumulate available information about the carbohydrates and their applications, and disseminate this information to users. With more than 15, 000 glycan microarrays or slides from CFG have been used by researchers in about 3000 array experiments that make CFG the world's largest catalog for protein-glycan interactions (Cummings and Pierce, 2014).

Table 1.2. A list of databases with a description of their function.

Databases	**Description**
UniCarbKB http://unicarbkb.org) (Campbell et al., 2013)	UniCarbKB aims to help towards our understanding of structures, pathways and networks involved in glycosylation and glyco-mediated processes by integrating structural, experimental and functional glycoscience information.
Xeno-glycomics database (XDB) http://bioinformatics.snu.ac.kr/xdb. (Park et al., 2013)	XDB contains cell- or tissue-specific pig glycomes analysed with mass spectrometry-based techniques, including comprehensive pig glycan information on chemical structures, mass values, types and relative quantities. It provides qualitative and quantitative information on glycomes characterised for transplantation from pig-to-humans important for biomedical research
KEGG Glycan http://www.genome.jp/kegg/glycan/ (Aoki-Kinoshita and Kanehisa, 2015)	The KEGG GLYCAN database is a collection of experimentally determined glycan structures and is categorised as KEGG pathway maps for glycans, glycans in cancer pathways, glycosyltransferases, glycan structure database, KCaM search tool and KegDraw tool
GlycoSuite http://www.glycosuite.com (Cooper et al., 2003)	It provides information on the glycan type, core type, linkages and anomeric configurations, mass, composition and the analytical methods used by the researchers to determine the glycan structure. The details about native and recombinant sources are provided, that includes species, tissue and/or cell type, cell line, strain, life stage, disease, and if known the protein to which the glycan structures are attached. There are links to SWISS-PROT/TrEMBL and PubMed where applicable. Recent developments include the implementation of searching by 2D structure and substructure, disease and reference. The database is updated twice a year, and now contains over 7,650 entries.
GlycoBase http://glycobase.ucd.ie (Campbell et al., 2008)	GlycoBase is a relational database which contains the HPLC elution positions (expressed as glucose unit values) for over 350 2AB-labeled *N*-linked glycan structures by a combination of NP-HPLC with exo-glycosidase sequencing and mass spectrometry

	(MALDI-MS, ESI-MS, ESI-MS/MS, LC-MS, LC-ESI-MS/MS)
Consortium for Functional Glycomics Glycan Database (CFGD)	CFGD offers detailed structural and chemical information for thousands of synthetic glycans as well as glycans isolated from biological sources. Each glycan structure in the database is linked to relevant entries in CFG and external databases (including primary data and information about binding proteins, where available). Links are also provided to a 3D modeling feature, references, and other information. The starting data in the CFG portal was established using the commercial GlycoMinds to which new structures are added based on experimental evidence.
GlycomeDB www.glycome-db.org (Ranzinger et al., 2008)	GlycomeDB through its cross-linking and inter-conversion of the carbohydrate sequences of all freely available glycan databases (CFG, KEGG, GLYCOSCIENCES.de, BCSDB & CCSD) to GlycoCT provides an overview of all carbohydrate structures in the different databases and crosslinks common structures in the different databases. One can search for a particular structure in the meta database and get information about the occurrence of this structure in the five carbohydrate structure databases.
Japan Consortium for Glycobiology and Glycotechnology DataBase (JCGGDB)	JCGGDB is a portal that integrates all glycan-related data (glycoprotein, glycolipid, GAGs, polysaccharides, etc.) set-up in Japan. The data is sourced from large-quantity synthesis of glycogenes and glycans, analysis and detection of glycan structure and glycoprotein, glycan-related differentiation markers, glycan functions, glycan-related diseases and transgenic and knockout animals, etc.
EUROCarbDB http://www.ebi.ac.uk/eurocarb. (von der Lieth et al., 2011)	EUROCarbDB is a relational database containing glycan structures, their biological context and, when available, primary and interpreted analytical data from high- performance liquid chromatography, mass spectrometry and nuclear magnetic resonance experiments. The database is complemented by a suite of glycoinformatics tools, specifically designed to assist the elucidation and submission of glycan structure and experimental data when used in conjunction with contemporary carbohydrate research workflows.

GlycoRDF http://www.glycoinfo.org/GlycoRDF/ (Ranzinger et al., 2014)	GlycoRDF standard Resource Description Framework (RDF) representation for glycomics data, focused on glycan sequences and related biological source, publications and experimental data. This RDF standard is defined by the GlycoRDF ontology and is used by database providers to generate common machine-readable exports of the data stored in their databases.
Qrator (Eavenson et al., 2015)	Qrator, a web-based application that uses a combination of external literature and database references, user annotations and canonical trees to assist and guide researchers in making informed decisions while curating glycans. Using this application, curation of large numbers of *N*-glycans, *O*-glycans and glycosphingolipids has been done.
The Carbohydrate-Active Enzymes database (CAZy; http://www.cazy.org) (Lairson et al., 2008, Lombard et al., 2014)	CAZy provides online and continuously updated access to a sequence-based family classification and is the only comprehensive resource that correlates the sequence, structure and molecular mechanism of carbohydrate-active enzymes such as GTs glycoside hydrolases, polysaccharide lyases, and carbohydrate esterases.

1.5.2. Gel electrophoresis staining methods

Gel electrophoresis can be used for the separation a mixture of glycoproteins using sodium dodecyl sulfate polyacrylamide gel electrophoresis (SDS-PAGE), isoelectric focusing (IEF) or 2-dimensional (2-D) gel electrophoresis, which is a combination of both SDS-PAGE and IEF. Proteins separated by electrophoresis on SDS-PAGE can be stained using Coomassie blue or silver. Coomassie Blue R250 is an anionic dye that stoichiometrically binds to proteins, and can be used for estimation of relative abundance of proteins. It hence provides a useful method for differential expression analysis of (2-DE) gels. Coomassie Blue staining is a relatively simple but less sensitive method for protein detection than silver staining. Silver staining can detect proteins in the nanomolar range. Proteins bind silver ions and lead to the reduction of silver ion to metallic silver that being insoluble builds up a visible image.

Glycoproteins after electrophoresis on SDS-PAGE can be detected using staining methods such as periodic acid-Schiff's reagent (PAS). Periodic acid oxidises two vicinal diol groups to form an aldehyde that reacts with the Schiff's reagent and imparts a magenta colour (Zacharius et al., 1969). The PAS stain is widely used in the histology of mucins, glycoproteins and other polysaccharides (Kumar and Kiernan, 2010). There are some commercially available fluorescent stains that utilise oxidation for the attachment of fluorescent hydrazide that then requires no further reduction step, for example, using Pro-Q Emerald 488 dye (Hart et al., 2003).

Alcian blue (AB) is used to stain mucins. AB is a group of polyvalent basic dyes that are water-soluble and turn blue upon forming reversible bonds between the cationic dye and the negative sites of polysaccharides. The blue colour is due to the presence of copper in AB. AB solution can be used for further characterisation of the subtypes of acidic mucins present in a tissue by varying the pH of the solution. All acidic mucins, whether carboxylated or sulfated will ionize at pH of 2.5 to produce anionic groups. In contrast, mucins that contain predominately carboxylated carbohydrates will stain strongly with AB at pH 2.5 but not at a pH of 1.0. The carboxyl groups do not ionize at this lower pH and as a result the mucins will display neutral characteristics. The cations on AB form salt bridges with the acid groups of acid mucopolysaccharides. (Wardi and Michos, 1972, Green et al., 1973). AB cannot be used for the staining of glycoproteins that carry insufficient charge.

1.5.3. Lectin-based glycan detection

Lectins are classified into different groups according to the monosaccharide for which they exhibit the highest affinity (Table 1.3). The affinity of the lectins for monosaccharides is weak, as the reported association constants are in the millimolar range, but they can be selective (Ambrosi et al., 2005). This implies that lectins specific for Gal do not react with Man and *vice versa*. However, the selectivity of lectins for monosaccharides is not always exclusive. For example, certain variations at the C-2 position of the pyranose ring may be tolerated, resulting in that certain lectins that bind Man can also interact with Glc, and certain lectins that bind Gal can also interact with GalNAc (Ambrosi et al., 2005). Certain lectins preferentially bind to either the α or the β anomer, whereas others lack anomeric specificity (Ambrosi et

al., 2005). For example, lectin Con A specifically binds to the α –anomer of Glc and Man, but not to the β anomer of either (Mody et al., 1995).

Table 1.3. Examples of lectins from different sources and their specificities.

Abbreviation	Species	Common name	Major Ligand(s)
AIA, Jacalin	*Artocarpus integrifolia*	Jack fruit lectin	Gal (~sialylation independent)
DSA	*Datura stramonium*	Jimson weed lectin	GlcNAc
LEL	*Lycopersicum eculentum*	Tomato lectin	GlcNAc-β-(1, 4)-GlcNAc
ConA	*Canavalia ensiformis*	Jack bean lectin	Man, Glc, GlcNAc
WGA	*Triticum vulgaris*	Wheat germ agglutinin	NeuAc/GlcNAc
MAA	*Maackia amurensis*	Maackia agglutinin	Sialic acid-α-(2, 3)-
SNA-I	*Sambucus nigra*	Sambucus lectin-I	Sialic acid-α-(2, 6)-
RCA-I/120	*Ricinus communis*	Castor bean lectin I	Gal-β-(1, 4)-GlcNAc
UEA-I	*Ulex europaeus*	Gorse lectin-I	α-Fuc-(1, 2)

Lectins have been used as a valuable tool for detection, isolation and characterisation of glycoconjugates, primarily glycoproteins. Lectins are labelled with tags such as biotin, fluorescence or alkaline phosphate are for detection and probing. They are used for histochemistry of cells and tissues and for the examination of changes that occur on cell surfaces during physiological and pathological processes, from cell differentiation to cancer. (Sharon and Lis, 2004). For separation, fractionation and characterisation of glycoproteins and animal cells, including B and T lymphocytes, lectin affinity columns can be used where lectins are covalently bound to matrices (sepharose or agarose membranes or magnetic beads). Lectins can be used as detection tools for glycoproteins after separation by SDS-PAGE gels blotted onto a membrane.

1.5.3.1. Lectin microarrays

Lectins have been employed for high throughput analysis due to their ability to discriminate between different carbohydrate moieties. Lectin microarrays have been developed where lectins are immobilised on glass slides similar to antibody

microarrays (Hirabayashi et al., 2014). Lectins are immobilised either via covalent bonding or physical adsorption. Lectin microarray-based carbohydrate profiling has given promising results with a range of sample types, including glycopeptides, glycoproteins, live mammalian cell-surface glycome, formalin-embedded tissue sections and bacteria (Gerlach et al., 2013, Landemarre et al., 2013). One of the biggest advantages of lectin microarrays over the other existing carbohydrate profiling methods such as LC-MS lies in its ability to analyse quantitatively the complex glycans in both pure and crude form (Hu and Wong, 2009). Lectin microarrays can detect both *N*- and *O*-linked glycans simultaneously providing more complete information on the glycome being analysed.

The analysis of lectin microarray data has been challenging due to the broad specificities of lectins and the relative higher background issues. Normalisation of the microarray data is performed to eliminate the bias arising from microarray to microarray. Depending on the purpose of the study, max, mean, particular lectin or median normalisation method can be used (Tateno et al., 2010). There are no specific packages yet available for the analysis and clustering of the lectin microarray data but the normalised, unfiltered lectin microarray data can be subjected to multi-scale bootstrap re-sampling prior to hierarchical clustering analysis in the R 'pvclust' environment (http://cran.r-project.org/web/packages/pvclust/index.html). It is employed for the estimation of certainty for each of the *p*-value calculations for clusters obtained from the bootstrapped data (Ross et al., 2016, O'Riordan et al., 2014). In appendix 3 of the thesis, lectin microarray analysis was carried to understand glycosylation pattern changes for buttermilk over time.

1.6. Scope of the thesis

Glycosylation affects the developmental, biological and pathological processes in numerous ways. The knowledge of glycosylation in biological cell models is critical to understand their importance in cell biology. The overall aim of the current work is to understand the role of glycosylation in different biological systems using different cell models as follows.

Chapter 2. Effect of PTMs on OPN in vascular biology

OPN is a phospho-glycoprotein that plays multiple biological roles in vascular biology. It had been earlier characterised for the presence of PTMs, however the biological studies to understand the importance of PTMs across panel of OPN molecules from different sources is missing in vascular biology. In this chapter, different OPN molecules produced in different expression systems were characterised using digestion studies and lectin microarray analysis and respective glycoforms and phoshoforms were generated. These glycoforms were tested for their angiogenic properties by performing functional bioassays such as proliferation assay, tubule formation and angiogenesis assay using an endothelial cell model.

Chapter 3. Immunomodulatory effects of natural compounds

Due to the known side effects of the available immunomodulatory drugs, there has been an emphasis on exploring immunomodulatory drugs with less side effects and more targeted functions. To achieve this, six naturally derived oligo- and poly-saccharides were screened for their immunomodulatory properties in a monocytic cell line and in human whole blood culture. A panel of chemokines and cytokines were studied at different time points (0, 6, 12, 24 and 48 h) upon incubation with test carbohydrates to examine pro- and anti-inflammatory effects of the oligo- and poly-saccharides.

Chapter 4. Glycomic and proteomic analysis of ECM secreted by MS-5 stromal cells

MS-5 supports the survival and expansion of hESCs by providing ECM for hESCs to grow and secrete various signalling molecules to maintain their undifferentiated state. However, the composition of secreted ECM and affect of different culturing methods for MS-5 cells are not completely known. Therefore, ECM produced by MS-5 cells under normoxic and hypoxic conditions were analysed by mass

spectrometry. *In silico* analyses identified differentially regulated proteins constituting the proteomic and glycomic profile of ECM. Gene ontology for the enrichment of cellular component and ECM related pathways were established. The differences in ECM components produced under normoxic and hypoxic conditions were examined using lectin staining and lectins blots of the whole proteome of ECM.

Chapter 5. Conclusion and future perspectives

Overall conclusions from chapter 2, 3 and 4 were drawn from studying different effects of glycosylation on biological models. Future perspectives about individual study undertaken are discussed.

In addition to the main chapters, shorter projects were carried out during my PhD studies, which are detailed in the appendices.

Appendix 1

Appendix 1 describes the cloning, expression and purification of human OPN sequence in *E. coli.* It was carried out to generate OPN devoid of any PTMs.

Appendix 2

The six oligo- and poly-saccharides from Chapter 3 were tested for their anti-angiogenic properties using endothelial cells as the model system. This work was done to compare the angiogenic properties of natural compounds to angiogenic protein, OPN. The results demonstrated anti-angiogenic properties of these natural compounds.

Appendix 3

A manuscript is presented where I performed statistical analysis for lectin microarray data. Bovine buttermilk, a viable source of bovine milk fat globule membrane was profiled using lectin microarrays and lectin blots. Heat maps were generated using bootstrapping method for lectin microarray data to understand glycosylation pattern changes for buttermilk over time.

Appendix 4

A list of outputs from my thesis work including poster and oral presentations, and manuscripts published and in preparation.

1.7. References

ABRAHAM, E. & CHANG, Y.-H. 1992. Haemorrhage-induced alterations in function and cytokine production of T cells and T cell subpopulations. *Clinical & Experimental Immunology,* 90**,** 497-502.

AEBI, M. 2013. N-linked protein glycosylation in the ER. *Biochimica et Biophysica Acta (BBA)-Molecular Cell Research,* 1833**,** 2430-2437.

AL-SHAMI, R., SORENSEN, E. S., EK-RYLANDER, B., ANDERSSON, G., CARSON, D. D. & FARACH-CARSON, M. C. 2005. Phosphorylated osteopontin promotes migration of human choriocarcinoma cells via a p70 S6 kinase-dependent pathway. *Journal of Cellular Biochemistry,* 94**,** 1218-1233.

ALI, T., KAITHA, S., MAHMOOD, S., FTESI, A., STONE, J. & BRONZE, M. S. 2013. Clinical use of anti-TNF therapy and increased risk of infections. *Drug Healthc Patient Saf,* 5**,** 79-99.

ALLAN, G., OUADID-AHIDOUCH, H., SANCHEZ-FERNANDEZ, E. M., RISQUEZ-CUADRO, R., FERNANDEZ, J. M. G., ORTIZ-MELLET, C. & AHIDOUCH, A. 2013. New castanospermine glycoside analogues inhibit breast cancer cell proliferation and induce apoptosis without affecting normal cells. *PloS one,* 8**,** e76411.

AMBROSI, M., CAMERON, N. R. & DAVIS, B. G. 2005. Lectins: tools for the molecular understanding of the glycocode. *Organic & Biomolecular Chemistry,* 3**,** 1593-1608.

AOKI-KINOSHITA, K. F. & KANEHISA, M. 2015. Glycomic Analysis Using KEGG GLYCAN. *Glycoinformatics***,** 97-107.

APWEILER, R., HERMJAKOB, H. & SHARON, N. 1999. On the frequency of protein glycosylation, as deduced from analysis of the SWISS-PROT database. *Biochimica et Biophysica Acta (BBA)-General Subjects,* 1473**,** 4-8.

AW, D., SILVA, A. B. & PALMER, D. B. 2007. Immunosenescence: emerging challenges for an ageing population. *Immunology,* 120**,** 435-46.

BALDWIN, A. D. & KIICK, K. L. 2010. Polysaccharide-modified synthetic polymeric biomaterials. *Peptide Science,* 94**,** 128-140.

BENNETT, E. P., MANDEL, U., CLAUSEN, H., GERKEN, T. A., FRITZ, T. A. & TABAK, L. A. 2012. Control of mucin-type O-glycosylation: a classification of the polypeptide GalNAc-transferase gene family. *Glycobiology,* 22**,** 736-756.

BERTHIER, R., PRANDINI, M. H., SCHWEITZER, A., THEVENON, D., MARTIN-SISTERON, H. & UZAN, G. 1997. The MS-5 murine stromal cell line and hematopoietic growth factors synergize to support the megakaryocytic differentiation of embryonic stem cells. *Experimental hematology,* 25**,** 481-490.

BONE, R. C., BALK, R. A., CERRA, F. B., DELLINGER, R. P., FEIN, A. M., KNAUS, W. A., SCHEIN, R. M. & SIBBALD, W. J. 1992. Definitions for sepsis and organ failure and guidelines for the use of innovative therapies in sepsis. The ACCP/SCCM Consensus Conference Committee. American College of Chest Physicians/Society of Critical Care Medicine. *Chest,* 101**,** 1644-55.

BOOMER, J. S., GREEN, J. M. & HOTCHKISS, R. S. 2014. The changing immune system in sepsis: Is individualized immuno-modulatory therapy the answer? *Virulence,* 5**,** 45-56.

BOSCHER, C., DENNIS, J. W. & NABI, I. R. 2011. Glycosylation, Galectins and Cellular Signaling. *Current Opinion in Cell Biology,* 23**,** 383-392.

BOYSE, E. A. & OLD, L. J. 1969. Some aspects of normal and abnormal cell surface genetics. *Annual Review of Genetics,* 3**,** 269-290.

BRANDLEY, B. K. & SCHNAAR, R. L. 1986. Cell-surface carbohydrates in cell recognition and response. *Journal of Leukocyte Biology,* 40**,** 97-111.

BRIMBLE, S. N., SHERRER, E. S., UHL, E. W., WANG, E., KELLY, S., MERRILL, A. H., ROBINS, A. J. & SCHULZ, T. C. 2007. The Cell Surface Glycosphingolipids SSEA-3 and SSEA-4 Are Not Essential for Human ESC Pluripotency. *Stem Cells,* 25**,** 54-62.

BROCKHAUSEN, I. 1995. Biosynthesis 3. Biosynthesis of O-glycans of the N-acetylgalactosamine-Œ±-Ser/Thr linkage type. *New Comprehensive Biochemistry,* 29**,** 201-259.

BROCKHAUSEN, I. 2006. Mucin-type O-glycans in human colon and breast cancer: glycodynamics and functions. *EMBO reports,* 7**,** 599-604.

BROCKHAUSEN, I. & KUHNS, W. 1997. Biosynthesis of O-glycans. *Glycoproteins and Human Disease.* Springer.

CAMPBELL, M. P., PETERSON, R., MARIETHOZ, J., GASTEIGER, E., AKUNE, Y., AOKI-KINOSHITA, K. F., LISACEK, F. & PACKER, N. H. 2013. UniCarbKB: building a knowledge platform for glycoproteomics. *Nucleic Acids Research***,** gkt1128.

CAMPBELL, M. P., ROYLE, L., RADCLIFFE, C. M., DWEK, R. A. & RUDD, P. M. 2008. GlycoBase and autoGU: tools for HPLC-based glycan analysis. *Bioinformatics,* 24**,** 1214-1216.

CHOUMERIANOU, D. M., DIMITRIOU, H. & KALMANTI, M. 2008. Stem cells: promises versus limitations. *Tissue Engineering Part B: Reviews,* 14**,** 53-60.

CHRISTENSEN, B., NIELSEN, M. S., HASELMANN, K. F., PETERSEN, T. E. & SØRENSEN, E. S. 2005. Post-translationally modified residues of native human osteopontin are located in clusters: identification of 36 phosphorylation and five O-glycosylation sites and their biological implications. *Biochemical Journal,* 390**,** 285.

CIVIN, C. I. & GORE, S. D. 1993. Antigenic analysis of hematopoiesis: a review. *Journal of Hematotherapy,* 2**,** 137-144.

COOPER, C. A., JOSHI, H. J., HARRISON, M. J., WILKINS, M. R. & PACKER, N. H. 2003. GlycoSuiteDB: a curated relational database of glycoprotein glycan structures and their biological sources. 2003 update. *Nucleic Acids Research,* 31**,** 511-513.

CRAIG, A. M., SMITH, J. & DENHARDT, D. 1989. Osteopontin, a transformation-associated cell adhesion phosphoprotein, is induced by 12-O-tetradecanoylphorbol 13-acetate in mouse epidermis. *Journal of Biological Chemistry,* 264**,** 9682-9689.

CUMMINGS, R. D. 2009. The repertoire of glycan determinants in the human glycome. *Molecular BioSystems,* 5**,** 1087-1104.

CUMMINGS, R. D. & PIERCE, J. M. 2014. The challenge and promise of glycomics. *Chemistry & biology,* 21**,** 1-15.

DAVIES, G. J., GLOSTER, T. M. & HENRISSAT, B. 2005. Recent structural insights into the expanding world of carbohydrate-active enzymes. *Current Opinion in Structural Biology,* 15**,** 637-645.

DELL, A., GALADARI, A., SASTRE, F. & HITCHEN, P. 2011. Similarities and differences in the glycosylation mechanisms in prokaryotes and eukaryotes. *International Journal of Microbiology,* 2010.

DENHARDT, D. T. & GUO, X. 1993. Osteopontin: a protein with diverse functions. *The FASEB journal,* 7**,** 1475-1482.

DIMITROFF, C. J., LEE, J. Y., FUHLBRIGGE, R. C. & SACKSTEIN, R. 2000. A distinct glycoform of CD44 is an L-selectin ligand on human hematopoietic cells. *Proceedings of the National Academy of Sciences,* 97**,** 13841-13846.

EAVENSON, M., KOCHUT, K. J., MILLER, J. A., RANZINGER, R., TIEMEYER, M., AOKI, K. & YORK, W. S. 2015. Qrator: A web-based curation tool for glycan structures. *Glycobiology,* 25**,** 66-73.

ELLGAARD, L. & HELENIUS, A. 2001. ER quality control: towards an understanding at the molecular level. *Current Opinion in Cell Biology,* 13**,** 431-437.

FATTOM, A. I., HORWITH, G., FULLER, S., PROPST, M. & NASO, R. 2004. Development of StaphVAX™, a polysaccharide conjugate vaccine against S. aureus infection: from the lab bench to phase III clinical trials. *Vaccine,* 22**,** 880-887.

FEARS, C. Y. & WOODS, A. 2006. The role of syndecans in disease and wound healing. *Matrix Biology,* 25**,** 443-456.

FRY, D. E. 2012. Sepsis, systemic inflammatory response, and multiple organ dysfunction: the mystery continues. *Am Surg,* 78**,** 1-8.

FUSTER, M. M. & ESKO, J. D. 2005. The sweet and sour of cancer: glycans as novel therapeutic targets. *Nature Reviews Cancer,* 5**,** 526-542.

GANG, E. J., BOSNAKOVSKI, D., FIGUEIREDO, C. A., VISSER, J. W. & PERLINGEIRO, R. C. 2007. SSEA-4 identifies mesenchymal stem cells from bone marrow. *Blood,* 109**,** 1743-1751.

GEA-BANACLOCHE, J. C., OPAL, S. M., JORGENSEN, J., CARCILLO, J. A., SEPKOWITZ, K. A. & CORDONNIER, C. 2004. Sepsis associated with immunosuppressive medications: an evidence-based review. *Crit Care Med,* 32**,** S578-90.

GENTILE, L. F., CUENCA, A. G., EFRON, P. A., ANG, D., BIHORAC, A., MCKINLEY, B. A., MOLDAWER, L. L. & MOORE, F. A. 2012. Persistent inflammation and immunosuppression: a common syndrome and new horizon for surgical intensive care. *J Trauma Acute Care Surg,* 72**,** 1491-501.

GERICKE, A., QIN, C., SPEVAK, L., FUJIMOTO, Y., BUTLER, W., S√∏RENSEN, E. & BOSKEY, A. 2005. Importance of phosphorylation for osteopontin regulation of biomineralization. *Calcified tissue international,* 77**,** 45-54.

GERLACH, J. Q., KRUEGER, A., GALLOGLY, S., HANLEY, S. A., HOGAN, M. C., WARD, C. J., JOSHI, L. & GRIFFIN, M. D. 2013. Surface glycosylation profiles of urine extracellular vesicles. *PloS one,* 8**,** e74801.

GHAREHBAGHIAN, A., HAQUE, K. M., TRUMAN, C., EVANS, R., MORSE, R., NEWMAN, J., BANNISTER, G., ROGERS, C. & BRADLEY, B. A. 2004. Effect of autologous salvaged blood on postoperative natural killer cell precursor frequency. *Lancet,* 363**,** 1025-30.

GHAZARIAN, H., IDONI, B. & OPPENHEIMER, S. B. 2011. A glycobiology review: carbohydrates, lectins and implications in cancer therapeutics. *Acta histochemica,* 113**,** 236-247.

GHOSH, T., CHATTOPADHYAY, K., MARSCHALL, M., KARMAKAR, P., MANDAL, P. & RAY, B. 2009. Focus on antivirally active sulfated polysaccharides: from structure,Äìactivity analysis to clinical evaluation. *Glycobiology,* 19**,** 2-15.

GINALDI, L., LORETO, M. F., CORSI, M. P., MODESTI, M. & DE MARTINIS, M. 2001. Immunosenescence and infectious diseases. *Microbes Infect,* 3**,** 851-7.

GOSPODAROWICZ, D. 1974. Localisation of a fibroblast growth factor and its effect alone and with hydrocortisone on 3T3 cell growth. *Nature,* 249**,** 123-127.

GREEN, M., PASTEWKA, J. & PEACOCK, A. 1973. Differential staining of phosphoproteins on polyacrylamide gels with a cationic carbocyanine dye. *Analytical Biochemistry,* 56**,** 43-51.

HÄLLEBERG NYMAN, M., JOHANSSON, J.-E., PERSSON, K. & GUSTAFSSON, M. 2011. A prospective study of nosocomial urinary tract infection in hip fracture patients. *Journal of clinical nursing,* 20**,** 2531-2539.

HAMILTON, S. R. & GERNGROSS, T. U. 2007. Glycosylation engineering in yeast: the advent of fully humanized yeast. *Current opinion in biotechnology,* 18**,** 387-392.

HAMMOND, C., BRAAKMAN, I. & HELENIUS, A. 1994. Role of N-linked oligosaccharides, glucose trimming and calnexin during glycoprotein folding in the endoplasmic reticulum. *Proc. Natl. Acad. Sci. USA,* 91**,** 913-917.

HARRIS, R. J. & SPELLMAN, M. W. 1993. O-linked fucose and other post-translational modifications unique to EGF modules. *Glycobiology,* 3**,** 219-224.

HART, C., SCHULENBERG, B., STEINBERG, T. H., LEUNG, W. Ä. & PATTON, W. F. 2003. Detection of glycoproteins in polyacrylamide gels and on electroblots using Pro-Q Emerald 488 dye, a fluorescent periodate Schiff-base stain. *Electrophoresis,* 24**,** 588-598.

HENDERSON, J., DRAPER, J., BAILLIE, H., FISHEL, S., THOMSON, J., MOORE, H. & ANDREWS, P. 2002. Preimplantation human embryos and embryonic stem cells show comparable expression of stage-specific embryonic antigens. *Stem Cells,* 20**,** 329-337.

HIRABAYASHI, J., KUNO, A. & TATENO, H. 2014. Development and applications of the lectin microarray. *SialoGlyco Chemistry and Biology II.* Springer.

HOTCHKISS, R. S., MONNERET, G. & PAYEN, D. 2013. Immunosuppression in sepsis: a novel understanding of the disorder and a new therapeutic approach. *The Lancet infectious diseases,* 13**,** 260-268.

HU, S. & WONG, D. T. 2009. Lectin microarray. *PROTEOMICS-Clinical Applications,* 3**,** 148-154.

ISLAM, N., WHITEHOUSE, M., MEHENDALE, S., HALL, M., TIERNEY, J., O'CONNELL, E., BLOM, A., BANNISTER, G., HINDE, J. & CEREDIG, R. 2014.

Post-traumatic immunosuppression is reversed by anti-coagulated salvaged blood transfusion: deductions from studying immune status after knee arthroplasty. *Clinical & Experimental Immunology,* 177**,** 509-520.

JENKINS, N., PAREKH, R. B. & JAMES, D. C. 1996. Getting the glycosylation right: implications for the biotechnology industry. *Nature Biotechnology,* 14**,** 975-981.

JONES, M. B., ROSENBERG, J. N., BETENBAUGH, M. J. & KRAG, S. S. 2009. Structure and synthesis of polyisoprenoids used in N-glycosylation across the three domains of life. *Biochimica et Biophysica Acta (BBA)-General Subjects,* 1790**,** 485-494.

JONO, S., PEINADO, C. & GIACHELLI, C. M. 2000. Phosphorylation of osteopontin is required for inhibition of vascular smooth muscle cell calcification. *Journal of Biological Chemistry,* 275**,** 20197-20203.

KANNAGI, R., COCHRAN, N. A., ISHIGAMI, F., HAKOMORI, S.-I., ANDREWS, P., KNOWLES, B. B. & SOLTER, D. 1983. Stage-specific embryonic antigens (SSEA-3 and-4) are epitopes of a unique globo-series ganglioside isolated from human teratocarcinoma cells. *The EMBO journal,* 2**,** 2355.

KAWASHIMA, H. 2006. Roles of sulfated glycans in lymphocyte homing. *Biological and Pharmaceutical Bulletin,* 29**,** 2343-2349.

KEYKHOSRAVANI, M., DOHERTY-KIRBY, A., ZHANG, C., BREWER, D., GOLDBERG, H. A., HUNTER, G. K. & LAJOIE, G. 2005. Comprehensive identification of post-translational modifications of rat bone osteopontin by mass spectrometry. *Biochemistry,* 44**,** 6990-7003.

KHAN, S., LOPEZ,ÄÊCHUA, C., ZHANG, J., FISHER, L., S√∏RENSEN, E. & DENHARDT, D. 2002. Soluble osteopontin inhibits apoptosis of adherent endothelial cells deprived of growth factors*. *Journal of cellular biochemistry,* 85**,** 728-736.

KLEINMAN, H. K. & MARTIN, G. R. Matrigel: basement membrane matrix with biological activity. Seminars in Cancer Biology, 2005. Elsevier, 378-386.

KORNFELD, R. & KORNFELD, S. 1985. Assembly of asparagine-linked oligosaccharides. *Annual Review of Biochemistry,* 54**,** 631-664.

KUMAR, G. L. & KIERNAN, J. A. 2010. Special stains and H&E. *Connection***,** 14.

LAINE, R. A. 1997. Chapter 1. The Information-Storing Potential of the Sugar Code. *Glycosciences: Status and Perspectives***,** 1-14.

LAIRSON, L., HENRISSAT, B., DAVIES, G. & WITHERS, S. 2008. Glycosyltransferases: structures, functions, and mechanisms. *Biochemistry,* 77**,** 521.

LANCTOT, P. M., GAGE, F. H. & VARKI, A. P. 2007. The glycans of stem cells. *Current Opinion in Chemical Biology,* 11**,** 373-380.

LANDEMARRE, L., CANCELLIERI, P. & DUVERGER, E. 2013. Cell surface lectin array: parameters affecting cell glycan signature. *Glycoconjugate Journal,* 30**,** 195-203.

LASKY, L. A. 1992. Selectins: interpreters of cell-specific carbohydrate information during inflammation. *Science,* 258**,** 964-969.

LINHARDT, R. J. & TOIDA, T. 1997. Heparin oligosaccharides: new analogues development and applications. Marcel Dekker: New York, NY, USA.

LIS, H. & SHARON, N. 1998. Lectins: carbohydrate-specific proteins that mediate cellular recognition. *Chemical Reviews,* 98**,** 637-674.

LIZAK, C., GERBER, S., NUMAO, S., AEBI, M. & LOCHER, K. P. 2011. X-ray structure of a bacterial oligosaccharyltransferase. *Nature,* 474**,** 350-355.

LOMBARD, V., RAMULU, H. G., DRULA, E., COUTINHO, P. M. & HENRISSAT, B. 2014. The carbohydrate-active enzymes database (CAZy) in 2013. *Nucleic Acids Research,* 42**,** D490-D495.

MA, S., XIE, N., LI, W., YUAN, B., SHI, Y. & WANG, Y. 2014. Immunobiology of mesenchymal stem cells. *Cell Death & Differentiation,* 21**,** 216-225.

MINAI,TEHRANI, A., CHANG, S.-H., PARK, S. B. & CHO, M. H. 2013. The O-glycosylation mutant osteopontin alters lung cancer cell growth and migration in vitro and in vivo. *International Journal of Molecular Medicine,* 32**,** 1137-1149.

MODY, R., ANTARAM JOSHI, S. H. & CHANEY, W. 1995. Use of lectins as diagnostic and therapeutic tools for cancer. *Journal of pharmacological and Toxicological Methods,* 33**,** 1-10.

MONDAL, G., CHATTERJEE, U., CHAWLA, Y. K. & CHATTERJEE, B. P. 2011. Alterations of glycan branching and differential expression of sialic acid on alpha fetoprotein among hepatitis patients. *Glycoconjugate journal,* 28**,** 1-9.

MOREMEN, K. W., TIEMEYER, M. & NAIRN, A. V. 2012. Vertebrate protein glycosylation: diversity, synthesis and function. *Nature Reviews Molecular Cell Biology,* 13**,** 448-462.

MURAMATSU, T. & MURAMATSU, H. 2004. Carbohydrate antigens expressed on stem cells and early embryonic cells. *Glycoconjugate Journal,* 21**,** 41-45.

NACHBAR, M., OPPENHEIM, J. & THOMAS, J. 1980. Lectins in the US Diet. Isolation and characterization of a lectin from the tomato (Lycopersicon esculentum). *Journal of Biological Chemistry,* 255**,** 2056-2061.

NAUTA, A. J. & FIBBE, W. E. 2007. Immunomodulatory properties of mesenchymal stromal cells. *Blood,* 110**,** 3499-3506.

NEMIR, M., DEVOUGE, M. W. & MUKHERJEE, B. 1989. Normal rat kidney cells secrete both phosphorylated and nonphosphorylated forms of osteopontin showing different physiological properties. *Journal of Biological Chemistry,* 264**,** 18202-18208.

NOVAK, M. & VETVICKA, V. 2008. β-glucans, history, and the present: immunomodulatory aspects and mechanisms of action. *Journal of immunotoxicology,* 5**,** 47-57.

O'RIORDAN, N., GERLACH, J. Q., KILCOYNE, M., O'CALLAGHAN, J., KANE, M., HICKEY, R. M. & JOSHI, L. 2014. Profiling temporal changes in bovine milk lactoferrin glycosylation using lectin microarrays. *Food chemistry,* 165**,** 388-396.

OHTSUBO, K. & MARTH, J. D. 2006. Glycosylation in cellular mechanisms of health and disease. *Cell,* 126**,** 855-867.

PAPPA, K. I. & ANAGNOU, N. P. 2009. Novel sources of fetal stem cells: where do they fit on the developmental continuum?

PARK, H.-M., PARK, J.-H., KIM, Y.-W., KIM, K.-J., JEONG, H.-J., JANG, K.-S., KIM, B.-G. & KIM, Y.-G. 2013. The Xeno-glycomics database (XDB): a relational database of qualitative and quantitative pig glycome repertoire. *Bioinformatics,* 29**,** 2950-2952.

PÉREZ, S. & MULLOY, B. 2005. Prospects for glycoinformatics. *Current opinion in structural biology,* 15**,** 517-524.

PEREZ-VILAR, J. & HILL, R. L. 1999. The structure and assembly of secreted mucins. *Journal of Biological Chemistry,* 274**,** 31751-31754.

PONTA, H., SHERMAN, L. & HERRLICH, P. A. 2003. CD44: from adhesion molecules to signalling regulators. *Nature Reviews Molecular Cell Biology,* 4**,** 33-45.

PRADO-LOPEZ, S., DUFFY, M. M., BAUSTIAN, C., ALAGESAN, S., HANLEY, S. A., STOCCA, A., GRIFFIN, M. D. & CEREDIG, R. 2014. The influence of

hypoxia on the differentiation capacities and immunosuppressive properties of clonal mouse mesenchymal stromal cell lines. *Immunology and Cell Biology*.

RABINOVICH, G. A., VAN KOOYK, Y. & COBB, B. A. 2012. Glycobiology of immune responses. *Annals of the New York Academy of Sciences,* 1253**,** 1-15.

RANZINGER, R., AOKI-KINOSHITA, K. F., CAMPBELL, M. P., KAWANO, S., LUTTEKE, T., OKUDA, S., SHINMACHI, D., SHIKANAI, T., SAWAKI, H. & TOUKACH, P. 2014. GlycoRDF: an ontology to standardize glycomics data in RDF. *Bioinformatics***,** 31/6/919.

RANZINGER, R., HERGET, S., WETTER, T. & VON DER LIETH, C.-W. 2008. GlycomeDB‚Äìintegration of open-access carbohydrate structure databases. *BMC Bioinformatics,* 9**,** 384.

RAZZOUK, S., BRUNN, J., QIN, C., TYE, C., GOLDBERG, H. & BUTLER, W. 2002. Osteopontin posttranslational modifications, possibly phosphorylation, are required for in vitro bone resorption but not osteoclast adhesion. *Bone,* 30**,** 40.

ROSS, S. A., GERLACH, J. Q., GILL, S. K., LANE, J. A., KILCOYNE, M., HICKEY, R. M. & JOSHI, L. 2016. Temporal alterations in the bovine buttermilk glycome from parturition to milk maturation. *Food Chemistry,* 211**,** 329-338.

RYŠLAVÁ, HELENA, DOUBNEROVÁ, V., KAVAN, D. & VANĚKA, O. 2013. Effect of posttranslational modifications on enzyme function and assembly. *Journal of Proteomics,* 92**,** 80-109.

SACKSTEIN, R. 2004. The bone marrow is akin to skin: HCELL and the biology of hematopoietic stem cell homing. *Journal of Investigative Dermatology,* 122**,** 1061-1069.

SALIH, E., ASHKAR, S., GERSTENFELD, L. C. & GLIMCHER, M. J. 1997. Identification of the phosphorylated sites of metabolically 32P-labeled osteopontin from cultured chicken osteoblasts. *Journal of Biological Chemistry,* 272**,** 13966-13973.

SALIH, E., ZHOU, H. Y. & GLIMCHER, M. J. 1996. Phosphorylation of purified bovine bone sialoprotein and osteopontin by protein kinases. *Journal of Biological Chemistry,* 271**,** 16897-16905.

SCHEPETKIN, I. A. & QUINN, M. T. 2006. Botanical polysaccharides: macrophage immunomodulation and therapeutic potential. *International immunopharmacology,* 6**,** 317-333.

SCHWARZBAUER, J. 1999. Basement membrane: Putting up the barriers. *Current Biology,* 9**,** R242-R244.

SETHURAMAN, N. & STADHEIM, T. A. 2006. Challenges in therapeutic glycoprotein production. *Current Opinion in Biotechnology,* 17**,** 341-346.

SGADARI, C., ANGIOLILLO, A. & TOSATO, G. 1996. Inhibition of angiogenesis by interleukin-12 is mediated by the interferon-inducible protein 10. *Blood,* 87**,** 3877-3882.

SHARON, N. 1996. Carbohydrate-Lectin Interactions in Infectious Disease. *Toward Anti-Adhesion Therapy for Microbial Diseases.* Springer.

SHARON, N. & LIS, H. 2004. History of lectins: from hemagglutinins to biological recognition molecules. *Glycobiology,* 14**,** 53R-62R.

SHORR, A. F. & JACKSON, W. L. 2005. Transfusion practice and nosocomial infection: assessing the evidence. *Curr Opin Crit Care,* 11**,** 468-72.

SILVERBOARD, H., AISIKU, I., MARTIN, G. S., ADAMS, M., ROZYCKI, G. & MOSS, M. 2005. The role of acute blood transfusion in the development of acute respiratory distress syndrome in patients with severe trauma. *J Trauma,* 59**,** 717-23.

SINGH, M., ANANTHULA, S., MILHORN, D. M., KRISHNASWAMY, G. & SINGH, K. 2007. Osteopontin: a novel inflammatory mediator of cardiovascular disease. *Front Biosci,* 12**,** 214-221.

SINGHAL, S., POWLES, R., KULKARNI, S., TRELEAVEN, J., SIROHI, B., MILLAR, B., SHEPHERD, V., SASO, R., ROWLAND, A. & LONG, S. 2000. Comparison of marrow and blood cell yields from the same donors in a double-blind, randomized study of allogeneic marrow vs blood stem cell transplantation. *Bone Marrow Transplantation,* 25**,** 501-505.

SODEK, J., GANSS, B. & MCKEE, M. 2000. Osteopontin. *Critical Reviews in Oral Biology & Medicine,* 11**,** 279-303.

SOLTER, D. & KNOWLES, B. B. 1978. Monoclonal antibody defining a stage-specific mouse embryonic antigen (SSEA-1). *Proceedings of the National Academy of Sciences,* 75**,** 5565-5569.

SØRENSEN, E. S., PETERSEN, T. E. & HØJRUP, P. 1995. Posttranslational modifications of bovine osteopontin: identification of twenty-eight phosphorylation and three O-glycosylation sites. *Protein Science,* 4**,** 2040-2049.

STEEN, P. V. D., RUDD, P. M., DWEK, R. A. & OPDENAKKER, G. 1998. Concepts and principles of O-linked glycosylation. *Critical Reviews in Biochemistry and Molecular Biology,* 33**,** 151-208.

STOWELL, S. R., JU, T. & CUMMINGS, R. D. 2015. Protein glycosylation in cancer. *Annual review of pathology,* 10**,** 473.

STRASSER, R. 2016. Plant protein glycosylation. *Glycobiology*, cww023.

SUGRUE, T., LOWNDES, N. F. & CEREDIG, R. 2014. Hypoxia enhances the radioresistance of mouse mesenchymal stromal cells. *Stem Cells,* 32**,** 2188-2200.

SVAROVSKY, S. A. & JOSHI, L. 2008. Biocombinatorial selection of carbohydrate binding agents of therapeutic significance. *Current drug discovery technologies,* 5**,** 20-28.

SVENSSON, L., ASZÓDI, A., REINHOLT, F. P., FÄSSLER , R., HEINEGÅRD, D. & OLDBERG, Å. 1999. Fibromodulin-null mice have abnormal collagen fibrils, tissue organization, and altered lumican deposition in tendon. *Journal of Biological Chemistry,* 274**,** 9636-9647.

TAKAHASHI, M., KUROKI, Y., OHTSUBO, K. & TANIGUCHI, N. 2009. Core fucose and bisecting GlcNAc, the direct modifiers of the N-glycan core: their functions and target proteins. *Carbohydrate Research,* 344**,** 1387-1390.

TATENO, H., KUNO, A., ITAKURA, Y. & HIRABAYASHI, J. 2010. Chapter Eight-A Versatile Technology for Cellular Glycomics Using Lectin Microarray. *Methods in enzymology,* 478**,** 181-195.

TAUB, D. D., LLOYD, A. R., CONLON, K., WANG, J. M., ORTALDO, J., HARADA, A., MATSUSHIMA, K., KELVIN, D. & OPPENHEIM, J. 1993. Recombinant human interferon-inducible protein 10 is a chemoattractant for human monocytes and T lymphocytes and promotes T cell adhesion to endothelial cells. *The Journal of Experimental Medicine,* 177**,** 1809-1814.

TAYLOR, M. E. & DRICKAMER, K. 2011. *Introduction to Glycobiology*, Oxford university press.

THOMAS, E. D., LOCHTE JR, H. L., LU, W. C. & FERREBEE, J. W. 1957. Intravenous infusion of bone marrow in patients receiving radiation and chemotherapy. *New England Journal of Medicine,* 257**,** 491-496.

THOMSON, S. P. & WILLIAMS, D. B. 2005. Delineation of the lectin site of the molecular chaperone calreticulin. *Cell Stress & Chaperones,* 10**,** 242.

TIGANIS, T., LEAVER, D. D., HAM, K., FRIEDHUBER, A., STEWART, P. & DZIADEK, M. 1992. Functional and morphological changes induced by tunicamycin in dividing and confluent endothelial cells. *Experimental cell research,* 198**,** 191-200.

TIWARI, A., TURSKY, M. L., MUSHAHARY, D., WASNIK, S., COLLIER, F. M., SUMA, K., KIRKLAND, M. A. & PANDE, G. 2013. Ex vivo expansion of haematopoietic stem/progenitor cells from human umbilical cord blood on acellular

scaffolds prepared from MS-5 stromal cell line. *Journal of Tissue Engineering and Regenerative Medicine,* 7**,** 871-883.

TZIANABOS, A. O. 2000. Polysaccharide immunomodulators as therapeutic agents: structural aspects and biologic function. *Clinical microbiology reviews,* 13**,** 523-533.

VARKI, A., CUMMINGS, R. D., ESKO, J. D., FREEZE, H. H., STANLEY, P., BERTOZZI, C. R., HART, G. W., ETZLER, M. E. & SASISEKHARAN, R. 2009. Glycomics. *Essentials of Glycobiology***,** 679-690.

VAUGHAN, E. E., LIEW, A., MASHAYEKHI, K., DOCKERY, P., MCDERMOTT, J., KEALY, B., FLYNN, A., DUFFY, A., COLEMAN, C. & O'REGAN, A. 2012b. Pretreatment of endothelial progenitor cells with osteopontin enhances cell therapy for peripheral vascular disease. *Cell transplantation,* 21**,** 1095-1107.

VEMBAR, S. S. & BRODSKY, J. L. 2008. One step at a time: endoplasmic reticulum-associated degradation. *Nature Reviews Molecular Cell Biology,* 9**,** 944-957.

VILLARROEL, J. P., GUAN, Y., WERLIN, E., SELAK, M. A., BECKER, L. B. & SIMS, C. A. 2013. Hemorrhagic shock and resuscitation are associated with peripheral blood mononuclear cell mitochondrial dysfunction and immunosuppression. *J Trauma Acute Care Surg,* 75**,** 24-31.

VON DER LIETH, C.-W., FREIRE, A. A., BLANK, D., CAMPBELL, M. P., CERONI, A., DAMERELL, D. R., DELL, A., DWEK, R. A., ERNST, B. & FOGH, R. 2011. EUROCarbDB: an open-access platform for glycoinformatics. *Glycobiology,* 21**,** 493-502.

WADA, I., RINDRESS, D., CAMERON, P., OU, W., DOHERTY, J. N., LOUVARD, D., BELL, A., DIGNARD, D., THOMAS, D. & BERGERON, J. 1991. SSR alpha and associated calnexin are major calcium binding proteins of the endoplasmic reticulum membrane. *Journal of Biological Chemistry,* 266**,** 19599-19610.

WALSH, C. 2006. *Posttranslational modification of proteins: expanding nature's inventory*, Roberts and Company Publishers Englewood, CO.

WANG, K. X. & DENHARDT, D. T. 2008. Osteopontin: role in immune regulation and stress responses. *Cytokine & growth factor reviews,* 19**,** 333-345.

WARDI, A. H. & MICHOS, G. A. 1972. Alcian blue staining of glycoproteins in acrylamide disc electrophoresis. *Analytical Biochemistry,* 49**,** 607-609.

WASNIK, S., TIWARI, A., KIRKLAND, M. A. & PANDE, G. 2012. *3 Osteohematopoietic Stem Cell Niches in Bone Marrow*.

WILDT, S. & GERNGROSS, T. U. 2005. The humanization of N-glycosylation pathways in yeast. *Nature Reviews Microbiology,* 3**,** 119-128.

WILKE, S., KRAUSZE, J., GOSSEN, M., GROEBE, L., JAGER, V., GHERARDI, E., VAN DEN HEUVEL, J. & BUSSOW, K. 2010. Glycoprotein production for structure analysis with stable, glycosylation mutant CHO cell lines established by fluorescence-activated cell sorting. *Protein Science,* 19**,** 1264-1271.

WINTERBURN, P. 1972. The significance of glycosylated proteins. *Nature,* 236**,** 147-151.

WOBUS, A. M. & BOHELER, K. R. 2005. Embryonic stem cells: prospects for developmental biology and cell therapy. *Physiological reviews,* 85**,** 635-678.

WOODS, A. 2001. Syndecans: transmembrane modulators of adhesion and matrix assembly. *Journal of Clinical Investigation,* 107**,** 935.

XIA, L., JU, T., WESTMUCKETT, A., AN, G., IVANCIU, L., MCDANIEL, J. M., LUPU, F., CUMMINGS, R. D. & MCEVER, R. P. 2004. Defective angiogenesis and fatal embryonic hemorrhage in mice lacking core 1–derived O-glycans. *The Journal of cell biology,* 164**,** 451-459.

ZACHARIUS, R. M., ZELL, T. E., MORRISON, J. H. & WOODLOCK, J. J. 1969. Glycoprotein staining following electrophoresis on acrylamide gels. *Analytical Biochemistry,* 30**,** 148-152.

CHAPTER 2

EFFECTS OF POST-TRANSLATIONAL MODIFICATIONS OF OSTEOPONTIN IN VASCULAR BIOLOGY

2.1. Introduction

OPN is a phosphorylated glycoprotein expressed in various tissues and cell types and it is regulated by such many factors as hormones, growth factors and tumour factors including the physiological conditions of the cell. It has been shown that OPN augments the angiogenic potential of endothelial progenitor cells and plays an important role in vascular biology. In this current chapter, the importance of PTMs on OPN molecules in their biological function was studied using a model endothelial cell line.

2.1.1. OPN structure

OPN has been categorized as a member of the small integrin binding ligand *N*-linked glycoprotein (SIBLING) family of related proteins. The SIBLING proteins share close similarities in secretion, phosphorylation and acidic nature (Fisher et al., 2001). The OPN gene is reported to exist as single copy gene in humans and mouse, but it also exists in various isoforms as a result of alternative splicing, alternative translation, alternative cleavage and different PTMs (Craig et al., 1989). OPN has a polypeptide backbone of up to 300 amino acid residues (Sgadari et al., 1996). The Mr of OPN differs among species and expression systems due to differences in PTMs such as glycosylation and phosphorylation. The pleiotropic nature of OPN can be attributed to its various peptide isoforms, its PTMs and the range of cellular interactions it participates in.

The gene for OPN was identified and described in the supernatants of transformed cell and was called secreted phosphoprotein 1 (SPP1) (Senger et al., 1979). In humans, the SPP1 gene maps to chromosome 4 located at 4q22.1 and has 7 exons in total, where 6 are coding exons and 1 is non-coding exon. Other than two known isoforms, five different splice variants of human OPN are also known to exist (Table 2.2) and have different biological activities. Due to lack of any secondary or tertiary structure, OPN falls in the category of Intrinsically Disordered Proteins (IDPs), a class of biologically active proteins without well-folded structures yet upon binding can dynamically adopt different functional conformations (Kurzbach et al., 2013). Algorithms designed specifically to predict the secondary structures of protein have suggested the possible existence of α-helical regions in the carboxyl terminal

portions of the molecules and areas of β-sheets on either sides of GRDGS sequence (Sodek et al., 2000), but these predications have not been validated experimentally. However, structural studies for OPN indicate no specific structural arrangement.

OPN has a conserved arginine-glycine-aspartic acid (RGD) domain similar to some ECM proteins such as fibronectin and vitronectin (Oldberg et al., 1986). OPN binds to various integrins, including αvβ3, αvβ1, and α5β1, using its RGD domain and it binds to the CD44 receptor with its RGD domain for attachment and chemotaxis (Weber et al., 1996). In Figure 2.1, different features of OPN are viewed in the Protein database (PDB) viewer (http://www.rcsb.org/pdb/home/home.do) to demonstrate the typical complexity of OPN at the protein level, but OPN may differ in amino acid composition further based on its originating tissues and cells. OPN is expressed disparately in tissues including kidney (Kohri et al., 1993), bone (Oldberg et al., 1986), biological fluids such as breast milk, (Senger et al., 1989), urine, blood and seminal fluid, and on epithelial surfaces (Brown et al., 1992).

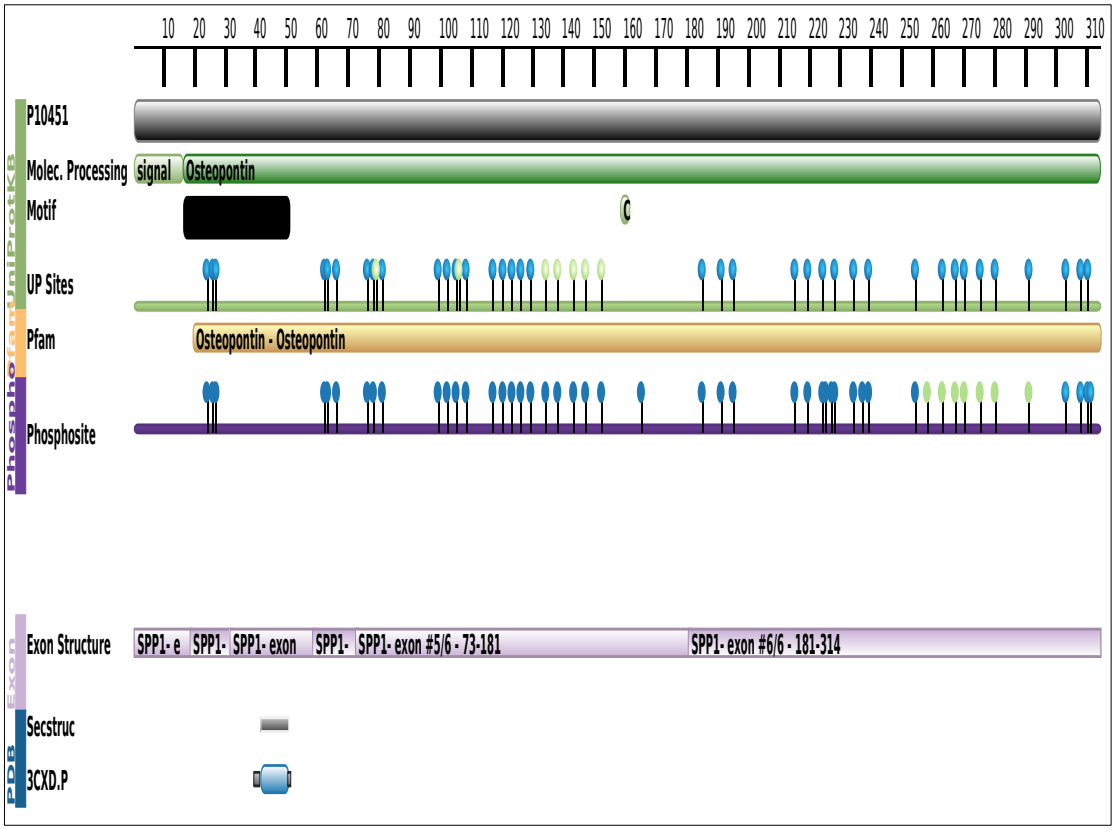

Figure 2.1. Modified PDB schematic representation of complexity of OPN and its potential PTMs. The data used to create this schematic representation was derived

from multiple sources; data in green originates from UniProtKB (http://www.uniprot.org/uniprot/), data in yellow originates from Pfam, data in purple originates from Phosphosite, data in lilac represent the genomic exon structure projected onto the UniProt sequence and data in blue originates from PDB and Secstruc. Secondary structure is projected from representative PDB entries onto the UniProt sequence.

2.1.2. PTMs of OPN

In silico predictions were made for three mammalian OPNs (human, mouse and bovine) using various bioinformatics tools to predict their potential PTM sites (Figure 2.2 and Table 2.1). A sequence alignment was made to compare the polypeptides of all three OPNs using their amino acid sequences as retrieved from the UniProt database (UniProt IDs for human, mouse and bovine OPNs are P10451, P10923 and P31096, respectively) along with human OPN that was expressed in *E. coli* sequence without signal peptide. More than 60% identity was found among the different OPNs as previously reported (Sodek et al., 2000) (Figure 2.2). However, the homology among the sequences for the conserved sequences is higher.

NetOGlyc (http://www.cbs.dtu.dk/services/NetOGlyc/) NetNGlyc (http://www.cbs.dtu.dk/services/NetNGlyc/), and Phosphosite (http://www.phosphosite.org/) are online programs used to predict *O*-linked and *N*-linked glycosylation sites and phosphorylation sites, respectively. The NetOGlyc server produces predictions of mucin *O*-linked glycosylation sites in mammalian proteins while the NetNGlyc server predicts *N*-linked glycosylation sites in human proteins that examine the sequence context of Asn-Xaa-Ser/Thr sequons.

Table 2.1. PTM predictions for OPN from three species as determined by NetOGly, NetNGly and Phosphosite.

Species	***O*-linked**	***N*-linked**	**Phosphorylation**
Human	5	2	40
Mouse	10	1	46
Bovine	11	1	43

These *in silico* predictions can provide insight about the potential OPN PTMs (Table 2.1). The available information on the presence or absence of PTMs on OPN reported in literature is compiled in Table 1.1. To fully understand OPN's heterogeneous nature, it is necessary to characterise each individual glycoprotein population depending on the preparation and source. The *in silicio* predictions provide an indication about the presence of potential sites that can be modified post translationally. However, these potential sites can exhibit differences in their PTMs depending on the tissues, physiological and pathological condition of the cell.

Due to OPN's various PTMs (Table 1.1), the apparent Mr can range from 45 to 75 kDa, although the functional domains are conserved across the species. Although the different OPN isoforms, splice variants and glycoforms have been previously characterized, it is still essential to characterise the particular OPN selected before experimental use. Hence, a confirmatory characterisation is needed depending on the source and method of expression of purification of OPN molecules.

Table 2.2. OPN and its various known splice variants

Isoforms of OPN	Other names	Amino acids	Mr
Isoform A (identifier: P10451-1)	OPN-a, OP1B	314	35,423
Isoform A (identifier: P10451-2)	OPN-b, OP1A	58-71, 300	33,844
Isoform C (identifier: P10451-3)	OPN-c	31-57, 287	32,355
Isoform D (identifier: P10451-4)	-	95-116, 292	33,017
Isoform 5 (identifier: P10451-5)	-	59-72, 300	33,843

OPN contains several cell adhesion domains, which are as follows

- arginine-glycine-aspartate containing domain (RGD)–interacting with $\alpha v\beta 3$, $\alpha v\beta 1$, $\alpha v\beta 5$ (Liaw et al., 1995).
- a cryptic-serine-valine-valine-tyrosine-glutamic-acid-leucine-arginine (SVVYGLR) -cleaved by thrombin cleavage.

- a matrix metalloproteinase (MMP) cleavage site. Upon cleavage by MMP-3 and MMP-7, the adhesive and migratory activity of OPN increases compared to full-length OPN (Valdimarsdóttir, 2004).
- leucine-proline-valine (LPV)
- two conserved N-terminal domains with the heparin binding homology.
- two highly conserved glutamine residues aiding in cross linkage between itself or other proteins by transglutamination (Sørensen et al., 1994).

The thrombin cleavage site located six amino acids to the C-terminal side of the RGD motif, is conserved in all species (Smith et al., 1996, Yokosaki et al., 1999).

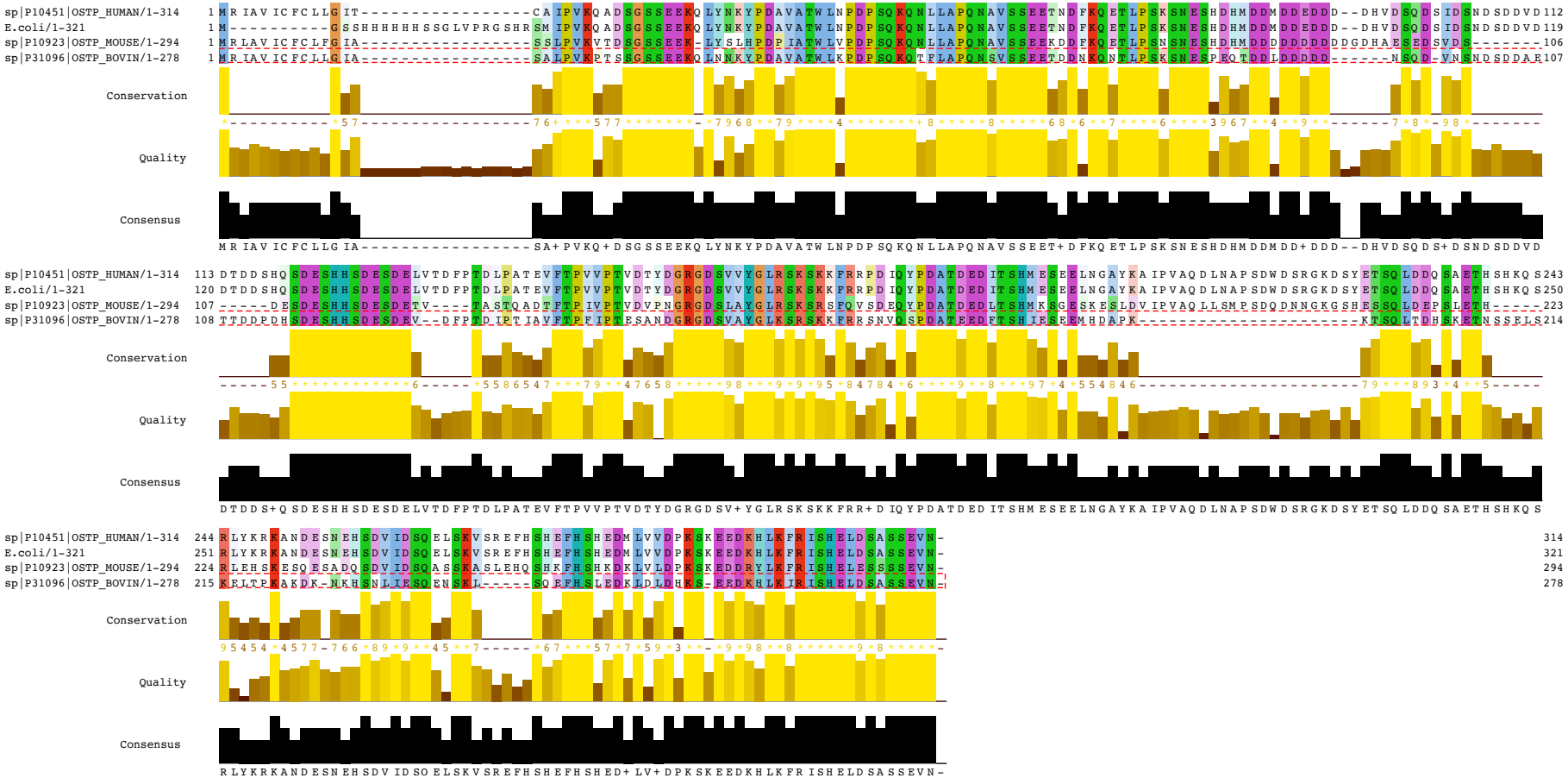

Figure 2.2. Amino acid sequences for mouse, human, bovine and *E. coli* expressed OPN were aligned using MAFFT version 7. The alignment shows the conservation across the sequences. The colour coding of the sequences has been done according to the amino acids

2.1.3. Functions of OPN and importance of its PTMs

Two different isoforms of OPN have been reported in mammals; secreted OPN (sOPN) and intracellular OPN (iOPN). sOPN is expressed by many different cell types, including macrophages, neutrophils, dendritic cells (DCs), natural killer cells, and T and B lymphocytes, while iOPN is expressed by antigen presenting cells (APCs), including macrophages and DCs (Inoue and Shinohara, 2011). In the immune system, OPN has been recognized as an early T-lymphocyte activation 1 cytokine molecule and is demonstrated to play an important role in the development of type-1 immunity against bacterial infections within 48 hours (Ashkar et al., 2000). It functions as a T helper 1 (Th1) cytokine and promotes cell-mediated immune responses. OPN has been identified as a biomarker for various types of cancers and inflammatory diseases (Sumpio et al., 2002, Pardali et al., 2010).

Since the discovery of OPN as a bone matrix protein in 1985, follow-on work has included identification of the binding sequence, expression profiling and elucidation of *in vivo* function (Denhardt and Guo, 1993). Alterations in phosphorylation and glycosylation can lead to different binding affinities to cell receptors. Phosphorylation of OPN has been reported as necessary for various physiological activities such as migration of cancer cells (Al-Shami et al., 2005), cell adhesion and bone resorption by osteoclasts (Razzouk et al., 2002). Native OPN purified from rat neonatal smooth muscle cell cultures inhibits smooth muscle cell calcification but neither the dephosphorylated OPN or OPN expressed in *E. coli* (and therefore devoid of eukaryotic PTMs) can perform similarly (Jono et al., 2000). Also, native OPN, but not the dephosphorylated forms of OPN, affect the *de novo* formation or regulation of mineralisation by hydroxyapatite deposition (Gericke et al., 2005). With respect to glycosylation, decreased sialylation has been reported to reduce the binding of OPN to its receptor in the case of ras-transformed cells. Concomitantly, mutations at the mucin type *O*-linked glycosylation sites inhibited downstream signalling in non-small cell lung cancer models *in vitro* and *in vivo* (Minai,Tehrani et al., 2013). The roles of OPN and its PTMs are explored in different biological models. However, a detailed comparison among the OPN molecules, and its glycoforms and phosphoforms using a same platform and assay conditions have never been attempted using HUVECs as a model cell line in vascular biology.

2.1.3. HUVECS

The endothelium, made up of endothelial cells, maintains vascular homeostasis by modulating vascular tone, regulating interaction between different cell types and local cellular growth, and mediating the inflammatory responses to local injury (Karimova and Pinsky, 2001). Endothelial cells provide an anatomical barrier to prevent the extravasation of circulating blood into the vessel wall. They play major roles in angiogenesis and vasculogenesis. HUVECs are a model system for the study of the regulation of endothelial cell function and the role of the endothelium in the response of the blood vessel wall to stretch, shear forces and angiogenesis. During vasculogenesis, formation of blood vessels occurs *de novo* while angiogenesis refers to formation of new blood vessels from pre-existing ones (Risau and Lemmon, 1988, Sumpio et al., 2002). The process of vasculogenesis only takes place during embryonic development while angiogenesis occurs in the adult human body in order to maintain integrity of tissues and physiological homeostasis during inflammation, wound healing and menstruation (Folkman, 1995, Folkman, 1997). In addition, angiogenesis is an important process for tumours as tumours are dependent on a blood supply of nutrition for them to be able to grow, survive and metastasize (Valdimarsdóttir, 2004). Angiogenesis is initiated by the proliferation of the endothelial cells either by the action of different growth factors or hypoxic conditions. Endothelial cells maintain their quiescent state in the absence of angiogenic stimuli. They can be activated to perform different angiogenesis roles upon activation with pro-angiogenic factors such as OPN.

The roles of OPN and its PTMs have not been explored to understand their importance in the different step of angiogenesis process, which was carried in the present study. Specific enzymatic digestions were performed on OPN from several sources and expression hosts to characterise the OPN molecules and generate alternative glycoforms and the dephosphorylated form. All of the forms of OPN were tested on HUVECs to assess the functional activities of the glycoforms. Proliferation, tubule formation and angiogenesis assays were performed to differentiate between angiogenic properties of OPN glycoforms.

2.2. Materials and Methods

2.2.1. Materials

Three different commercial OPN molecules were used in this study; human recombinant OPN (rhOPN) expressed in NS0 cells and bovine OPN (bOPN) purified from bovine milk were from R&D Systems (Minneapolis, MN, U.S.A.) and OPN expressed in *E. coli* (eOPN) from Prospec (Rehovot, Israel). Neuraminidase from *Clostridium perfringens* was bought from Calbiochem (La Jolla, U.S.A.), *endo*–α–*N*-acetylgalactosaminidase (O-glycanase) was purchased from New England Biolabs Ltd. (Hitchin, U.K.) and alkaline phosphatase (AP) from calf intestine mucosa and thiazolyl blue tetrazolium blue (MTT) were bought from Sigma-Aldrich Co. (Wicklow, Ireland). The Pro-Q® Diamond Phosphoprotein Blot Stain Kit was from Life technologies (Carlsbad, CA, U.S.A.). NuPAGE 4–12% Bis-Tris gels and MOPS running buffer, Pierce™ Coomassie (Bradford) Protein Assay Kit and Pierce™ Silver Stain Kit were bought from Life Technologies (Carlsbad, CA, U.S.A.). Rabbit polyclonal anti PI3K p58α/β/γ (sc-292114), phospho-PI3K p85α (Tyr 457) (sc-293115), AKT 1/2/3/(H-136) (sc-8312), β-actin, mouse monoclonal anti-phospho AKT 1/2/3 (11E6) (sc-81433) antibodies were purchased from Santa Cruz Biotechnology (CA, U.S.A). Enhanced chemiluminescent (ECL) substrate WesternBright™ ECL substrate (Advansta, Menlo Park, CA, USA) and polyvinylidene difluoride (PVDF) membrane were obtained from Millipore (Billerica, MA, USA). TranSignal Human Cytokine Antibody Array 3.0 kit was purchased from Panomics (Redwood City, CA, U.S.A). Matrigel® was bought from BD Biosciences (Oxford, U.K.). Transwell chambers (pore size 8.0 μm) were bought from Costar, Corning Inc., (NY, U.S.A). Endothelial Basal Medium-2 (EBM-2, cat. no. CC-3156) and Endothelial Growth Media (EGM-2 when supplemented with SingleQuot kit (cat. no. CC-3162) were bought from Lonza (Basal, Switzerland). Human umbilical vein endothelial cells (HUVECs) were purchased from ATCC (Rockville, U.S.A.).

2.2.2. Cell culture

HUVECs were grown in the EGM-2 media supplemented with the provided Singlequot cocktail. Cells were passaged with 0.25% trypsin and 1 mM EDTA every

3-4 days and culture were replaced with fresh EGM-2 media. Confluent, serum-deprived HUVECs in *passages* 5 to 10 were used in the studies described below.

2.2.3. Modification of OPN glycoforms

All OPN preparations (bOPN, rhOPN, eOPN and hOPN, 2 μg each) were digested with 0.5 U of neuraminidase at 37 °C for 2 h in PBS, pH 4.6 and then followed by peptide-*N*-glycosidase F (PNGase F) digestion after initial denaturation in 10X denaturing Buffer for 10 minutes at 94° C and follow on incubation for 1 h with supplied 10X NP-40 and 10X G7 buffers or 0.05 mU of O-glycanase in 50 mM sodium phosphate, pH 6.0, at 37 °C overnight. Enzymatically modified products were electrophoresed on 4-12% SDS polyacrylamide gels under non-reducing conditions in MOPS running buffer at 150 V for 1.5 h. The gels were visualized using Pierce™ Silver Stain Kit as per manufacturer's instructions. Using the same protocol, glycoforms of bOPN and rhOPN were generated for testing them for biological assays (Table 2.3).

2.2.4. Dephosphorylation of OPN

OPN preparations (bOPN, rhOPN and eOPN, 2 μg each) were treated with 2.5 U of AP at 37 °C for 1 h in 10 mM of ammonium bicarbonate (NH_4HCO_3), pH 8.5. The digested products were electrophoresed on 4-12% SDS-NuPAGE gels under non-reducing conditions in MOPS running buffer at 150 V for 1.5 h. The gels were silver stained as described in section 2.2.3. Confirmation of the dephosphorylation of OPN molecules was performed by staining with the Pro-Q® Diamond stain kit where casein, a phosphorylated protein, was used as the positive control. Using the same protocol, phosphoforms of bOPN and rhOPN were generated (Table 2.3).

Table 2.3. Codes for OPN molecules from different sources and their generated glycoforms and phosphoforms.

Molecule	**Code**	**Digestion**
Bovine OPN from milk	bOPN	-
	bOPN N	Neuraminidase
	bOPN NO	Neuraminidase and O-glycanse
	bOPN PNGase F	bOPN PF
	bOPN AP	Alkaline phosphatase
Recombinant OPN produced in NS0 cells	rhOPN	-
	rhOPN N	Neuraminidase
	rhOPN NO	Neuraminidase and O-glycanse
	rhOPN PNGase F	rhOPN PF
	rhOPN AP	Alkaline phosphatase
Recombinant OPN produced in *E. coli*	eOPN	-
Human OPN from breast milk	hOPN	-

2.2.5. Lectin microarray construction

Proprietary lectin microarrays (v2.3.0) were constructed as described previously (Gerlach et al., 2014, Kilcoyne et al., 2012a). Forty eight lectins sourced from multiple vendors were diluted to 0.5 mg/mL in PBS supplemented with 1 mM of respective haptenic sugar to maintain binding site integrity (Table 2.5) and printed on Nexterion H (Schott, Mainz, Germany) functionalized glass slides using a Scienion S3 non-contact spotter (Scienion, Berlin, Germany). During printing, the following conditions were maintained: 62% (+/- 2%) relative humidity, 20 °C. Following printing, slides were incubated in a humidity chamber overnight at room temperature to ensure completion of conjugation. Unoccupied functional groups were deactivated by incubation with 100 mM ethanolamine in 50 mM sodium borate, pH 8.0. Slides

were then washed with TBS with 0.05% Tween-20 (TBS-T) three times and once with PBS, centrifuged dry (450 x g, 5 min) and stored dry at 4 °C with desiccant until use.

2.2.5. Glycoprofiling of OPN on lectin microarray

BOPN, rhOPN, eOPN and fetuin were labelled with DyLight^{TM} 550 NHS-ester activated fluorescent dye. All the labelling steps were performed in the dark to avoid photobleaching. Unincorporated dye was removed from labelled OPN by sequential washes using PBS in a 10 kDa molecular weight cutoff (MWCO) (Amicon, Thermo-Fisher). (Kilcoyne et al., 2012a, Kilcoyne et al., 2014). After titrations were made with different concentrations of OPNs 2 μg/mL of OPN was used for triplicate profiling on the lectin microarray. OPN samples were applied to microarrays using an eight-well gasket slide and incubation cassette system (Agilent Technologies, Cork, Ireland). 70 μL of each labelled glycoform dilution, in Tris-buffered saline supplemented with Ca^{2+} and Mg^{2+} ions (TBS; 20 mM Tris-HCl, 100 mM NaCl, 1 mM $CaCl_2$, 1 mM $MgCl_2$, pH 7.2) with 0.05% Tween-20 (TBS-T), was applied to each well of the gasket. The microarray slide was sandwiched with the gasket, the cassette was assembled and placed in a rotating incubation oven (23 °C, approximately 4 rpm) for 1 h. Incubation chambers were disassembled under TBS-T, and microarrays were washed in a Coplin jar twice in TBS-T for 2 min each and once with TBS. Microarrays were dried by centrifugation (450 x *g*) and imaged immediately using an Agilent G2505B microarray scanner at 5 μm resolution (532 nm laser, 100% laser power, 90% PMT).

2.2.5. Microarray data extraction and analysis

Data extraction was performed essentially as previously described (Kilcoyne et al., 2012b, Kilcoyne et al., 2014). Raw intensity values were extracted from high-resolution *.tif files using GenePix Pro v6.1.0.4 (Molecular Devices, Berkshire, UK) and a proprietary *.gal file (containing feature spot addresses and identities) using adaptive diameter (70–130%) circular alignment based on 230 mm features and were exported as text to Excel (Version 2010, Microsoft, Dublin, Ireland). Local background-corrected median feature intensity data (F543median-B543) was

analysed. The median values, derived from data from six replicate spots per subarray, was handled as a single data point for graphical and statistical analyses.

Lectin microarray intensity values were normalized to the median total intensity value for all features across all subarrays in a single experiment. Unsupervised, hierarchical clustering of the lectin microarray data was performed with Hierarchical Clustering Explorer v3 (http://www.cs.umd.edu/hcil/hce/hce3.html). Normalized data was clustered with parameters such as no pre-filtering, complete linkage, and Euclidean distance.

2.2.6. Proliferation assay

HUVECS (1 x 10^4) were seeded in each well of a 96 well-plate and incubated overnight to adhere in EGM-2 media. The following day, serum-rich media (EGM-2) was replaced with serum-free media (EBM-2) with increasing concentrations (0, 7.81 15.63, 31.25, 62.5, 125, 250, 500, and 1000 nM) of bOPN and rhOPN for 24 and 48 h at 37 °C. HUVECs in serum free media with 1% FBS were referred as the control. Cells were further incubated with MTT (0.5 mg/mL) at 37 °C for 4 h. After incubation, media was removed and the purplish-blue crystals formed by the adherent cells were dissolved at room temperature. The absorbance was measured at 570 nm using a spectrophotometric SpectraMax M^5 reader. This was done to obtain an optimised concentration of bOPN and rhOPN that significantly increased the cell proliferation.

The optimised concentration of 125 nM of bOPN and rhOPN was further used to test the glycoforms using MTT assay. For generation of glycoforms of bOPN and rhOPN, the concentration of OPN molecules was adjusted to 125 nM for controls and the generated glycoforms while performing digestions with glycosidase and AP enzymes to remove certain residues or oligosaccharides and phosphates. The glycoforms of bOPN, rhOPN along eOPN were incubated with serum-deprived HUVECs for 24 h and 48 h. The experiments were performed in triplicate.

2.2.7. Matrigel® assay

Capillary tube formation by HUVECs in Matrigel® was the basis for this assay. Matrigel®, thawed at 4 °C overnight (50 μL/mL), was aliquoted into a 96-well plate and allowed to stand at room temperature for 60 min to polymerize. HUVECs were trypsinized and 5 x 10^4 cells in culture medium (EBM-2) per well with optimised concentrations of 5 μg/mL of bOPN, rhOPN and eOPN were plated onto polymerized Matrigel® in triplicate. The plate was incubated at 37 °C at 5% CO_2 for 24, 40 and 64 h. Tube formation in the Matrigel® was observed using confocal microscopy at the endpoint for each assay. Quantification of the length of capillary tubes in each well was performed using a freeware plugin angiogenesis analyzer toolset for National Institutes of Health ImageJ software (Carpentier, 2012).

2.2.8. Angiogenesis antibody assay

HUVECs were plated at a density of 50 x 10^4 with 2 μg/mL bOPN or eOPN in a 6 well plate. Supernatants were collected after 8 h of incubation by centrifuging cells at 500 *g* for 10 min and the cell pellet was discarded. Cytokine angiogenesis antibody array membranes were blocked with 1% BSA in TBST for 1 h at room temperature and then washed and incubated with about 1 mL of conditioned media for 2 h at room temperature as per manufacturer's instructions. The membranes were washed three times with wash buffer before being incubated with a biotin-conjugated anti-cytokine mix of panel of activators and inhibitors of angiogenesis against membrane bound cytokines. Following the primary incubation, the membranes were washed as above and incubated with HRP conjugated streptavidin (1:1000 dilution) for 45 min at room temperature. The membranes were then incubated with HRP detection substrate and imaged using an image analysis system (Flurochem; Alpha Innotech Corporation, San Leandro, CA) at different exposure times. The imaged were saved digitally as. tiff files and used for the analysis.

2.2.9. Signalling pathway analysis

HUVECs (50 x 10^3) were incubated with .5 μM of untreated bOPN, bOPN N, bOPN NO, bOPN AP, or eOPN at for 30 min in serum-free media. Cells were lysed using radio-immunoprecipitation assay (RIPA) buffer (Tris 50 mM, NaCl 150 mM, 0.1% SDS, 0.5% sodium deoxycholate, 1% Triton^{TM} X-100, pH 8). Protein was quantified

using the BCA assay (Kruger, 1994). HUVEC lysates (50 μg protein) were electrophoresed on 8% SDS-PAGE gels in SDS running buffer and transferred using a semi-dry blotter 1.5 mA/cm^2 for 30 min to PVDF membranes (0.45 μm). Cathode (0.3M aminocaproic acid, 0.03M Tris, 0.0375% SDS) and anode (0.3M Tris, 0.1M glycine, 0.0375% SDS) buffers facilitated the transfer of the proteins from the gel to the PVDF membrane. Following blocking with 1% BSA in PBS, the membrane was probed with primary antibodies, p-AKT or p-PI3K in 1:200 dilution (100 μg/μL stock concentrations) stripped using mild strip buffer (15 g glycine, 1 g SDS, 10 mL Tween 20 in 1 L ultrapure water, pH 2.2), re-probed with either PI3K or AKT antibodies in 1:200 dilution and then visualized using chemiluminescence reagents. Anti β-actin antibody was used for probing the total protein as the loading control. The blots were imaged using a ChemiDoc® imaging system (Bio-Rad, Hercules, CA, U.S.A.) and quantified using Quantity One version 4.6.1 software (Bio-Rad). For densitometry analysis (intensity/area) ratios were considered to evaluate the signal differences between the treatments.

2.2.10. Statistical analysis

Statistical analysis was performed using Prism (version 5.0.1, GraphPad Software Inc., La Jolla, CA, USA). One way and two-way ANOVA was performed to assess the time-dependent statistical variations and effects of different OPN molecules.

2.3. Results

2.3.1. Characterization of OPN

OPN preparations were subjected to the action of different endo- and exo-glycosidases to cleave, in a stepwise manner, selected terminal and internal linkages of the glycan moieties from the glycoprotein and to generate glycoforms for performing functional assays using HUVECs. These preparations were also treated with AP to generate dephosphorylated OPN isoforms. Figure 2.3A shows bOPN and respective digestions separated on a 4-12% gel. bOPN had an apparent molecular mass of 68 kDa and when it was digested with neuraminidase, there was a slight shift toward lower relative Mr on the gel, but with the consecutive digestion with O-glycanase, the bOPN band was shifted to approximately 55 kDa. A shift to lower Mr was also apparent upon AP digestion (Figure 2.3 A). RhOPN was also resolved at

approximately 68 kDa and was shifted to approximately to 55 kDa after *O*-glycanase treatment but not after AP treatment (Figure 2.3 B). Both bOPN and rhOPN when treated with β-galactosidase did not show any further shift on the gel compared to neuraminidase treatment of bOPN and rhOPN respectively. Neuraminidase digestion cleaves the terminal sialic acids that are negatively charged entities and it makes the neuramindase digested products run lower due to not only the losing molecular weight of sialic acids but charges. When the neuraminidase-digested hOPN and rhOPN were further digested with β-galactosidase, neligible shift in the molecular band was reported on the SDS-PAGE. hOPN showed "fuzzy" bands which suggested a Mr distribution, likely due to a heterogeneous PTMs, and it resolved at higher Mr than both bOPN (Figure 2.3C) and rhOPN. hOPN however showed similar changes upon digestion with neuraminidase, O-glycanase and AP. Thus, based on these observations, bOPN, hOPN and rhOPN were modified with sialylated mucin core type 1 oligosaccharide. (Table 2.4).

Digestion with AP was also performed for all OPN isoforms, bOPN AP, rhOPN AP, and eOPN AP were separated on 4-12 % SDS-PAGE and SDS-PAGE was stained using ProQ Diamond kit staining. However, only bOPN and the positive control, casein, demonstrated the presence of phosphorylation (Figure 2.4A). This confirmed the absence of phosphorylation on rhOPN and eOPN (Figure 2.4B, Table 2.4). These digestion studies confirmed the presence of sialic acids, *O*-glycans and phosphorylation on bOPN, presence of sialic acid and *O*-glycans on rhOPN and absence of phosphates summarised in Table 2.4. EOPN was not affected upon the treatment with the glycosidases or phosphatase confirmed the absence of these PTMs on the bacterially-expressed protein.

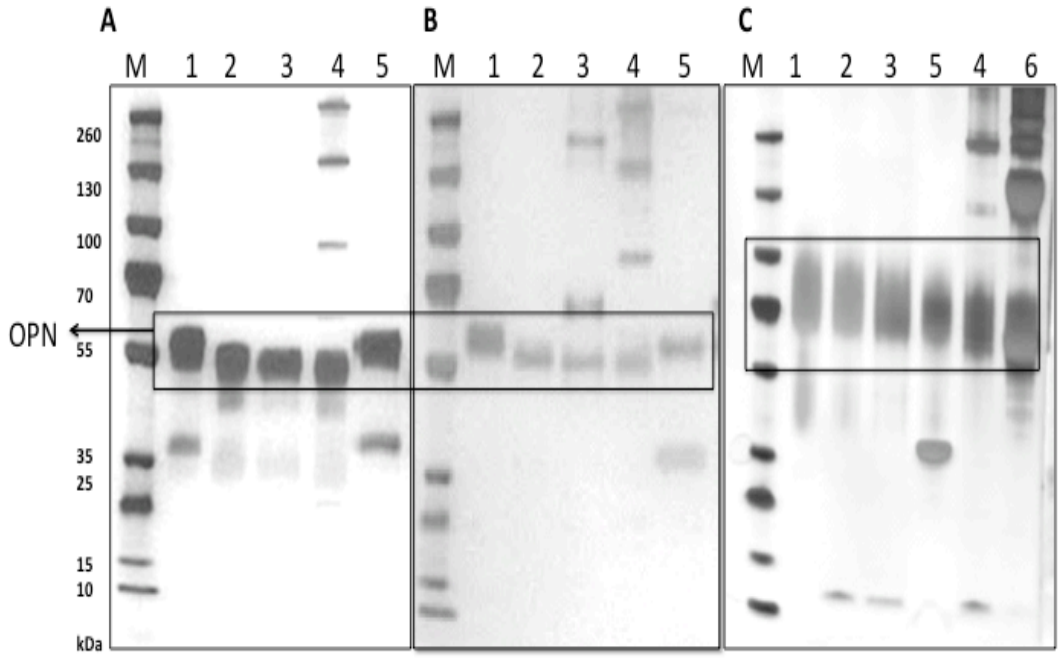

Figure 2.3. Resolution of OPN isoforms on 4-12% Bis-Tris SDS-PAGE after silver staining, bOPN (A), rhOPN (B) and hOPN (C), 2 μg of each OPN molecule was digested with neuraminidase enzyme (lane 2), neuraminidase and β–galactosidase (lane 3), neuraminidase and *O*-glycanase (lane 4), PNGase F (lane 5) and AP (lane 6) and run on 4-12% SDS-NuPAGE gels. Undigested OPN was loaded in lane 1 of A to C.

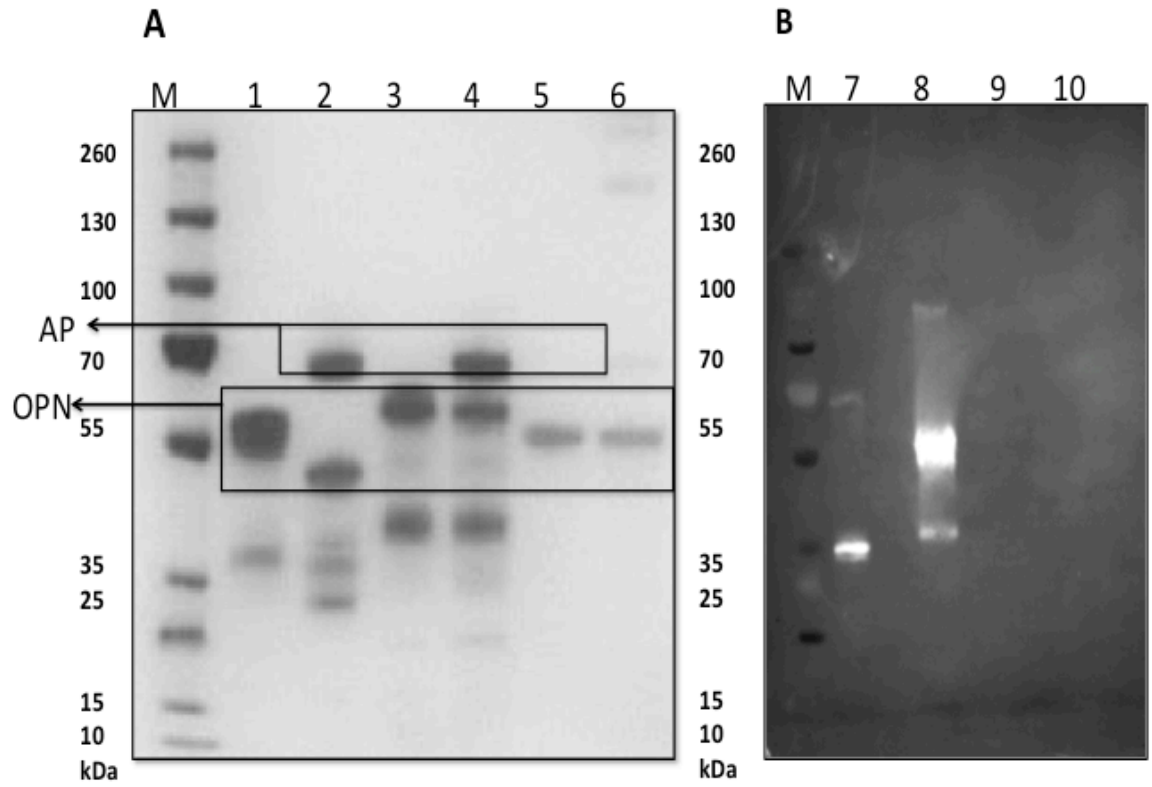

Figure 2.4. Dephosphorylation of OPN from different sources. bOPN (lane 1), bOPN digested with AP (lane 2), rhOPN (lane 3), rhOPN digested with AP (lane 4), eOPN (lane 5), eOPN digested with AP (lane 6) were run on separate 4-12% SDS NuPAGE gel and was visualized with silver stain (A). Casein (lane 7), bOPN (lane 8), rhOPN (lane 9) and eOPN (lane 10) were visualized for phosphorylation using the ProQ Diamond kit (B).

Table 2.4. Summary for digestion studies carried for OPN molecules from different sources, where † denotes presence of PTMs and †† denotes relatively higher presence of PTMs among all the OPN molecules.

Modifications	**bOPN**	**rhOPN**	**hOPN**	**eOPN**
Sialic acid	††	††	†	-
N-linked glycans	-	-	-	-
O-linked glycans	††	†	†	-
Phosphates	††	-	†	-

2.3.2. Lectin glycoprofiling of OPN

Lectin microarray profiling provides a method to distinguish OPN molecules based on their glycosylation. Relative binding intensities of OPN isoforms for 48 lectins with a range of known specificities (Table 2.5) were utilised for generation of the heat map (Figure 2.5). Fetuin was used as a control protein and the digestions studies were performed as confirmation of generation of its glycoforms along the OPN molecules. 15 lectins out of 48 lectins defined the variations among all the molecules incubated on lectin microarray. Feutin controls and AP treated fetuin showed different glyco-profile compared to neuraminidase and O-glycanase digested fetuin. Higher binding with GNA, HHA, SNA and CAA lectins were found for control and AP digested feutin suggesting the *N*-linked and *O*-linked oligosaccharides present on feutin. This binding was lowered for feutin neuraminidase treated (FN) and feutin neuraminidase and O-glycanase treated (FNO), and higher binding for MPA, ACA, Calsapa, RCA and DSA lectin was found. SNA-II lectin also showed relatively higher binding for FN and FNO.

Table 2.5. Lectins printed, their binding specificities, their simple print sugars (1 mM) and the supplying company.

Abbreviation	Source	Species	Common name	Binding specificity*	Print sugar	Supplier
AIA, Jacalin	Plant	*Artocarpus integrifolia*	Jack fruit lectin	Gal, Gal-β-(1,3)-GalNAc (sialylation independent)	Gal	EY Labs
RPbAI	Plant	*Robinia pseudoacacia*	Black locust lectin	Gal	Gal	EY Labs
PA-I	Bacteria	*Pseudomonas aeruginosa*	Pseudomonas lectin	Gal, Gal derivatives	Gal	Sigma Aldrich
SNA-II	Plant	*Sambucus nigra*	Sambucus lectin-II	Gal/GalNAc	Gal	EY Labs
SJA	Plant	*Sophora japonica*	Pagoda tree lectin	β-GalNAc	Gal	EY Labs
DBA	Plant	*Dolichos biflorus*	Horse gram lectin	GalNAc	Gal	EY Labs
GHA	Plant	*Glechoma hederacea*	Ground ivy lectin	GalNAc	Gal	EY Labs
SBA	Plant	*Glycine max*	Soy bean lectin	GalNAc	Gal	EY Labs
VVA-B4	Plant	*Vicia villosa*	Hairy vetch lectin	GalNAc	Gal	EY Labs
BPA	Plant	*Bauhinia purpurea*	Camels foot tree lectin	GalNAc/Gal	Gal	EY Labs
WFA	Plant	*Wisteria floribunda*	Japanese wisteria lectin	GalNAc/sulfated GalNAc	Gal	EY Labs
HPA	Animal	*Helix pomatia*	Edible snail lectin	α-GalNAc	Gal	EY Labs
GSL-I-A4	Plant	*Griffonia simplicifolia*	Griffonia isolectin I A4	GalNAc	Gal	EY Labs
ACA	Plant	*Amaranthus caudatus*	Amaranthin	Sialylated/Gal-β-(1,3)-GalNAc	Lac	Vector Labs
ABL	Fungus	*Agaricus bisporus*	Edible mushroom lectin	Gal-β(1,3)-GalNAc, GlcNAc	Lac	EY Labs
PNA	Plant	*Arachis hypogaea*	Peanut lectin	Gal-β-(1,3)-GalNAc	Lac	EY Labs
GSL-II	Plant	*Griffonia simplicifolia*	Griffonia lectin-II	GlcNAc	GlcNAc	EY Labs
sWGA	Plant	*Triticum vulgaris*	Succinyl WGA	GlcNAc	GlcNAc	EY Labs
DSA	Plant	*Datura stramonium*	Jimson weed lectin	GlcNAc	GlcNAc	EY Labs
STA	Plant	*Solanum tuberosum*	Potato lectin	GlcNAc oligomers	GlcNAc	EY Labs
LEL	Plant	*Lycopersicum eculentum*	Tomato lectin	GlcNAc-β-(1,4)-GlcNAc	GlcNAc	EY Labs
Calsepa	Plant	*Calystegia sepium*	Bindweed lectin	Man/Maltose	Man	EY Labs
NPA	Plant	*Narcissus pseudonarcissus*	Daffodil lectin	α-(1,6)-Man	Man	EY Labs
GNA	Plant	*Galanthus nivalis*	Snowdrop lectin	Man-α-(1,3)-	Man	EY Labs
HHA	Plant	*Hippeastrum hybrid*	Amaryllis agglutinin	Man-α-(1,3)-Man-α-(1,6)-	Man	EY Labs

ConA	Plant	*Canavalia ensiformis*	Jack bean lectin	Man, Glc, GlcNAc	Man	EY Labs
Lch-B	Plant	*Lens culinaris*	Lentil isolectin B	Man, core fucosylated, agalactosylated biantennary *N*-glycans	Man	EY Labs
Lch-A	Plant	*Lens culinaris*	Lentil isolectin A	Man/Glc	Man	EY Labs
PSA	Plant	*Pisum sativum*	Pea lectin	Man, core fucosylated trimannosyl *N*-glycans	Man	EY Labs
WGA	Plant	*Triticum vulgaris*	Wheat germ agglutinin	NeuAc/GlcNAc	GlcNAc	EY Labs
MAA	Plant	*Maackia amurensis*	Maackia agglutinin	Sialic acid-α-(2,3)-linked	Lac	EY Labs
SNA-I	Plant	*Sambucus nigra*	Sambucus lectin-I	Sialic acid-α-(2,6)-linked	Lac	EY Labs
CCA	Animal	*Cancer antennarius*	California crab lectin	*O*-acetyl sialic acids	Lac	EY Labs
PHA-L	Plant	*Phaseolus vulgaris*	Kidney bean leukoagglutinin	Tri- and tetraantennary β-Gal/Gal-β-(1,4)-GlcNAc	Lac	EY Labs
PCA	Plant	*Phaseolus coccineus*	Scarlet runner bean lectin	GlcNAc in complex oligosaccharides	Lac	Sigma Aldrich
PHA-E	Plant	*Phaseolus vulgaris*	Kidney bean erythroagglutinin	Biantennary with bisecting GlcNAc,β-Gal/Gal-β-(1,4)-GlcNAc	Lac	EY Labs
RCA-I/120	Plant	*Ricinus communis*	Castor bean lectin I	Gal-β-(1,4)-GlcNAc	Gal	Vector Labs
CPA	Plant	*Cicer arietinum*	Chickpea lectin	Complex oligosaccharides	Lac	EY Labs
CAA	Plant	*Caragana arborescens*	Pea tree lectin	Gal-β-(1,4)-GlcNAc	Lac	EY Labs
ECA	Plant	*Erythrina cristagalli*	Cocks comb/coral tree lectin	Gal-β-(1,4)-GlcNAc oligomers	Lac	EY Labs
AAL	Fungi	*Aleuria aurantia*	Orange peel fungus lectin	Fuc-α-(1,6)- and Fuc-α-(1,3)-linked	Fuc	Vector Labs
LTA	Plant	*Lotus tetragonolobus*	Lotus lectin	Fuc-α-(1,3)-, Fuc-α-(1→6)- and Fuc-α-(1→2)-linked	Fuc	EY Labs
UEA-I	Plant	*Ulex europaeus*	Gorse lectin-I	Fuc-α-(1,2)-linked	Fuc	EY Labs
EEA	Plant	*Euonymous europaeus*	Spindle tree lectin	Terminal α-linked Gal	Gal	EY Labs
GSL-I-B4	Plant	*Griffonia simplicifolia*	Griffonia lectin-I	Exclusively to terminal α-linked Gal	Gal	EY Labs
MPA	Plant	*Maclura pomifera*	Osage orange lectin	Terminal α-linked Gal	Gal	EY Labs
VRA	Plant	*Vigna radiata*	Mung bean lectin	Terminal α-linked Gal	Gal	EY Labs
MOA	Fungus	*Marasmius oreades*	Fairy ring mushroom lectin	Terminal α-linked Gal	Gal	EY Labs

* Reported recognition based on literature consensus or experimental evidence generated within our laboratory.

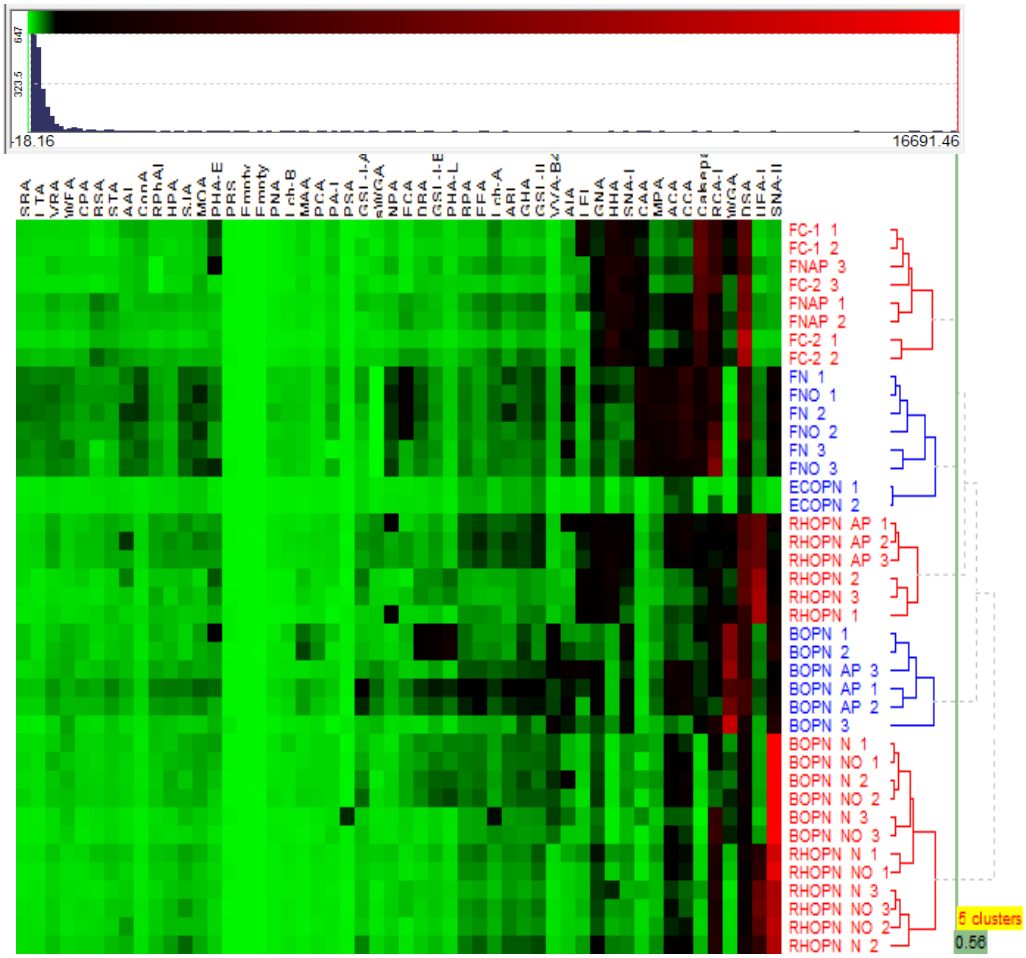

Figure 2.5. Lectin microarray profiling for bOPN, rhOPN, eOPN and their respective glycoforms. The lectin binding profiles were generated for all glycoforms produced by enzymatic treatment. Here FC-1 and FC-2 are fetuin, a glycoprotein standard with a known binding profile, FN is fetuin treated with neuraminidase, FNO is fetuin treated with neuraminidase and O-glycanse, FNAP is fetuin treated with neuraminidase and AP.

As expected, due to the complete absence of glycosylation on the eOPN, there was relatively extremely low eOPN binding to lectins compared to fetuin and OPN with known glycosylation (bOPN and rhOPN, Figure 2.5). UEA-I and DSA lectin overall showed higher relative intensities with rhOPN than bOPN. As UEA-I is known to bind to Fuc in an α-(1, 2) linkage, the presence of α-(1, 2)-fucosylation was indicated rhOPN (Table 2.5) and DSA suggested specific binding to GlcNAc particularly to β-(1, 4)-linked GlcNAc residues in rhOPN (Figure 2.5, Table 2.5). DSA also binds poly-*N*-acetyllactosamine (poly-LacNAc), which extends both *N*-, and mucin type *O*-linked structures however there are no *N*-linked modifications

reported for OPN. In the case of bOPN, WGA, RCA-I and SNA-II lectins showed relatively higher intensities compared to rhOPN. RCA-I binds to Gal in a β-(1, 4)-linkage (Hauke and Korr, 1993) and again most likely demonstrated the presence of polyLacNAc structures. WGA has a reported affinity for both sialic acid and GlcNAc with additional binding affinity to poly-LacNAc structures (Bhavanandan and Katlic, 1979). WGA binding indicated the presence of sialylation on the *O*-linked structures, but the low MAA or SNA-I binding on both rhOPN and bOPN suggested that the potential (Hirabayashi, 2015) presence of sialic acid is minimal. Thus, it is most likely that mucin type core 1 and 2 were present on bOPN and rhOPN extended by poly-LacNAc. The intensity data for UEA-I and DSA suggested rhOPN had more core fucosylation in *O*-linked oligosacchrides than bOPN.

2.3.3. Influence of OPN PTMs on HUVEC proliferation

OPN has been previously reported to increase cell proliferation in neural cells (Lin and Yang-Yen, 2001) but the proliferative effects of OPN on HUEVCs are not extensively explored. To assess the effects of OPN PTMs on endothelial cell proliferation, HUVECS were incubated with increasing concentrations of bOPN and rhOPN to determine a concentration that significantly increased cell proliferation using the MTT assay. bOPN and rhOPN led to increase in the cell absorbance values indicative of increased cell proliferation both 24 and 48 h cultures. bOPN at 1000 nM and rhOPN at 500 nM had greatest effects for increased cell proliferation of 22% and 37% respectively. However, among the enzymatically modified forms of bOPN and rhOPN (bOPN N, bOPN NO, bOPN AP, bOPN N, bOPN NO and bOPN AP), there were no significant differences in absorbance values at the tested concentrations, except for 125 nM at 48 h (Figure 2.6).

bOPN and rhOPN and bOPN N, bOPN NO, bOPN AP rhOPN and eOPN were incubated with serum free HUVECs at 125 nM for 24 and 48 h. The difference between control and OPN treatment were significant, but no significant differences were reported between the native OPN molecules and the glycoforms. However, there were significant time-dependent differences between OPN molecules and glycoforms at 48 h compared to 24 h (Figure 2.7). There were no significant differences among the glycoforms of bOPN observed for the proliferation activity of the glycoforms of OPN. But the absorbance values for bOPN N and bOPN NO were

lower compared to bOPN at 24 h. Also, all the OPN glycoforms performed better over control suggesting a role of OPN in cell proliferation.

Taken together, these results implied that the proliferative effects of OPN on HUVEC cells were protein related, as OPN treatment increased HUVEC cell proliferation independent of its PTMs.

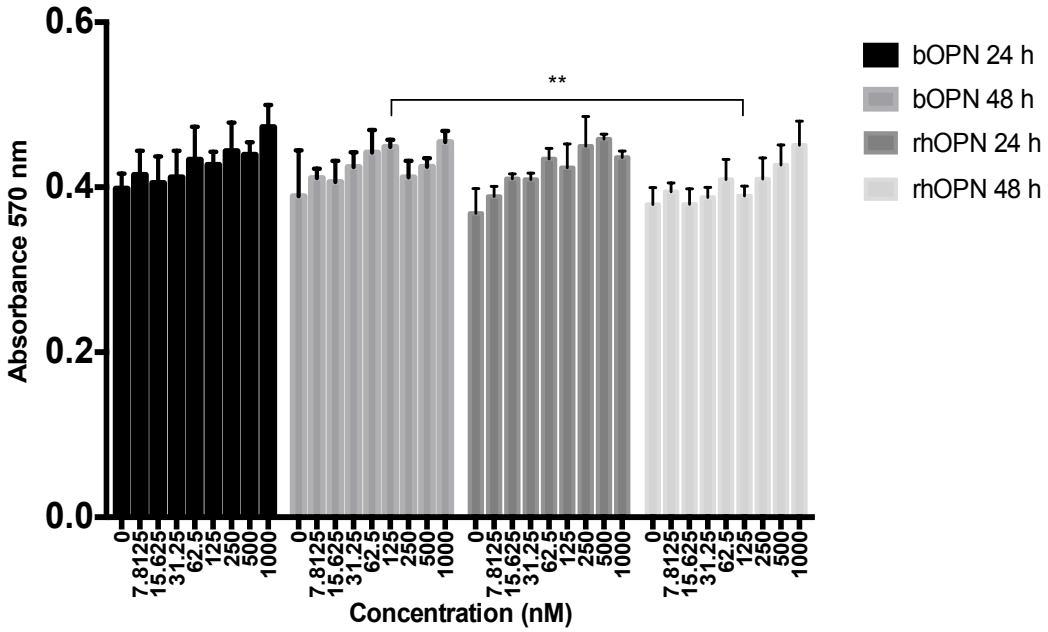

Figure 2.6. Cell proliferation was determined by MTT assay in HUVECs in response to bOPN and rhOPN concentration at two timepoints. HUVECs were seeded on 96 well plates at a density of 1 x 10^4 cells. After attachment and starvation, cells were treated with different concentrations of bOPN and rhOPN for 24 and 48 h. Low serum media (1% FBS) was used in the control. Data are expressed as mean ± s.d and ** is p value < 0.05.

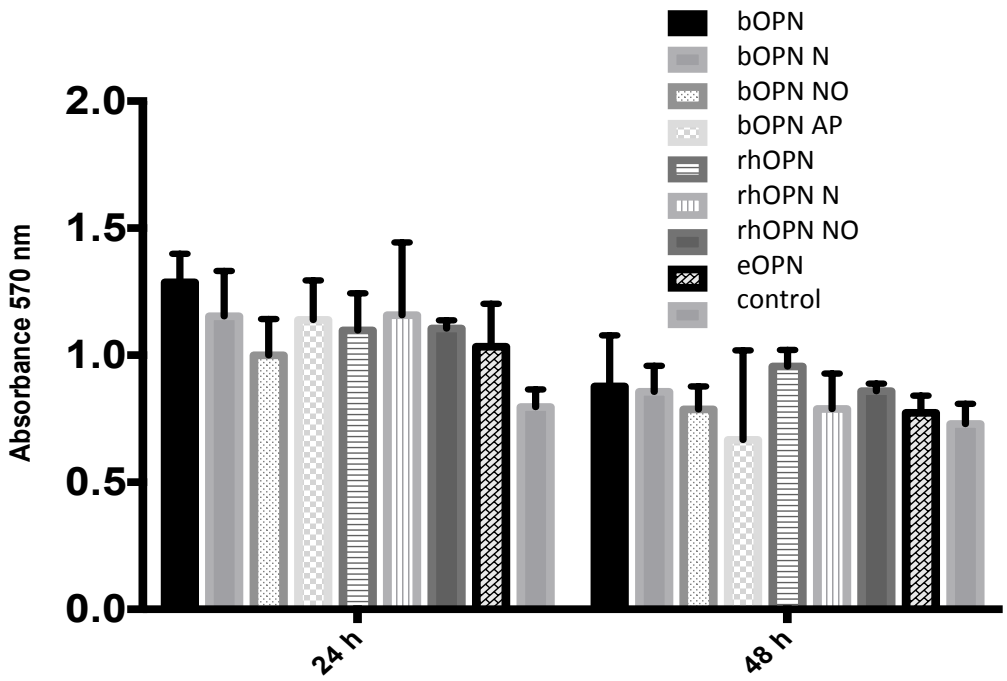

Figure 2.7. Cell proliferation was determined by MTT assay of HUVECs. HUVECs were seeded on 96 well plates at a density of 1 x 10^4 cells. After attachment and starvation, cells were treated with different glycoforms of bOPN, rhOPN and eOPN (each at 125 nM) for 24 and 48 h. Low serum media (1% FBS) was used in control. Data are expressed as mean ± s.d.

2.3.4. Influence of OPN PTMs on tubule formation

OPN has been previously evaluated for its effects on *in vitro* vasculogenesis using Matrigel® (Vaughan et al., 2012a). Here bOPN, rhOPN and eOPN were screened with HUVECs for their ability to form tubules on the Matrigel®. The optimised cell number of 5 x 10^4 cells per well was plated on the Matrigel®, incubated for 24, 40 and 64 h and the number of tubules formed at each time point was manually counted. The number of tubules formed at 24 h was not significantly different between bOPN, rhOPN and eOPN and the control, but the number of tubules at the later time points i.e 64 h was lower for all conditions and varied significantly among all test conditions.

The number of tubules that remained at 40 and 64 h were plotted against the number of tubules at 24 h for each condition in percentage of tubules remaining (Figure 2.8). Significant differences were shown for bOPN but not for rhOPN or eOPN at 40 h against control at 24 h, which indicated the increased stability of tubules maintained

by bOPN. However significant differences in the ability to maintain number of tubules were found for bOPN, rhOPN and eOPN at 40 h compared to control at 40 h. These data suggested the ability of OPN isoforms to maintain tubule structures over time compared to control conditions. However, no significant differences between OPNs from different sources for tubule maintenance were observed which indicated that this ability was due to the protein rather than the PTMs of OPN.

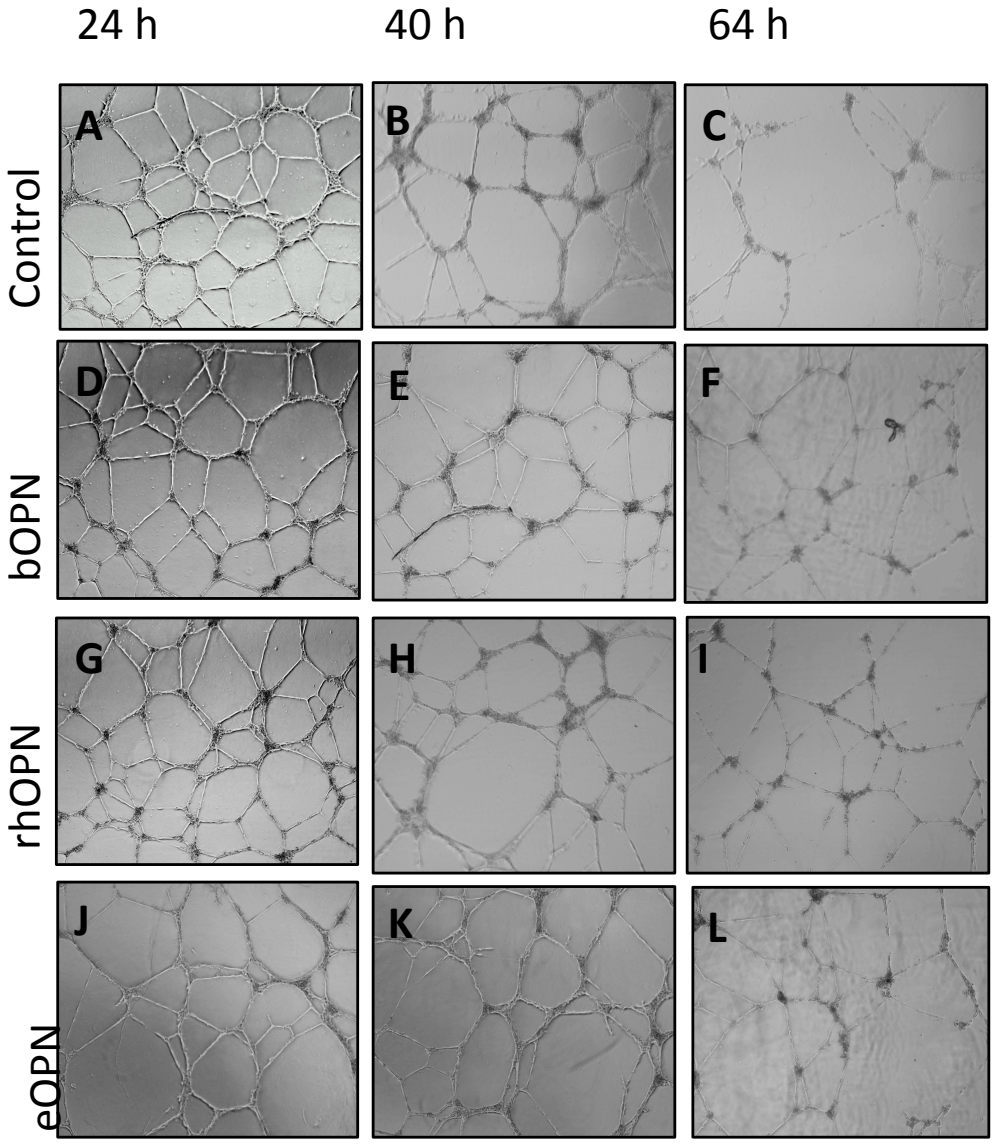

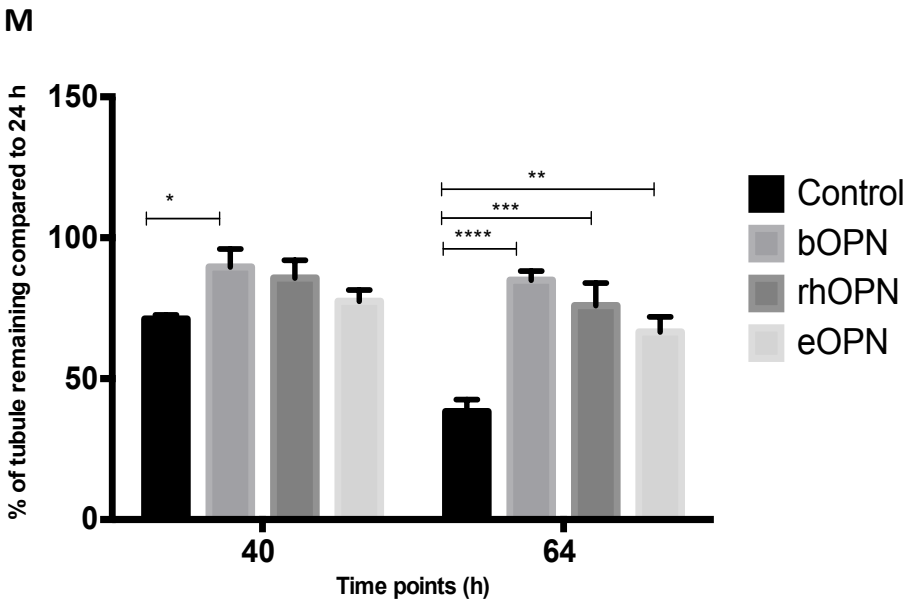

Figure 2.8. HUVEC capillary tube formation *in vitro* induced by OPN and the maintained stability of the tubules. HUVECs were plated on Matrigel® (50 μL each well) at a density of 5 x 10^4 cells per well and treated (5 μg/mL) with bOPN, rhOPN and eOPN (**A to L**). Capillary tube formation images was taken after 24, 40 and 64 h using an inverted microscope and counted using angiogenesis analyser software. (**M**) The data with number of tubules was plotted against 24 h data and represented as mean ± s.d (M). * denotes a p-value < 0.5, ** a p-value < 0.05, *** a p-value 0.005 and **** a p-value < 0.0005.

2.3.5. Angiogenic profiles

Endothelial cells maintain their quiescent state in the absence of angiogenic stimuli maintaining low endothelial cell turnover in healthy adult organism. Upon activation by stimuli such as OPN, release of cytokines and chemokines affect the endothelial cell activation status. They can be positive or negative regulators of angiogenesis. To study this, supernatants from HUVECs incubated with bOPN and eOPN were assayed for angiogenic cytokine expression using an angiogenesis cytokine array (Figure 2.9 and Table 2.6). BOPN was the most glycosylated form of OPN used in this study (section 2.2.1) and eOPN is not modified with any PTMs.

The activators of angiogenic factors, i.e. fibroblast growth factor-β (FGF-β) and interleukin-6 (IL-6), were expressed by HUVECs upon treatment with both bOPN

and eOPN, while interleukin-12 (IL-12), an angiogenic inhibitor, and interferon gamma-induced protein 10 (IP-10) were expressed in response to bOPN but not eOPN. IL-12, a unique cytokine that forms a positive and negative feedback loop in neovascularisation, can also induce the expression of IP-10 in mouse splenocytes suggesting a role of IL-12 in inducing IP-10 expression in certain other cell types (Sgadari et al., 1996). IP-10 has been reported act as chemoattractant and in promoting T-cell adhesion to endothelial cells (Taub et al., 1993).

Following this first observation, various angiogenic factors such as IL-6, IL-1β, TNF-α, IL-8, MCP-1 and MIP-1α were selected for screening the effects of various OPN molecules and their glycoforms. The supernatants collected upon incubation of HUVECs with different isoforms and their glyco- and phospho-forms were used for the sandwich ELISAs. However, there were no significant differences found among the treatments with different forms of OPN. Due to limited availability of OPN isoforms, only one biological replicate with three technical repeats was used for ELISA. Thus, the ELISA results were not conclusive and are not shown.

Table 2.6. List of activators and inhibitors for angiogenesis process for humans that are present on the angiogenesis array.

	1	**2**	**3**	**4**	**5**	**6**	**7**	**8**
A	pos	pos	pos	pos	pos	pos	pos	Pos
B	Ang	Ang	IL-1α	IL-1α	FGFα	FGFα	IFNy	IFNy
C	G-CSF	G-CSF	IL-1β	IL-1β	FGFβ	FGFβ	IL-12	IL-12
D	HGF	HGF	IL-6	IL-6	TNF-α	TNF-α	IP-10	IP-10
E	Leptin	Leptin	IL-8	IL-8	TGF-α	TGF-α	TIMP-1	TIMP-1
F	VEGF	VEGF	PIGF	PIGF	neg	neg	TIMP-2	TIMP-2

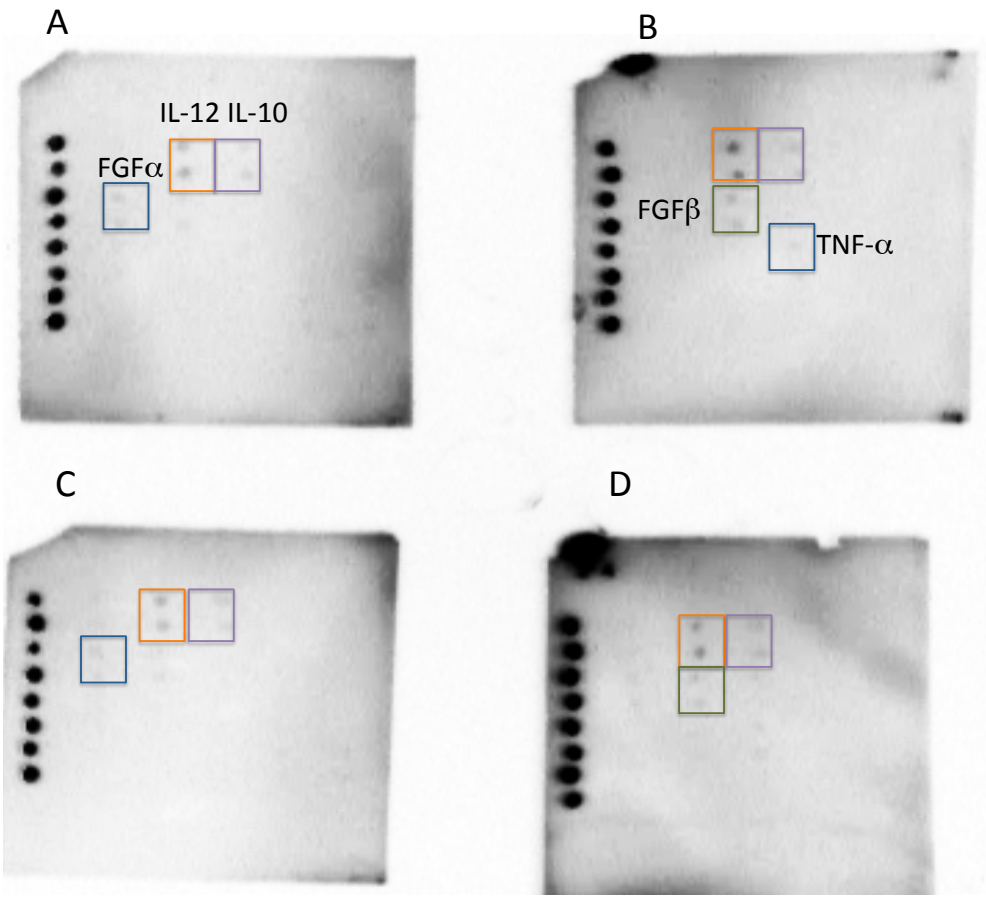

Figure 2.9. Expression of angiogenic factors upon incubation of bOPN and eOPN with serum-deprived HUVECs were measured compared to cell and media controls. The cell supernatants were incubated on an angiogenesis cytokine array where A) SFM, b) bOPN in SFM c) eOPN in SFM d) HUVECS in SFM.

2.3.6. Signalling pathway analysis

OPN has cytoprotective, survival and pro-angiogenic roles and it is known to activate the downstream PI3K/AKT pathway (Carpentier, 2012) (Figure 2.10). The effects of OPN on the kinase signalling pathway PI3K/AKT have been studied in glioma cells (Urtasun et al., 2012), a murine IL-3-dependent pro-B-cell line (Carpentier, 2012), hepatic stellate cells (Urtasun et al., 2012) and endothelial cells (Carpentier, 2012) but the PI3K/AKT signalling pathway in endothelial cells in response to OPN and its glycoforms has never been studied before.

BOPN and its generated glycoforms (bOPN N, bOPN NO and bOPN AP) and eOPN were incubated with serum-deprived HUVECs for 30 min. The total protein

extracted from HUVECS lysate was quantified and loaded on the SDS-PAGE and probed for p-PI3K and p-AKT pathway activation markers by Western blotting. The signal intensity for p-PI3K was higher for bOPN compared to the glycoforms bOPN (7%) and bOPN NO (9%) and desphosphorylated bOPN (12 %) AP following a trend but the signals were not significantly different (Figure 12.11 (C). The signals of p-PI3K and p-AKT were observed upon incubation with eOPN but the expression intensity was lower compared to bOPN by 12% and 48 % respectively (Figure 2.11, B and C).

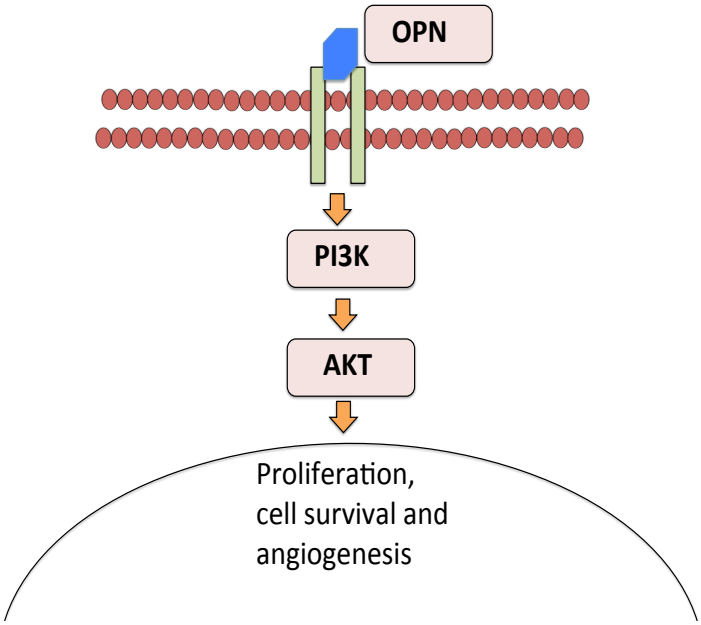

Figure 2.10. OPN on binding to the receptors on endothelial cells trigger PI3K/AKT pathway.

The signal for p-AKT ranged from no to low intensity signal upon incubation with bOPN AP (n=9). The differences between the signal intensities for either p-PI3K or p-AKT upon incubation with different glycoforms of bOPN were not significant. However, lower intensity signals for p-AKT signals were observed upon treatment bOPN N (9%) and similar intensity to bOPN NO glycoforms compared to their respective untreated parental OPN, statistical analysis showed that no significant differences between the intensities for the p-PI3K and p-AKT signals when compared among the glycoforms of bOPN (Figure 2.11, B and C). In contrast to previous reports (Wang et al., 2011), low intensity signals for p-PI3K and p-AKT were observed in the control condition, i.e. when HUVECs were not activated for the

PI3K/AKT signalling pathway. This observation suggested that p-PI3K/ p-AKT signalling pathway was constitutively on prior to the incubation of bOPN and its glycoforms. Nevertheless, OPN had an effect on the activation of pPI3K/P-AKT pathway similar or less compared to controls but always higher than eOPN.

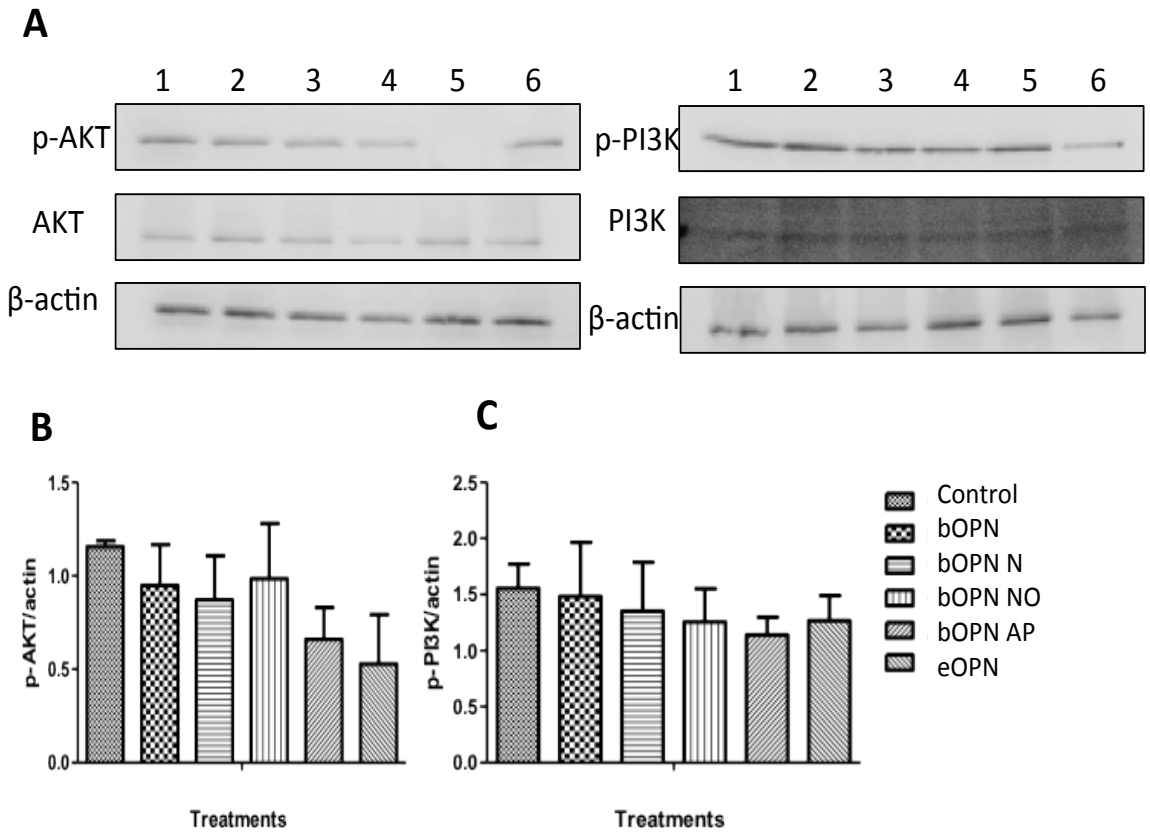

Figure 2.11. pPI3K/pAKT pathway analysis upon incubation with different OPN molecules. HUVECs (1 x 10^6 cells) were cultured in the presence bOPN and its glycoforms (5 μM) for 30 min (no treatment (lane 1), bOPN (lane 2), bOPN N (lane 3), bOPN NO (lane 4), bOPN AP (lane 5), eOPN (lane 6), and then lysed with RIPA lysis buffer. Cell lysates were applied to 8% SDS–PAGE. PI3K p85α (Tyr 457) and AKT 1/2/3 activation was detected by Western blotting. PI3K p58α/β/γ and AKT 1/2/3 were used as the internal control and β-actin was also detected as another internal and loading control (A). Densiometry analyses for p-AKT/actin (B) and p-PI3K (C) among all the treatments were performed.

2.4. Discussion

Many forms and sources of OPN that are biologically present make it difficult to study with pieces spread across many roles throughout matrix and vascular biology. The wide diversity of roles played by OPN has been attributed to structural variations due to its tissue/cell sources; splice variants and PTMs and associated physiology or pathology. OPN molecules from different origins with diverse PTMs have been studied independently and not across the same platform to understand the roles of PTMs on OPN. Hence, in the present work, OPN from different sources was characterised for the presence of glycosylation and phosphorylation and the effects of these PTMs in different aspects of angiogenesis were studied.

OPN derived from human milk is reported to have 5 *O*-linked glycans and 36 phosphate groups (Christensen et al., 2005). OPN from bovine milk is reported to have 3 *O*-linked glycans and 28 phosphorylation sites (Sørensen et al., 1995). Similarly, OPN from rat bone or rat kidney differ in their glycosylation sites and phosphorylation sites. OPN from rat bone has 4 *O*-linked glycans and 29 phosphorylation sites (Keykhosravani et al., 2005) but rat kidney cells can secrete either the phosphorylated or non-phosphorylated OPN forms in ras-transformed cells (Nemir et al., 1989). In this work, three different commercially available forms of OPN were established to have different PTMs, or in the case of eOPN, no glycosylation or phosphorylation at all. The digestion studies performed for the various OPN molecules verified the absence of *N*-linked glycans. Digestion studies showed the presence of different *O*-linked glycosylation and presence of phosphorylation on the bOPN while phosphates were absent on the rhOPN produced in murine NS0 cells. These results are in accordance with the published details of bOPN.

In order to identify the presence of different glycan moieties and overall glycoprofile on the individual forms of OPN molecules, lectin microarray profiling was performed. Lectin microarray data further confirmed the differences in rhOPN, bOPN and eOPN with overall small differences in the glyco- and phospho-forms of rhOPN and bOPN. These differences were observed in the degree of fucosylation, GlcNAc and degree of sialic acid, mainly when digested with O-glycanse. BOPN

and rhOPN was found to have mucin core type 1 and 2 structures extended by poly-LacNAc. This data is in agreement with respect to comparison with the earlier published lectin microarray data for rhOPN (Li et al., 2015).

Endothelial cells organise themselves into tubule structures that are composed of extracellular factors such as the adhesive glycoproteins laminin, fibronectin and collagen. OPN has not been previously tested for its angiogenic capabilities nor is the influence of its PTMs on angiogenesis known. Endothelial cells lie in close proximity to the basement membrane and have the ability to form the tubule like structures on the Matrigel® basement (Kleinman and Martin, 2005). Matrigel® is a gelatinous protein mixture derived from mouse tumour cells and is commonly used as a basement membrane matrix in the study of stem cell biology because it can maintain stem cells in an undifferentiated state. Angiogenesis can be modelled *in vitro* by short-term cultures of endothelial cells on Matrigel®. The tubule formation assay is quick and can be used to model endothelial cell behaviour upon incubation with different test compounds or for investigating the effects of drugs prior to these drugs being developed into clinical therapies. In the tubule formation assay for HUVECs on Matrigel®, the basement membrane helps to facilitate all the necessary steps for angiogenesis such as adhesion, migration, alignment and capillary like structure formation. Of all the tested OPN forms, no significant differences in the number of tubules formed were observed at the earlier time points. However, OPN facilitated the survival of a higher number of tubules at the later time points, which was due to the protein portion of OPN rather than any influence of its PTMs. OPN has been tested earlier for its ability to form tubules in Matrigel® assay but its glycoforms have not been tested.

When endothelial cells invade the ECM, they secrete proteases that degrade the ECM, called matrix metalloproteases (MMPs). During the activation of endothelial cells in angiogenesis, pro-angiogenic factors such as vascular-endothelial growth factor (VEGF) and basic fibroblast growth factor (bFGF) are released to stimulate the process. The differences between HUVEC-expressed angiogenic factors upon treatment with different OPN forms were negligible. OPN has been earlier shown to induce the secretion of angiogenic protein such as IL-6, TGF-α and FGF-α in EPCs (Vaughan et al., 2012b).

Previously, functional studies of OPN have shown that its PTMs play a role in increased cell adhesion, migration and the activation of various kinase pathways (Carpentier, 2012, Lin and Yang-Yen, 2001). Absence of *O*-glycosylation in threonine-proline rich areas is known to increase the phosphorylation of OPN and affect its cell adhesive properties (Yoshinobu et al., 2014). The *O*-glycosylation of OPN has been known to play important role in tumour biology (Minai-Tehrani et al., 2013). Hence, the glycosylation sites of OPN have been targeted and then mutated to suppress the lung tumorigenesis in a murine model of human non-small cell lung cancer (Minai-Tehrani et al., 2013). The signalling pathway expression analysis was performed to assess the effects of bOPN and its glycoforms on p-PI3K/p-AKT pathway as both these signalling pathways play important role in various biological functions including proliferation, adhesion, migration, and survival in angiogenesis process. Although no significant differences were observed, there was an increased expression signal following a trend of p-PI3K and p-AKT upon the incubation with bOPN and its generated glycoforms. Dephosphorylated forms of the bOPN led to the reduction in signal for the p-AKT pathway compared to control and other glycoforms. It may be indicative of role of phosphorylation on bOPN towards the activation of p-AKT pathway. However, down-regulation in expression of p-AKT for eOPN was also observed, which suggested that the activation of pPI3K/pAKT could be initiated by the protein backbone of OPN without any additional modifications.

With the increase in OPN biological research over last few years, there are discrepancies arising among these studies. There are various functional and biological studies to determine the effect of OPN PTMs on the cells *in vitro* which may contribute to these varying conclusions (Yoshinobu et al., 2014, Brown et al., 1992, Wang and Denhardt, 2008). The concentration of either the complete proteins or its generated variants may not be explicitly mentioned or the concentration used was not in the range for *in vivo* experimentation. Currently, there are very few studies, which include OPN purified from different sources. Using different OPN molecules and their glycoforms as was done in this work provides a better assessment of their biological roles and can direct more informed and meaningful subsequent studies.

In conclusion, the functional effects of OPN from three sources and their enzyme-generated glycoforms were tested in various biological assays including the proliferation of HUVECs, tubule formation and the secretion of angiogenic factors. There were no significant differences in biological effects between the various glycoforms of OPN and eOPN, suggesting that the PTMs of OPN did not significantly contribute towards the overall effect of OPN in these assays. These results were obtained for HUEVCs that has intracellular OPN (iOPN) and hence required higher concentration of OPN to provide significant response in the cell assays. A primary cell line with no expression of iOPN could provide an alternative to understand the roles of PTMs on OPN. This study provided a coherent platform to study the roles of different OPN molecules and their glycoforms in the process of angiogenesis. This work can be further expanded by incorporation of OPN proteolytic fragments and its various isoforms to explore their importance in biological models.

Comments: OPN was found to be down regulated in EPCs from diabetic type I patients versus EPCs from healthy controls. However, HUVECs were used, as an alterantive cell line for studying the effect glycosylation of OPN to EPCs as EPCs were not readily availabile. Also, hOPN molecule was not used in the biological assays to compare it to bOPN, rhOPN and eOPN because of its unavailability.

2.5. References

AL-SHAMI, R., SORENSEN, E. S., EK-RYLANDER, B., ANDERSSON, G., CARSON, D. D. & FARACH-CARSON, M. C. 2005. Phosphorylated osteopontin promotes migration of human choriocarcinoma cells via a p70 S6 kinase-dependent pathway. *Journal of Cellular Biochemistry,* 94**,** 1218-1233.

ASHKAR, S., WEBER, G. F., PANOUTSAKOPOULOU, V., SANCHIRICO, M. E., JANSSON, M., ZAWAIDEH, S., RITTLING, S. R., DENHARDT, D. T., GLIMCHER, M. J. & CANTOR, H. 2000. Eta-1 (osteopontin): an early component of type-1 (cell-mediated) immunity. *Science,* 287**,** 860-864.

BHAVANANDAN, V. P. & KATLIC, A. W. 1979. The interaction of wheat germ agglutinin with sialoglycoproteins. The role of sialic acid. *Journal of Biological Chemistry,* 254**,** 4000-4008.

BROWN, L. F., BERSE, B., VAN DE WATER, L., PAPADOPOULOS-SERGIOU, A., PERRUZZI, C., MANSEAU, E., DVORAK, H. & SENGER, D. 1992. Expression and distribution of osteopontin in human tissues: widespread association with luminal epithelial surfaces. *Molecular biology of the cell,* 3**,** 1169.

CARPENTIER, G. 2012. Contribution: angiogenesis analyzer. *ImageJ News,* 5.

CHRISTENSEN, B., NIELSEN, M. S., HASELMANN, K. F., PETERSEN, T. E. & SØRENSEN, E. S. 2005. Post-translationally modified residues of native human osteopontin are located in clusters: identification of 36 phosphorylation and five O-glycosylation sites and their biological implications. *Biochemical Journal,* 390**,** 285.

CRAIG, A. M., SMITH, J. & DENHARDT, D. 1989. Osteopontin, a transformation-associated cell adhesion phosphoprotein, is induced by 12-O-tetradecanoylphorbol 13-acetate in mouse epidermis. *Journal of Biological Chemistry,* 264**,** 9682-9689.

DENHARDT, D. T. & GUO, X. 1993. Osteopontin: a protein with diverse functions. *The FASEB journal,* 7**,** 1475-1482.

FISHER, L., TORCHIA, D., FOHR, B., YOUNG, M. & FEDARKO, N. 2001. Flexible structures of SIBLING proteins, bone sialoprotein, and osteopontin. *Biochemical and biophysical research communications,* 280**,** 460-465.

FOLKMAN, J. 1995. Angiogenesis in cancer, vascular, rheumatoid and other disease. *Nature Medicine,* 1**,** 27-30.

FOLKMAN, J. 1997. Angiogenesis and angiogenesis inhibition: an overview. *Regulation of Angiogenesis.* Springer.

GERICKE, A., QIN, C., SPEVAK, L., FUJIMOTO, Y., BUTLER, W., S√ ∏RENSEN, E. & BOSKEY, A. 2005. Importance of phosphorylation for osteopontin regulation of biomineralization. *Calcified tissue international,* 77**,** 45-54.

GERLACH, J. Q., KILCOYNE, M. & JOSHI, L. 2014. Microarray evaluation of the effects of lectin and glycoprotein orientation and data filtering on glycoform discrimination. *Analytical Methods,* 6**,** 440-449.

HAUKE, C. & KORR, H. 1993. RCA-I lectin histochemistry after trypsinisation enables the identification of microglial cells in thin paraffin sections of the mouse brain. *Journal of neuroscience methods,* 50**,** 273-277.

HIRABAYASHI, J. 2015. Historical and Practical Aspects of Development of Lectin Microarray Technique Lectin microarray. *Glycoscience: Biology and Medicine.* Springer.

INOUE, M. & SHINOHARA, M. L. 2011. Intracellular osteopontin (iOPN) and immunity. *Immunologic research,* 49**,** 160-172.

JONO, S., PEINADO, C. & GIACHELLI, C. M. 2000. Phosphorylation of osteopontin is required for inhibition of vascular smooth muscle cell calcification. *Journal of Biological Chemistry,* 275**,** 20197-20203.

KARIMOVA, A. & PINSKY, D. J. 2001. The endothelial response to oxygen deprivation: biology and clinical implications. *Intensive care medicine,* 27**,** 19-31.

KEYKHOSRAVANI, M., DOHERTY-KIRBY, A., ZHANG, C., BREWER, D., GOLDBERG, H. A., HUNTER, G. K. & LAJOIE, G. 2005. Comprehensive identification of post-translational modifications of rat bone osteopontin by mass spectrometry. *Biochemistry,* 44**,** 6990-7003.

KILCOYNE, M., GERLACH, J. Q., GOUGH, R., GALLAGHER, M. E., KANE, M., CARRINGTON, S. D. & JOSHI, L. 2012a. Construction of a natural mucin microarray and interrogation for biologically relevant glyco-epitopes. *Analytical Chemistry,* 84**,** 3330-3338.

KILCOYNE, M., GERLACH, J. Q., KANE, M. & JOSHI, L. 2012b. Surface chemistry and linker effects on lectin‚Äìcarbohydrate recognition for glycan microarrays. *Analytical Methods,* 4**,** 2721-2728.

KILCOYNE, M., TWOMEY, M. E., GERLACH, J. Q., KANE, M., MORAN, A. P. & JOSHI, L. 2014. Campylobacter jejuni strain discrimination and temperature-dependent glycome expression profiling by lectin microarray. *Carbohydrate Research,* 389**,** 123-133.

KLEINMAN, H. K. & MARTIN, G. R. Matrigel: basement membrane matrix with biological activity. Seminars in Cancer Biology, 2005. Elsevier, 378-386.

KOHRI, K., ET AL., NOMURA, S., KITAMURA, Y., NAGATA, T., YOSHIOKA, K., IGUCHI, M., YAMATE, T., UMEKAWA, T., SUZUKI, Y. & SINOHARA, H. 1993. Structure and expression of the mRNA encoding urinary stone protein (osteopontin). *Journal of Biological Chemistry,* 268**,** 15180-15184.

KRUGER, N. J. 1994. The Bradford method for protein quantitation. *Basic protein and peptide protocols***,** 9-15.

KURZBACH, D., PLATZER, G., SCHWARZ, T. C., HENEN, M. A., KONRAT, R. & HINDERBERGER, D. 2013. Cooperative unfolding of compact conformations of the intrinsically disordered protein osteopontin. *Biochemistry,* 52**,** 5167-5175.

LI, H., SHEN, H., YAN, G., ZHANG, Y., LIU, M., FANG, P., YU, H. & YANG, P. 2015. Site-specific structural characterization of O-glycosylation and identification of phosphorylation sites of recombinant osteopontin. *Biochimica et Biophysica Acta (BBA)-Proteins and Proteomics,* 1854**,** 581-591.

LIAW, L., SKINNER, M. P., RAINES, E. W., ROSS, R., CHERESH, D. A., SCHWARTZ, S. M. & GIACHELLI, C. M. 1995. The adhesive and migratory effects of osteopontin are mediated via distinct cell surface integrins. Role of alpha v beta 3 in smooth muscle cell migration to osteopontin in vitro. *Journal of Clinical Investigation,* 95**,** 713.

LIN, Y.-H. & YANG-YEN, H.-F. 2001. The osteopontin-CD44 survival signal involves activation of the phosphatidylinositol 3-kinase/Akt signaling pathway. *Journal of Biological Chemistry,* 276**,** 46024-46030.

MINAI-TEHRANI, A., CHANG, S.-H., KWON, J.-T., HWANG, S.-K., KIM, J.-E., SHIN, J.-Y., YU, K.-N., PARK, S.-J., JIANG, H.-L. & KIM, J.-H. 2013. Aerosol delivery of lentivirus-mediated O-glycosylation mutant osteopontin suppresses lung tumorigenesis in K-ras LA1 mice. *Cellular Oncology,* 36**,** 15-26.

MINAI,TEHRANI, A., CHANG, S.-H., PARK, S. B. & CHO, M. H. 2013. The O-glycosylation mutant osteopontin alters lung cancer cell growth and migration in vitro and in vivo. *International Journal of Molecular Medicine,* 32**,** 1137-1149.

NEMIR, M., DEVOUGE, M. W. & MUKHERJEE, B. 1989. Normal rat kidney cells secrete both phosphorylated and nonphosphorylated forms of osteopontin showing different physiological properties. *Journal of Biological Chemistry,* 264**,** 18202-18208.

OLDBERG, A., FRANZEN, A. & HEINEGARD, D. 1986. Cloning and sequence analysis of rat bone sialoprotein (osteopontin) cDNA reveals an Arg-Gly-Asp cell-binding sequence. *Proceedings of the National Academy of Sciences,* 83**,** 8819-8823.

PARDALI, E., GOUMANS, M.-J. & TEN DIJKE, P. 2010. Signaling by members of the TGF-β family in vascular morphogenesis and disease. *Trends in Cell Biology,* 20**,** 556-567.

RAZZOUK, S., BRUNN, J., QIN, C., TYE, C., GOLDBERG, H. & BUTLER, W. 2002. Osteopontin posttranslational modifications, possibly phosphorylation, are required for in vitro bone resorption but not osteoclast adhesion. *Bone,* 30**,** 40.

RISAU, W. & LEMMON, V. 1988. Changes in the vascular extracellular matrix during embryonic vasculogenesis and angiogenesis. *Developmental Biology,* 125**,** 441-450.

SENGER, D. R., PERRUZZI, C. A., PAPADOPOULOS, A. & TENEN, D. G. 1989. Purification of a human milk protein closely similar to tumor-secreted phosphoproteins and osteopontin. *Biochimica et Biophysica Acta (BBA)-Protein Structure and Molecular Enzymology,* 996**,** 43-48.

SENGER, D. R., WIRTH, D. F. & HYNES, R. O. 1979. Transformed mammalian cells secrete specific proteins and phosphoproteins. *Cell,* 16**,** 885-893.

SGADARI, C., ANGIOLILLO, A. & TOSATO, G. 1996. Inhibition of angiogenesis by interleukin-12 is mediated by the interferon-inducible protein 10. *Blood,* 87**,** 3877-3882.

SMITH, L. L., CHEUNG, H. K., LING, L. E., CHEN, J., SHEPPARD, D., PYTELA, R. & GIACHELLI, C. M. 1996. Osteopontin N-terminal domain contains a cryptic adhesive sequence recognized by α9β1 Integrin. *Journal of Biological Chemistry,* 271**,** 28485.

SODEK, J., GANSS, B. & MCKEE, M. 2000. Osteopontin. *Critical Reviews in Oral Biology & Medicine,* 11**,** 279-303.

SØRENSEN, E., RASMUSSEN, L., MØLLER, L., JENSEN, P., HØJRUP, P. & PETERSEN, T. 1994. Localization of transglutaminase-reactive glutamine residues in bovine osteopontin. *Biochemical Journal,* 304**,** 13.

SØRENSEN, E. S., PETERSEN, T. E. & HØJRUP, P. 1995. Posttranslational modifications of bovine osteopontin: identification of twenty-eight phosphorylation and three O-glycosylation sites. *Protein Science,* 4**,** 2040-2049.

SUMPIO, B. E., RILEY, J. T. & DARDIK, A. 2002. Cells in focus: endothelial cell. *The International Journal of Biochemistry & Cell Biology,* 34**,** 1508-1512.

TAUB, D. D., LLOYD, A. R., CONLON, K., WANG, J. M., ORTALDO, J., HARADA, A., MATSUSHIMA, K., KELVIN, D. & OPPENHEIM, J. 1993. Recombinant human interferon-inducible protein 10 is a chemoattractant for human

monocytes and T lymphocytes and promotes T cell adhesion to endothelial cells. *The Journal of Experimental Medicine,* 177**,** 1809-1814.

URTASUN, R., LOPATEGI, A., GEORGE, J., LEUNG, T. Ä., LU, Y., WANG, X., GE, X., FIEL, M. I. & NIETO, N. 2012. Osteopontin, an oxidant stress sensitive cytokine, up-regulates collagen-I via integrin αVβ3 engagement and PI3K/pAkt/NFκB signaling. *Hepatology,* 55**,** 594-608.

VALDIMARSDÓTTIR, G. 2004. TGFβ Signal Transduction in Endothelial Cells.

VAUGHAN, E., LIEW, A., MASHAYEKHI, K., DOCKERY, P., MCDERMOTT, J., KEALY, B., FLYNN, A., DUFFY, A., COLEMAN, C. & O'REGAN, A. 2012a. Pretreatment of endothelial progenitor cells with osteopontin enhances cell therapy for peripheral vascular disease. *Cell transplantation,* 21**,** 1095-1107.

VAUGHAN, E., LIEW, A., MASHAYEKHI, K., DOCKERY, P., MCDERMOTT, J., KEALY, B., FLYNN, A., DUFFY, A., O'REGAN, C. & BARRY, F. 2012b. Pre-treatment of Endothelial Progenitor Cells with Osteopontin Enhances Cell Therapy for Peripheral Vascular Disease. *Cell transplantation*.

WANG, K. X. & DENHARDT, D. T. 2008. Osteopontin: role in immune regulation and stress responses. *Cytokine & growth factor reviews,* 19**,** 333-345.

WANG, Y., YAN, W., LU, X., QIAN, C., ZHANG, J., LI, P., SHI, L., ZHAO, P., FU, Z. & PU, P. 2011. Overexpression of osteopontin induces angiogenesis of endothelial progenitor cells via the avβ3/PI3K/AKT/eNOS/NO signaling pathway in glioma cells. *European journal of cell biology,* 90**,** 642-648.

WEBER, G. F., ASHKAR, S., GLIMCHER, M. J. & CANTOR, H. 1996. Receptor-ligand interaction between CD44 and osteopontin (Eta-1). *Science,* 271**,** 509-512.

YOKOSAKI, Y., MATSUURA, N., SASAKI, T., MURAKAMI, I., SCHNEIDER, H., HIGASHIYAMA, S., SAITOH, Y., YAMAKIDO, M., TAOOKA, Y. & SHEPPARD, D. 1999. The Integrin α9β1 Binds to a Novel Recognition Sequence (SVVYGLR) in the Thrombin-cleaved Amino-terminal Fragment of Osteopontin. *Journal of Biological Chemistry,* 274**,** 36328.

YOSHINOBU, K., MAYUMI, K., KANA, M.-M., MIDORI, K., YOSHIKI, Y. & YASUHIRO, H. 2014. Osteopontin O-glycosylation contributes to its phosphorylation and cell-adhesion properties. *Biochemical Journal,* 463**,** 93-102.

CHAPTER 3

IMMUNOMODULATORY PROPERTIES OF NATURAL OLIGO- AND POLY-SACCHARIDES*

*This chapter has been expanded on the published article;
Gill, Satbir Kaur, Nahidul Islam, Iain Shaw, Andreia Ribeiro, Benjamin Bradley, Michelle Kilcoyne, Rhodri Ceredig, and Lokesh Joshi. "Immunomodulatory effects of natural polysaccharides assessed in human whole blood culture and THP-1 cells show greater sensitivity of whole blood culture." International immunopharmacology 36 (2016): 315-323.

3.1. Introduction

Infections and physical traumas affect the immune status of the organism, inducing an initial inflammatory cascade followed by a transient anti-inflammatory response (Hirsiger et al., 2012). Activated monocytes and macrophages produce inflammatory mediators including cytokines and chemokines to overcome the trauma or biological insult. Immunomodulators are potential therapeutics to maintain immunological balance in patients with infectious and non-infectious traumas, and diseases such as autoimmune disease or cancer. Several immunomodulatory drugs are available but some have known side effects (Bascones-Martinez et al., 2014). Immunomodulatory drugs of the natural origin with less side effects and more targeted functions are needed.

3.1.1. Polysaccharides and their roles

Polysaccharides have a wide range of roles. Their main functions comprise of food storage or as structural components. The important storage poly-saccharides in plants are starch and inulin while glycogen is important in animals. Poly-saccharides have various other uses in the food industry including their use as stabilizers, thickeners and emulsifiers in food, beverages and animal feed (Paul et al., 1986, Campos et al., 2013). Other than energy storage and structural functions, specific carbohydrates participate in cell-cell recognition, adhesion, and immune response and wound healing. The biological properties of poly-saccharides are governed by their chemical structures, identity of the comprising residues, linkages, length of the polysaccharide backbone, degree of branching, molecular mass, substituent position, identity and degree and overall charge of the molecule (Wijesekara et al., 2011). They have diverse biological effects including anti-tumour, anti-viral, anti-complementary, anti-coagulant, anti-oxidant and immunomodulatory properties (Koyanagi et al., 2003, Nergard et al., 2005, Fedorov et al., 2013, Schepetkin and Quinn, 2006, Lee et al., 2012, Dore et al., 2013). Their use is also well established in tissue engineering, for drug delivery and in therapeutic applications (Tiwari et al., 2014).

Poly-accharides or oligosaccharides from different sources have been earlier tested for their immunomodulatory properties. For example, heparin is widely used clinically as an anticoagulant since 1930s. The structure-function relationship for

anti-coagulant properties and mechanism of action of heparin has been elucidated and various modifications of sulfation patterns are reported to be responsible for the cellular uptake (Raman et al., 2013). Fucoidan has demonstrated biological properties like antithrombic, antiviral, antitumor and immunomodulatory activities and vary in their sulfation patterns, and consequently in their overall charge, composition and three-dimensional conformation. (Zhang et al., 2014, Zhang et al., 2015). Depending on the structural variation of the same poly-saccharides, they could have multiple or even opposing effects on the biological system, primarily stimulating the immune system. Pectins of different structures have different immunomodulatory properties (Popov and Ovodov, 2013).

A class of poly-saccharides β-glucans stimulate a wide range of immune responses, such as cytokine release, generation of ROS and immunostimulation effects (Chlubnova et al., 2011). However, due to the poor solubility and the direct leukocyte activating action of β-glucans, these compounds have experienced limited clinical usefulness. However, modified forms of β-glucans, e.g. soluble β-(1,6)-branched- β -(1,3)-glucans, have been shown to enhance microbicidal activities of neutrophils and macrophages (Schepetkin and Quinn, 2006).

In the present study, six naturally derived poly- and oligo-saccharides (fucoidan, fructan, heteroglycan, galacturonan, mannan and xyloglucan) (Table 3.1) were screened for their immunomodulatory effects.

Table 3.1. Name, type (P, polysaccharide; O, oligosaccharide), origin, abbreviation and structures for poly- and oligo- saccharides.

Name	Type	Origin	Abbrev.	Structure
Fucoidan	P	*Ascophyllum nodosum*	FUC	Linear, highly sulfated [→3]-L-Fuc-α-(1→)$_n$ with some α-(1→4)-linked Fuc
Fructan/ Inulin	O	Jerusalem artichoke	INL	Linear, β-(2→1)-linked fructose with terminal Glc
Sulfated heteropolysaccharides	P	*Caulerpa racemosa*	HGL	Linear, α-(1→4)-linked glucan and sulfated xyloarabinogalactan.
Apio-galacturonan	P	*Zostera marina*	GAL	Branched, α-(1 → 4)-linked D-galacturonic acid (GalA) substituted with *β* -D-apiose and β-D-apiose-(1 → 5)-β-D-apiose side chains at C-2 and/or C-3.
Xyloglucan	O	Biomass (Apple)	xGLU	Branched, β-D-(1→4)-linked glucan with D-Xyl α-linked at C-6 of approximatively 75% of the glucosyl residues. Some Xyl residues substituted at C-2 with Gal or [→2)-Fuc-α-(1→2)-Gal-β-(1→n] moieties
Mannan	O	Biomass (Ivory nuts)	MAN	Linear, β-(1→4)-mannan

3.1.2. Cell models

Cells of the immune system exhibit the ability to secrete cytokines and chemokines and are used to test the immunomodulatory properties of potential compounds. Cell models widely used for assessing immunomodulatory properties are; *in vitro* homogenous immortalised cell lines such as THP-1 cell line and *ex vivo* heterogeneous cell population as human whole blood culture. THP-1 cell line is readily available monocytic cell line and easy to culture in RPMI-1640 media. Human whole culture mimics the *in vivo* environment where all the cells of immune

system exist in proximity and provides a cost effective method. Hence, in this work, the THP-1 cell line and human whole blood culture were used to study the effect of the six oligo- and poly-saccharides (Table 3.1) for their immunomodulatory properties.

The Limulus Amebocyte Lysate (LAL) assay was carried out to determine the purity of the samples and absence of endotoxin contamination in samples. However, the LAL assay is known to react with other molecules including β-glucans, yeast mannans, branched dextrans and pectic polysaccharides. However, one of the samples of our test panel, GAL, reacted positively in the LAL assay based on its structure, despite the lack of endotoxin in the samples. Thus, this assay is not a useful measurement of endotoxin contamination when dealing with biologically active poly- and oligo-saccharides.

While the LAL assay is more sensitive than SDS-PAGE combined with silver stain, the latter method can reach a sensitivity of 4 ng [3]. 10 μg (by weight) of each sample was loaded on to the gels and silver staining did not show any typical LPS banding (ladder-like banding) (not shown) which implied any potential contamination of less than 0.04%. One of our test panel, xGLU, was certified as endotoxin-free by the manufacturer. (Elicityl, batch E1308-08 EC08). Any potential contamination by LPS would be apparent by 1H NMR analysis and all of the other samples were analysed by the manufacturer (Elicityl) by this method. Hence, it is very unlikely that the samples were contaminated by endotoxin.

In addition, the pattern of response of each of the test panel is different from that of even the lowest concentration of LPS (10 ng) tested between the two test systems. The comparative effects of test compounds and LPS (both concentration, 10 ng/mL and 100 ng/mL) are shown by the heatmaps in Figures 5 and S5. For example, INL had greatest response in the HWBC system with some responses overlapping those of LPS. In the THP-1 system, INL had a very low response in contrast to LPS, which had strong response in both systems in contrast to LPS, which had strong response in both systems.

3.1.2.1. THP-1 cell line

The THP-1 cell line is a human-derived myeloid leukaemia cell line, which is widely used to investigate the roles of monocytes and macrophages in the cardiovascular system. It was originally cultured from the peripheral blood of an infant boy suffering from acute monocytic leukaemia, a disease that leads to the unimpeded growth of monocytes (Tsuchiya et al., 1980). It was characterised as a leukocytic cell line due to the presence of markers common to monocytic cells. THP-1 cell line can be better choice over other immortalized human monocytic cell lines, such as U937 and Mono Mac-6 cells, due to less genetic variability owing to their homogenous genetic background (Chanput et al., 2014). THP-1 cells also have higher transfection efficiency that makes their genetic modifications easier for studying specific protein functions (Chanput et al., 2014, Qin, 2012). THP-1 cells that exist in a monocytic state can be differentiated into a macrophage-like phenotype using phorbol-12-myristate-13-acetate, 1α, 25-dihydroxyvitamin D3 or macrophage colony-stimulating factor (M-CSF) (Schwende et al., 1996).

Peripheral blood mononuclear cells (PBMC) are the populations of immune cells include lymphocytes (T cells, B cells, and NK cells), monocytes, and dendritic cells. PBMC derived monocytes and macrophages are also used for the screening of various test compounds. However, THP-1 has various advantages over human PBMC derived monocytes or macrophages such as lower doubling time, homogenous background, higher passage number over the limited PBMC-derived monocytes (Chanput et al., 2014). Absence of any infectious virus or toxic products in the THP-1 cells stocks makes their culturing and utilisation as a model cell system easier than PBMCs. They have been widely utilised as an *in vitro* model for mechanistic studies of inflammation due to exposure to drugs, test compounds or naturally-derived poly-saccharides and to investigate different drug treatments in different diseases (Chanput et al., 2010, Smiderle et al., 2011). Apart from studying THP-1 as monocytes or stimulated to macrophages, they have also been studied in co-culture systems with other cell types such as cancer cells to understand the interactions between the monocytes and the cancer cells to design immuno-therapies.

3.2.2.2. Human whole blood culture

Human whole blood culture (HWBC) produces all the blood components (both cellular and humoral) of human blood. HWBC contains all the essential components for the stimulation of both innate and T-cell mediated immunity, hence mimicking the *in vivo* condition. PBMC-derived monocytes have been widely used for the testing of compounds and they have a mixture of monocytes, T-, B-, and NK-cells but compared to HWBC, they have skewed ratios of monocytes to lymphocyte ratios (De Groote et al., 1992). The isolation of PBMCs from HWBC is time consuming and devoid of many other factors such as cytokines, hormones and cell types which are present in HWBC. HWBC can be utilised for cell assays immediately after sampling from the blood and from comparatively less volume of blood otherwise required for the isolation of PBMCs. The culturing of monocytic cell lines further needs the addition of fetal calf serum (FBS), which contains various hormones and nutrients that can lead to changes in the immunological responses of the cells towards the test compounds. HWBC could also be advantageous over *in vivo* animal studies as animal testing does not always mirror the response in humans due to genetic dissimilarity in the immuno-functionality between animals and humans (Mestas and Hughes, 2004, Rice, 2012).

3.2.2.3. Assessing immunomodulation by inflammatory response

Following injury, local immune cells secrete different chemokines to trigger the recruitment of immune cells such as neutrophils, monocytes and mesenchymal stromal cells to the site of injury. Thus, IL-8, which is the most commonly studied chemokine, MCP-1, which helps in recruiting monocytes and MIP-1α were measured following treatment of the models with potential immunomodulators in the present study. Following stress, the human body also triggers immediate release of IL-1β and TNF-α by the local and the newly recruited innate immune cells. IL-6 is an inflammatory cytokine and is secreted at the site of injury/stress. Recent observations suggest IL-6 as a complex cytokine that plays a dual role (pro- and anti-inflammatory) depending on presence of the receptors and cell type. Therefore IL-6 was selected as an additional pro-inflammatory biomarker in this study in parallel to IL-1β. IL-10 and IL-13 are widely studied anti-inflammatory cytokines (Islam et al., 2014). Monocytes can secrete IL-10 to maintain an anti-inflammatory environment.

In the present study, six naturally derived poly- and oligo-saccharides (Table 3.1) were hence screened for their ability to secrete anti- and pro- inflammatory ctyokines and chemokines when incubated with HWBC and THP-1 cells.

3.2. Material and Methods

3.2.1. Materials

Six lyophilized oligo- and poly- saccharides: inulin (INL), galacturonan (GAL), mannan (MAN), heteroglycan (HGL), fucoidon (FUC) and xyloglucan (xGLU) (Table 3.1) were purchased from Elicityl (Crolles, France) and all except MAN were reconstituted to 1 mg/mL in phosphate buffered saline (PBS, pH 7.2). MAN (2 mg) was first dissolved in 500 μL of 5% sodium hydroxide and then diluted in PBS to 1 mg/mL. RPMI-1640 media, fetal bovine serum (FBS), L-glutamine, periodic acid, Alcian Blue 8GX, Schiff's reagent for aldehydes (catalogue number 84655) and bovine serum albumin (BSA) were from Sigma-Aldrich Co. (Wicklow, Ireland). Penicillin-streptomycin (10,000 U/mL penicillin and 10 mg/mL streptomycin), NuPAGE® Tris-acetate (3–8%) gels and NuPAGE® LDS sample buffer were from Life Technologies (Carlsbad, CA, U.S.A.). Ultrapure lipopolysaccharide (LPS) from *E. coli* 0111:B4 was from Invivogen (San Diego, CA, USA). Sterile pyrogen-free 96-well flat-bottom microplates from Nunc Maxisorp (Roskilde, Denmark) were used for the enzyme-linked immunosorbent assays (ELISA). Cytokine (IL-1β, IL-6, TNF-α, IL-10 and IL-13) and chemokine (IL-8, MCP-1 and MIP-1α) ELISA DuoSet® kits were purchased from R&D Systems (Abingdon, U.K.). Vacutainer® cell preparation tube (CPT^{TM}) heparin-coated tubes were obtained from Becton Dickinson Bioscience (San Jose, CA, U.S.A.). Brefeldin A (BFA) solution (3 mg/mL in methanol) and the fluorescently labelled mouse anti-human antibodies anti-CD45 conjugated to peridinin-chlorophyll protein-Cyanine5.5 (CD45-PerCP-Cy5.5) (catalogue number 45-0459-42), anti-CD14 conjugated to allophycocyanin (CD14-APC) (catalogue number 17-0149-42) and anti-cytoplasmic TNF-α conjugated to phycoerythrin (Cy-TNF-α-PE) (catalogue number 12-7349-41), were from eBioscience (San Diego, CA, U.S.A.). IntraPrep^{TM} kit (catalogue number: A07802) was purchased from Beckman Coulter (High Wycombe, U.K.). The THP-1 cell line was purchased from the American Type Culture Collection (ATCC) (Rockville, MD). All other reagents

were from Sigma-Aldrich Co. and were of the highest grade available unless otherwise noted.

3.2.2. Poly- and oligo-saccharide characterization

The poly- and oligo-saccharides were prepared in NuPAGE® LDS sample buffer with 25 mM dithiothreitol, heated at 95 °C for 5 min and 10 μg of each compound was loaded on a 3-8% Tris-acetate polyacrylamide gel and then electrophoretically separated with MES buffer (150 V, 1 h). The gels were stained with Coomassie Brilliant Blue R-250 (CBB) and destained in 40% methanol, 10% acetic acid solution. Separate electrophoresed gels were also stained with periodic acid Schiff's reagent (PAS) (Kilcoyne et al., 2011, Zacharius et al., 1969) with some modifications as follows. After electrophoresis, the gels were rinsed in deionised water, fixed with 30% ethanol and 5% acetic acid solution for 1 h, then rinsed twice in 10% ethanol for 5 min each rinse followed for two further rinses in deionized water for 15 min each. The gels were then oxidized separately by incubation in 25 mL of 1% periodic acid for 1 h in three different buffers, 7% acetic acid buffer (pH 2.5), 50 mM sodium acetate (pH 4) or 50 mM sodium phosphate (pH 7). The gels were washed three times in 3% acetic acid for 5 min per wash, incubated in 20 mL Schiff's reagent for aldehydes for 1 h and washed three times in deionised water for 5 min each. Alcian Blue 8GX (AB) staining was also performed. After electrophoresis, washed gels were incubated with 0.125% AB in 10% acetic acid and 25% ethanol for 15 min at 50 °C and then rinsed with 5% acetic acid and 10% ethanol in distilled water with gentle agitation (Wardi and Michos, 1972). All gels were imaged immediately after development.

3.2.3. HWBC

Peripheral human venous blood was collected in CPT^{TM} heparin-coated tubes with signed informed consent from three healthy donors under a protocol approved by the National University of Ireland Galway Research Ethics Committee. Human blood culture was performed as previously described with minor modifications (Yaqoob et al., 1999), heparinized blood samples were diluted in a 1:10 ratio in RPMI-1640 and were then cultured with a final concentration of 10 and 100 ng/mL of LPS. Diluted blood cultures were also incubated with various concentrations (1, 5, and 10 μg/mL)

of the six poly- and oligo-saccharides and assayed for cytokine and chemokine response at given time-points. At 1 and 5 μg/mL of poly- and oligo- saccharide, cytokine and chemokine concentrations were below the detection limit and thus 10 μg/mL was selected as the optimised concentration for use in both model systems. All treatments were carried out for incubation periods of 6, 12 and 24 h at 37 °C in 5% CO_2. Following centrifugation for 5 min at 15,295 *g* the pelleted cells were discarded and the supernatants were collected and stored at -80 °C until further use.

3.2.4. Cell culture

Aliquots of cryopreserved human monocytic cell line THP-1 were thawed by plunging sealed ampoules into a 37 °C water bath, then diluted with culture medium (RPMI-1640 supplemented with 10% heat inactivated FBS, 1 mM L-glutamine, 100 ng/mL streptomycin and 100 U/mL penicillin) and cultured in 175 cm^2 flasks in a humidified atmosphere at 5% CO_2 at 37 °C. Cells were passaged when they reached 80% confluency. After 6 to 8 passages, the cells were suspended in fresh culture medium, and adjusted to 1 x 10^6 viable cells/mL. Cells were then incubated for 0, 6, 12, 24 and 48 h at 37 °C and 5% CO_2 in a humidified incubator with LPS at 10 and 100 ng/mL and test compounds at 10 μg/mL and un-stimulated control cells at a density of 1 x 10^6 cells/mL. HWBC consisted of a mixture of large number of red blood cells, platelets and other immune cells with approximately 40,000 CD14+CD45+ monocytes/ mL of diluted blood. Following centrifugation as above, pelleted cells were discarded and supernatants were collected and stored at -80 °C until further use.

3.2.5. Cytokine and chemokine quantification

ELISA was performed to measure the levels of IL-1β, IL-6, IL-8, TNF-α, MCP-1 and MIP-1α in the collected supernatants from both THP-1 cells and HWBC using ELISA DuoSet® kits following the manufacturer's instructions except that the supernatants were incubated overnight on the ELISA plates that were coated with capture antibodies. Briefly, primary antibodies were captured on 96-well plates and incubated overnight at room temperature. Blocking buffer (1% BSA in PBS, pH 7.2) was then added to each well and left for 2 h at room temperature. Plates were washed three times with wash buffer (PBS with 0.05% Tween 20) prior to the addition of

standards and supernatant samples to the plate in duplicates. After incubations of 2 h, detection antibody was added to the plates and kept in the dark at room temperature for another 2 h. Streptavidin-HRP was then added to the plate and incubated in the dark for 20-30 min at room temperature. After five washes, bound streptavidin-HRP was detected by adding the substrate trimethyl blue. Cytokine and chemokine quantifications were performed using three biological replicates of the HWBC culture and analysing in duplicate (for three patients separately). The average of each sample was then calculated and mean and standard deviation (SD) of the averages of three donors was obtained from these data sets. The enzyme-substrate reaction was stopped by 1 M sulfuric acid and absorbance was read at 450 nm. Concentrations of each analyte were quantified from standard curves.

3.2.6. Intracellular TNF-α quantification

For intracellular expression of TNF-α in human blood monocytes, heparinised blood (4 mL) collected from two healthy donors was diluted 10 times in RPMI-1640 medium supplemented with BFA (final concentration 2 nM). HWBC samples were cultured for 6 h at 37 °C and 5% CO_2 and monocytes were labelled in the dark at room temperature for 15 min with 17.5 ng/test each of anti-CD14-APC (clone 61D3) and anti-CD45-PerCPCy5.5 (clone 2D1) antibodies. Fluorescence-activated cell sorting (FACS) buffer was prepared with 2% FBS and 0.05% sodium azide in PBS. Following staining, cells were fixed with 60 μL of Reagent-1 from Intraprep™ kit for each sample, mixed thoroughly and incubated for 10 min at room temperature in the dark. Following this, 200 μL of FACS buffer was added in each tube, mixed well and centrifuged at 250 *g* for 5 min and supernatant was decanted. White blood cells were permeabilized and red blood cells were lysed using 50 μL of Reagent-2/sample of IntraPrep™ kit by vigrous mixing at room temperature. Anti-human CyTNF-α-PE was then added to the HWBC (17.5 ng/test, i.e 0.7 μL), vortexed and incubated for 15 min at room temperature in the dark. Cells were then re-suspended with 600 μL of PBS and centrifuged at 250 *g* for 5 min. Supernatant was discarded and washed with PBS once again. Finally, 60 μL of FACS buffer was added to the cells.

Following the same procedure as above, THP-1 cells were incubated with anti-human CyTNF-α-PE for 15 min in the dark at room temperature, washed with PBS

and re-suspended in FACS buffer. FACS analysis was performed for labelled monocytes from HWBC and THP-1 cells on a BD Accuri^{TM} C6 flow cytometer (Becton Dickinson Bioscience, San Jose, CA, U.S.A.). Data was collected for 10,000 events for each sample using C-Flow software.

The monocytes were defined by sequential gating on all CD45+ CD14+ cells in HWBC by triggering FL3 and FL4 emission detectors, respectively, and cytoplasmic TNF-α expressing monocytes were enumerated within the CD14+ population. The number and percentage of TNF-α expressing CD14+ cells and the mean fluorescence intensity (MFI) were recorded for each sample.

3.2.7. Statistical analysis

Statistical analysis was performed using Prism (version 5.0.1, GraphPad Software Inc., La Jolla, CA, USA). Two-way ANOVA was performed to assess the time-dependent statistical variations. Paired t-tests were performed on percentage TNF-α expression by monocytes in HWBC to assess variations between oligo- and poly-saccharide treatment by comparing each with the no treatment values. The matrix of poly-saccharides for the secreted cytokines and chemokines values for both THP-1 (Table 3.3) and HWBC (Table 3.4) were used for the generation of heat maps using R programing language (http://www.r-project.org/). The concentration values below the detection limit were considered null (0) for the calculation purposes and dendrograms were placed along the heat map for the ordering of the data.

3.3 Results

A panel of poly- and oligo-saccharides (Table 3.1) were selected for assessment of immunomodulatory ability. These compounds covered a range of structures, which were explored for their immunomodulatory responses. These compounds were assessed in two model systems, THP-1 cell culture and HWBC from three healthy donors. The concentrations of pro-inflammatory cytokines (IL-1β, IL-6 and tumour necrosis factor-α (TNF-α)), anti-inflammatory cytokines (IL-10 and IL-13) and chemokines (IL-8, monocyte chemoattractant protein-1 (MCP-1) and macrophage inflammatory protein 1-α (MIP1-α) were measured at different time points to

understand the immunomodulatory responses by the tested poly- and oligo-saccharides.

3.3.1. Characterisation of poly- and oligo-saccharides

As poly- and oligo-saccharides from varying sources can influence the Mr, degree of substitution and physical properties of the purified carbohydrates and the Mr range given by the manufacturer was quite wide, the test compounds (Table 3.1) were initially characterised for their apparent molecular mass and physical properties. A lack of CBB staining of the electrophoresed gels confirmed the absence of protein contamination in the oligo- and poly- saccharide preparations (Figure 3.1, Table 3.2). AB staining detects charged poly-saccharides, which include FUC, GAL and HGL in the test panel. AB stained FUC and HGL as expected but not GAL (Figure 3.1 B, Table 3.2). GAL is composed of galacturonic acid (D-GalA) and apiose, and the GalA residues impart a negative charge. However, AB binds to molecules due to their polyanionic nature rather than the constituent groups in the backbone chain (Whiteman, 1973) and the Mr of GAL is even lower than 1 kDa, and possibly ran off the gel. Varying the pH of periodate oxidation led to different results for PAS staining. At pH 2.5, only FUC was detected, while at both pH 4 and 7, FUC and HGL were detected (Figure 3.1 and Table 3.2). INL, despite the presence of vicinal hydroxyl groups, did not evolve any colour. This may be due to its low Mr that ranges from 162 Da to 164 kDa and it hence it might have ran off the gel (Azis et al., 1999). Neither MAN nor xGLU reacted with PAS despite the presence of suitable structures for both compounds. MAN was dissolved in NaOH and latter diluted in PBS. The NaOH most likely depolymerized the higher molecular mass MAN and thus the remaining lower molecular mass MAN was not retained on the gel.

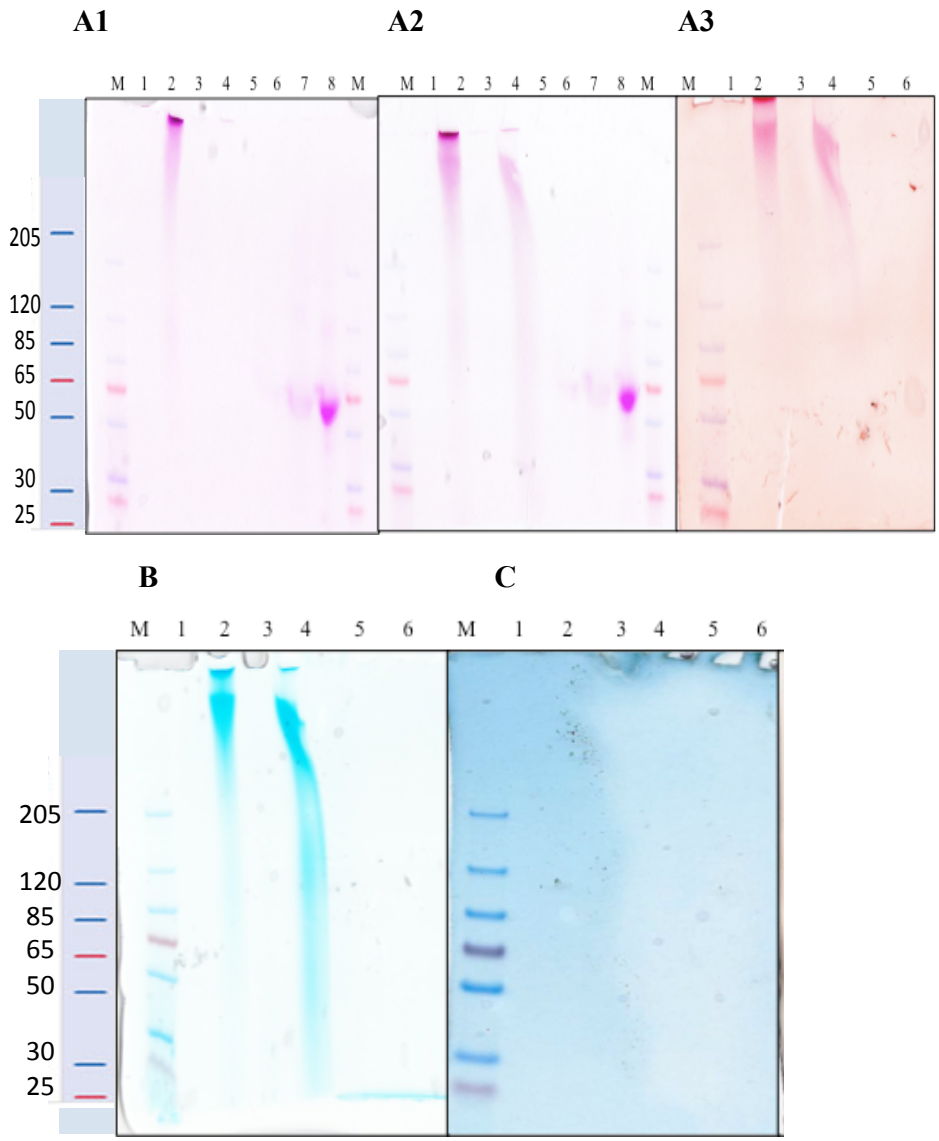

Figure 3.1. The oligo and poly- saccharides INL (lane 1), FUC (lane 2), GAL (lane 3), HGL (lane 4), MAN (lane 5) and xGLU (lane 6) and BSA (lane 7) and fetuin (lane 8) separated on 3-8% Tris-acetate gel using MES buffer. Characterisation of oligo- and poly- saccharides using PAS staining at different pHs (A1= pH 2.5, A2= pH 4.0 and A3 pH = 7.0), Alcian blue (B) and Coomassie blue (C).

Table 3.2. Compound characterisation using various stains. CBB, Coomassie Brilliant Blue; AB, Alcian Blue; PAS, periodic acid-Schiff's reagent; (+), staining; (–), absence of staining, ND, not detected, NA, information not available. Reported Mr is as reported by the manufacturer.

Compounds	Reported Mr (kDa)	Apparent Mr (kDa)	CBB	AB	PAS		
					pH 2.2	pH 4.0	pH 7.0
INL	164	ND	-	-	-	-	-
FUC	3 – 320	> 205	-	+	+	+	+
GAL	<250	ND	-	-	-	-	-
HGL	NA	> 205	-	+	-	+	+
MAN	324 Da - <1	ND	-	-	-	-	-
xGLU	312 Da – 50	ND	-	-	-	-	-

3.3.2. Cell morphology analysis

To demonstrate that the test compounds did not have any toxic effects on cells, the THP-1 cells were imaged by light microscopy for any morphological changes before and after incubation with the oligo- and poly-saccharides. No morphological changes were observed for THP-1 cells as a result of incubation with LPS and compounds, which indicated that there were no morphological variations between treatment groups nor apoptotic effects caused by the test compounds or LPS treatments. HWBC was opaque red and could not be photographed due to the limitation of light microscopy.

3.3.3. Optimization of dose concentrations and whole blood dilution factor

Different concentrations of each oligo- and polysaccharide (1, 5, and 10 μg/mL) for all incubation periods (0, 6, 12, and 24 h for HWBC and 0, 6, 12, 24, and 48 h for THP-1 cells) were selected to determine the optimal concentrations of compounds that would give detectable levels for all selected cytokines and chemokines for ELISAs. Three different concentrations of LPS (1, 10, and 100 ng/mL) were tested for the response within ELISA for the respective cytokine/chemokine standard range. HWBC was diluted in PBS at two different dilution factors (DF) (10 and 20) to find the appropriate DF to carry out further experiments. Concentrations of secreted cytokines and chemokines in the supernatants were assayed. As the concentrations of studied cytokines and chemokines at the selected time points were below detection

limit when the polysaccharide concentration were 1 and 5 μg/mL, all experiments were continued with 10 μg/mL of each polysaccharide in both THP-1 and WBC. As 1 ng/mL of LPS resulted in an undetectable concentration for cytokines at the various time points), LPS at 10 ng/mL of concentration was used as control for the following experiments carried out upon incubation with oligo- and poly-saccharides. HWBC at 20DF showed undetectable ranges for different cytokines), the experiments were continued with a HWBC at 10 DF.

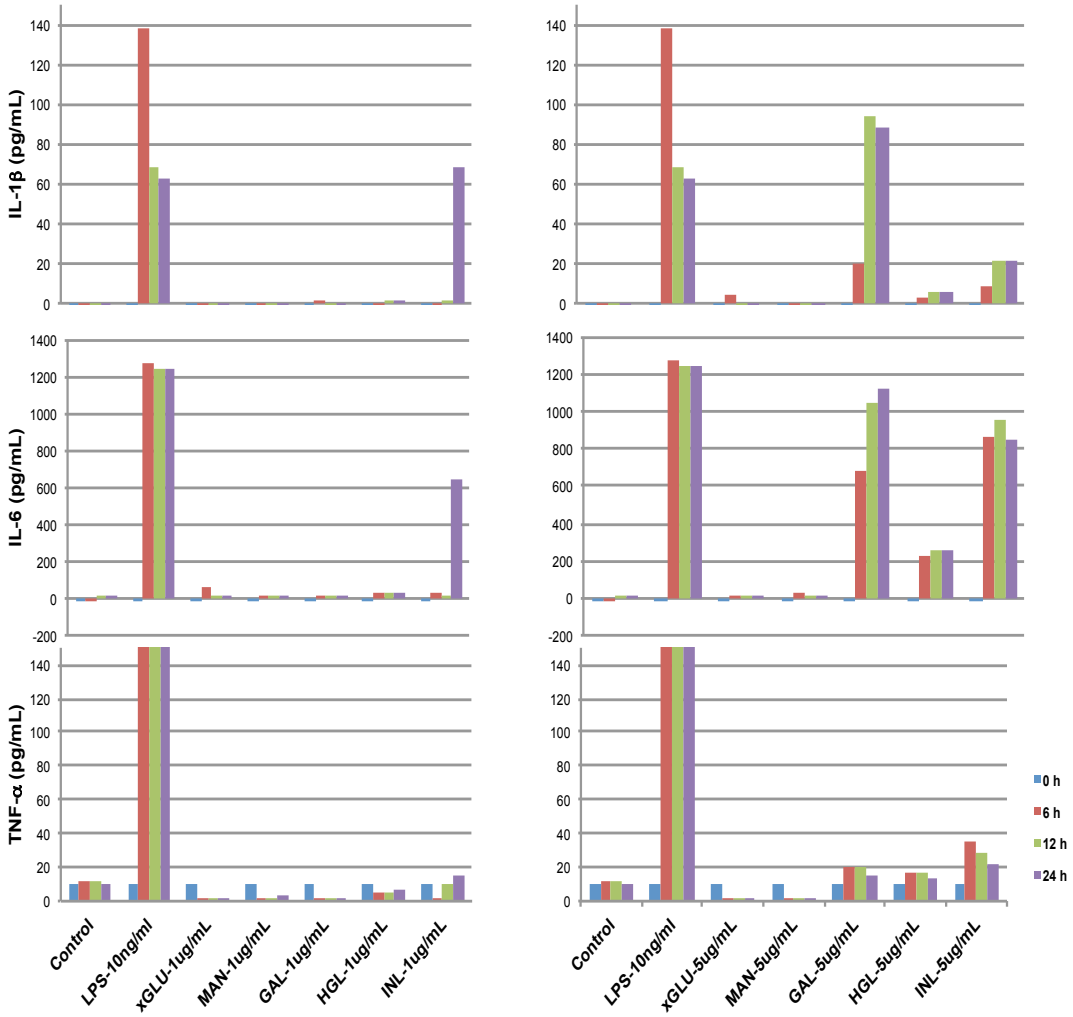

Figure 3.2. Cytokine production was measured secreted by HWBC in response to co-incubation with 1 and 5 μg/mL (optimisation concentrations) of oligo- and poly-saccharides at 0, 6, 12 and 24 h.

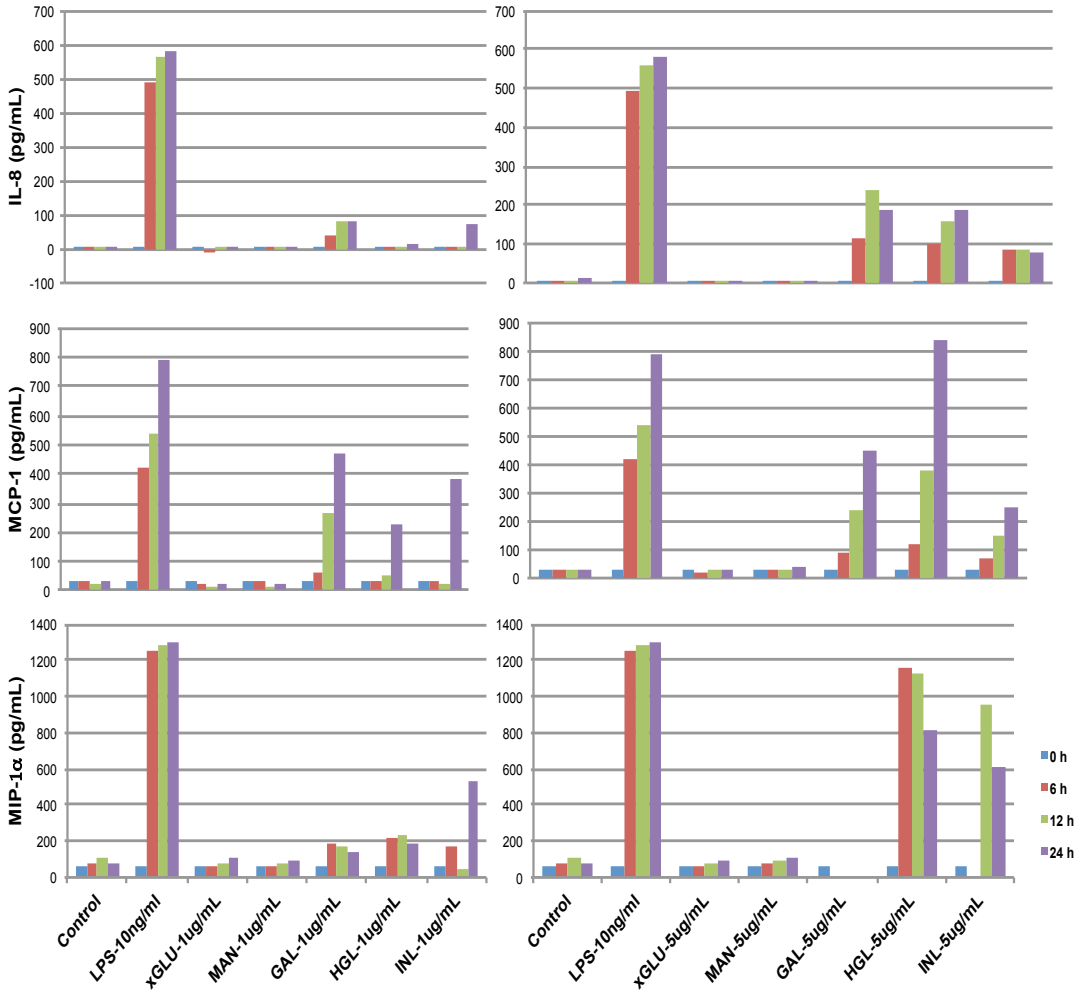

Figure 3.3. Chemokine production was measured by HWBC in response to co-incubation with 1 and 5 μg/mL (optimisation concentrations) oligo- and poly-saccharides. 0, 6, 12 and 24 h.

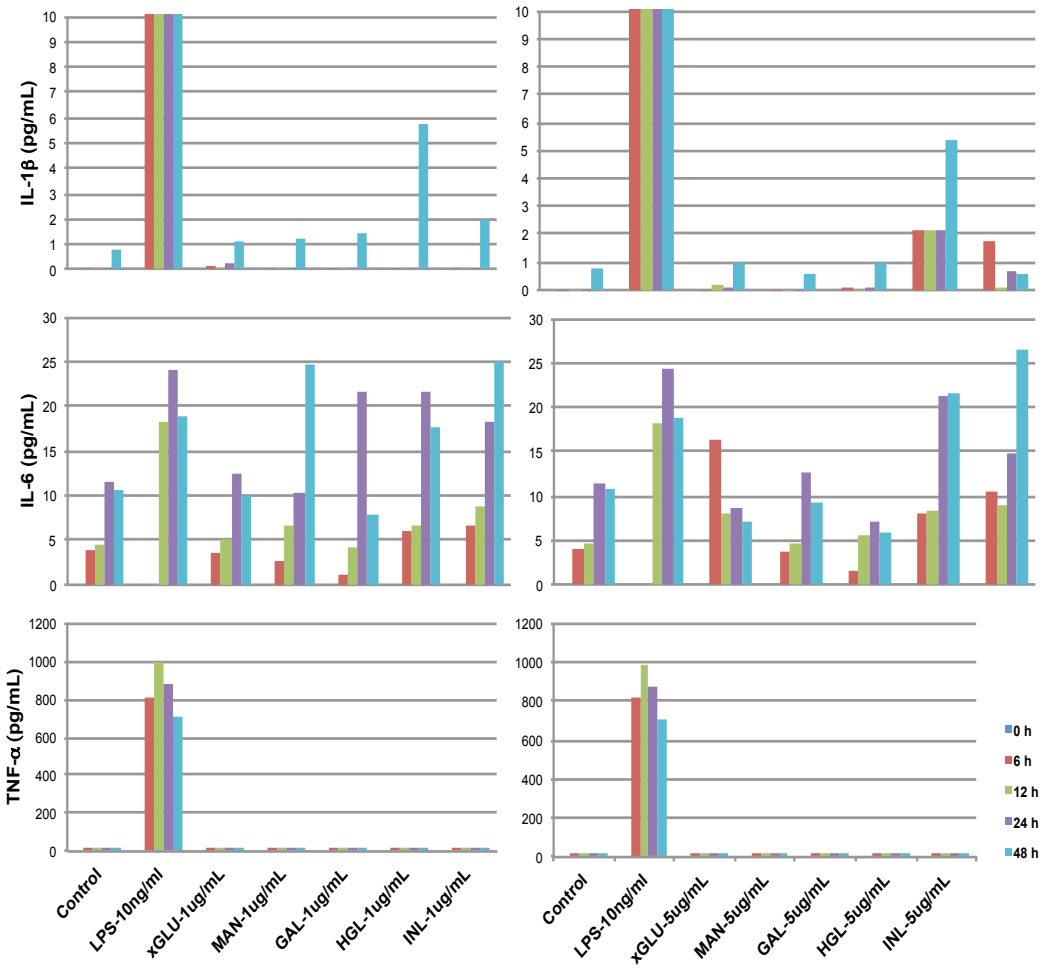

Figure 3.4. Cytokine production was measured secreted by THP-1 cells in response to co-incubation with 1 and 5 μg/mL (optimisation concentrations) oligo- and poly-saccharides at 0, 6, 12 and 24 h.

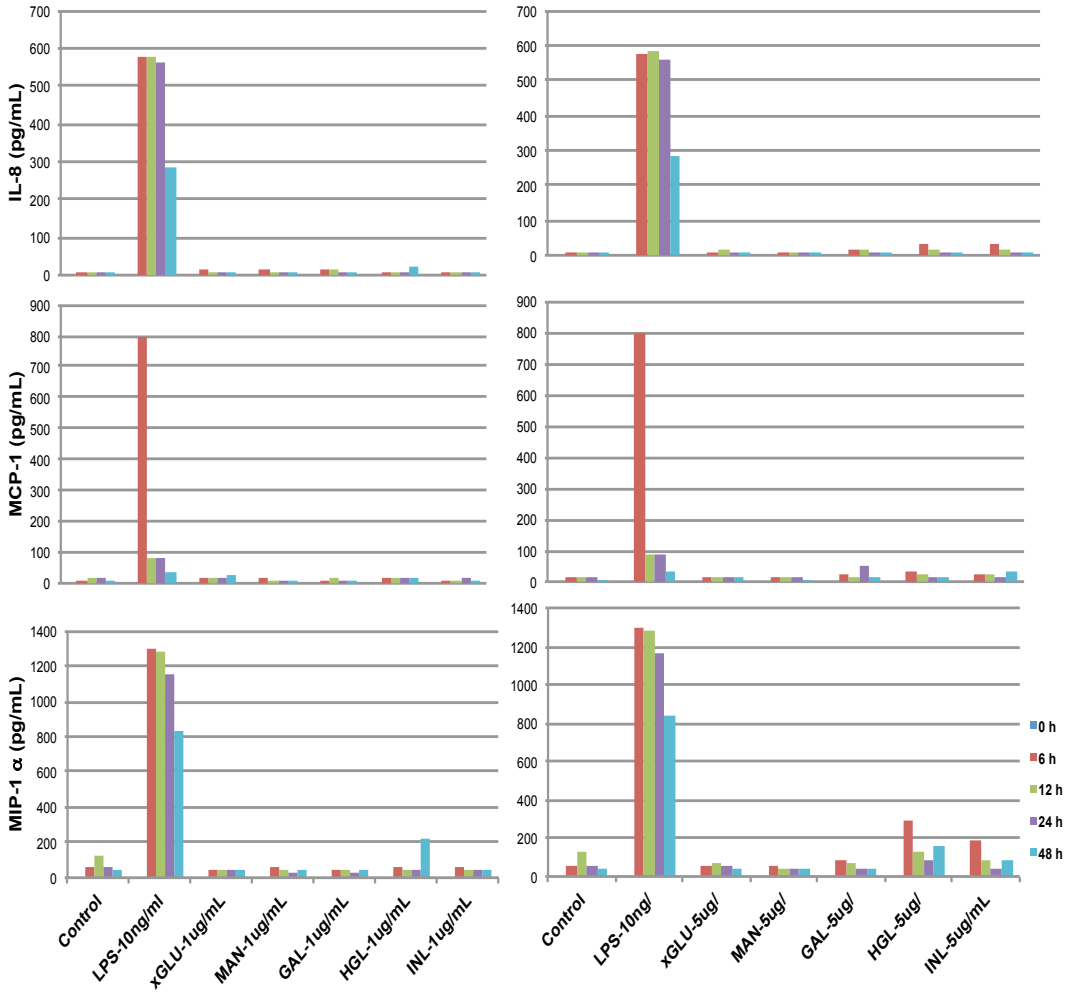

Figure 3.5. Cytokine production was measured secreted by THP-1 cells in response to co-incubation with 1 and 5 μg/mL (optimisation concentrations) oligo- and poly-saccharides at 0, 6, 12, 24 and 48 h.

3.3.4. Effect of LPS

Supernatants were collected from HWBC until 24 hours of incubation after treatment as the constituents of HWBC started degrading and differentiating and the cells began to die at later time points. However, the immortalised THP-1 cells were incubated for 48 hours.

Stimulating HWBC with both concentrations of LPS (10 and 100 ng/mL) significantly increased production of all measured pro-inflammatory cytokines, IL-1β, IL-6 and TNF-α, and chemokines, IL-8, MCP-1 and macrophage inflammatory protein-1α (MIP-1α), at 6 h post- stimulation (Figure 3.6, Tables 3.3 and 3.4) (p-value < 0.02 to <0.0001) for cytokine and chemokines except for IL-6 which had

high error bars). The concentrations of all secreted cytokines and chemokines continued to increase slightly up to 24 h for both concentrations of LPS, except for IL-6 which remained constant for 10 ng/mL of LPS at 6 h with 6425.6 ± 8037 pg/mL, 12 h at 6400.6 ± 8070.4 pg/mL and 24 h at 6430 ± 8073.5 pg/mL mg/mL LPS and 100 ng/mL of LPS at 6 h 8506.1 ± 11663.4 ng/mL, 12 h at 8502.7 ± 11684.4 pg/mL and 24 h at 8520.9 ± 11707 ng/mL. The concentrations of IL-6 varied over time with 10 ng/mL and 100 ng/mL of LPS incubation.

In contrast, THP-1 cells secreted lower overall concentrations of cytokines and chemokines upon LPS stimulation in comparison to HWBC, except for TNF-α and MIP-1α, which showed similar magnitudes in response in both cell models. However, the overall concentration trend increased over time in the THP-1 cells (Figure 3.6). All measured pro-inflammatory cytokine concentrations increased at the 6 h time point and only increased marginally at all later time points for THP-1 cells, except for IL-6 which was undetectable at all time points assessed (Figure 3.6, Table 3.3). On the other hand, IL-8 and MIP-1α concentrations stayed unchanged after their initial increase at 6 h until 48 h for 100 ng/mL LPS stimulation for THP-1 cells and dropped slightly by 48 h for the 10 ng/mL LPS stimulation. For MCP-1, the concentrations varied from 36.27+4.19 to 190 pg/mL from 6 h to 12 h and stayed constant from 24 h to 48 at 84.47 ± 64.69 pg/mL and 84.76 ± 9.79 respectively upon incubation with 10 ng/mL (Figure 3.6).

The anti-inflammatory cytokines IL-10 and IL-13 did not have a measurable response and their concentrations were below the LLOD (i.e. response was below 10 pg/mL). Due to their low concentrations when incubated with LPS, these cytokines were not tested upon incubation of cells with oligo- and poly-saccharides.

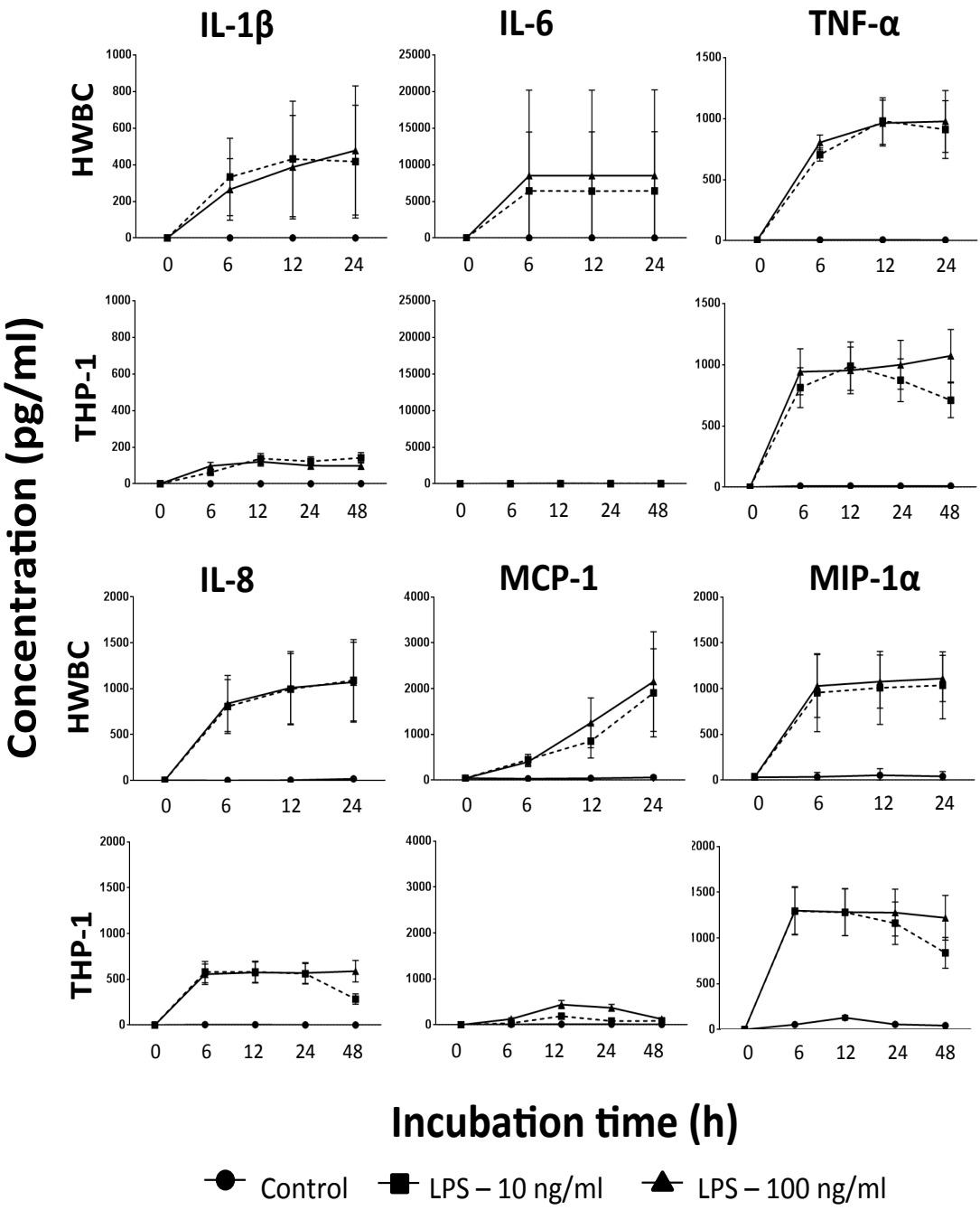

Figure 3.6. Cytokine and chemokine production by HWBC (top and third row) and THP-1 cells (second and fourth) rows in response to the incubation with LPS at 10 ng/mL and 100 ng/mL. HWBC were incubated for 6, 12 and 24 h and THP-1 cells for 6, 12, 14 and 48 h.

Table 3.3. Concentrations of cytokines and chemokines (ng/mL) produced by THP-1 cells upon incubation with 10 μg/mL of oligo- and poly-saccharides.

	Time (h)	THP-1 cells supernatants (Untreated and Treated Samples) following different incubation periods								
		Control	LPS (10 ng/ml)	LPS (100 ng/ml)	xGLU	MAN	GAL	HGL	INL	FUC
Cytokines										
IL-1 β ng/mL (Mean ± SEM) (LLOD: 3.5)	0	n.d.	n.d.		n.d.	n.d.	n.d.	n.d.	n.d.	n.d.
	6	n.d.	62.1 ± 7.2		n.d.	n.d.	n.d.	8.8	n.d.	-
	12	n.d.	137.9 ± 15.9		n.d.	n.d.	n.d.	5.9 ± 0.1	n.d.	-
	24	n.d.	122.7 ± 14.2		n.d.	n.d.	n.d.	7.2 ± 7.1	n.d.	-
	48	n.d.	141.7 ± 16.4		n.d.	n.d.	5.8 ± 3	11.6 ± 0.1	4.19	-
IL-6 ng/mL (Mean ± SEM) (LLOD: 9)	0	n.d.	n.d.	n.d.	n.d.	n.d.	n.d.	n.d.	n.d.	n.d.
	6	n.d.	12.1 ± 1.4	35.6 ± 4.1	n.d.	n.d.	n.d.	n.d.	n.d.	n.d.
	12	n.d.	18.1 ± 2.1	52.6 ± 6.1	n.d.	n.d.	13.6 ± 10	n.d.	n.d.	n.d.
	24	11.9 ± 6.6	24.2 ± 2.8	39.3 ± 4.5	30.5 ± 15.7	n.d.	31.9 ± 10.7	11.6 ± 1.1	18.7 ± 2	n.d.
	48	10.7 ± 5.3	18.7 ± 2.2	29.4 ± 3.4	9.4 ± 3.6	n.d.	11.6 ± 5.6	n.d.	31.7 ± 16.9	n.d.
TNF-α ng/mL (Mean ± SEM) (LLOD: 15.6)	0	n.d.	n.d.	n.d.	n.d.	n.d.	n.d.	n.d.	n.d.	n.d.
	6	n.d.	812.7 ± 93.8	942.1 ± 108.8	n.d.	n.d.	n.d.	36.3 ± 3.3	10.41	n.d.
	12	n.d.	988.6 ± 114.2	952.9 ± 110.0	n.d.	n.d.	n.d.	31.5 ± 2.8	10	n.d.
	24	n.d.	872.9 ± 100.8	999.1 ± 115.4	n.d.	n.d.	n.d.	31.4 ± 1.9	10	n.d.
	48	n.d.	709.3 ± 81.9	1072.2 ± 123.8	n.d.	n.d.	n.d.	41.4 ± 3.3	11.1	n.d.
Chemokines										
IL-8 ng/mL (Mean ± SEM) (LLOD: 27)	0	n.d.	n.d.	n.d.	n.d.	n.d.	n.d.	n.d.	n.d.	n.d.
	6	n.d.	579.5 ± 66.9	555.2 ± 64.1	n.d.	n.d.	n.d.	86.5 ± 3.6	30.3 ± 12.2	n.d.
	12	n.d.	581.0 ± 67.1	574.3 ± 66.3	n.d.	n.d.	n.d.	50.8 ± 0.9	30.2 ± 2	n.d.
	24	n.d.	560.2 ± 64.7	568.6 ± 65.7	n.d.	n.d.	n.d.	25.6	n.d.	n.d.
	48	n.d.	283.6 ± 32.7	588.1 ± 67.9	n.d.	n.d.	n.d.	36.3 ± 1.3	n.d.	n.d.
MCP-1 ng/mL (Mean ± SEM)	0	n.d.	n.d.	n.d.	n.d.	n.d.	n.d.	n.d.	n.d.	n.d.
	6	n.d.	36.3 ± 4.2	128 ± 14.8	19.9 ± 6.5	n.d.	15.3	44.5 ± 1.8	19.7 ± 2.9	58.87
	12	n.d.	190.5 ± 22.00	442.5 ± 51.1	n.d.	15.9 ± 1.8	22.4 ± 0.5	38.2 ± 3.3	23.7 ± 5.3	37.4 ± 12.7

(LLOD: 15.6)	24	n.d.	84.5 ± 64.7	371.7 ± 42.9	19 ± 5.7	n.d.	20.9 ± 2.8	51.1 ± 30.2	20 ± 0.3	37.40 ± 5.2
	48	n.d.	84.8 ± 9.8	125.5 ± 14.5	15.7 ± 3	n.d.	17.2± 3.9	32.5 ± 11.7	32.1 ± 19.7	24.8
MIP-1α	0	n.d.	n.d.	n.d.	n.d.	n.d.	n.d.	n.d.	n.d.	n.d.
ng/mL	6	54.5 ± 5.3	1294.3 ± 149.4	1299.9 ± 150.1	52.4 ± 1.5	85.8 ± 21.2	75.6 ± 3.9	624.5 ± 54.6	173.7 ± 48.1	
(Mean ± SEM)	12	129.8 ± 24.1	1280.4 ± 147.9	1283 ± 148.2	37.4 ± 0.4	38.7 ± 2.4	65.1 ± 6.4	259.1 ± 12.1	132.1 ± 7.6	10.6
(LLOD: 7.1)	24	57.1 ± 4.4	1161.2 ± 134.1	1277.6 ± 147.5	33.2 ± 4.7	32.25 ± 4.56	38.9 ± 0.8	148.6 ± 3.6	62.75 ± 2.7	
	48	43.9 ± 9	837.6 ± 96.7	1220.3 ± 140.9	41.1 ± 1	34.81 ± 1.18	135.9 ± 85	416.6 ± 8.1	112.9 ± 52.9	17.1

Table 3.4. Concentrations (ng/mL) of cytokines and chemokines produced by HWBC cells upon incubation with 10 μg/mL of oligo- and poly-saccharides.

	Time (h)	HWBC supernatants following incubation (Mean ± SD)								
		Control	LPS (10 ng/ml)	LPS (100 ng/ml)	xGLU	MAN	GAL	HGL	INL	FUC
Cytokines										
IL-1 β (Mean ± SD) (LLOD: 3.5)	0	n.d.	n.d.	n.d.	n.d.	n.d.	n.d.	n.d.	n.d.	n.d.
	6	n.d.	332.8 ± 211	265.2 ± 168.2	n.d.	n.d.	16.5 ± 3.3	37.7 ± 25.6	37.9 ± 12.9	59.4 ± 37.5
	12	n.d.	431.4 ± 315.2	386.9 ± 282.7	n.d.	n.d.	46.2 ± 52.3	45 ± 29	192 ± 74.8	141.9 ± 166.6
	24	n.d.	417.3 ± 307.8	477.9 ± 352.5	n.d.	n.d.	32.6 ± 31.4	40.8 ± 6.2	140.9 ± 13.6	112.9 ± 127.709
IL-6 (Mean ± SD) (LLOD: 9)	0	n.d.	n.d.		n.d.	n.d.	n.d.	n.d.	n.d.	n.d.
	6	n.d.	6425.6 ± 8037	8506.1 ± 11663.4	n.d.	n.d.	708.9 ± 309.3	1617.5 ± 1414.2	1440.5 ± 855	843.7 ± 167.5
	12	n.d.	6400.6 ± 8070.4	8502.5 ± 11684.4	n.d.	n.d.	791.5 ± 431.5	1517.2 ± 1077.7	3445.9 ± 3848.8	1263.9 ± 570.2
	24	n.d.	6430 ± 8073.5	8520.9 ± 11707.0	n.d.	n.d.	873 ± 521.3	1815.3 ± 1640.7	3389.4 ± 3773.2	1242 ± 628
TNF-α (Mean ± SD) (LLOD: 15.6)	0	n.d.	n.d.	n.d.	n.d.	n.d.	n.d.	n.d.	n.d.	n.d.
	6	n.d.	705 ± 58.4	804.4 ± 60.9	n.d.	n.d.	42.1 ± 5.3	157.2 ± 112.9	98.6 ± 34.6	117 ± 34.8
	12	n.d.	980. ± 191.1	963.4 ± 187.8	n.d.	n.d.	34.5 ± 6.3	128.9 ± 87.8	225 ± 115.5	136.2 ± 78
	24	n.d.	910.4 ± 236.4	976.8 ± 253.6	n.d.	n.d.	22.5 ± 10	94.949 ± 75.219	129.9 ± 52.5	109.1 ± 72.5
Chemokines										
IL-8 (Mean ± SD) (LLOD: 27)	0	n.d.	n.d.	n.d.	n.d.	n.d.	n.d.	n.d.	n.d.	n.d.
	6	n.d.	805.3 ± 294.2	837.8 ± 306.1	n.d.	n.d.	110.5 ± 32.9	521.119 ± 153.7	191 ± 85.1	203.6 ± 65.9
	12	n.d.	994.6 ± 387.1	1009.9 ± 393	n.d.	n.d.	116.1 ± 47.5	596.9 ± 102.1	415 ± 198.8	206.6 ± 71.7
	24	n.d.	1091 ± 443.5	1070.8 ± 435.3	n.d.	n.d.	136.5 ±	691.4 ± 44.2	391.3 ± 391.3	221.9 ± 121.8

							96.6			
MCP-1 (Mean ± SD) (LLOD: 15.6)	0	37.08 ± 7.69	37.1 ± 7.7	37.1 ± 7.7	37.1 ± 7.7	37.1 ± 7.7	37.1 ± 7.7	37.1 ± 7.7	37.1 ± 7.7	37.1 ± 7.7
	6	30.48 ± 2.34	447.3 ± 115.3	398.2 ± 102.6	52.7 ± 40.3	56.2 ± 39.9	166.1 ± 89.8	454.6 ± 250.3	182.4 ± 70.4	172 ± 107.2
	12	32.13 ± 9.82	853.3 ± 396.9	1251.6 ± 542.7	50.9 ± 33.7	72.3 ± 42.5	357.6 ± 255.6	1399.1 ± 763.9	422 ± 167	534.6 ± 251.7
	24	38.01 ± 5.95	1907.5 ± 963.7	2154.4 ± 1088.5	48.7 ± 26.1	47.3 ± 24.7	686.7 ± 378.7	1799.7 ± 949.9	820 ± 329.3	1182.7 ± 482.5
MIP-1α (Mean ± SD) (LLOD: 7.1)	0	30.76 ± 42.33	30.8 ± 42.3	30.8 ± 42.3	30.7 ± 42.3	30.7 ± 44.3	30.7 ± 42.3	30.8 ± 42.3	30.8 ± 42.3	30.8 ± 42.3
	6	36.6 ± 48.7	955.7 ± 425.5	1028.4 ± 343	33.16 ± 44.1	42 ± 55.8	740.5 ± 679	898.7 ± 491.2	806.1 ± 667.7	348.2 ± 125.9
	12	53.5 ± 71.5	1008.2 ± 398.7	1076.3 ± 289.7	43.62 ± 58.5	41.8 ± 52.1	705.5 ± 722.8	885.4 ± 531.9	851.8 ± 605.6	285 ± 85.1
	24	41.3 ± 53.4	1035.5 ± 366	1110.5 ± 252.3	60.01 ± 81.3	50.3 ± 65.9	489.9 ± 567.2	842.1 ± 568.4	820 ± 621.8	230.8 ± 22.1
n.d. = not determined (below detection limit); SEM = standard error of the mean; LLOD = lower limit of detection										

3.3.5. Effect of poly- and oligo-saccharides on secreted cytokine production in HWBC and THP-1 culture

Compared with the unstimulated cells in the HWBC cell model, four (FUC, INL HGL and GAL) of the six poly- and oligo-saccharides showed significant increases in production of all assessed pro-inflammatory cytokines (IL-1β ($p = <0.0001$), IL-6 ($p = 0.02$) and TNF-α ($p = <0.0001$)) over time (Figure 3.7 and Table 3.4). Time-dependent elevations in the concentrations of IL-1β and TNF-α were observed in HWBC ($p = <0.0001$) treated with these four compounds. The cytokine secretion profiles for all three blood donors followed a similar trend upon incubation with the compounds (Figure 3.8). INL stimulated the greatest production of cytokines (for example. IL-6 at 12 h with 3445.9 ± 3848.8 ng/mL) whereas GAL the lowest concentration of cytokine secretion ($p = 0.02$, for example, IL-1β at 6 h with 16.48 ± 3.3 ng/mL) in HWBC.

For THP-1 cells, the production of the cytokines IL-1β, IL-6 and TNF-α was very limited in response to treatment by the oligo- and poly-saccharide panel and secreted cytokine concentrations of IL-1β and IL-6 were below the limit of detection (3.6 pg/mL and 9 pg/mL respectively) at all incubation times tested (Table 3.3). The concentration of TNF-α was above the LLOD unlike the other two cytokines upon incubation with HGL with 36.34 ± 3.9 pg/mL at 6 h, 31.5 ± 2.8 pg/mL at 12 h, 31.4 ± 1.91 at 24 h and 41.41 ± 3.25 pg/mL at 48 h, which stayed constant over time.

Of all compounds, the branched oligosaccharide xGLU and linear oligosaccharide MAN did not have any effect on the production of pro-inflammatory cytokines in either HWBC or THP-1 cell culture.

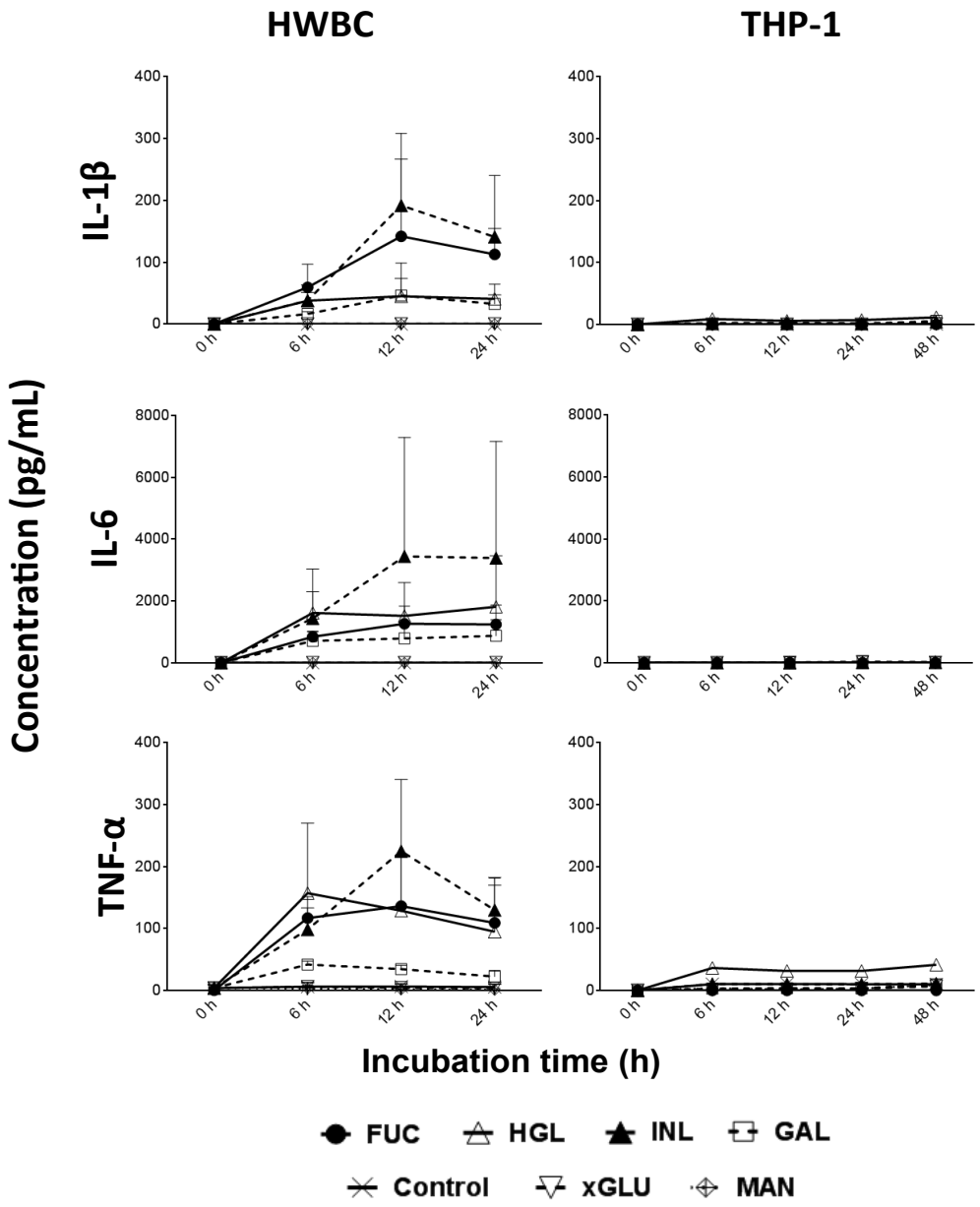

Figure 3.7. Cytokine production by HWBC (left) and THP-1 cells (right) in response to co-incubation with 10 μg/mL oligo- and poly-saccharides. THP-1 cells were incubated for 6, 12, 14 and 48 h while HWBC were incubated for 6, 12 and 24 h.

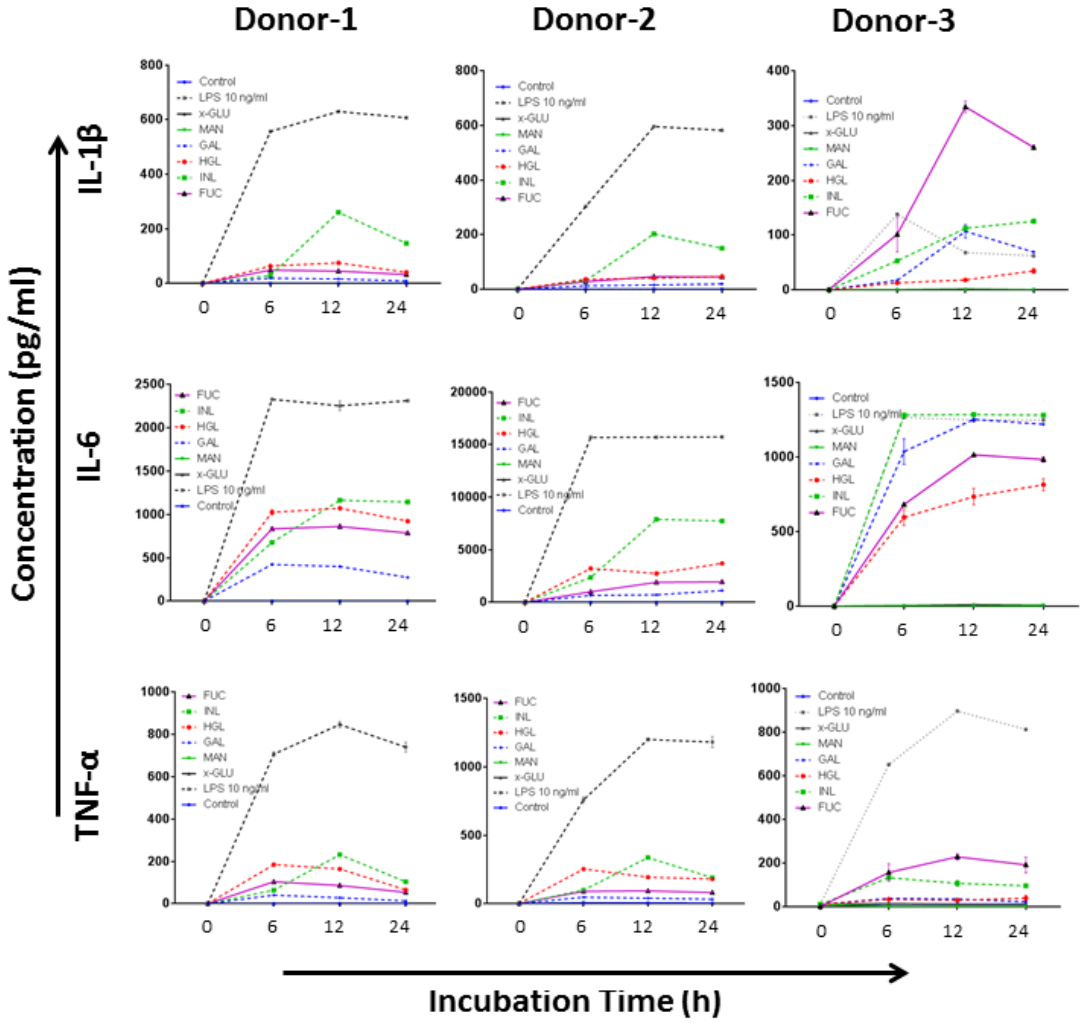

Figure 3.8 Concentrations of cytokines produced by HWBC in response to co-incubation with 10 µg/mL oligo- and poly-saccharides for 6, 12 and 24 h. Results expressed as mean ± SD for individual donors (n=3).

3.3.6. Effect of poly- and oligo-saccharides on secreted chemokine production in HWBC and THP-1 culture

The concentration of secreted chemokines significantly increased over time in HWBC upon treatment with FUC, INL HGL and GAL but the high error bars denote individual variation, although the pattern of the onset of chemokine secretion was the same across all the volunteers (Figures 3.9 and 3.10). HGL induced the greatest chemokine production in HWBC for MCP-1 (686.7 ± 378.7 pg/mL at 24 h) whereas GAL had the least effect on any chemokine except for MIP-1α. The concentration of MIP-1α increased significantly at 6 h ($p = 0.04$) in response to FUC, INL and HGL, and remained high until the 24 h time point. Treatment with GAL showed slight decrease in MIP-1α concentrations at 24 h from 6 h (Figures 3.9 and 3.10). Time-dependent significant elevations in the concentration of IL-8 ($p = 0.0003$) were observed following incubation periods of 6 h, 12 h and highest concentrations were observed at 24 h. The concentrations of IL-8 were highest at 24 h (691.4 ± 44.2 pg/mL) and concentrations of MIP-1α increased significantly at 6 h 6 h (898.7 ± 491.2 pg/mL), which stayed constant until 24 h when incubated with HGL.

In THP-1 cells, the general concentration responses of IL-8, MCP-1 and MIP-1α to poly- and oligo-saccharide treatments were very low to undetectable compared to HWBC. The expression of both IL-8 and MIP-1α increased at 6 h when treated with HGL to 86.5 ± 3.6 and 624.5 ± 54.6 pg/mL, respectively. Interestingly, MIP-1α concentration was significantly elevated at 6 h compared to control when treated with either HGL or INL, decreased at 24 h to 148.6 ± 3.6 pg/mL and increased again by 48 h to 416.6 ± 8.1 pg/mL. However, production of IL-8 and MCP-1 by THP-1 cells was inconsistent between the incubation times and treatments, with undetectable ranges. HGL led to low detectable concentrations of TNF-α at 6 h that stayed unchanged till 48 h.

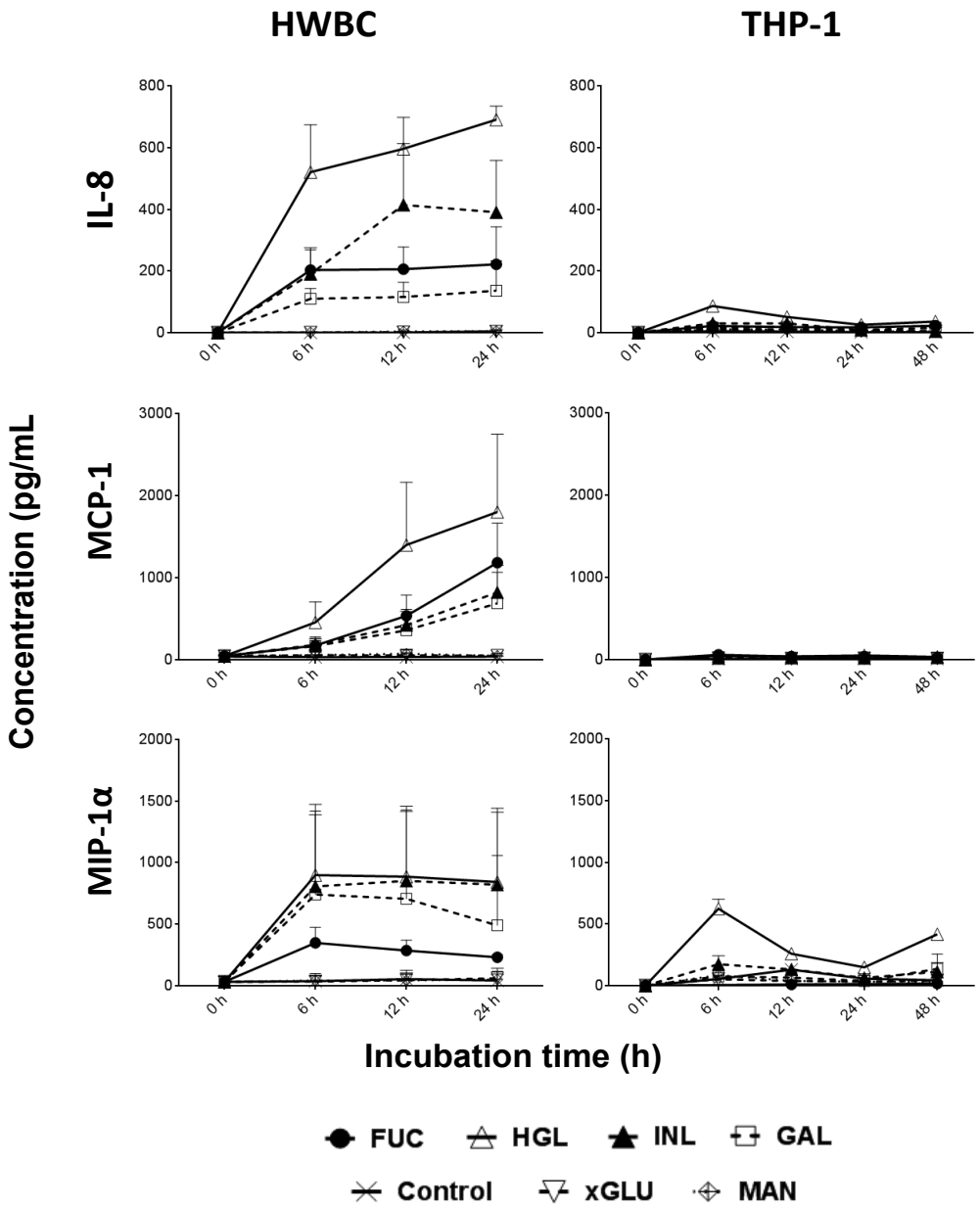

Figure 3.9. Chemokine production by HWBC (left) and THP-1 cells (right) in response to co-incubation with 10 μg/mL oligo- and poly-saccharides. THP-1 cells were incubated for 6, 12, 14 and 48 h while HWBC were incubated for 6, 12 and 24 h.

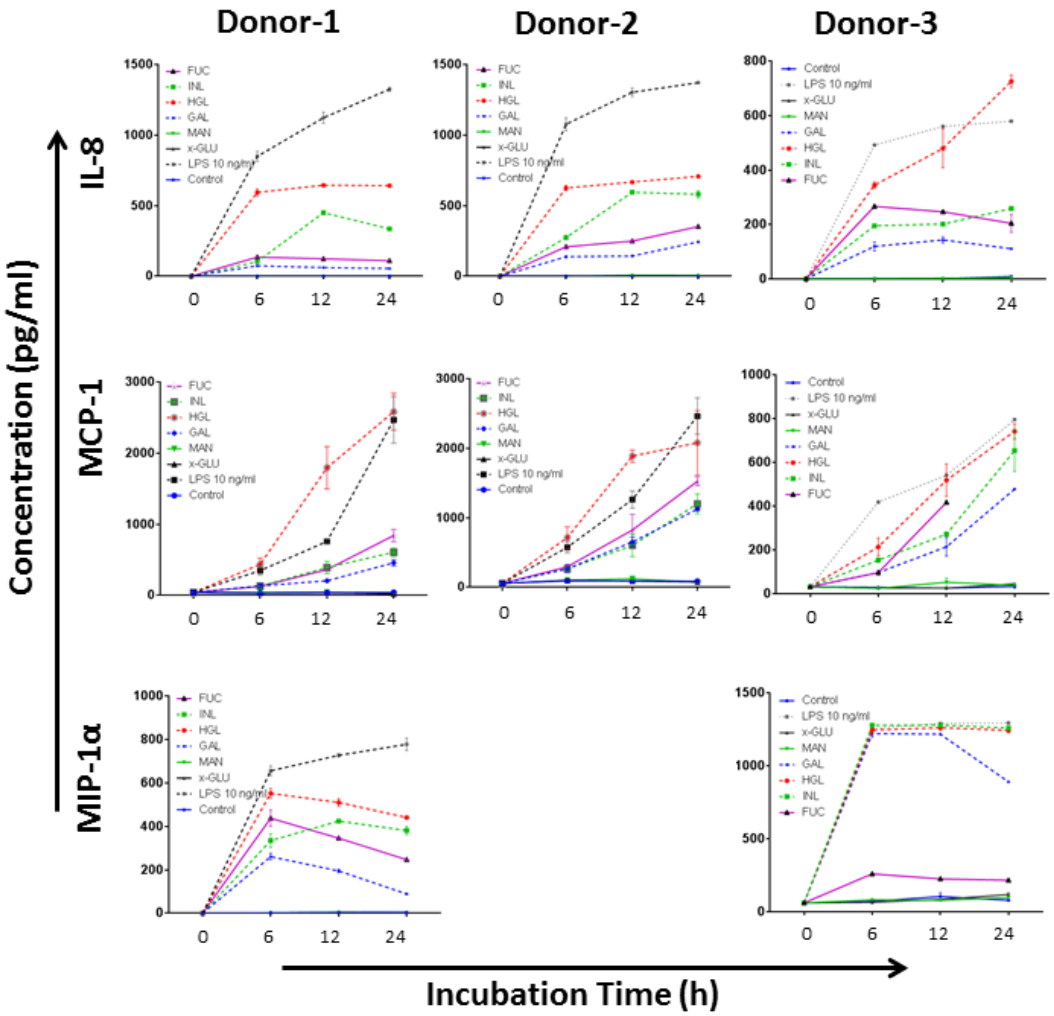

Figure 3.10. Concentrations of chemokines produced by HWBC in response to co-incubation with 10 µg/mL oligo- and poly-saccharides for 6, 12 and 24 h. Results are expressed as mean ± SD for individual donors (n=3).

3.4.7. Overall effect of poly- and oligo-saccharides on secreted chemokines and cytokines

The overall analyses upon incubation with oligo and poly-saccharides on the HWBC and THP-1 are compiled in graphical outputs represented in form of heat maps (Figure 3.11). These representative heat maps present the effect of oligo and poly-saccharides on secretion of cytokines and chemokines by THP-1 cells and HWBC, where colour mapping facilitate visual assessment of the correlation coefficients. The colour in each cell represents the ELISA responses ranging low to high values indicated by green shades to red shades. INL and HGL had the greatest effect on the secretion of cytokines and chemokines respectively proceeded by FUC and GAL at similar levels as shown by the dendrogram on the heat map for HWBC (Figure 3.11 A). MAN and xGLU had no effect on the secretion of either cytokines or chemokines when compared to control, also shown by the dendrogram. The heat map for THP-1 was representative of the low responses of the poly-saccharides (as shown by the lower value colour key compared to colour key for HWBC) except HGL, which secreted detectable chemokines upon incubation with THP-1 cells (Figure 3.11 B). The heat maps were generated with LPS and the 0 h time point for both HWBC and THP-1 cells (Figure 3.12) where LPS lies on a different branch of the dendrogram due to significantly higher responses than the oligo and poly-saccharides in two model systems.

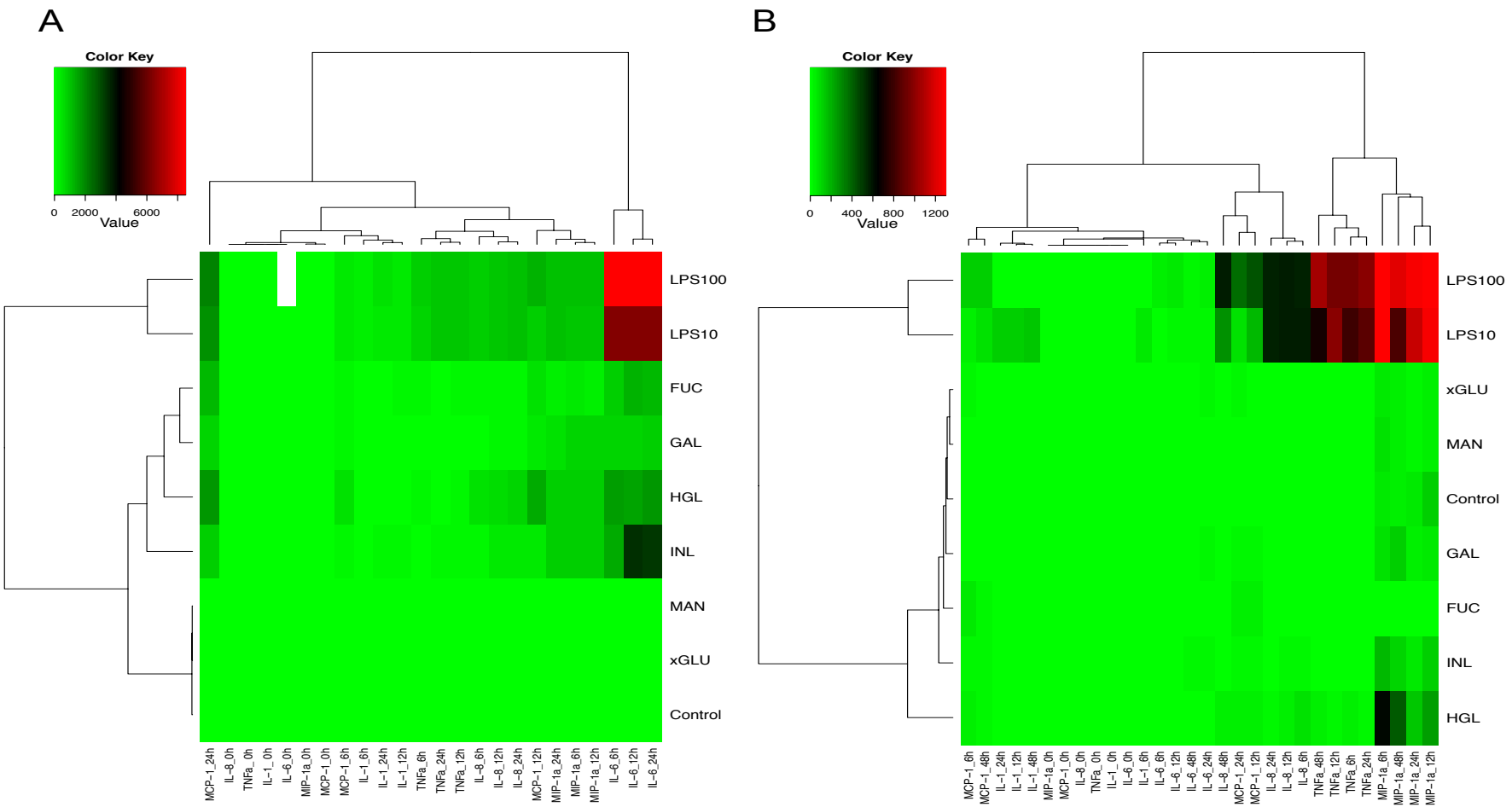

Figure 3.11. Hierarchical clustering of the relative expression of the cytokines and chemokines upon incubation with 10 μg/mL oligo- and poly-saccharides and 10 ng/ml LPS. A heat map representation is graphed for HWBC (A) and THP-1 cells (B).

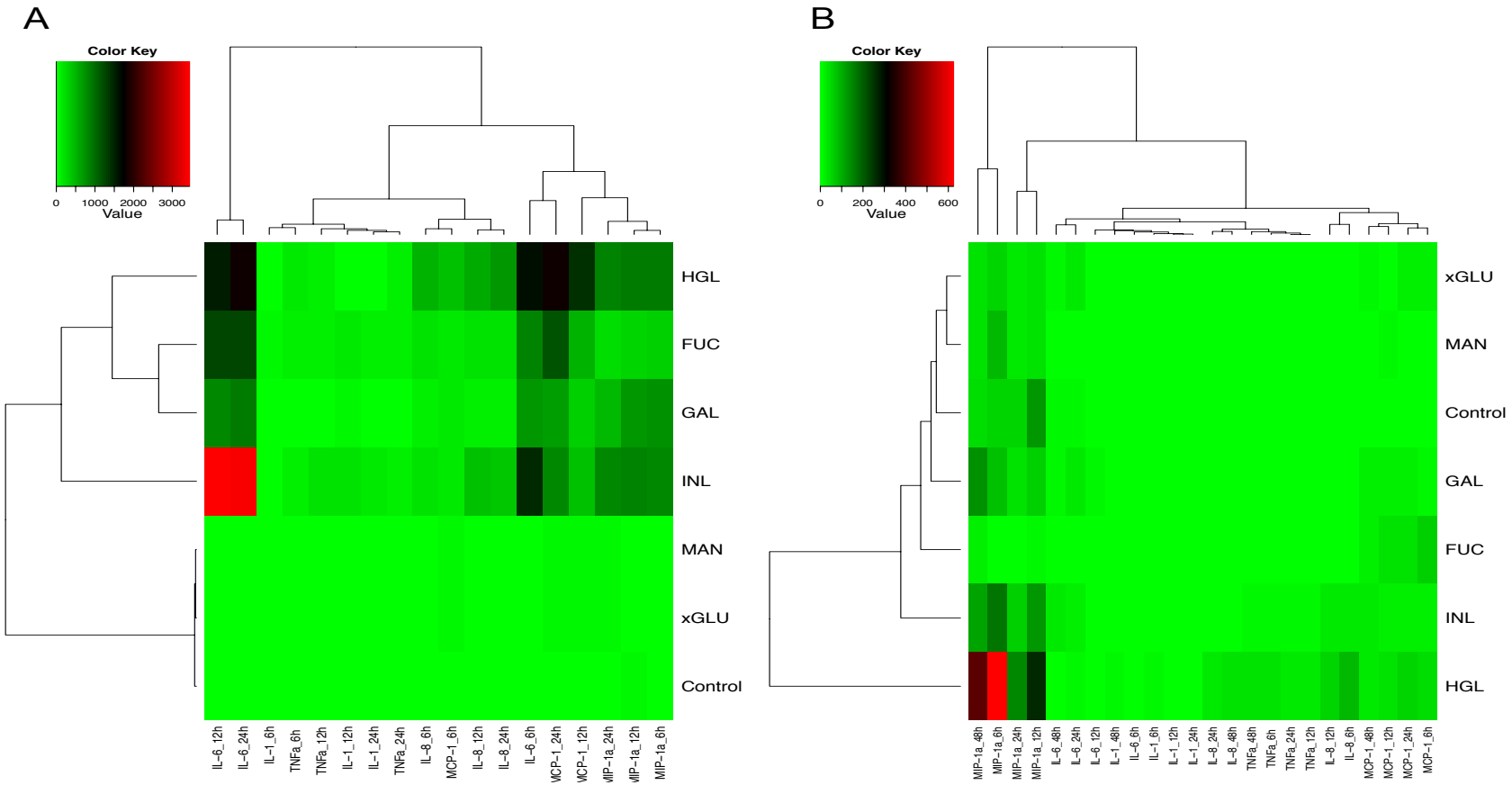

Figure 3.12. Hierarchical clustering of the relative expression of the cytokines and chemokines upon incubation with 10 μg/mL oligo- and poly-saccharides. A heat map representation is graphed for HWBC (A) and THP-1 cells (B).

3.3.7. Effect of poly- and oligo-saccharides on intracellular TNF-α expression

The effects of all poly- and oligo-saccharides on intracellular TNF-α expression in monocytes in HWBC and THP-1 cells following 6 h incubation were also investigated using FACS analysis. The intracellular expression of TNF-α in monocytes was also compared to the secreted TNF-α concentration upon incubation with test compounds. Intracellular detection using flow cytometry avoids the influence of the extracellular environment and provides information about the contribution that each cell type makes towards the secretion of cytokines (Sewell et al., 1997, Prussin, 1996).

In order to determine which sub-population of HWBC contributed most to TNF-α production, the expression of iTNF-α was tested in several HWBC sub-populations, including the CD3+ T-cells (both CD4+ and CD8+, together and separately), CD19+ B-cells and natural killer cells, after LPS stimulation for 6 h. None of these cell types showed any significant iTNF-α expression compared to control (data not shown). The percentage of intracellular TNF-α expressed by the monocytic cell population in HWBC upon incubation with different oligo- and poly-saccharides was calculated (Table 3.5). A significant increase in intracellular TNF-α expression by HWBC monocytes was found when they were treated with GAL, HGL, INL and FUC (Figure 3.13 and Figure 3.14) with a mean increase of 8.5-, 15.8-, 14.5-, and 13-fold in percentage of TNF-α expressing monocytes, respectively, compared to untreated control. xGLU and MAN, with mean change of 4.8% (1.2 fold) and 4.3% (no fold change) compared with untreated control, respectively, had no effect on TNF-α expression. In three volunteers, the monocyte concentration varied less than 10% and in these, 1 mL of blood contained on average 1.8×10^5 CD45+/CD14+ monocytes as determined by flow cytometry analysis. Therefore, when diluted ten-fold, the number of monocytes present in the HWBC iTNF-α assays, as well as the assay for secreted cytokines and chemokines was 1.8×10^4.

As THP-1 cells secreted only very low concentrations of TNF-α and furthermore are comprised of a single homogenous population, iTNF-α expression was not determined for THP-1 cells.

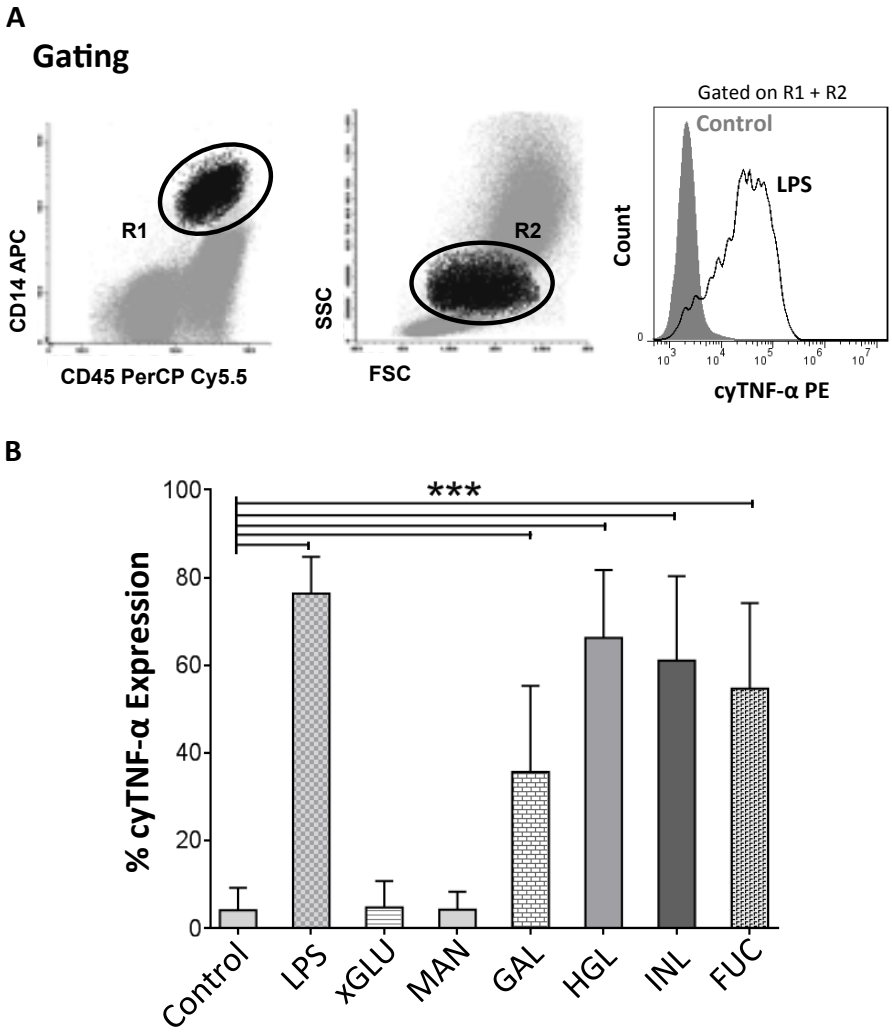

Figure 3.13. Intracellular TNF-α production by gated HWBC for monocytes (A) after labelling with human anti-CD45 and CD14 antibodies in response co-incubation with 10 μg/mL oligo- and poly-saccharides. The bar chart represents the % cytoplasmic TNF-α expressed by monocytes following 4 h of incubation time, where *** indicates the p value <0.001 (B).

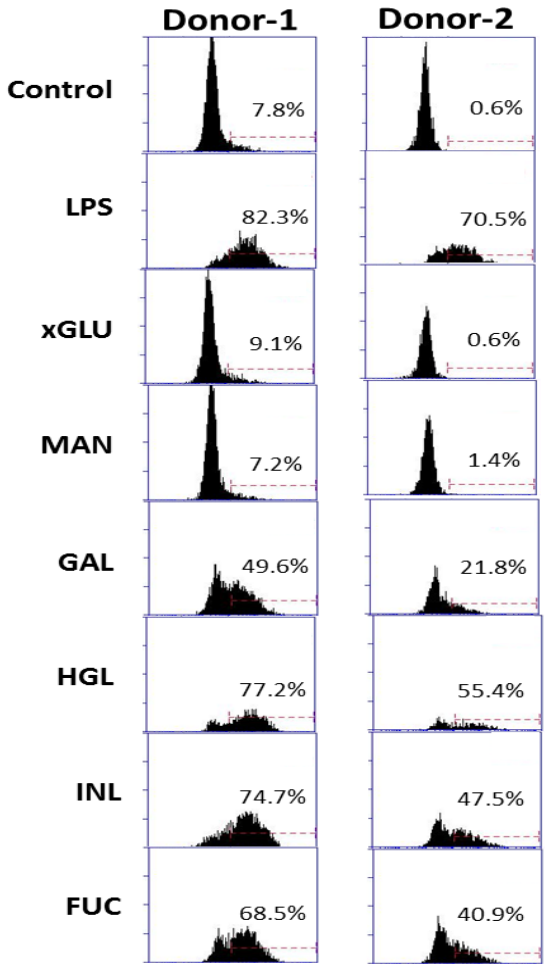

Figure 3.14. Intracellular TNF-α expression by monocytes in HWBC in response to co-incubation with 10 μg/mL oligo- and poly-saccharides or LPS for 6 h. Results expressed for individual donors (n=2) as percentage (%) of monocytes that express TNF-α comparing with total monocytes in HWBC

3.4. Discussion

As structural variations influence biological activity, the characterisation of the test panel for apparent Mr and biochemical properties revealed more specific details about the poly- and oligo-saccharides employed in this study which can facilitate better comparison with future studies and better correlation of biological activity with defined chemical properties and structures, e.g. charge and Mr.

The objective of this study was to assess the immunomodulatory properties of naturally derived poly- and oligo-saccharides in two model systems, THP-1 cells and HWBC. While cell lines can elucidate mechanisms and can be a good choice to identify specific molecular pathways, they cannot completely predict clinical efficacy due to the lack of coherent complex and multi-functional cells. In contrast, HWBC is a heterogeneous population of blood cells and other soluble mediators in the plasma. HWBC cannot confirm any specific triggered pathway on any stimulus due to the involvement of various cell types in the culture but it can account for individual donor variations and mimic human *in vivo* conditions. In addition, HWBC provide the most relevant physiological conditions and components essential for the stimulation of both innate and adaptive immunity (Brookes et al., 2014). HWBC also provides more compatible approach for screening and monitoring of drugs during clinical trials (Hanekom et al., 2004).

Upon incubation of LPS and the panel of poly- and oligo-saccharides, HWBC was more responsive than THP-1 cells as reflected by higher concentrations of pro-inflammatory cytokines and chemokines in the supernatant. LPS (also known as endotoxin) is the principal component of the outer membrane of gram-negative bacteria. It participates in the initiation of the septic syndrome that occur in gram-negative infections (Bosshart and Heinzelmann, 2007).

Individual variations between the responses in the HWBC model from three healthy donors were observed, but the concentration trends of cytokines and chemokines over time were similar. The most responsive poly- and oligo-saccharides were INL and HGL for cytokine and chemokine expression, respectively, in the HWBC model.

In the present study, INL, a type of fructan, showed the highest secretion concentrations for all the inflammatory cytokines (IL-1β, IL-6 and TNF-α). In addition to its role in triggering inflammatory activities through activating inflammasomes, INL also showed substantial time-dependent secretions for all of the studied chemokines, which indicated that INL might also have a potential role in the recruitment of immune cells to the site of inflammation. Fructans with β-(2→1)-linkages, irrespective of different chain lengths, activate the inflammatory cascades and initiate signalling cascades (Vogt et al., 2013). They bind to Toll-like receptor-2 (TLR-2) and partly to TLR-4, -5, -7, -8, and also have good binding affinity with the nucleotide-binding oligomerisation domain-containing proteins (NODs) (Vogt et al., 2014). Similarly, treatment with HGL resulted in the highest secretions of all studied chemokines (IL-8, MCP-1 and MIP-1α) and may indicate a role of this polysaccharide in the recruitment of immune cells. Additionally, HGL resulted in considerable production of the pro-inflammatory cytokines. This indicated that HGL might trigger the inflammatory cascades by cytokine-mediated immune pathways.

FUC was a second major stimulant for cytokine expression and both INL and FUC stimulated chemokine expression in HWBC. THP-1 cells were not responsive for cytokine and chemokine secretions when incubated with test compounds except HGL that stimulated the THP-1 cells to secrete chemokines to a detectable range. FUC extracted from *Ascophyllum nodosum* is a highly sulfated fucoidan which has been used as an anticoagulant (Pomin et al., 2005). In contrast to the known anti-inflammatory effects of FUC (Lee et al., 2012), the present study demonstrated the pro-inflammatory effects of FUC on HWBC and THP-1 cells. The opposite immunomodulatory properties of FUC can be attributed to its structural differences depending on the sources and the method of extraction and also the test model system as reported earlier by various groups (Raghavendran et al., 2011, Jang et al., 2014). Both FUC and HGL have varying degrees of sulfation that may be responsible for their ability to induce cytokine production. Varying the sulfation on FUC has emphasized its anti-tumour and anti-angiogenic properties (Koyanagi et al., 2003). Sulfated poly-saccharides have been exclusively studied for their physiological and biological activities, including anticoagulant, anti-viral, anti-tumour, and anti-inflammatory and antioxidant effects (Wijesinghe and Jeon, 2012, Siqueira et al., 2011, Dore et al., 2013).

GAL is a major constituent of pectins and is present in the cell walls of some aquatic monocots such as *Zostera marina*. The immunomodulatory properties of pectins depend on the D-GalA content (Popov and Ovodov, 2013) and GAL used in the present study had 62% D-GalA and an $[\rightarrow 4)$-α-D-GalA-$(1\rightarrow]_n$ backbone which presumably induced the secretion of pro-inflammatory cytokines and chemokines.

INL, HGL, FUC and GAL also had significant effects on the expression of the iTNF-α at 6 h in HWBC and the results were comparable to the TNF-α profiles at 6 h in supernatants of HWBC. Overall, INL, HGL, FUC and GAL also had significant effects on iTNF-α expression in HWBC monocytes and the results were comparable to the secreted TNF-α profiles at 6 h of HWBC, which was not surprising considering that monocytes were the main cell sub-population, which expressed TNF-α in HWBC. HGL was the most stimulatory compound for the secretion of both iTNF-α and secreted TNF-α followed by INL. Interestingly, there were high SD values between donors for the HWBC assays, notwithstanding the similar number of monocytes present between donors, but this may be due to the variability of monocyte activation state between individuals. HGL also had little effect on the concentration of the secreted TNF-α in the THP-1 cells, despite the approximately 55 times less monocytes assayed in HWBC compared to THP-1 cells (1.8 x 104 compared to 1 x 106 cells per mL, respectively). Different compositions of the cell line medias can contribute to alterations of the immune responses.

MAN and xGLU did not show any effect on cytokine and chemokine secretion profiles either in HWBC or THP-1. Following incubation for 6 h with these test compounds, there was no difference in iTNF-α expression by HWBC or THP-1 cells. Thus, four (INL, FUC, HGL and GAL) out of the six studied poly- and oligo-saccharides have pro-inflammatory properties that can be explored further in boosting patient immunity. These four compounds have different structures but similar effects on the secretion of pro inflammatory cytokines and chemokines in HWBC but minimal effects on THP-1 cells. This may indicate a common mode of action by heterogeneous population of all blood cells in HWBC. The concentration range of the secreted chemokines and cytokines in HWBC is also much higher

compared to THP-1 cells. INL and HGL had the greatest effect on the secretion of cytokines and chemokines, respectively, followed by FUC and GAL. THP-1 cells had relatively very low responses upon the incubation of the oligo and poly-saccharides except HGL, which on incubation with THP-1 cells secreted a detectable range of chemokines. INL has been also used as potent humoral and cellular immune adjuvant and is effective at boosting cellular immune responses without the toxicity exhibited by other adjuvants (Petrovsky and Aguilar, 2004). Macrophages have glucan and mannan receptors, activation of which stimulates phagocytosis and cytokine secretion. To further investigate the mechanism of immunostimualtion by these nautral polysaccharides, the ligands on immune cells can be further investigated.

The genetic background and immune status differences between *in vivo* animal models and humans have led to the failure of many drugs in human trials (Mestas and Hughes, 2004). Side effects and unforeseen complications such as the Tegenero disaster have also been reported, where immunomodulatory anti-CD28 monoclonal antibody (mAb) (TGN1412) triggered an immediate systemic inflammatory response and a serious adverse event referred to as a "cytokine storm" during first clinical trials (Suntharalingam et al., 2006). Differences in dose administration for the *in vivo* studies and missing homology between the preclinical studies in primates and man led to the failure of CD28 in phase I clinical trials. Screening of drugs/compounds *ex vivo* using HWBC can provide more information about the cytokine and chemokine profiles of humans and the differences in the distribution of immune cells in rodents and humans makes *ex vivo* screening important before human clinical trials.

The relative insensitivity of the THP-1 cells compared to HWBC in response to both LPS and the test panel, despite the dramatically lower number of monocytes assayed in HWBC compared to THP-1 cells, indicated that HWBC could be a model that is more predictive of the in vivo situation. One possibility that could account for the insensitivity of THP-1 cells is that they have been in culture for decades and could have lost some of the components involved in intracellular signalling. Another possibility is that THP-1 cells do not represent genuine resting monocytes. Monocytes are produced in the bone marrow and migrate into tissues where they rapidly differentiate. Therefore, blood monocytes are primed to differentiate and

produce cytokines. THP-1 cells are an established myelomonocytic cell line and perhaps do not represent the equivalent blood monocyte. That THP-1 cells are less sensitive than monocytes clearly have important implications for testing potential drugs for their immunomodulatory ability, in that false negative results would be obtained using THP-1 cells.

In conclusion, we suggest that HWBC is a better model than THP-1 cells to test compounds for their immunomodulatory ability. We also present INL and HGL as potentially effective immunomodulatory therapeutics.

3.5. References

AGARWAL, S., PIESCO, N., JOHNS, L. & RICCELLI, A. 1995. Differential Expression of IL-1β, TNF-α, IL-6, and IL-8 in Human Monocytes in Response to Lipopolysaccharides from Different Microbes. *Journal of dental research,* 74, 1057-1065.

AZIS, B., CHIN, B., DEACON, M., HARDING, S. & PAVLOV, G. 1999. Size and shape of inulin in dimethyl sulphoxide solution. *Carbohydrate Polymers,* 38, 231-234.

BASCONES-MARTINEZ, A., MATTILA, R., GOMEZ-FONT, R. & MEURMAN, J. H. 2014. Immunomodulatory drugs: Oral and systemic adverse effects. *Medicina oral, patologia oral y cirugia bucal,* 19, e24.

BOSSHART, H. & HEINZELMANN, M. 2007. Targeting Bacterial Endotoxin. *Annals of the New York Academy of Sciences,* 1096, 1-17.

BROOKES, R. H., HAKIMI, J., HA, Y., ABOUTORABIAN, S., AUSAR, S. F., HASIJA, M., SMITH, S. G., TODRYK, S. M., DOCKRELL, H. M. & RAHMAN, N. 2014. Screening vaccine formulations for biological activity using fresh human whole blood. *Human vaccines & immunotherapeutics,* 10, 1129-1135.

CAMPOS, J. M., MONTENEGRO STAMFORD, T. N. L. C., SARUBBO, L. A., DE LUNA, J. M., RUFINO, R. D. & BANAT, I. M. 2013. Microbial biosurfactants as additives for food industries. *Biotechnology progress,* 29, 1097-1108.

CHANPUT, W., MES, J., VREEBURG, R. A., SAVELKOUL, H. F. & WICHERS, H. J. 2010. Transcription profiles of LPS-stimulated THP-1 monocytes and macrophages: a tool to study inflammation modulating effects of food-derived compounds. *Food & Function,* 1, 254-261.

CHANPUT, W., MES, J. J. & WICHERS, H. J. 2014. THP-1 cell line: An in vitro cell model for immune modulation approach. *International immunopharmacology,* 23, 37-45.

CHLUBNOVA, ILONA, SYLLA, B., NUGIER-CHAUVIN, C., DANIELLOU, R., LEGENTIL, L., KRALOVA, B. & FERRIARES, V. 2011. Natural glycans and glycoconjugates as immunomodulating agents. *Natural Product Reports,* 28, 937-952.

DE GROOTE, D., ZANGERLE, P.-F. S., GEVAERT, Y., FASSOTTE, M.-F., BEGUIN, Y., NOIZAT-PIRENNE, F., PIRENNE, J., GATHY, R. E., LOPEZ, M. & DEHART, I. 1992. Direct stimulation of cytokines (IL-1 beta, TNF-alpha, IL-6, IL-2, IFN-gamma and GM-CSF) in whole blood. I. Comparison with isolated PBMC stimulation. *Cytokine,* 4, 239-248.

DORE, C. M. P. G., ALVES, M. G. D. C. F., WILL, L. S. E. P. R., COSTA, T. G., SABRY, D. A., DE SOUZA RÊGO, L. A. R., ACCARDO, C. M., ROCHA, H. A. O., FILGUEIRA, L. G. A. & LEITE, E. L. 2013. A sulfated polysaccharide, fucans, isolated from brown algae Sargassum vulgare with anticoagulant, antithrombotic, antioxidant and anti-inflammatory effects. *Carbohydrate Polymers,* 91, 467-475.

FEDOROV, S. N., ERMAKOVA, S. P., ZVYAGINTSEVA, T. N. & STONIK, V. A. 2013. Anticancer and cancer preventive properties of marine polysaccharides: some results and prospects. *Marine drugs,* 11, 4876-4901.

HANEKOM, W. A., HUGHES, J., MAVINKURVE, M., MENDILLO, M., WATKINS, M., GAMIELDIEN, H., GELDERBLOEM, S. J., SIDIBANA, M., MANSOOR, N. & DAVIDS, V. 2004. Novel application of a whole blood intracellular cytokine detection assay to quantitate specific T-cell frequency in field studies. *Journal of immunological methods,* 291, 185-195.

HIRSIGER, S., SIMMEN, H.-P., WERNER, C. M. M., WANNER, G. A. & RITTIRSCH, D. 2012. Danger signals activating the immune response after trauma. *Mediators of inflammation,* 2012.

ISLAM, N., WHITEHOUSE, M., MEHENDALE, S., HALL, M., TIERNEY, J., O'CONNELL, E., BLOM, A., BANNISTER, G., HINDE, J. & CEREDIG, R. 2014. Post-traumatic immunosuppression is reversed by anti-coagulated salvaged blood transfusion: deductions from studying immune status after knee arthroplasty. *Clinical & Experimental Immunology,* 177, 509-520.

JANG, J.-Y., MOON, S.-Y. & JOO, H.-G. 2014. Differential effects of fucoidans with low and high molecular weight on the viability and function of spleen cells. *Food and Chemical Toxicology,* 68, 234-238.

KILCOYNE, M., GERLACH, J. Q., FARRELL, M. P., BHAVANANDAN, V. P. & JOSHI, L. 2011. Periodic acid-Schiff's reagent assay for carbohydrates in a microtitre plate format. *Analytical biochemistry,* 416, 18-26.

KOYANAGI, S., TANIGAWA, N., NAKAGAWA, H., SOEDA, S. & SHIMENO, H. 2003. Oversulfation of fucoidan enhances its anti-angiogenic and antitumor activities. *Biochemical pharmacology,* 65, 173-179.

LEE, S.-H., KO, C.-I., AHN, G., YOU, S., KIM, J.-S., HEU, M. S., KIM, J., JEE, Y. & JEON, Y.-J. 2012. Molecular characteristics and anti-inflammatory activity of the fucoidan extracted from Ecklonia cava. *Carbohydrate Polymers,* 89, 599-606.

MATHIAK, G., KABIR, K., GRASS, G., KELLER, H., STEINRINGER, E., MINOR, T., RANGGER, C. & NEVILLE, L. F. 2003. Lipopolysaccharides from different bacterial sources elicit disparate cytokine responses in whole blood assays. *International journal of molecular medicine,* 11, 41-44.

MESTAS, J. & HUGHES, C. C. 2004. Of mice and not men: differences between mouse and human immunology. *The Journal of Immunology,* 172, 2731-2738.

NERGARD, C. S., MATSUMOTO, T., INNGJERDINGEN, M., INNGJERDINGEN, K., HOKPUTSA, S., HARDING, S. E., MICHAELSEN, T. E., DIALLO, D., KIYOHARA, H. & PAULSEN, B. S. 2005. Structural and immunological studies of a pectin and a pectic arabinogalactan from Vernonia kotschyana Sch. Bip. ex Walp.(Asteraceae). *Carbohydrate research,* 340, 115-130.

PAUL, F., MORIN, A. & MONSAN, P. 1986. Microbial polysaccharides with actual potential industrial applications. *Biotechnology advances,* 4, 245-259.

PETROVSKY, N. & AGUILAR, J. C. 2004. Vaccine adjuvants: current state and future trends. *Immunology and cell biology,* 82**,** 488-496.

POMIN, V. H., PEREIRA, M. S., VALENTE, A.-P., TOLLEFSEN, D. M., PAVÃO, M. S. & MOURÃO, P. A. 2005. Selective cleavage and anticoagulant activity of a sulfated fucan: stereospecific removal of a 2-sulfate ester from the polysaccharide by mild acid hydrolysis, preparation of oligosaccharides, and heparin cofactor II-dependent anticoagulant activity. *Glycobiology,* 15, 369-381.

POPOV, S. & OVODOV, Y. S. 2013. Polypotency of the immunomodulatory effect of pectins. *Biochemistry (Moscow),* 78, 823-835.

PRUSSIN, C. 1996. Cytokine flow cytometry: Assessing cytokine production at the single cell level. *Clinical Immunology Newsletter,* 16, 85-91.

QIN, Z. 2012. The use of THP-1 cells as a model for mimicking the function and regulation of monocytes and macrophages in the vasculature. *Atherosclerosis,* 221, 2-11.

RAGHAVENDRAN, H. R. B., SRINIVASAN, P. & REKHA, S. 2011. Immunomodulatory activity of fucoidan against aspirin-induced gastric mucosal damage in rats. *International immunopharmacology,* 11, 157-163.

RAMAN, K., MENCIO, C., DESAI, U. R. & KUBERAN, B. 2013. Sulfation patterns determine cellular internalization of heparin-like polysaccharides. *Molecular pharmaceutics,* 10, 1442-1449.

RICE, J. 2012. Animal models: Not close enough. *Nature,* 484, S9-S9.

SCHEPETKIN, I. A. & QUINN, M. T. 2006. Botanical polysaccharides: macrophage immunomodulation and therapeutic potential. *International immunopharmacology,* 6, 317-333.

SCHWENDE, H., FITZKE, E., AMBS, P. & DIETER, P. 1996. Differences in the state of differentiation of THP-1 cells induced by phorbol ester and 1, 25-dihydroxyvitamin D3. *Journal of leukocyte biology,* 59, 555-561.

SEWELL, W. C., NORTH, M. E., WEBSTER, A. D. B. & FARRANT, J. 1997. Determination of intracellular cytokines by flow-cytometry following whole-blood culture. *Journal of immunological methods,* 209, 67-74.

SIQUEIRA, R. M. C., DA SILVA, M. S., DE ALENCAR, D. B., PIRES, A. D. F., DE ALENCAR, N. M., PEREIRA, M. G., CAVADA, B. S., SAMPAIO, A. H., FARIAS, W. R. & ASSREUY, A. M. S. 2011. In vivo anti-inflammatory effect of a sulfated polysaccharide isolated from the marine brown algae Lobophora variegata. *Pharmaceutical Biology,* 49, 167-174.

SMIDERLE, F. R., RUTHES, A. C., VAN ARKEL, J., CHANPUT, W., IACOMINI, M., WICHERS, H. J. & VAN GRIENSVEN, L. J. 2011. Polysaccharides from Agaricus bisporus and Agaricus brasiliensis show similarities in their structures and their immunomodulatory effects on human monocytic THP-1 cells. *BMC complementary and alternative medicine,* 11, 58.

SUNTHARALINGAM, G., PERRY, M. R., WARD, S., BRETT, S. J., CASTELLO-CORTES, A., BRUNNER, M. D. & PANOSKALTSIS, N. 2006. Cytokine storm in a phase 1 trial of the anti-CD28 monoclonal antibody TGN1412. *New England Journal of Medicine,* 355, 1018-1028.

TIWARI, P., PANTHARI, P., KATARE, D. P. & KHARKWAL, H. 2014. Natural polymers in drug delivery. *World Journal of Pharmacy and Pharmaceutical Sciences,* 3, 1395-1409.

TSUCHIYA, S., YAMABE, M., YAMAGUCHI, Y., KOBAYASHI, Y., KONNO, T. & TADA, K. 1980. Establishment and characterization of a human acute monocytic leukemia cell line (THP,Äê1). *International journal of cancer,* 26, 171-176.

VOGT, L., RAMASAMY, U., MEYER, D., PULLENS, G., VENEMA, K., FAAS, M. M., SCHOLS, H. A. & DE VOS, P. 2013. Immune modulation by different types of beta 2→1-fructans is toll-like receptor dependent. *PloS one,* 8, e68367.

VOGT, L. M., MEYER, D., PULLENS, G., FAAS, M. M., VENEMA, K., RAMASAMY, U., SCHOLS, H. A. & DE VOS, P. 2014. Toll-like receptor 2 activation by β2→1-fructans protects barrier function of T84 human intestinal epithelial cells in a chain length-dependent manner. *The Journal of nutrition*, jn. 114.191643.

WARDI, A. H. & MICHOS, G. A. 1972. Alcian blue staining of glycoproteins in acrylamide disc electrophoresis. *Analytical biochemistry,* 49, 607-609.

WHITEMAN, P. 1973. The quantitative determination of glycosaminoglycans in urine with Alcian Blue 8GX. *Biochem. J,* 131, 351-357.

WIJESEKARA, I., PANGESTUTI, R. & KIM, S.-K. 2011. Biological activities and potential health benefits of sulfated polysaccharides derived from marine algae. *Carbohydrate Polymers,* 84, 14-21.

WIJESINGHE, W. & JEON, Y.-J. 2012. Biological activities and potential industrial applications of fucose rich sulfated polysaccharides and fucoidans isolated from brown seaweeds: A review. *Carbohydrate Polymers,* 88, 13-20.

YAQOOB, P., NEWSHOLME, E. A. & CALDER, P. C. 1999. Comparison of cytokine production in cultures of whole human blood and purified mononuclear cells. *Cytokine,* 11, 600-605.

ZACHARIUS, R. M., ZELL, T. E., MORRISON, J. H. & WOODLOCK, J. J. 1969. Glycoprotein staining following electrophoresis on acrylamide gels. *Analytical biochemistry,* 30, 148-152.

ZHANG, Z., TILL, S., JIANG, C., KNAPPE, S., REUTTERER, S., SCHEIFLINGER, F., SZABO, C. M. & DOCKAL, M. 2014. Structure-activity relationship of the pro-and anticoagulant effects of Fucus vesiculosus fucoidan. *Thromb Haemost,* 111, 429-437.

ZHANG, Z., TILL, S., KNAPPE, S., QUINN, C., CATARELLO, J., RAY, G. J., SCHEIFLINGER, F., SZABO, C. M. & DOCKAL, M. 2015. Screening of complex fucoidans from four brown algae species as procoagulant agents. *Carbohydrate Polymers,* 115, 677-685.

CHAPTER 4

PROTEOMIC AND GLYCOMIC ANALYSES OF EXTRACELLULAR MATRIX SECRETED BY MS-5 CELLS

4.1. Introduction

Stem cells are capable of self-renewal and multi-lineage differentiation potential. These features of stem cells make them invaluable tools in cell based therapies and regenerative medicine. They also exhibit stable division in culture that makes them ideal targets for *in vitro* manipulation. The growth of pluripotent stem cells in *in vitro* conditions needs an optimal balance of biochemical signals for their survival, proliferation, and self-renewal. There are different approaches for culturing stem cells such as with feeder cells or feeder cell free environments used in laboratories to maintain the survival and undifferentiated state of adult stem. The undifferentiated stem cells can be used in transplantation-based therapies.

4.1.1 Feeder cells

Feeder cells are growth arrested adherent cells that provide a sticky surface for stem cells to attach and secrete nutrients into the culture medium for stem cells to maintain their undifferentiated state. Feeder cells are prevented from overgrowing themselves either by gamma irradiation or by treatment with mitomycin C so that they maintain non-multiplying state but stay metabolically active. The metabolically active feeder cells provide active signals or express specific ligands necessary for the stem cells cultured over them.

Human embryonic stem cells (hESCs), like all other cells in the body, attach to the ECM produced by feeder cells or attach directly to feeder cells in order to survive, proliferate, migrate and differentiate or stay in an undifferentiated state. The first hESCs were cultured on mitotically inactivated mouse embryonic fibroblasts (mEF) (Thomson et al., 1998). mEFs can be used optimally between passages 3 to 6, after which they begin to senesce and lose their capacity to support the hESCs grown over them. The advantage of mEFs is that they provide a consistent source of feeder cells. Some of the successfully used feeder cells lines are the immortalised mEF cell line, Sertoli and SIM mouse embryo-derived thioguanine- and ouabain-resistant (STO). Whether human feeder cells or other mammalian cell lines are used to support the undifferentiated state of hESCs, there are differences in the way they support these cells. The difference in composition of ECM secreted by feeder cells and the environmental conditions in which feeder cells are cultured lead to variations in self-

renewal and differentiation capacities of the hESCs growing on feeder cells. Some of the issues can be solved by the feeder-free cultures in the form of soluble factor enriched secretome or the ECM secreted by feeder cells.

4.1.2. Feeder-free cultures

The possible future use of hESCs in the clinical and industrial arenas could potentially be expanded with a reproducible, well-defined, and animal-free culture system. There has been progress in the development of substitutes for serum and for feeder layers, such as culturing cells in serum-free culture conditions (Amit et al., 2000), maintenance of the cells in an undifferentiated state on commercial Matrigel® matrix with 100% mEF conditioned medium (Xu et al., 2001) and substituting the use of mouse feeder cells with human cells.

4.1.2.1. Secretome

Secretome or conditioned media is a term used to define the complete set of secreted proteins by any cell including feeder cells. Secreted proteins, such as numerous enzymes, growth factors, cytokines and hormones or other soluble mediators, control and regulate different biological and physiological properties and provide a niche to the overlaying stem cells (Lim and Bodnar, 2002). The communication between the feeder free cultures and stem cells is attained by these secreted factors from the feeder cells that also contribute towards the stem cell fate decisions (Kaur-Bollinger et al., 2012). Thus conditioned media contains all the nutrients and metabolites important for culturing hESCs. Several different conditioned medium compositions have been tested for their ability to sustain undifferentiated hESC, for example 20% FBS for STO cells. The use of conditioned media has been of great value in establishing the feeder cell-free culture of hESCs, but several novel methods have been developed recently to use more defined media to support culture of hESCs without feeders and, in some cases, without Matrigel®

4.1.2.2. ECM

ECM is a complex network of secreted macromolecules that interact with the microenvironment. It was once considered as an inert supportive scaffold for packing purposes of material but now the role of ECM is also well established in controlling

the cell behaviour. It consists of structural and functional macromolecules such as PGs, fibrous proteins and glycoproteins. Collagens are the most abundant proteins in mammal in ECM (Ricard-Blum, 2011). The organisation and the distribution of ECM are dependent on the tissue type. The interaction between cells and the matrix occurs via specialised matrix molecules and corresponding receptor molecules on the attached cells. Glycoproteins with RGD domain (including OPN, studied in chapter 2) are recognised by the integrins and mediates the cell adhesion. The carbohydrates present on the cells further mediate the cell adhesion and, growth and cell spreading upon binding to the carbohydrate binding proteins; lectins. It participates in physiological roles such as providing the nutrients to cells, acts as a reservoir for physiological mediators and help in mediating cellular function through interaction with cell surface receptors (Bosnakovski et al., 2006). However, it is difficult to elucidate the key interactions between cells and matrix because even most ECM proteins have multiple structural domains that can engage with a variety of cell-surface receptors. ECM initiates crucial biochemical and biomechanical signals required for tissue morphogenesis, differentiation and homeostasis (Frantz et al., 2010). Hence, the ECM plays an important role in determining the interaction of cells with their microenvironment via cell signalling. It consists of complex mesh of proteins which together promote cell recruitment, adhesion, migration, proliferation and differentiation (Bourgine et al., 2013).

There is evidence suggesting the role of growth factors and cytokines as inducers and mediators of stem cell differentiation, however, little is known regarding the influence of ECM on cell differentiation [63]. To understand the importance of ECM, different feeder-free systems acting as ECM for culturing hESC have been established. The first feeder free cultures used were Matrigel®, laminin-coating and mEF conditioned media (Xu et al., 2001). Matrigel® is a basement membrane matrix, rich in types I and IV collagens, laminin, entactin, heparan sulfate proteoglycan, matrix metalloproteinases, undefined growth factors, and chemical compounds (Kleinman et al., 1982). MEFs provide substrate for the stem cells to attach and grow and assist in maintaining their pluripotency. A desired feeder free culture therefor must have suitable substrate as well as soluble growth factors. It is also known that the growth conditions such as gradient of oxygen concentration can affect the structural composition of ECM produced by feeder cells.

4.1.2. MS-5 cells

MS-5 cells are a continuously growing clone of mouse mesenchymal stromal cells (MSC). They were derived from Dexter-type murine long-term marrow culture, which supports colony forming unit-spleen (CFU-S) maintenance (Dexter et al., 1977). They act synergistically with human growth factors to stimulate the formation of blast colonies and macroscopic colonies from $CD34^{+}CD38^{-}$ primitive progenitors in short-term methylcellulose assays (Breems et al., 1998, Issaad et al., 1993). They have been extensively used as a model of MSC because their proteome is enriched in pro-angiogenic factors and supportive of overlying HSC and progenitor cell survival and differentiation. MS-5 cells support human haematopoiesis (Bennaceur-Griscelli et al., 2001) and human blood vessel development. They play important roles in maintaining the endothelial component of the HSC niche and regulating the fate of HSC/HPC.

MS-5 cells produce ECM, which make them a suitable candidate for studying the ECM compositional differences when they are cultured in different environmental conditions. It has been suggested that the haematopoietic niche is hypoxic and the limited oxygen concentration maintain stem cell characteristic for longer and increases cell proliferation and colony forming potential. (Saller et al., 2012). The effect of hypoxic conditions on differentiation of MS-5 and other continuously growing mouse MSC lines (Prado-Lopez et al., 2014) and the DNA damage response of MS-5 (Sugrue et al., 2014) has been investigated. Gene expression experiments suggest that MSC cultured on ECM in hypoxia retained elevated levels of certain stem cell genes (Prado-Lopez et al., 2014).

4.1.3. Oxygen concentration

The concentration of oxygen (O_2) is an important factor that affects stem cell behaviour *in vivo* and *in vitro*. O_2 content under which ECM is prepared *in vitro* can change the differentiation fate of cells cultured on top of feeder cells (Tiwari et al., 2013). Oxygen tension in the bone marrow is about 2-7%, with highest O_2 concentration near the sinusoids, which are small blood capillaries lined by endothelial cells. It has been shown that the cultures maintained in atmospheric O_2 of 21% has poorer growth compared to cultures in low (5%) O_2 concentrations. Stem cells located closer to sinusoids are exposed to higher O_2 concentrations and various

factors carried in the blood, and are more likely to undergo differentiation (Nodwell et al., 2005). ECM is important component for hematopoietic niche and any changes in the ECM compostion, if prepared under the varying oxygen concentration lead to the different stem cell properties

4.1.4. Aim of the study

With an aim to maintain stem cell cultures in the undifferentiated state for long time, many different approaches have been used such as addition of such as activator or inhibitor in pluripotency related signaling pathway, regulation of cell culturing environment like culture on feeder cell layer, use of feeder cell conditioned medium and hypoxia during short time (Grayson et al., 2007). Culturing of feeder cells under hypoxic compared to normoxic conditions have been demonstrated to contribute towards the better survival and expansion of stem cells by expression of adhesion molecules and the secretion of ECM (Prado-Lopez et al., 2014, Tiwari et al., 2013).

In order to gain knowledge about the compositional proteomic and glycomic differences between the ECM prepared under hypoxic and normoxic conditions, a proteomic study of the ECM secreted by MS-5 cells was undertaken. Proteomic analysis can further provide an insight into the proteome and glycome involved in adhesion, angiogenesis and activation pathways to maintain cellular functions. MS analysis of ECM prepared by MS-5 cells under normoxia (21% O_2) and hypoxia (5% O_2) was performed. The aim of this research was to better understand compositional changes of MS-5 ECM produced under the two conditions with emphasis on the changes in the glycosylation profile under hypoxic compared to normoxic conditions. The long-term goal of these studies is to identify ECM molecules that signal MS-5 cells to retain their stemness.

4.2. Material and methods

4.2.1. Materials

T-75 cm^2 flask, pre-coated with 1% gelatine and Corning® Costar® cell culture plates (48 wells or 24 wells), and 4'6-diamidino-2-phenylindole dihydrochloride (DAPI) were from Sigma Aldrich Co. (Wicklow, Ireland). DMEM low glucose, GlutaMax and 10% FBS (DE14-801F) was from Lonza (Basel, Switzerland).

Mitomycin C was from Acros Organics (Geel, Belgium). 1% Penicillin/Streptomycin and GIBCO® Dulbecco's Phosphate-Buffered Saline (DPBS) were from Thermo Fisher Scientific Inc (Epsom, U.K.). Centricon-3 and Microcon-3 concentration units were from Millipore (Hertfordshire, U.K.). Dulbecco's modified eagle medium nutrient mixture F-12 (DMEMF-12) was from Invitrogen (Carlsbad, CA, U.S.A.). Fluorescein isothiocyanate (FITC)- or tetramethylrhodamine isothiocyanate (TRITC)-conjugated lectins and biotinylated lectins were from EY Labs. All other reagents were from Sigma-Aldrich Co. and were of the highest grade available unless otherwise noted.

4.2.2. Cell lines and cell culture

The mouse stromal cell line, MS-5, was cultured under 21% or 5% O_2 concentration in MSC media consisting of DMEMF-12, 10% FBS and Penicillin/Streptomycin. Cells (1 x 10^6) were cultured in previously optimised cell conditions with less cell death and maximisation of the ECM preparation (Prado-Lopez et al., 2014) .

4.2.3. Preparation of ECM from MS-5 cells

ECM for proteomic characterisation was prepared by buffer extraction of mMSCs using previous methods (Hedman et al., 1979, Cukierman et al., 2001, Escobedo-Lucea et al., 2012) with some modifications. In brief, the mMSCs clones, MS-5.C2 were cultured at density 25 x 10^4 cells per T-75 cm^2 flask, pre-coated with 1% gelatine under either 21% or 5% O_2. Cultures were maintained in DMEM low glucose supplemented with GlutaMAX, 10% FBS and 1% Penicillin/Streptomycin. The cells were cultured for 3 days and then treated with 10 µg/mL mitomycin C. The cells were then washed twice with DPBS and fresh media was added allowing the cell to secrete ECM for 4 days. Cells were treated with a lysis buffer (10 mM Tris, 2 mM EDTA, pH 8.0) and incubated overnight with gentle rocking at 4 ºC. The ECM was then washed five times with DPBS. This protocol was repeated twice under the same conditions and the recovered ECM was pooled.

De-cellularised ECMs were treated with 10 mM DTT in 5 M sodium guanidine for 1 h at 4ºC on an orbital shaker to remove proteins from ECMs. The matrix was collected by scraping the flask and then centrifuged for 20 min at 4,000 x *g* to

precipitate the insoluble material. The clean material was stored at -80 ºC and sent for proteomic analysis at University of Bristol Proteomics Facility, School of Medical Sciences (Bristol, U.K.).

4.2.4. LC-MS analysis

The gel lane was cut into 3 slices and each slice subjected to in-gel tryptic digestion using a ProGest automated digestion unit (Digilab U.K.). The resulting peptides were fractionated using a Dionex Ultimate 3000 nanoHPLC system in line with an LTQ-Orbitrap Velos mass spectrometer (Thermo Scientific). Peptides in 1% (v/v) formic acid were injected onto an Acclaim PepMap C18 nano-trap column (Dionex). After washing with 0.5% (v/v) acetonitrile, 0.1% (v/v) formic acid peptides were resolved on a 250 mm × 75 μm Acclaim PepMap C18 reverse phase analytical column (Dionex) over a 150 min organic gradient, using 7 gradient segments (1-6 % solvent B over 1 min, 6-15% B over 58 min, 15-32% B over 58 min., 32-40% B over 3 min, 40-90% B over 1 min, held at 90% B for 6 min and then reduced to 1% B over 1 min) with a flow rate of 300 μL/ min. Solvent A was 0.1% formic acid and Solvent B was aqueous 80% acetonitrile in 0.1% formic acid. Peptides were ionised by nano-electrospray ionization at 2.0 kV using a stainless steel emitter with an internal diameter of 30 μM (Thermo Scientific) and a capillary temperature of 250 °C. Tandem mass spectra were acquired using an LTQ- Orbitrap Velos mass spectrometer controlled by Xcalibur 2.1 software (Thermo Scientific) and operated in data-dependent acquisition mode. The Orbitrap was set to analyse the survey scans at 60,000 resolution (at m/z 400) in the mass range m/z 300 to 2000 and the top twenty multiply charged ions in each duty cycle selected for MS/MS in the LTQ linear ion trap. Charge state filtering, where unassigned precursor ions were not selected for fragmentation, and dynamic exclusion (repeat count, 1; repeat duration, 30 s; exclusion list size, 500) was used. Fragmentation conditions in the LTQ were as follows: normalized collision energy, 40%; activation q, 0.25; activation time 10 ms; and minimum ion selection intensity, 500 count.

4.2.5. Data Analysis

The raw data files were processed and quantified using Proteome Discoverer software v1.2 (Thermo Scientific) and searched against the UniProt Mouse database

(81998 entries) using the SEQUEST (Ver. 28 Rev. 13) algorithm. Peptide precursor mass tolerance was set at 10 ppm, and MS/MS tolerance was set at 0.8 Da. Search criteria included carbamidomethylation of cysteine (+57.0214 Da) as a fixed modification and oxidation of methionine as variable modifications. Searches were performed with full tryptic digestion and a maximum of 1 missed cleavage was allowed. The reverse database search option was enabled and all peptide data was filtered to satisfy false discovery rate (FDR) of 5%. The Proteome Discoverer software generates a reverse "decoy" database from the same protein database and any peptides passing the initial filtering parameters that were derived from this decoy database are defined as false positive identifications. The minimum cross-correlation factor (Xcorr) filter was readjusted for each individual charge state separately to optimally meet the predetermined target FDR of 5% based on the number of random false positive matches from the reverse decoy database. Thus each data set has its own passing parameters.

4.2.6. Bioinformatics analysis

Peptide spectral matches (PSM) values across hypoxic and normoxic conditions were normalised to determine the fold changes among them (Elias et al., 2004). PSM provides an estimate about the spectra matched to peptides from the specific protein in the database. A list of unique proteins for each condition and common proteins among all the conditions was prepared using the Unix environment. The proteins less than two peptides across all cell lines were rejected for any fold change analysis. Gene Ontology (GO) analysis was carried out for peptide list for each cell line and growth condition using Gorilla software (http://cbl-gorilla.cs.technion.ac.il/) (Eden et al., 2009). For clarity, only top-level GO terms from the Cellular Component and Biological Process domains, second level GO terms from the Molecular Function domain, and KEGG Pathway terms were considered. Furthermore, only terms with enrichment value $\geq$ 1.5, Bonferroni-corrected p-value <0.05 were considered. Wherever Gorilla software was missing the annotation, another program DAVID (https://david.ncifcrf.gov/) was used along with it (Da Wei Huang and Lempicki, 2008). This combined analysis using two programs helped to include higher protein number in the study thereby increasing the confidence of the analysis. The functions

of the proteins included in the comparative list were also studied by STRING database (http://string-db.org/).

4.2.7. Histochemistry for ECM characterisation *in situ*

The matrix was prepared as in section 4.2 but in 48 well plates format. Matrix was stained with 0.125% alcian blue solution for 30 min and washed with dH_2O for 2 min to remove excess dye. The plates were washed three times in TBS-T and imaged at 10x on Olympus IX71 inverted fluorescent microscope with CellSans software.For lectin immunochemistry, ECM prepared in the plate were fixed in 4% paraformaldehyde for 20 min. The plates were washed three times with Tris buffered saline supplemented with Ca^{2+} and Mg^{2+} ions (TBS; 20 mM Tris-HCl, 100 mM NaCl, 1 mM $CaCl_2$, 1 mM $MgCl_2$, pH 7.2) with 0.05% Triton X-100 (TBS-T) and then blocked with 2% periodate-treated BSA (Sigma-Aldrich, cat. no. A7638, ≥99%) in TBS for 1 h. The wells were washed three times in TBS and then incubated for 1 h with a panel of FITC- or TRITC-conjugated lectins at concentration of 10 μg/mL each diluted in TBS (Table 4.1.). ECM was washed five times with TBS-T and counterstained with DAPI (1:1000 dilution in TBS) for 20 min. The wells were washed three times in TBS-T and imaged at 10x on an Olympus IX71 inverted fluorescent microscope with CellSans software. Three images were taken for each well and the experiment was performed in triplicates. The images were exported to ImageJ software (National Institutes of Health, http://rsbweb.nih.gov/ij/) and quantification was performed for fluorescence intensities of the nine images for each lectin staining. The intensity/area values were recorded for each image and the average fluorescence intensity values were plotted for normoxic and hypoxic conditions. For the relative quantification of lectin staining between hypoxia and normoxia, was assigned as 100%.

Table 4.1. List of lectins used for histochemistry or lectin blots.

Abbreviation	Species	Specificity	Inhibitory sugars	TRITC	FITC	Biotin
AAA	*Anguilla anguilla*	*α*-(1→2)-, *α*-(1→3) and *α*-(1→4)-linked Fuc	Fuc			√
LTA	*Lotus tetragonolobus*	*α*-(1→3)-, *α*-(1→6)- and *α*-(1→2)-linked Fuc	Fuc	√		√
UEA-I	*Ulex europaeus*	*α*-(1→2)-linked Fuc	Fuc	√		√
BPA	*Bauhinia purpurea*	GalNAc/Gal	GalNAc			√
DSA	*Datura stramonium*	*β* –(1, 4)-GlcNAc	Chitotriose > Chitobiose > GalNAc	√		√
PNA	*Arachis hypogaea*	Gal (Gal-*β*-(1→3)-GalNAc (T-antigen) > GalNAc > Lac > Gal, terminal *β*-Gal)	Lac > D-Gal	√		
ECA	*Erythrina cristagalli*	Gal-β-(1, 4)-GlcNAc oligomers	LacNAc>Lac>GalNAc>Gal			
MPA	*Maclura pomifera*	α-Gal and GalNAc	α-D-Gal, Gal-*α*(1, 6)Gl-c	√		
GS-I-B4	*Griffonia simplicifolia*	Exclusively α-Gal				
MAA	*Maackia amurensis*	Sialic acid-α-(2→3)-GalNAc	Lac	√	√	√
SNA-I	*Sambucus nigra*	Sialic acid-*α*-(2→6)-GalNAc > Lac, GalNAc > Gal	Lac	√		√
WFA	*Wisteria floribunda*	GalNAc, GalNAc-*α*-(1→6)-Gal > GalNAc-*α*-(1→3)-GalNAc (Forsmann antigen) > GalNAc >> Lac > Gal, GlcA-*α*-(1→3)-GalNAc, chondroitin sulfate	GalNAc >> Lac> Gal	√		√
Con A	*Canavalia ensiformis*	*α*-Man > *α*-Glc > *α*-GlcNAc, complex biantennary structures	Man	√		√

4.2.8. SDS-PAGE and lectin blots for total protein extracts

The total extract from the matrix was collected and mixed with reducing loading buffer and denatured at 95 °C for 5 min. This was separated on Novex 3-8% Tris-Acetate protein gels with MES running buffer for staining proteins using silver stain kit and in NuPAGE 4-12% Bis-Tris gels using MOPS running buffer at 150 V constant for approximately 1.5 h for lectin blots. Semi-dry transfer was performed at 1.5 mA/cm^2 for 45 min. Cathode (0.3 M aminocaproic acid, 0.03 M Tris, 0.0375% SDS) and anode (0.3 M Tris, 0.1 M glycine, 0.0375% SDS) buffers facilitated the transfer of the proteins from the gel to the PVDF membrane. Membranes were blocked directly after transfer with 2% BSA in TBS-T for 2 h at room temperature. Following washing with TBS-T, membranes were incubated with 1 μg/mL dilution of biotinylated lectins in TBS (Table 4.1.) overnight at 4 °C. The blots were then washed with TBS-T 3 times for 15 min and incubated with streptavidin conjugated to HRP (stock concentration 1 mg/mL) at a dilution of 1:15,000 in TBS-T for 1 h at room temperature. The blots were detected by WesternBright™ ECL HRP substrate kit (Advansta, Menlo Park, CA, USA) as per manufacturer's instructions and imaged on a gel documentation system (Alpha Innotech Co., San Leandro, CA). In parallel, the blots were incubated with lectins each with different specificity along with their inhibitory sugars such as Gal, Lac, GalNAc, GlcNAc, Man, and Fuc at a dilution of 50 mM (Table 4.1.) in TBS-T overnight in 4 °C and treated similarly as mentioned above.

4.3. Results

MS-5 cells were cultured to secrete ECM independently in two culture conditions, hypoxia and normoxia, and LC-MS of MS-5 ECM was performed by a facility in Bristol. The experiment was carried out in duplicate. Proteins identified by LC-MS were used for (i) *in silico* analysis to study their distribution in each condition, (ii) to understand the changes occurring in the ECM under the hypoxic conditions, and (iii) to understand the impact of hypoxic and normoxic growth conditions on the glycome composition of secreted ECM.

4.3.1. Distribution of proteins in normoxia and hypoxia

The spectral count data from the LC-MS with the identification of proteins in each hypoxia and normal was used for the overall distribution of proteins. The proteins with a spectral count of 2 or more were excluded from the analysis as a data-filtering step. The LC-MS analysis of secreted ECM components of MS-5 cells grown under hypoxia led to the identification of a total of 3,341 proteins in replicate 1 and 3,277 proteins were identified in replicate 2 with an overlap of 61% and 62% in two replicates, respectively. A greater number of proteins were identified in normoxic conditions, with replicate 1 had 3,972 proteins, while replicate 2 had 3,982 proteins. An overlap of 60% of protein identity was found between normoxic and hypoxic conditions. The spectral counts values of protein, i.e. the total numbers of spectra identified for a protein, identified in both the conditions were averaged between the duplicates (Figure 4.1) for subsequent analyses.

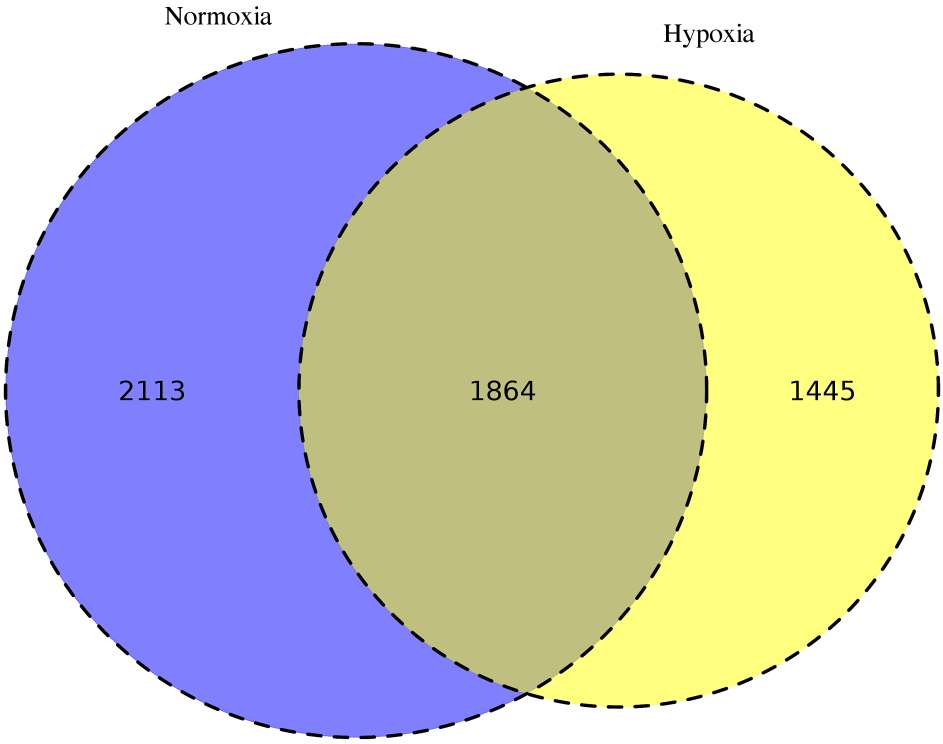

Figure 4.1. Distribution of proteins in hypoxia and normoxia for MS-5 proteomics data. Venn diagram presents the number of proteins exclusive to each condition and overlapping proteins.

4.3.2. Differentially regulated proteins

Averaged spectral counts of the identified proteins from two replicates were normalised across both conditions for calculating their fold changes across both conditions. After total intensity normalisation, the differentially expressed proteins with fold change higher than 1.2, were retrieved. The top 10 most up-regulated proteins in hypoxic versus normoxic conditions (Table 4.2) were found to be ECM components. The most up-regulated protein in this study was procollagen (fold change 5.2) followed by additional up-regulated proteins that included different types of collagens; collagen VI and IV isoforms, fibronectin, laminin, integrins, thrombospondin-1 and heparan sulfate proteoglycan (Table 4.2). This indicated that ECM composition was altered between two conditions.

The proteins translated either by glycosylation related genes or by the action of GTs were extracted from the proteins list with fold changes higher than 1.2 using the glycogene list available from the Consortium for Functional Glycomics (CFG, http://www.functionalglycomics.org/) A list of the top 10 most up-regulated glycosylation related proteins was prepared (Table 4.3). that included beta 1, 3 glucosyaltranferases (B3GLT), dolichol-phosphate mannosyltransferase (DPMI), alpha-1,3-mannosyl-glycoprotein, and 4-beta-*N*-acetylglucosaminyltransferase (MGAT4B), which participate in the biosynthesis of *N*-linked glycosylated structures and UDP-*N*-acetylglucosamine-peptide, *N*-acetylglucosaminyltransferase (OGTI) that participate in *O*-linked structures. This list contained glycosyl xylotranferases (XYLT1), mannose-1-phosphate guanyltransferase alpha (GMPPA), C-mannosyltransferase (DPY19L4) and sulfurtransferase (MPST).

Table 4.2. The most up regulated proteins of normoxia versus hypoxia.

Accession	AAs	Mr [kDa]	Calc. pI	Description	Ratio
E9Q718	758	86.8	6.89	Procollagen-lysine,2-oxoglutarate 5-dioxygenase 2 OS=Mus musculus GN=Plod2 PE=2 SV=1 - [E9Q718_MOUSE]	**5.2**
Q9Z0I9	1703	185.7	5.57	Collagen alpha3(VI) (Fragment) OS=Mus musculus GN=Col6a3 PE=2 SV=1 - [Q9Z0I9_MOUSE]	**4**
P08122	1707	167.2	8.48	Collagen alpha-2(IV) chain OS=Mus musculus GN=Col4a2 PE=2 SV=4 - [CO4A2_MOUSE]	**3.5**
Q02788	1034	110.3	6.42	Collagen alpha-2(VI) chain OS=Mus musculus GN=Col6a2 PE=2 SV=3 - [CO6A2_MOUSE]	**3.28**
P02463	1669	160.6	8.24	Collagen alpha-1(IV) chain OS=Mus musculus GN=Col4a1 PE=2 SV=4 - [CO4A1_MOUSE]	**2.6**
Q04857	1025	108.4	5.36	Collagen alpha-1(VI) chain OS=Mus musculus GN=Col6a1 PE=2 SV=1 - [CO6A1_MOUSE]	**2.5**
E9PX70	3064	333.5	5.8	Collagen alpha-1(XII) chain OS=Mus musculus GN=Col12a1 PE=2 SV=1 - [E9PX70_MOUSE]	**2**
Q00780	744	73.6	9.55	Collagen alpha-1(VIII) chain OS=Mus musculus GN=Col8a1 PE=1 SV=3 - [CO8A1_MOUSE]	**1.5**
P11276	2477	272.4	5.59	Fibronectin OS=Mus musculus GN=Fn1 PE=1 SV=4 - [FINC_MOUSE]	**1.6**
E0CXY0	540	59.1	6.55	Fibronectin type-III domain-containing protein 3A (Fragment) OS=Mus musculus GN=Fndc3a PE=2 SV=1 - [E0CXY0_MOUSE]	**2.5**
Q05793	3707	398	6.32	Basement membrane-specific heparan sulfate proteoglycan core protein OS=Mus musculus GN=Hspg2 PE=1 SV=1 - [PGBM_MOUSE]	**1.6**
B1B0C7	4375	468.7	6.48	Basement membrane-specific heparan sulfate proteoglycan core protein OS=Mus musculus GN=Hspg2 PE=2 SV=1 - [B1B0C7_MOUSE]	**1.5**
E5Q371	303	33.1	8.63	Integrin-associated protein OS=Mus musculus GN=Cd47 PE=2 SV=1 - [E5Q371_MOUSE]	**3**
P09055	798	88.2	5.94	Integrin beta-1 OS=Mus musculus GN=Itgb1 PE=1 SV=1 - [ITB1_MOUSE]	**2.7**
E9PY08	681	74.6	7.77	A disintegrin and metalloproteinase with thrombospondin motifs 1 (Fragment) OS=Mus musculus GN=Adamts1 PE=2 SV=1 - [E9PY08_MOUSE]	**2**
Q62470	1053	116.7	6.57	Integrin alpha-3 OS=Mus musculus GN=Itga3 PE=1 SV=1 - [ITA3_MOUSE]	**1.6**
Q61001	3718	403.8	6.73	Laminin subunit alpha-5 OS=Mus musculus GN=Lama5 PE=1 SV=4 - [LAMA5_MOUSE]	**2**

P02469	1786	197	4.94	Laminin subunit beta-1 OS=Mus musculus GN=Lamb1 PE=1 SV=3 - [LAMB1_MOUSE]	**1.7**
F8VQJ3	1607	177.1	5.19	Laminin subunit gamma-1 OS=Mus musculus GN=Lamc1 PE=2 SV=1 - [F8VQJ3_MOUSE]	**1.7**
P35441	1170	129.6	4.96	Thrombospondin-1 OS=Mus musculus GN=Thbs1 PE=1 SV=1 - [TSP1_MOUSE]	**2.2**
E9QNR5	1644	183.3	7.2	Thrombospondin type-1 domain-containing protein 7A OS=Mus musculus GN=Thsd7a PE=2 SV=1 - [E9QNR5_MOUSE]	**1.5**

Table 4.3. Differential expression of glycosylation related proteins and GTs in normoxia versus hypoxia.

Accession	**# AAs**	**Mr [kDa]**	**calc. pI**	**Description**
Q8BHT6	489	55.3	6.92	Beta-1,3-glucosyltransferase OS=Mus musculus GN=B3galtl PE=2 SV=3 - [B3GLT_MOUSE]
F8VPK6	953	107.2	9.29	Xylosyltransferase 1 OS=Mus musculus GN=Xylt1 PE=4 SV=1 - [F8VPK6_MOUSE]
Q59J91	607	69.5	6.4	Polypeptide N-acetylgalactosaminyltransferase 18 OS=Mus musculus GN=Galnt18 PE=2 SV=1 - [Q59J91_MOUSE]
A2AJQ2	496	57.7	8.27	Probable C-mannosyltransferase DPY19L4 (Fragment) OS=Mus musculus GN=Dpy19l4 PE=2 SV=1 - [A2AJQ2_MOUSE]
Q3UXG7	353	40	8.48	GDP-fucose protein O-fucosyltransferase 1 OS=Mus musculus GN=Pofut1 PE=2 SV=1 - [Q3UXG7_MOUSE]
O70152	260	29.2	9.51	Dolichol-phosphate mannosyltransferase OS=Mus musculus GN=Dpm1 PE=2 SV=1 - [DPM1_MOUSE]
Q812F8	548	63.3	7.88	Alpha-1,3-mannosyl-glycoprotein 4-beta-N-acetylglucosaminyltransferase B OS=Mus musculus GN=Mgat4b PE=2 SV=1 - [MGT4B_MOUSE]
Q922H4	420	46.2	7.62	Mannose-1-phosphate guanyltransferase alpha OS=Mus musculus GN=Gmppa PE=2 SV=1 - [GMPPA_MOUSE]
Q3UW66	297	33.1	6.47	Sulfurtransferase OS=Mus musculus GN=Mpst PE=2 SV=1 - [Q3UW66_MOUSE]
Q8CGY8-2	1036	115.7	6.65	Isoform 2 of UDP-N-acetylglucosamine--peptide N-acetylglucosaminyltransferase 110 kDa subunit OS=Mus musculus GN=Ogt - [OGT1_MOUSE]

4.3.3. GO analysis of identified proteins

GO provides ontologies to describe the attributes of gene products in the three non-overlapping domains of molecular biology. Proteins identified from LC-MS analysis and with fold change of 1.2 from both conditions were analysed for GO using GOrilla software (http://cbl-gorilla.cs.technion.ac.il/) and ECM constituted the major part of the Cellular Component in GO. This was followed by enrichment of intracellular component. The proteins were categorised into three groups; (i) ECM secreted proteins, (ii) cytoplasmic gene participants, and (iii) intracellular proteins. Differentially regulated proteins participated in molecular processes for secretion, migration and angiogenesis. GO component analysis results for shared proteins between hypoxia and normoxia (Figure 4.2, A), hypoxia alone (Figure 4.2, B) and normoxia alone (Figure 4.2, C) showed differences between the cellular component enrichment. Proteins with GO component including ECM and membrane bound proteins were reported with lower p-values in hypoxic than normoxic conditions. Go cellular component analysis with differences across the hypoxia and normoxia showed the effect of O_2 concentration leading to compositional differences in ECM preparation by MS-5 cells.

Differentially regulated proteins in hypoxia and normoxia were searched for GO with emphasis on ECM component. The most abundant proteins in the MS-5 cell lines were studied and the associated pathways were retrieved using KEGG database. There were 19 pathways associated with the overall up-regulated proteins including the ATP generating processes as glycolysis, tricarboxylic acid cycle, ATP synthesis and apoptosis signalling pathways (Table 4.4). This is in agreement with earlier reports that hypoxia, or indeed any kind of cell stress, affects the energy metabolism by triggering the energy synthesising pathways to overcome the nutrient shortage (Mason and Rathmell, 2011, Frezza et al., 2011). These proteins also demonstrate the continuous interaction that may be taking place between stem cells and the ECM, which are required in the adhesion, anchorage and homing of stem cells (Figure 4.3), focal adhesion (Figure 4.4) and leucocyte transendothelial migration pathway (Figure 4.5). All the proteins that were differentially regulated in the identified pathways are highlighted with red stars (Figure 4.3, 4.4 and 4.5). Differentially up-regulated proteins also participated in the signalling pathways triggered by HIF-1α activation

pathway. HIF-1α pathway is activated to maintain O_2 haemostasis and signalling events are mediated by interactions with integrins and PGs in the ECM (Cassavaugh and Lounsbury, 2011).

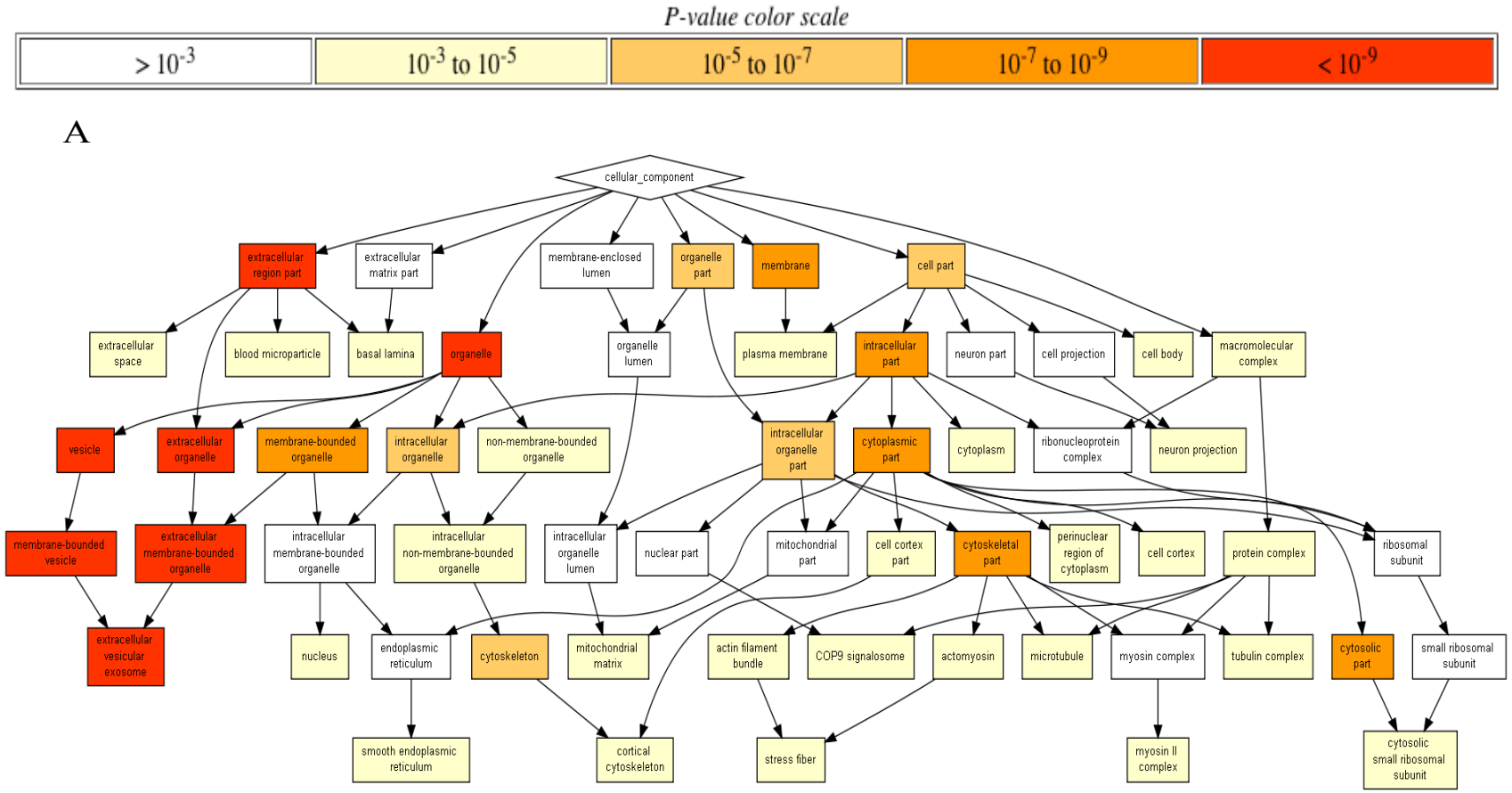

Figure 4.2 (A). GO for cellular component for MS-5 protein hypoxia versus normoxia.

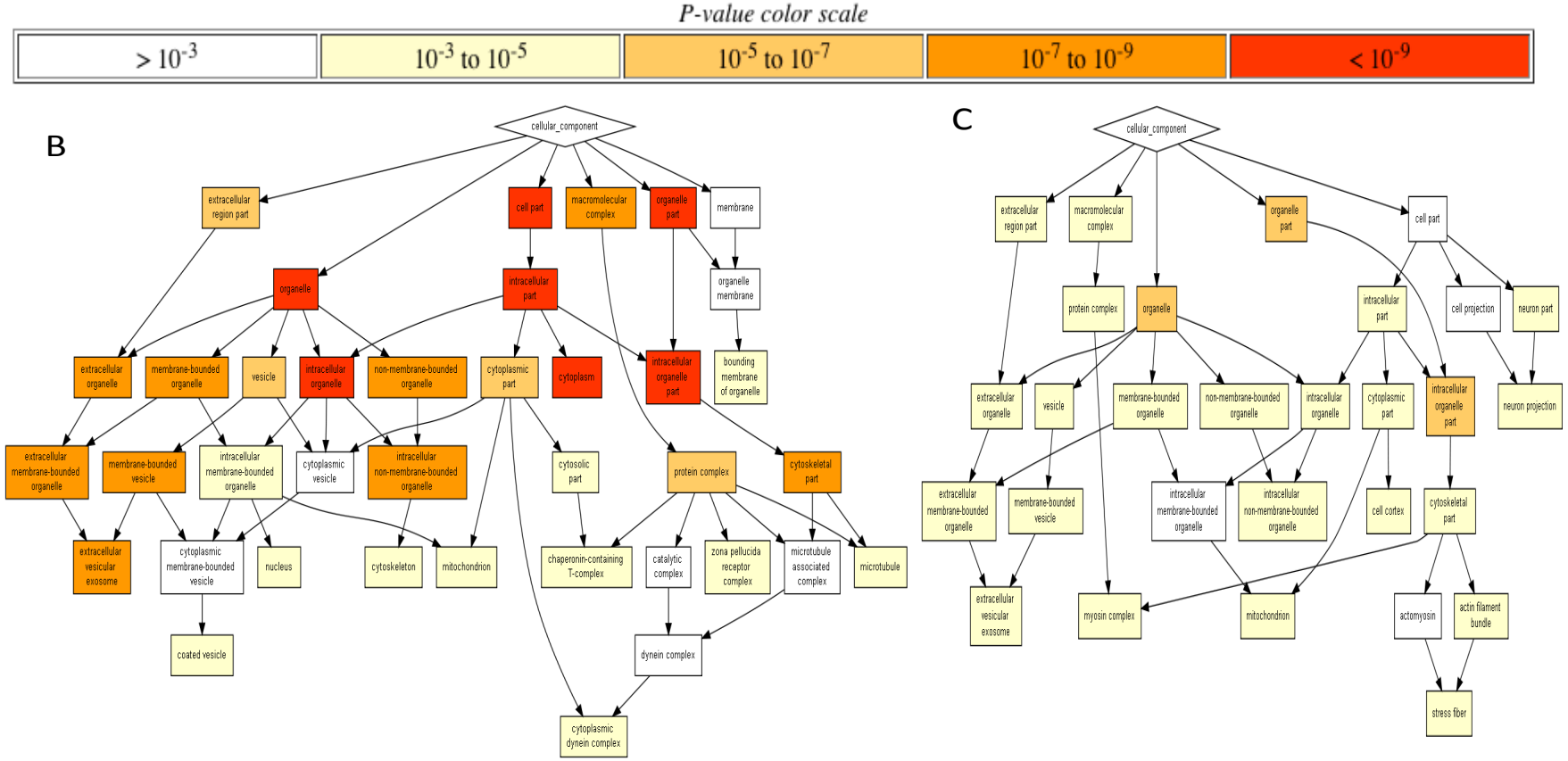

Figure 4.2. GO for cellular component for MS-5 protein hypoxia versus hypoxia only (B) and normoxia only (C)

Table 4.4. Pathways associated with differential regulated proteins in hypoxia versus normoxia.

	PATHWAYS
1	ECM receptor pathway
2	Focal adhesion pathway
3	Leukocyte trans-endothelial migration pathway
4	Apoptosis
5	ATP generating pathway (Glycolyis, TCA)
6	CCKR signalling pathway
7	Cadherin signalling pathway
8	Cytoskeleton regulation by Rho GTPase
9	Hedgehog pathway
10	Inflammation mediated by cytokine and chemokine signalling pathway
11	Integrin signalling pathway
12	Interferon gamma signalling pathway
13	Mannose metabolism
14	Nicotine acetylcholine receptor signalling pathway
15	Plasminogen activating cascade
16	Sulfate assimilation
17	P53 pathway
18	Calcium signalling pathway
19	Hypoxia response by HIF activation

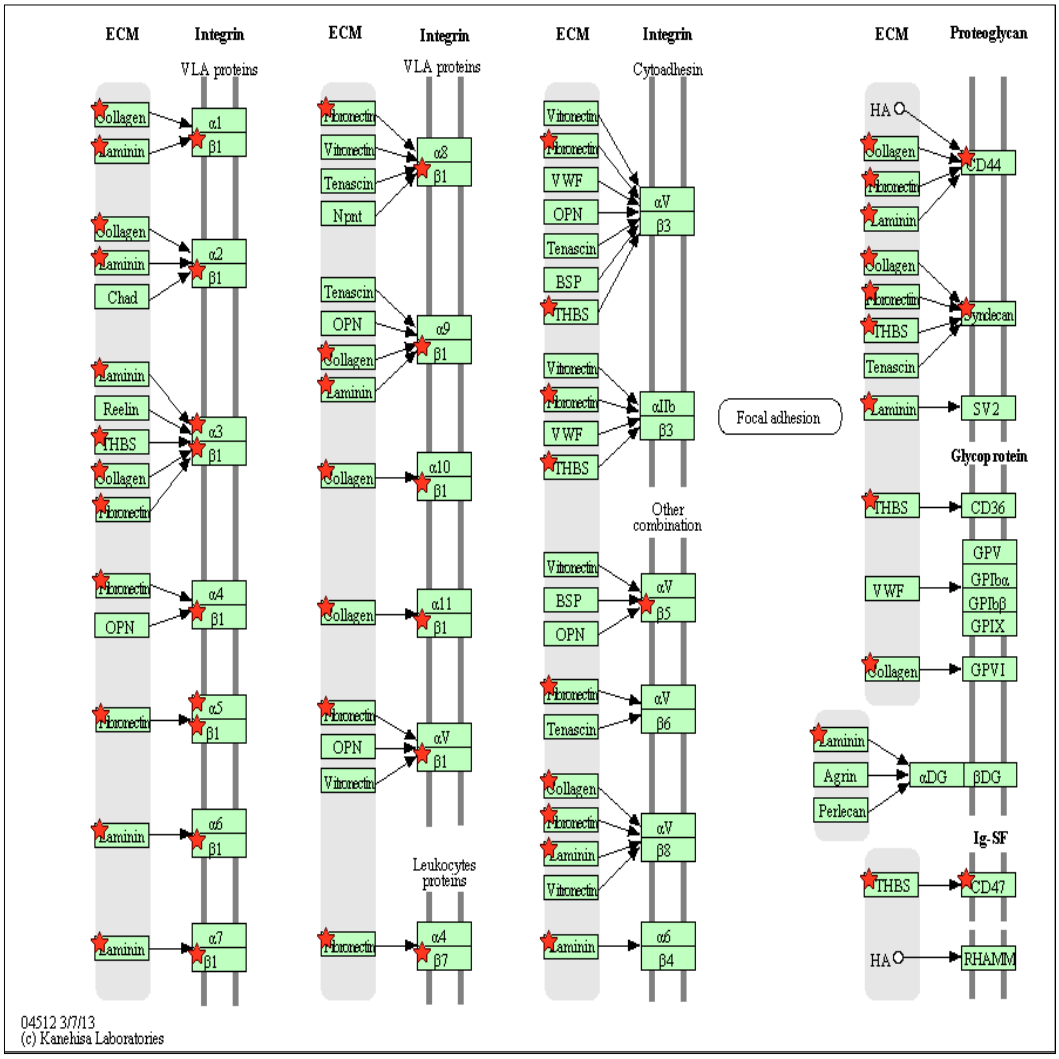

Figure 4.3. The differentially regulated proteins between normoxia and hypoxia that participated in ECM- receptor pathway are highlighted with red stars.

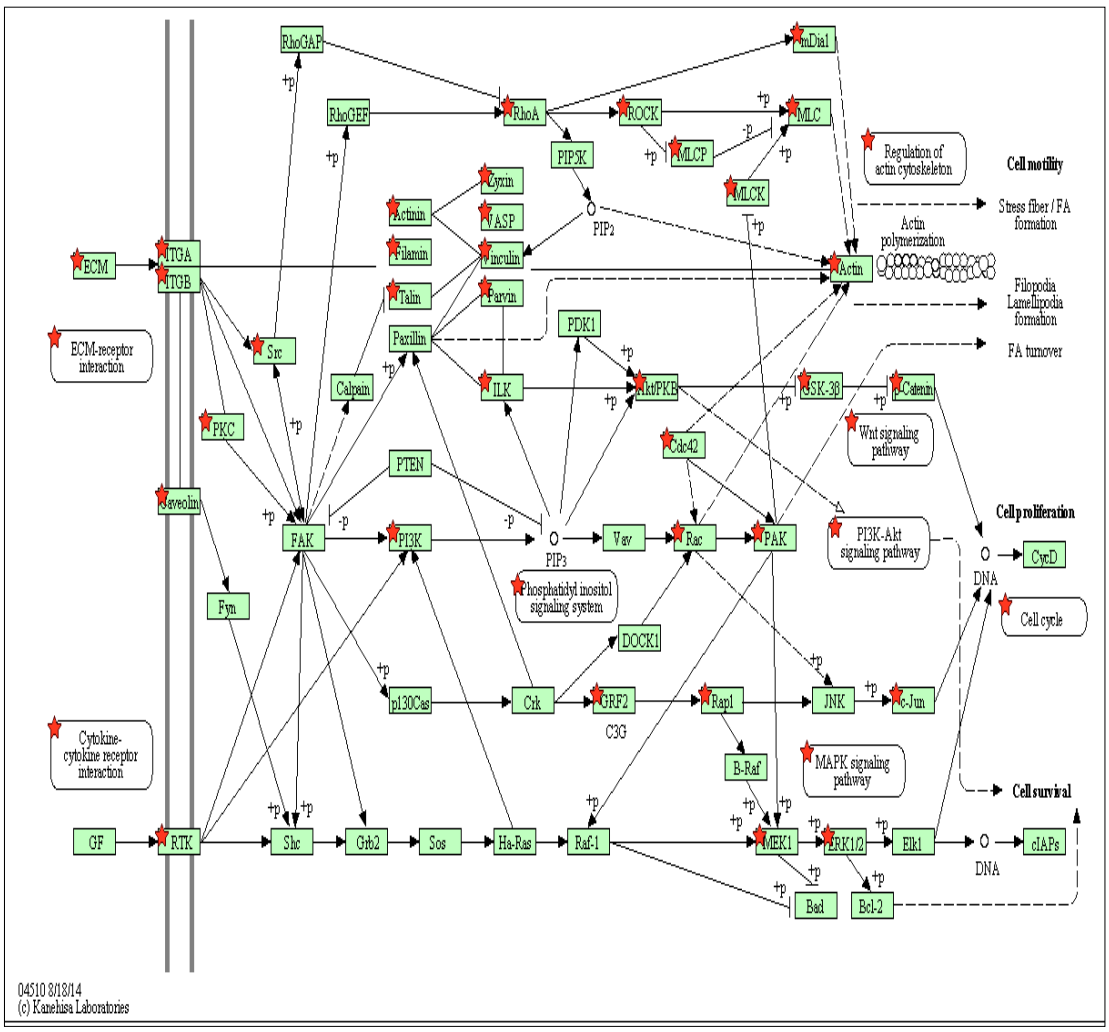

Figure 4.4. The differentially regulated proteins between normoxia and hypoxia that participated in focal adhesion pathway are highlighted with red stars.

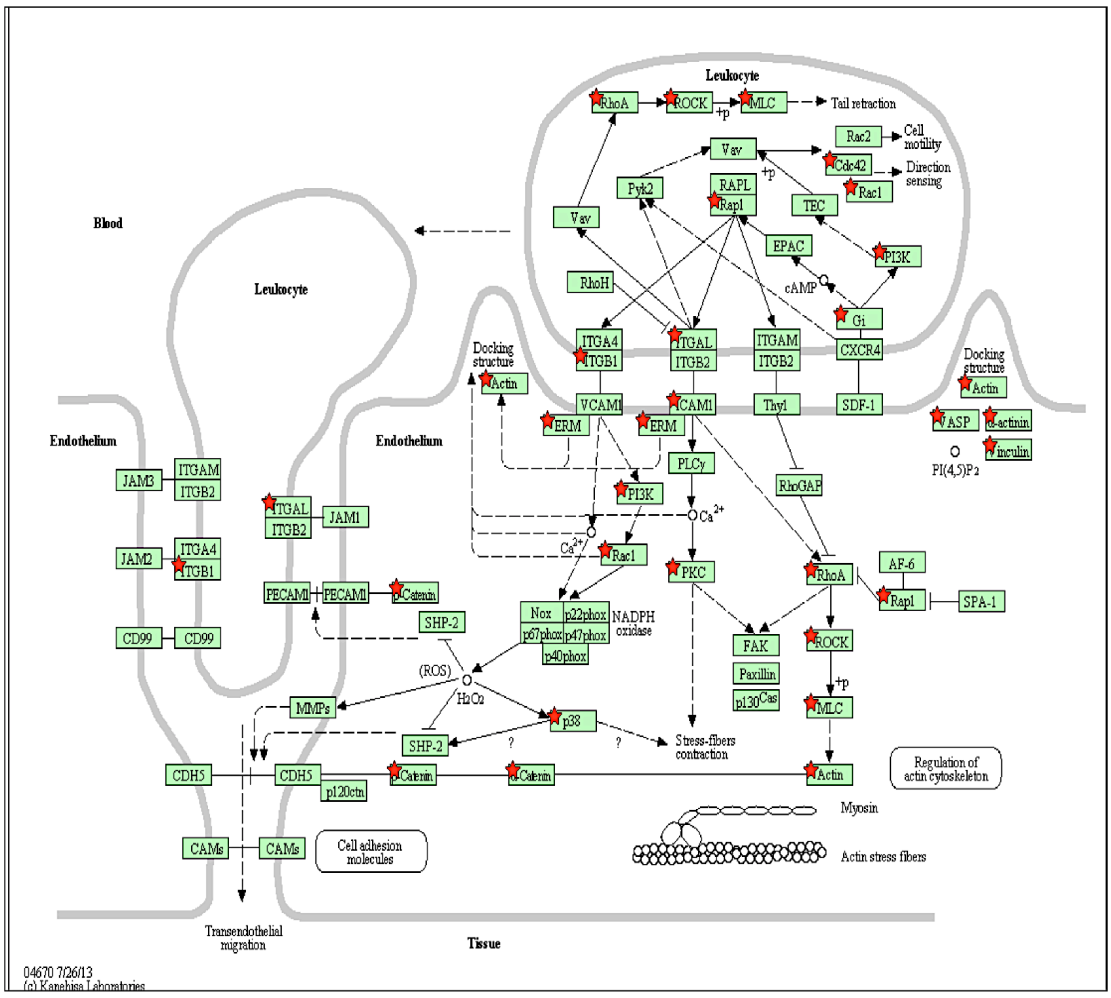

Figure 4.5. The differentially regulated proteins between normoxia and hypoxia that participated in Leucocyte transendothelial migration pathway are highlighted with red stars.

4.3.4. SDS-PAGE analysis

Total proteome extracted from the ECM prepared under both conditions was electrophoresed on two separate gels with different composition and resolving ranges, 4-12% and 3-8% respectively. The proteins were widely distributed with multiple and dense bands between 70 and 250 kDa on the 4-12% gel (Figure 4.6, A). To resolve these dense and high Mr proteins, 3-8% Tris-acetate gels were used, which identified protein distribution from 10 to 200 kDa with multiple bands. Both gradient gels demonstrated intense staining for high Mr proteins in hypoxia versus normoxia with more bands at high Mr and higher intensity compared to low Mr

bands. However, it does not confirm any qualitative differences between the proteins in two conditions (Figure 4.6).

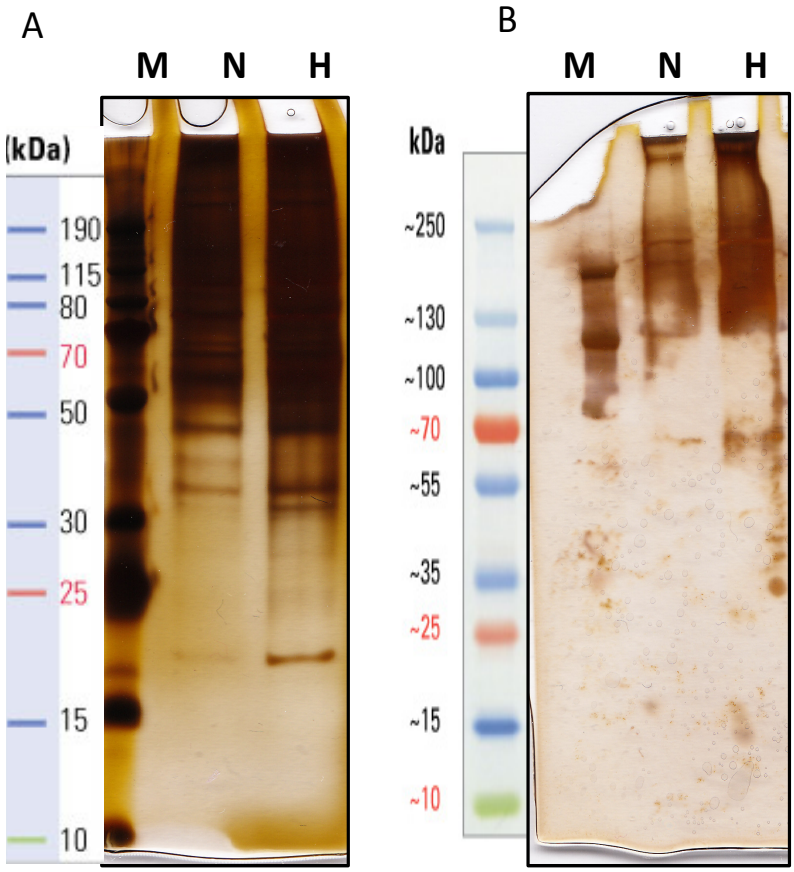

Figure 4.6. Silver staining of the total protein extract electrophoresed on (A) 3-8% and (B) 4-12% gel, where marker lane is M, hypoxic sample is H and normoxic sample is N.

4.3.5. Histochemistry of intact ECM under hypoxia and normoxia

AB staining of the ECM distinguished the morphology of ECM prepared under normoxia and hypoxia. Under normoxic conditions, the cell morphology stayed intact, i.e. MSC type, while under hypoxic conditions, matrix-forming structures were observed (Figure 4.7). Dark blue staining was observed for ECM produced in hypoxia, indicating the presence of potentially charged molecules suggestive of constituents of charged structures of ECM such as GAGs under this condition. Also, more cell nuclei were observed in normoxic conditions suggesting that the lysis buffer did not lyse the MS-5 cells upon secretion of ECM in normoxia.

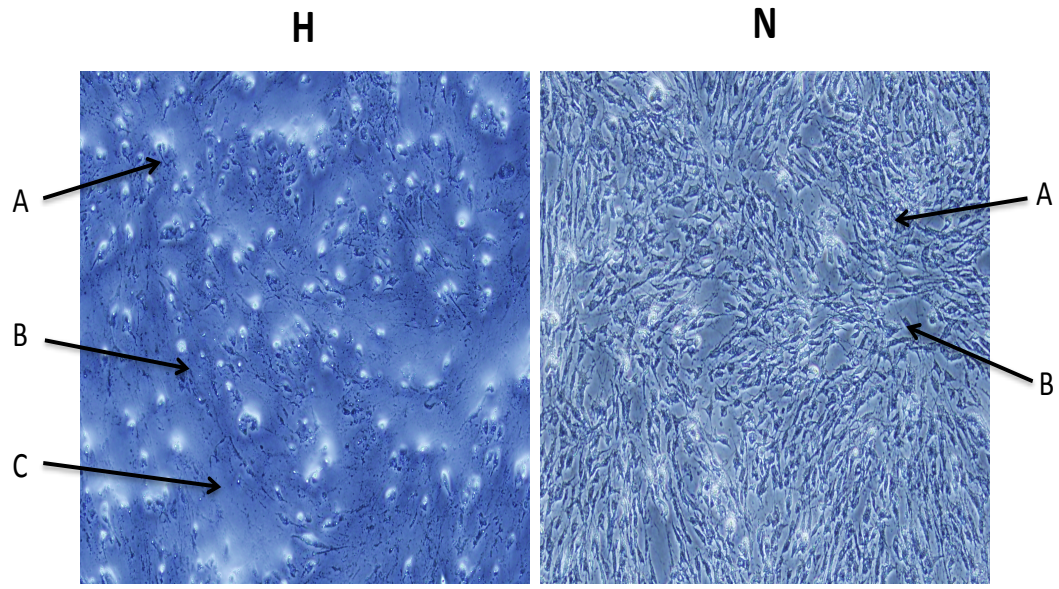

Figure 4.7. Alcian blue staining of ECM prepared under normoxic (N) and hypoxic (H) conditions, where cell staining (A), empty (B) and ECM (C) are shown for two conditions.

A panel of lectins was selected based on the list of GTs to differentiate glycomic composition between ECM prepared under normoxia and hypoxia (Table 4.3). A differential pattern of lectin staining was observed for ECM produced by MS-5 cells under hypoxia compared to normoxia (Figure 4.8 and 4.9). SNA-I and MAA lectins were used for the detection of sialylated structures, where these lectin staining indicated the presence of sialic acid in α-(2, 3)- or α-(2, 6)-linkages, respectively. Both SNA-I and MAA showed intense binding to ECM prepared under hypoxia compared to normoxia (Figure 4.8). This is in agreement with the higher AB staining data again indicative of charged structures such as sialylated structures present in hypoxic conditions detected by AB.

Con A preferentially binds to Man residues and generally indicates the presence of high mannose type *N*-linked oligosaccharides as occur on glycoproteins (Yoon et al., 2013). Con A showed higher binding in hypoxic ECM compared to normoxic ECM (Figure 4.8). WFA, which binds terminal *N*-GalNAc structures and can be used to indicate the presence of CS, showed higher binding of ECM prepared in hypoxia than normoxia. The Fuc -binding lectins UEA-I, AAA, and LTA have distinct and overlapping linkage specificities (Table 4.1). Intense binding intense was found for UEA-I lectin for ECM prepared under hypoxia (Figure 4.9). GS-I-B4 specifically

binds to terminal α-linked Gal residues but there were no differences in relative binding between the hypoxic and normoxic conditions. The binding intensity for DSA, which recognises GlcNAc structures, was higher in normoxic than hypoxic conditions (Figure 4.9).

The fluorescence intensity of each lectin was quantified for every image and relative fluorescence intensities were plotted for hypoxia versus normoxia, where lectin binding under normoxia was considered 100% (Figure 4.10). Significant differences for fluorescence intestines of Con A, MAA, WFA and ECA were reported, with p-value <0.0001 for hypoxia versus normoxia (Figure 4.10). However, no significant differences were observed for the lectins SNA-I, UEA-I, GS-I-B4 and DSA. These observations suggested an overall increase in sialylated, sulfated and mannosylated structures in hypoxia.

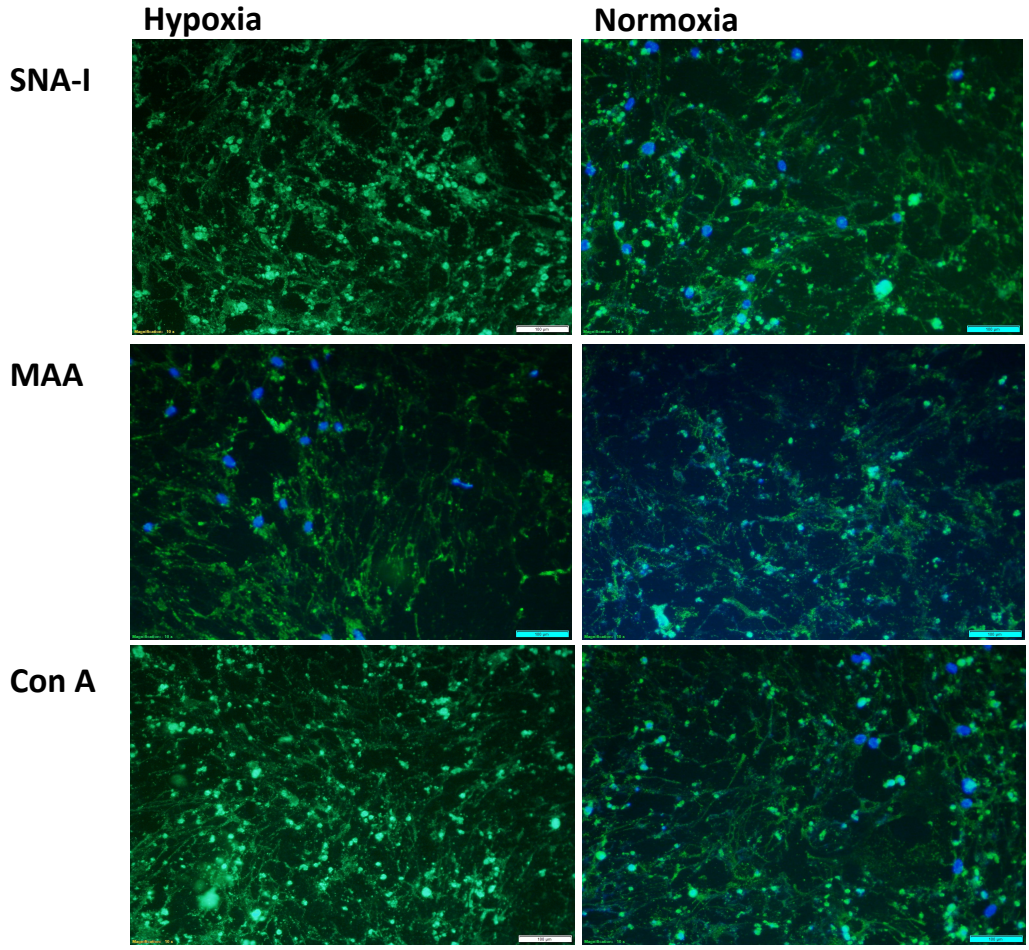

Figure 4.8. Histochemistry using lectins SNA-I, MAA and Con A for ECM produced under hypoxia and normoxia. The fluorescent green indicated staining with lectin while blue staining is DAPI staining for the nuclei of cells

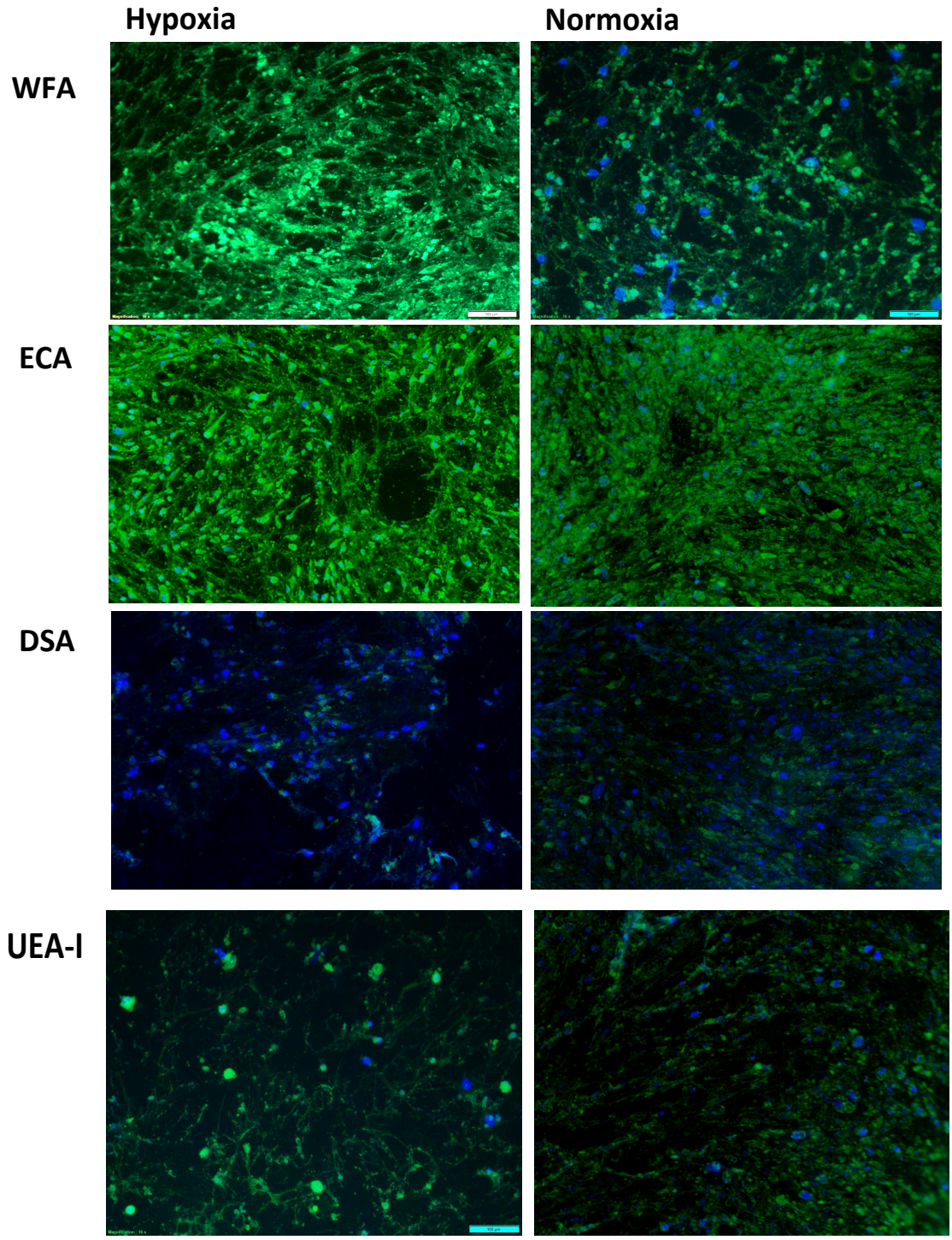

Figure 4.9. Histochemistry using lectins WFA, ECA, DSA and UEA-I for ECM produced under hypoxia and normoxia. The fluorescent green indicated staining with lectin while blue staining is DAPI staining for the nuclei of cells.

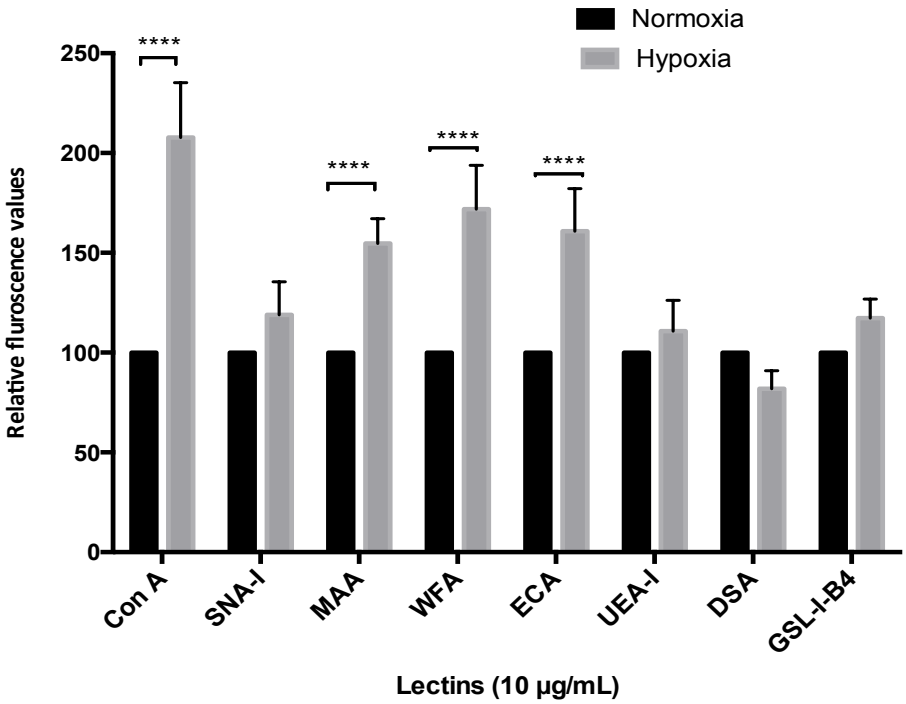

Figure 4.10. Quantification of lectin staining relative fluorescence intensities for ECM prepared normoxia versus hypoxia (n= 9, ANOVA, **** denotes significance of $p < 0.0001$).

4.3.6. Lectin blots

Lectin blots were performed for the total proteins extracted after the decellularisation of the ECM to analyse the overall glycomic changes that occur due to altered culturing conditions of MS-5 cells. Multiple bands were detected with lectins with stronger binding at low Mr. Lectins, AAA and LTA binding indicated two low Mr bands and a faint band at 60 and 35 kDa, respectively. UEA-I lectin blot showed multiple bands ranging between Mr of 10 to 130 kDa with intense binding in hypoxia *versus* normoxia. BPA and PNA lectins showed intense binding at lower Mr with a single band at 55 kDa in hypoxia but no qualitative differences were observed. Interestingly, quantitative and qualitative differences were observed for WFA binding with bands at different Mr for hypoxia and normoxia suggesting differences in the structures from one condition to another. Con A lectin showed no binding in normoxia but showed a single intense band in hypoxia. Similarly, quantitative differences were observed for MPA, GS-I-B4 and MAA lectins between two conditions.

Higher Con A binding was observed for ECM in hypoxia versus normoxia suggesting presence of mannosylated structures (Figure 4.9) in agreement with the lectin histochemistry results. Intense staining was observed by UEA-I followed by LTA and AAA staining in hypoxia suggesting differences in fucosylation from one culture condition to other. GS-I-B4 lectin detected more structures as shown by multiple bands appearing in the hypoxia and also BPA that recognises α-Gal and GalNAc led to higher staining in hypoxia. WFA lectin bound to different Mr bands between the hypoxia and normoxia suggesting changes of the structures on the proteins from one condition to another. These results also indicate dissimilar enrichment of the sulfated structures in hypoxia versus normoxia also suggested by the differential staining with AB.

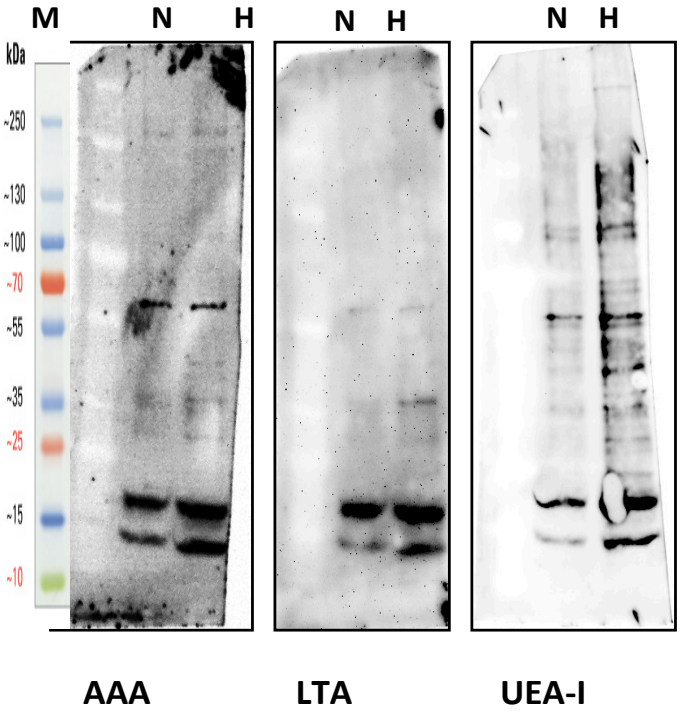

Figure 4.11. Total protein extract from ECM prepared under the normoxic (N) and hypoxic (H) conditions was separated on 4-12% SDS–PAGE. The gels were transferred to PVDF membrane and probed with AAA, LTA and UEA-I for detecting fucosylated structures.

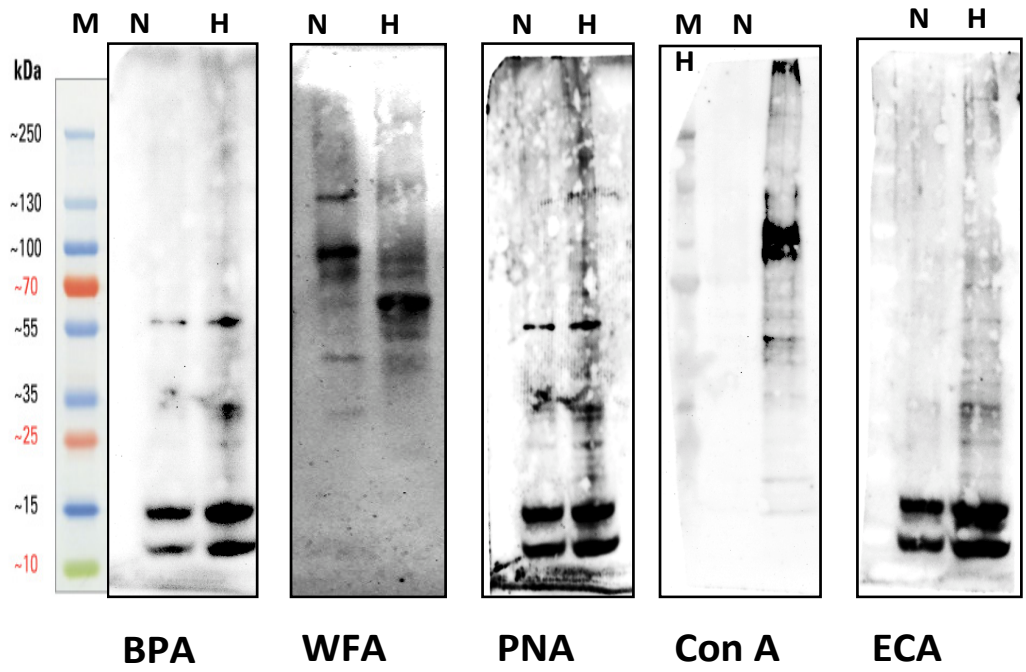

Figure 4.12. Total protein extract from ECM prepared under the normoxic (N) and hypoxic (H) conditions was separated on 4-12% SDS–PAGE. The gels were transferred to PVDF membrane and probed with BPA, WFA, PNA, Con A and ECA.

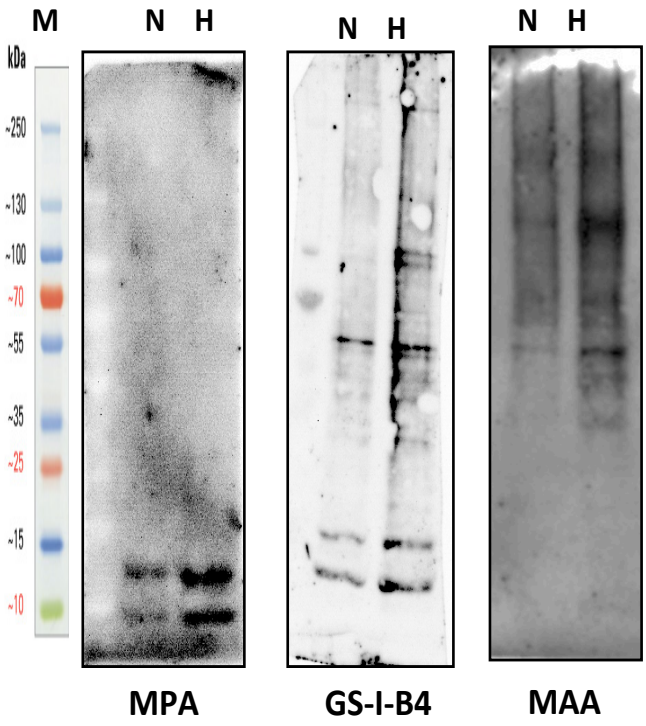

Figure 4.13. Total protein extract from ECM prepared under the normoxic (N) and hypoxic (H) conditions was separated on 4-12% SDS–PAGE. The gels were transferred to PVDF membrane and probed with MPA, GS-I-B4 and MAA.

Haptenic sugar inhibitions were performed to confirm carbohydrate mediated binding of the lectins. Lac was used to inhibit MAA binding and 50 mM inhibited binding completely. Similarly, Gal inhibited GS-I-B4 binding, and Fuc and MAN inhibited UEA-1 and Con A binding respectively (Figure 4.14). Thus, all lectin binding observed for lectin blotting was confirmed as carbohydrate-mediated.

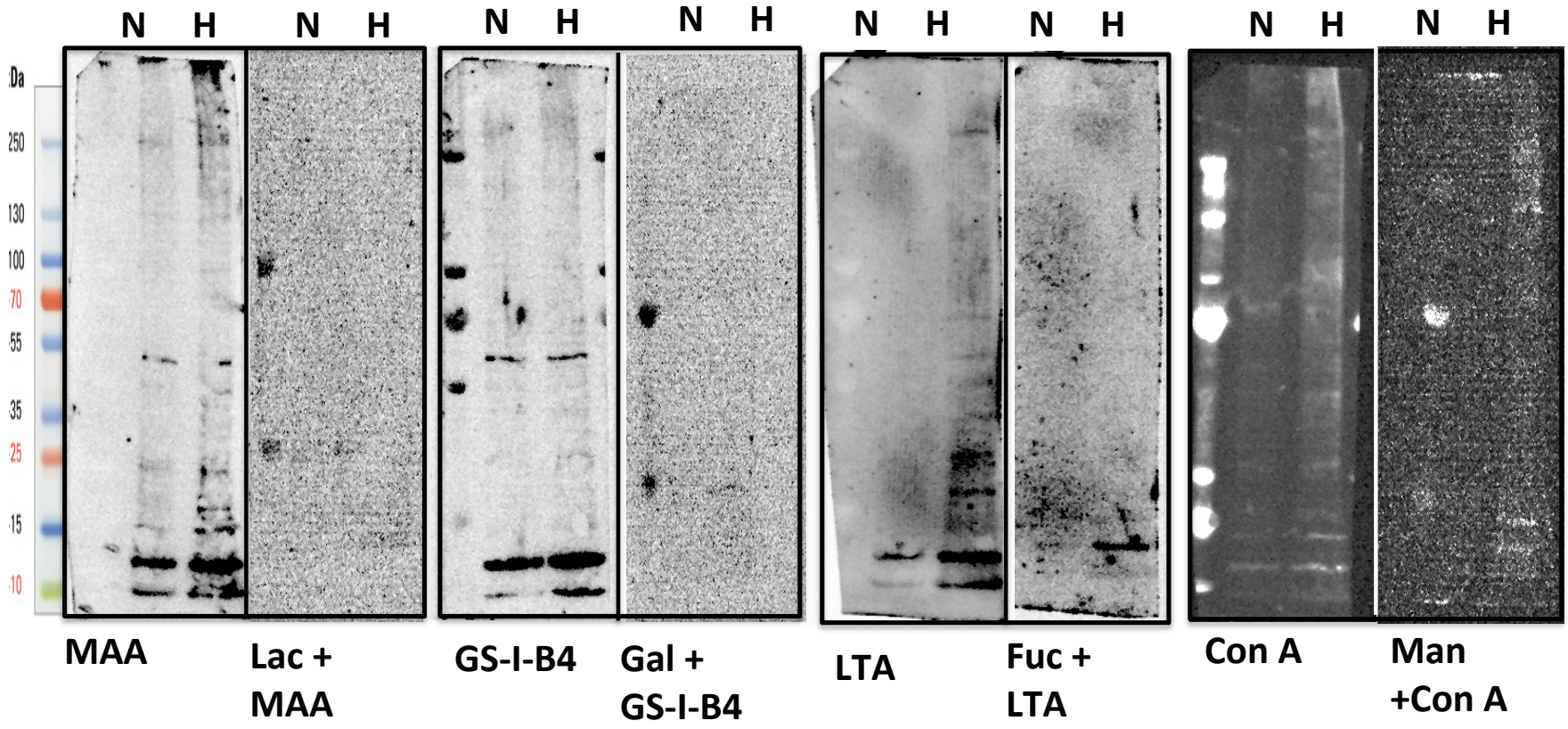

Figure 4.14. Total protein extract from ECM prepared under the normoxic (N) and hypoxic (H) conditions was separated on 4-12% SDS–PAGE. The gels were transferred to PVDF membrane and probed with different lectins and their corresponding inhibitory sugars.

4.4. Discussion

MS-5-derived ECM provides a three-dimensional matrix system and features, which are relevant to tissue physiology and cell behaviour *in vivo*. When maintained in hypoxia, MS-5 cells showed quantitative differences in the production of ECM protein. These cells have also demonstrated increased proliferation, increased expression of pluripotent genes and improved differentiation (Basciano et al., 2011). The differentiation capacities and immunosuppressive properties of MS-5 cells are also altered by hypoxia (Prado-Lopez et al., 2014).

The future of hESCs for stem cell based therapy is promising (Fitzpatrick and McDevitt, 2015). In order to expand hESC in *ex vivo* culture, they are either cultured in feeder cell-containing or feeder-free cultures. However, depending on the nature of the cell culturing and environmental conditions, the properties and the fate of the hESC cells grown on top of feeder cell-containing or feeder-free culture varies (Toh et al., 2010). In the present work, MS-5 cells used as a feeder cell line was cultured in hypoxic and normoxic conditions to study the effect of O_2 concentration on the composition changes of the ECM. MS-5 cells have the ability to secrete soluble factors and ECM that supports and maintains cells (Tiwari et al., 2013). To understand the compositional changes in ECM prepared under hypoxia and normoxia, LC-MS analysis was done followed by proteomic and glycomic analyses. Proteins with more than 2 identified peptides across the duplicates and each condition was used for the total intensity normalisation and fold change analysis. PSM information from the LC-MS was used for bioinformatics analysis to generate a list of differentially regulated proteins in hypoxia and normoxia. This information can potentially be employed for the preparation of selective yet reactive ECM for the hESC culture growth for clinical applications.

In silico analysis identified ECM related proteins such as collagens, fibronectin, laminins and PGs as aggercan, decorin and syndecan, those were most differentially expressed in hypoxic conditions. Pro-collagen and collagen isoforms, fibronectin, laminins and thrombospondin-1 were found most up regulated. Procollagen has N and C terminal propeptide domains (Table 5.2) that, when removed during post-translational processing, lead to production of collagen, mainly collagen type I (Chan

et al., 1990). The collagen superfamily has 28 types, of which collagen I is primary structural protein in mammalian tissue and is found ubiquitously across the animal and plant kingdom (Ricard-Blum, 2011, Van der Rest and Garrone, 1991). Collagen VI has growth factor-like properties and collagen IV is fundamental for the maintenance of integrity and function of basement membranes under conditions of increasing mechanical demands (Alitalo et al., 1982). ECM components can be either involved in structural organisation, such as collagens or as cell adhesion molecules, such as fibronectin and laminins and were identified with higher fold changes in ECM prepared under hypoxia. There are two types of fibronectin molecules; the soluble form found in blood and the insoluble form found in ECM (Hynes, 2012). Fibronectin provides structural integrity and acts as a biological glue mediating interactions between cells and other ECM proteins, or cell to cell contacts that are necessary for interaction between HSC and ECM. (Schultz and Wysocki, 2009). Laminins, together with collagen IV, are found in the basement membrane, an ECM structure that cover the basal aspect of the epithelium and separates it from underlying layers of connective tissue and muscle (Hohenester and Yurchenco, 2013). Laminins have different effects in the adjacent cells where they participate in cell differentiation, cell adhesion and cell migration (Bosman and Stamenkovic, 2003). They exert these effects through interactions with integrins. The presence of integrins in hypoxic conditions suggested the interaction between cells and ECM. Integrins and their transmembrane receptors are heterodimeric molecules composed of α and β subunits with extracellular domains, which bind to the ECM, and a cytoplasmic domain (Danen, 2000).

A list of glycosylation related proteins and GTs was also prepared (Table 4.3). This list included B3GLT that participates in protein glycosylation and synthesizes the Glc-β-(1,3)-Fuc disaccharide found on thrombospondin type-1 repeats (Kozma et al., 2006). DPM1 and MGAT4B, which participate in the *N*-linked glycosylation pathway, were also identified. DPMI transfers Man residue from GDP-Man to Dol-P to form Dol-P-Man and the MGAT4B participates in the transfer of GlcNAc to the core Man residues of *N*-linked oligosaccharides (http://www.uniprot.org/). These two proteins are essential for the production of tri- and tetra-antennary *N*-linked oligosaccharides. A range of lectins was selected based on details of the glycosylation related proteins and GTs from the LC-MS data to detect the differential

glycosylation patterns as an effect of these proteins. OGT1 catalyses the transfer of a single GlcNAc from UDP-GlcNAc to a Ser or Thr residue in cytoplasmic and nuclear proteins. Overall, proteins participating in *N*-linked or *O*-linked biosynthesis were up regulated in hypoxic conditions suggesting the production of highly sialylated and mannosylated structures in hypoxia. A panel of lectins thereafter was selected to differentiate between two ECM preparations.

GO ontology analysis identified different pathways associated with the differentially regulated proteins in hypoxia. The ECM-receptor pathway was identified that involved the interaction of transmembrane molecules, mainly integrins and laminins (Figure 4.3). These transmembrane molecules and other cell-surface-associated components mediate specific interactions between cells and the ECM. (Giancotti and Ruoslahti, 1999) These interactions exert direct or indirect control of cellular activities such as adhesion, migration, differentiation, proliferation, and apoptosis. In addition, integrins function as mechanoreceptors and provide a force-transmitting physical link between the ECM and the cytoskeleton (Schwartz et al., 1995). At the cell-ECM matrix contact points specialised structures called as focal adhesions are formed. Focal adhesions participate in the structural link between membrane receptors and the actin cytoskeleton, which are engaged as signalling molecules. However, the occurrences of the focal adhesions in *in vivo* conditions are rare and are sometimes referred as an artefact of the culture conditions (Burridge et al., 1988). Focal adhesion occurs due to the planar configuration imposed by the growth of cultured cells on flat and rigid substrates. As the MS-5 cells are plated on the plastic substrates, proteins identified in focal adhesion pathway (Figure 4.4) could have been an artefact in the experiment. However, there is occurrence of cytokine-receptor interaction within focal-adhesion pathway that may activate bioactive signalling molecules helpful towards the maintenance of ECM integrity.

Proteins identified in hypoxia were associated with extracellular components followed by intracellular components constituting half of the cellular component suggesting contamination of ECM with intracellular constituents. This emphasises that the methodology for ECM extraction was not restricted to the ECM proteins. Hence, depending on the method of ECM preparation and its extraction, differences in the composition of ECM will occur. Both in tissue and in culture, cells secreting

the ECM components are highly cross-linked, which makes it difficult to extract membrane proteins alone (Byron et al., 2013). However, cell culture secreted ECM offers the ease of use and the ability to assign ECM production to specific cell types. DAPI staining demonstrated numerous cell nuclei in ECM prepared under normoxia while limited nuclei were visible in hypoxia. This suggested the differences that could have arisen due to the decellularisation procedure used for ECMs prepared under hypoxia versus normoxia. The current procedure suffers from intracellular cell contamination problems, hence better ECM preparation and different approaches for the decellularisation of ECM are required to minimise the cell contamination.

Laminins, identified in analysed LC-MS proteomic data, are heavily glycosylated and constitutively present $\alpha(\beta)$-Gal-terminated and Man-rich oligosaccharides. Also GTs, MGATB4 and DPMI, participate in the production of high Man structures. These results indicate abundance of Man structures produced in hypoxia, which were detected by Con A lectin in both lectin histochemistry and lectin blotting for ECM prepared in hypoxic conditions. This result is in agreement with earlier reports with the importance of Man structures in ECM as it has been shown that surface coated with neoglycoprotein containing α-Man can stimulate growth of epidermal keratinocytes without feeder cells (Labský et al., 2003). Similarly, α-(2, 3)-linked and α-(2, 6)-linked sialic acids were identified using SNA-I and MAA lectins. MAA lectin showed intense binding for ECM prepared under hypoxic conditions suggesting the possibility of more α-(2, 3)-linked structures. Sialylation of ECM and its alterations influence cell behaviour by modifying cell adhesion, proliferation and differentiation. For the identification of fucosylated structures with different linkage, UEA-I, AAA and LTA lectins (Table 4.1, Figure 4.12) were used that led to no significant differences in the intensity of binding among lectin but slight differences across the culturing conditions. Fucosylation plays an important role in a variety of biological and pathological processes, cell adhesion and cell homing (Mody et al., 1995, Sackstein, 2012) and cell-cell interactions *via* lectins such as selectins (Chase et al., 2012). Across all the lectin blots, bands of low Mr were observed. The low Mr could possibly be disintegrin and metalloproteinase, saroglycan, galectin related proteins and integrins reported in the identified protein list. WFA lectin was quantitatively and qualitatively different in proteins resolved on SDS-PAGE for hypoxia compared to normoxia may indicate different enrichment of sulfated

structures as WFA binds to CSPG-GAGS and glycoproteins (Härtig et al., 1992). The lectin blotting and lectin staining results suggested the presence of higher sialylated, fucosylated and Gal terminal structures in hypoxia.

The composition of ECM secreted by MS-5 cells differs in its proteomic and glycomic composition in response to O_2 gradient. These proteins also demonstrate the continuous interaction that may be taking place between stem cells and the ECM, which are required in the adhesion, anchorage and homing of stem cells. This suggests that hypoxia leads to differential expression of various proteins and glycosylation related proteins that may supports hESC undifferentiated state and cell proliferation. The identified proteins and glycosylation related proteins could be further explored for their role in maintaining hESC growth and can be studied in the development of biomaterials and bioactive scaffolds in the field of tissue engineering.

4.5. References

ALITALO, K., KUISMANEN, E., MYLLYLÄ, R., KIISTALA, U., ASKO-SELJAVAARA, S. & VAHERI, A. 1982. Extracellular matrix proteins of human epidermal keratinocytes and feeder 3T3 cells. *The Journal of cell biology,* 94**,** 497-505.

AMIT, M., CARPENTER, M. K., INOKUMA, M. S., CHIU, C.-P., HARRIS, C. P., WAKNITZ, M. A., ITSKOVITZ-ELDOR, J. & THOMSON, J. A. 2000. Clonally derived human embryonic stem cell lines maintain pluripotency and proliferative potential for prolonged periods of culture. *Developmental Biology,* 227**,** 271-278.

BASCIANO, L., NEMOS, C., FOLIGUET, B., DE ISLA, N., DE CARVALHO, M., TRAN, N. & DALLOUL, A. 2011. Long term culture of mesenchymal stem cells in hypoxia promotes a genetic program maintaining their undifferentiated and multipotent status. *BMC Cell Biology,* 12**,** 1.

BENNACEUR-GRISCELLI, A., PONDARRÉ, CORINNE, SCHIAVON, V., VAINCHENKER, W. & COULOMBEL, L. 2001. Stromal cells retard the differentiation of CD34+ CD38low/neg human primitive progenitors exposed to cytokines independent of their mitotic history. *Blood,* 97**,** 435-441.

BOSMAN, F. T. & STAMENKOVIC, I. 2003. Functional structure and composition of the extracellular matrix. *The Journal of Pathology,* 200**,** 423-428.

BOSNAKOVSKI, D., MIZUNO, M., KIM, G., TAKAGI, S., OKUMURA, M. & FUJINAGA, T. 2006. Chondrogenic differentiation of bovine bone marrow mesenchymal stem cells (MSCs) in different hydrogels: influence of collagen type II extracellular matrix on MSC chondrogenesis. *Biotechnology and bioengineering,* 93**,** 1152-1163.

BOURGINE, P. E., PIPPENGER, B. E., TODOROV, A., TCHANG, L. & MARTIN, I. 2013. Tissue decellularization by activation of programmed cell death. *Biomaterials,* 34**,** 6099-6108.

BREEMS, D. A., BLOKLAND, E. A., SIEBEL, K. E., MAYEN, A. E., ENGELS, L. J. & PLOEMACHER, R. E. 1998. Stroma-contact prevents loss of hematopoietic stem cell quality during ex vivo expansion of CD34+ mobilized peripheral blood stem cells. *Blood,* 91**,** 111-117.

BURRIDGE, K., FATH, K., KELLY, T., NUCKOLLS, G. & TURNER, C. 1988. Focal adhesions: transmembrane junctions between the extracellular matrix and the cytoskeleton. *Annual Review of Cell Biology,* 4**,** 487-525.

BYRON, A., HUMPHRIES, J. D. & HUMPHRIES, M. J. 2013. Defining the extracellular matrix using proteomics. *International journal of experimental pathology,* 94**,** 75-92.

CASSAVAUGH, J. & LOUNSBURY, K. M. 2011. Hypoxia-mediated biological control. *Journal of Cellular Biochemistry,* 112**,** 735-744.

CHAN, D., LAMANDE, S. R., COLE, W. & BATEMAN, J. F. 1990. Regulation of procollagen synthesis and processing during ascorbate-induced extracellular matrix accumulation in vitro. *Biochem. J,* 269**,** 175-181.

CHASE, S., MAGNANI, J. & SIMON, S. 2012. E-selectin ligands as mechanosensitive receptors on neutrophils in health and disease. *Annals of biomedical engineering,* 40**,** 849-859.

CHEN, K. G., MALLON, B. S., MCKAY, R. D. G. & ROBEY, P. G. 2014. Human pluripotent stem cell culture: considerations for maintenance, expansion, and therapeutics. *Cell Stem Cell,* 14**,** 13-26.

CHENG, L., HAMMOND, H., YE, Z., ZHAN, X. & DRAVID, G. 2003. Human adult marrow cells support prolonged expansion of human embryonic stem cells in culture. *Stem Cells,* 21**,** 131-142.

CUKIERMAN, E., PANKOV, R., STEVENS, D. R. & YAMADA, K. M. 2001. Taking cell-matrix adhesions to the third dimension. *Science Signaling,* 294**,** 1708.

DA WEI HUANG, B. T. S. & LEMPICKI, R. A. 2008. Systematic and integrative analysis of large gene lists using DAVID bioinformatics resources. *Nature Protocols,* 4**,** 44-57.

DANEN, E. H. 2000. *Integrins: an overview of structural and functional aspects*, Landes Bioscience.

DEXTER, T. M., ALLEN, T. D. & LAJTHA, L. 1977. Conditions controlling the proliferation of haemopoietic stem cells in vitro. *Journal of Cellular Physiology,* 91**,** 335-344.

EDEN, E., NAVON, R., STEINFELD, I., LIPSON, D. & YAKHINI, Z. 2009. GOrilla: a tool for discovery and visualization of enriched GO terms in ranked gene lists. *BMC Bioinformatics,* 10**,** 48.

ELIAS, J. E., GIBBONS, F. D., KING, O. D., ROTH, F. P. & GYGI, S. P. 2004. Intensity-based protein identification by machine learning from a library of tandem mass spectra. *Nature Biotechnology,* 22**,** 214-219.

ESCOBEDO-LUCEA, C., AYUSO-SACIDO, A., XIONG, C., PRADO-LÓPEZ, SONIA, DEL PINO, M. S., MELGUIZO, D., BELLVER-ESTELLÉS, C., GONZALEZ-GRANERO, S., VALERO, M. L. & MORENO, R. 2012. Development of a Human Extracellular Matrix for Applications Related with Stem Cells and Tissue Engineering. *Stem Cell Reviews and Reports,* 8**,** 170-183.

FITZPATRICK, L. E. & MCDEVITT, T. C. 2015. Cell-derived matrices for tissue engineering and regenerative medicine applications. *Biomaterials Science,* 3**,** 12-24.

FRANTZ, C., STEWART, K. M. & WEAVER, V. M. 2010. The extracellular matrix at a glance. *Journal of Cell Science,* 123**,** 4195-4200.

FREZZA, C., ZHENG, L., TENNANT, D. A., PAPKOVSKY, D. B., HEDLEY, B. A., KALNA, G., WATSON, D. G. & GOTTLIEB, E. 2011. Metabolic profiling of hypoxic cells revealed a catabolic signature required for cell survival. *PloS one,* 6**,** e24411.

GENBACEV, O., KRTOLICA, A., ZDRAVKOVIC, T., BRUNETTE, E., POWELL, S., NATH, A., CACERES, E., MCMASTER, M., MCDONAGH, S. & LI, Y. 2005. Serum-free derivation of human embryonic stem cell lines on human placental fibroblast feeders. *Fertility and Sterility,* 83**,** 1517-1529.

GIANCOTTI, F. G. & RUOSLAHTI, E. 1999. Integrin signaling. *science,* 285**,** 1028-1033.

GRAYSON, W. L., ZHAO, F., BUNNELL, B. & MA, T. 2007. Hypoxia enhances proliferation and tissue formation of human mesenchymal stem cells. *Biochemical and biophysical research communications,* 358**,** 948-953.

HÄRTIG, W., BRAUER, K. & BRÜCKNER, G. 1992. Wisteria floribunda agglutinin-labelled nets surround parvalbumin-containing neurons. *Neuroreport,* 3**,** 869-872.

HEDMAN, K., KURKINEN, M., ALITALO, K., VAHERI, A., JOHANSSON, S. & HÖÖK, M. 1979. Isolation of the pericellular matrix of human fibroblast cultures. *The Journal of Cell Biology,* 81**,** 83-91.

HOHENESTER, E. & YURCHENCO, P. D. 2013. Laminins in basement membrane assembly. *Cell Adhesion & Migration,* 7**,** 56-63.

HYNES, R. O. 2012. *Fibronectins*, Springer Science & Business Media.

ISSAAD, C., CROISILLE, L., KATZ, A., VAINCHENKER, W. & COULOMBEL, L. 1993. A murine stromal cell line allows the proliferation of very primitive human CD34++/CD38-progenitor cells in long-term cultures and semisolid assays. *Blood,* 81**,** 2916-2924.

KAUR-BOLLINGER, P., GOTZE, K. S. & OOSTENDORP, R. A. 2012. Role of secreted factors in the regulation of hematopoietic stem cells by the bone marrow microenvironment. *Front Biosci,* 17**,** 876-91.

KLEINMAN, H. K., MCGARVEY, M. L., LIOTTA, L. A., ROBEY, P. G., TRYGGVASON, K. & MARTIN, G. R. 1982. Isolation and characterization of type

IV procollagen, laminin, and heparan sulfate proteoglycan from the EHS sarcoma. *Biochemistry,* 21**,** 6188-6193.

KOZMA, K., KEUSCH, J. J., HEGEMANN, B., LUTHER, K. B., KLEIN, D., HESS, D., HALTIWANGER, R. S. & HOFSTEENGE, J. 2006. Identification and Characterization of aβ1,3-Glucosyltransferase That Synthesizes the Glc-β1,3-Fuc Disaccharide on Thrombospondin Type 1 Repeats. *Journal of Biological Chemistry,* 281**,** 36742-36751.

LABSKÝ, J., DVOŘÁNKOVÁ, B., SMETANA, K., HOLÍKOVÁ, Z. & BROŽ, L. R. G., HANS-JOACHIM 2003. Mannosides as crucial part of bioactive supports for cultivation of human epidermal keratinocytes without feeder cells. *Biomaterials,* 24**,** 863-872.

LIM, J. W. E. & BODNAR, A. 2002. Proteome analysis of conditioned medium from mouse embryonic fibroblast feeder layers which support the growth of human embryonic stem cells. *Proteomics,* 2**,** 1187-1203.

MASON, E. F. & RATHMELL, J. C. 2011. Cell metabolism: an essential link between cell growth and apoptosis. *Biochimica et Biophysica Acta (BBA)-Molecular Cell Research,* 1813**,** 645-654.

MODY, R., ANTARAM JOSHI, S. H. & CHANEY, W. 1995. Use of lectins as diagnostic and therapeutic tools for cancer. *Journal of pharmacological and Toxicological Methods,* 33**,** 1-10.

NODWELL, A., CARMICHAEL, L., ROSS, M. & RICHARDSON, B. 2005. Placental compared with umbilical cord blood to assess fetal blood gas and acid-base status. *Obstetrics & Gynecology,* 105**,** 129-138.

NOMBELA-ARRIETA, C., WINKEL, B., CANTY, K. J., HARLEY, B., MAHONEY, J. E., PARK, S.-Y., LU, J., PROTOPOPOV, A. & SILBERSTEIN, L. E. 2013. Quantitative imaging of haematopoietic stem and progenitor cell localization and hypoxic status in the bone marrow microenvironment. *Nature Cell Biology,* 15**,** 533-543.

PRADO-LOPEZ, S., DUFFY, M. M., BAUSTIAN, C., ALAGESAN, S., HANLEY, S. A., STOCCA, A., GRIFFIN, M. D. & CEREDIG, R. 2014. The influence of hypoxia on the differentiation capacities and immunosuppressive properties of clonal mouse mesenchymal stromal cell lines. *Immunology and Cell Biology*.

RICARD-BLUM, S. 2011. The collagen family. *Cold Spring Harbor Perspectives in Biology,* 3**,** a004978.

RICHARDS, M., FONG, C.-Y., CHAN, W.-K., WONG, P.-C. & BONGSO, A. 2002. Human feeders support prolonged undifferentiated growth of human inner cell masses and embryonic stem cells. *Nature Biotechnology,* 20**,** 933-936.

SACKSTEIN, R. 2012. Glycoengineering of HCELL, the human bone marrow homing receptor: sweetly programming cell migration. *Annals of biomedical engineering,* 40**,** 766-776.

SALLER, M. M., PRALL, W. C., DOCHEVA, D., SCHÖNITZER, V., POPOV, T., ANZ, D., CLAUSEN-SCHAUMANN, H., MUTSCHLER, W., VOLKMER, E. & SCHIEKER, M. 2012. Increased stemness and migration of human mesenchymal stem cells in hypoxia is associated with altered integrin expression. *Biochemical and biophysical research communications,* 423**,** 379-385.

SCHULTZ, G. S. & WYSOCKI, A. 2009. Interactions between extracellular matrix and growth factors in wound healing. *Wound Repair and Regeneration,* 17**,** 153-162.

SCHWARTZ, M. A., SCHALLER, M. D. & GINSBERG, M. H. 1995. Integrins: emerging paradigms of signal transduction. *Annual review of cell and developmental biology,* 11**,** 549-599.

SUGRUE, T., LOWNDES, N. F. & CEREDIG, R. 2014. Hypoxia enhances the radioresistance of mouse mesenchymal stromal cells. *Stem Cells,* 32**,** 2188-2200.

THOMSON, J. A., ITSKOVITZ-ELDOR, J., SHAPIRO, S. S., WAKNITZ, M. A., SWIERGIEL, J. J., MARSHALL, V. S. & JONES, J. M. 1998. Embryonic stem cell lines derived from human blastocysts. *Science,* 282**,** 1145-1147.

TIWARI, A., TURSKY, M. L., MUSHAHARY, D., WASNIK, S., COLLIER, F. M., SUMA, K., KIRKLAND, M. A. & PANDE, G. 2013. Ex vivo expansion of haematopoietic stem/progenitor cells from human umbilical cord blood on acellular scaffolds prepared from MS-5 stromal cell line. *Journal of Tissue Engineering and Regenerative Medicine,* 7**,** 871-883.

TOH, Y.-C., BLAGOVIJÁ, K. & VOLDMAN, J. 2010. Advancing stem cell research with microtechnologies: opportunities and challenges. *Integrative Biology,* 2**,** 305-325.

VAN DER REST, M. & GARRONE, R. 1991. Collagen Family of Proteins. *The FASEB journal,* 5**,** 2814-2823.

XU, C., INOKUMA, M. S., DENHAM, J., GOLDS, K., KUNDU, P., GOLD, J. D. & CARPENTER, M. K. 2001. Feeder-free growth of undifferentiated human embryonic stem cells. *Nature Biotechnology,* 19**,** 971-974.

YOON, S.-J., UTKINA, N., SADILEK, M., YAGI, H., KATO, K. & HAKOMORI, S.-I. 2013. Self-recognition of high-mannose type glycans mediating adhesion of embryonal fibroblasts. *Glycoconjugate Journal,* 30**,** 485-496.

CHAPTER 5

CONCLUSIONS AND FUTURE DIRECTIONS

5.1. Conclusions and future perspectives

Carbohydrates confer advantageous physical and biological properties to natural compounds and proteins. Glycosylation results in the structural and functional diversification of a single protein to yield a set of glycosylation variants or glycoforms. In this thesis, glycosylation was used to manipulate biological functions of model systems using glycoproteins and natural compounds.

The work presented in this thesis has contributed to the understanding of the role of glycosylation in several biological models and three biological processes in particular;
i) PTMs on a glycoprotein, OPN, for their contribution to angiogenic properties,
ii) testing poly- and oligo-saccharides as potential immunomodulatory therapeutics, and,
iii) the effect of oxygen concentration on the glycomic composition of ECM produced by feeder cells that support the growth and expansion of hESCs.

The main conclusions drawn from each chapter are discussed in separate sections below and are followed by future perspectives for each chapter.

5.1.1. Effect of PTMs on OPN in endothelial biology

There is literature available either demonstrating the role of PTMs on OPN to contribute towards its angiogenic properties or independent of its PTMs (Denhardt and Guo, 1993, Jono et al., 2000, Yoshinobu et al., 2014). However, a study comparing OPN from various sources and expression systems and their glycoforms and phosphoforms, was missing. In this thesis, OPN and its generated phosphoforms and glycoforms were tested on HUVECs for studying differences in their angiogenic properties. Contrary to earlier reports based on other cell models, the OPN glycoforms and phosphoforms did not significantly alter studied angiogenic activities, proliferation, tubule formation, cytokines release or activation of kinase pathways compared to OPN lacking any PTMs.

5.1.1.1. Future directions

- These results presented in this thesis may imply that HUVECs are not the ideal cell

line for testing OPN and its glycoforms, as HUEVCs have constitutive expression of iOPN. The presence of iOPN mitigates the effects of OPN provided exogenously to HUVECs. Also, obtaining endothelial cells from primary isolates is difficult and their *in vitro* prolonged expansion leads to significant changes in activation state, karyotype, expression of cell surface antigens and growth properties.

- OPN, its isoforms, glycoforms and known active peptides (with RGD domain) can be compared in parallel on same platform for their angiogenic activities. This will provide an overall consensus about roles of PTMs on OPN.

- In parallel to HUEVCs, OPN and its variants can be tested on primary endothelial cells and additional endothelial cell lines such as human microvascular endothelial cell line (HMEC-1), human umbilical vein endothelial (ECV304) and a hybridoma of the epithelial cell line A549 and HUVEC (EaI-Iy926). Endothelial cells are not alike as they respond to growth factors and inhibitors differently depending on their source. Hence, testing more than one cell line will provide a clearer understanding of the role of PTMs on OPN in angiogenic activity.

- Biological assays, such as tubule formation and proliferation, are the quantitative assessment of the activity for testing potential useful compounds. These assays have some limitations such as in the tubule formation assay, it is difficult to generate identical tubules, which not only leads to considerable variability but also adds subjective bias as what is tubule or node for the tubule formation assay. Hence, quantitative methods for assessing tubules can be employed for assessment of angiogenic capacities of cells. This can be achieved by labelling the cells with fluorescent dye and thereafter the tubules formed can be easily counted after being captured by confocal microscope. The fluorescence intensities of the images can also be used for comparing between the control and the OPN incubated HUVECs.

  In addition, proliferation assays that employ MTT dye to study metabolic activity of cells can lead to overall bias due to some hyper metabolic cells in test wells, even when the same number of cells are added to each well. As an alternative, the ATP-based method is highly sensitive, reproducible and simple for the evaluation of cell viability and proliferation, which is based on the quantitation of cellular ATP (Petty

et al., 1995). Also, a DNA-based method, which is based on the measurement of cellular DNA to indicate the relative cell number, can be used as cellular DNA content is highly regulated (Wang et al., 2010).

- In parallel to functional assays, gene and protein expression analysis of the angiogenic factors upon incubation of OPN and its variants can be compared to understand the role of PTMs. An angiogenesis PCR array with multiple angiogenic factors (including ANGPT1, ANGPT2, ANPEP, TYMP, EREG, FGF1, FGF2, FIGF, FLT1, JAG1, KDR, LAMA5, NRP1, NRP2, PGF, PLXDC1, STAB1, VEGFA, and VEGFC) and transcription factors (HAND2 and SPHK1) can be utilised for studying the regulation of the biological processes of angiogenesis. The differential expression of genes upon incubation of cells with different glyco- and phospho-forms of OPN can further help in understanding the roles of OPN in biochemical pathways of angiogenesis.

- OPN and its glyco- and phospho-forms can be generated using lentiviral gene constructs by mutating the potential individual *O*-linked glycosylation and phosphorylation sites (Minai-Tehrani et al., 2013). These mutated OPNs can be tested for their downstream effects on signalling kinase pathways that includes p-PI3K/p-AKT and mTOR, which is a downstream effector in the PI3k/Akt signalling pathway, can control the activation of p70S6K and the phosphorylation of 4E-BP1, a suppressor of eIF4E. Lentiviral method of generation and expression of non-glycosylated or non-phosphorylated forms of OPN would likely overcome the issues of purification, stability and activity of OPN that persist when OPN is expressed in bacterial system.

5.1.2. Immunomodulatory effects of oligo- and poly-saccharides in HWBC and THP-1 cell line

In chapter 3, exogenous poly- and oligo-saccharides not native to the biological system were incubated with *in vitro,* THP-1 cells and *ex vivo* HWBC cell model systems to study their immunomodulatory properties. Out of six different oligo- and poly-saccharides (INL, GAL, xGLU, MAN, HGL and FUC) assessed, four (INL, GAL, HGL and FUC) had pro-inflammatory responses. It was demonstrated that

HWBC had a greater and more varied response to the compounds in comparison to THP-1 cell and was suggested that HWBC could serve as a better cell model system because of its closeness to an *in vivo* model.

5.1.2.1. Future directions

- INL, GAL, HGL and FUC can be validated for their immunomodulatory properties *in vitro* and *in vivo* using immunosuppressed models such as post-traumatic immunosuppression model. Thus, they can provide an explored further as potential therapeutics alternative to current classical antibiotic.

- Structural differences in oligo- and poly-saccharides arise due to different multiple sources and extraction and purification methods (Holtkamp et al., 2009) and structural variations of the carbohydrates contribute to multiple biological functions (Tzianabos, 2000). Therefore, these four compounds can be further studied for their structure-function relationship for immunomodulation. Fucoidans can exhibit both pro- and anti-immunostimulation properties due to differences in their structure, including composition of monosaccharides, presence and position of sulfate groups and molecular weight. Thus, the influence of such structural details of the tested compounds can be further explored contributing to their immunomodulatory properties.

- Polysaccharides activate intracellular signal transduction pathways upon binding to the surface receptors on immune cells. Hence, exploring the receptors on the cell surface and the binding affinities between polysaccharides and surface receptors on immune cells, macrophages and dendritic cells may provide the mechanism for modulation of immune response. This can be carried by targeting and studying the intrinsic signalling pathways such as toll like receptor pathway (TLR) that play a central role in the enhancement of immune response (Vogt et al., 2014, Tzianabos, 2000) .

5.1.3. Proteomic and glycomic analysis of ECM produced by MS-5 cells under hypoxia and normoxia

In chapter 4, ECM secreted by MS-5 cells that support human hematopoietic stem

and progenitor cell survival and differentiation was studied. Proteomic and glycomic analysis of decellularised MS-5 cell ECM under normoxic and hypoxic conditions identified differences in the enrichment of ECM-related molecules, and glycosylation related proteins and GTs, respectively. *In silico* analysis of LC-MS data from decellularised MS-5 cell ECM produced under normoxic and hypoxic conditions showed that the top-most affected pathways by hypoxia were the ECM-receptor interaction, focal adhesion and leucocyte transendothelial migration pathways. Differences in the enrichment of glycosylation related proteins and GTs were also identified which allowed the selection of relevant lectins to detect resulting glycosylation by histochemistry and lectin blotting. These data suggested that ECM prepared under hypoxia had more mannosylated, fucosylated, sulfated and sialylated structures than ECM produced under normoxia.

5.1.3.1. Future directions

- The identified ECM and glycosylation-related proteins in hypoxia compared to normoxia require validation by Western immunoblotting. Lectin blotting identified changes in the mannosylation, fucosylation, and sialylation patterns of ECM that can be correlated to the differential expression of proteins bearing these glycans as potential PTMs.

- Alcian blue histochemistry results demonstrated morphological differences in presence of GAG moieties for ECM prepared under hypoxia and normoxia. Upon treatment of ECMs with heparinise I, II, III and Chondroitinase ABC, the GAG structures present on ECM can be ablated. The removal GAGs can be confirmed by Alcian blue. The differences in the expansion and differentiation of stem cells grown on the ablated and non-ablated ECM will provide details about the role of GAGs in the expansion of stem cells.

- Intracellular contamination was observed when the secreted ECM by MS-5 cells analysed by LC-MS. It will be useful to develop methods to minimise the intracellular contamination such as suicidal gene approach. This approach utilises a suicide gene that causes cell death through apoptosis and is widely used in treatment of various cancers (Freytag et al., 1998, Bonini et al., 2007). This approach when

introduced in feeder cells cultures could lead to cell death resulting in intact ECM with significantly less intracellular contamination.

- This work can be expanded for further understanding of biochemical organisation of ECM secreted by MS-5 cells. Knowledge about the constituents, either proteins or carbohydrates of ECM, could help in the design of bioactive and biomimetic scaffolds mimicking the *in vitro* organisation of ECM for the expansion of stem cells.

5.2. Overall conclusions

With an interdisciplinary approach, diverse roles of carbohydrates were explored using different biological cell models. The studies described in this thesis helped to clarify the roles of PTMs, natural polysaccharides and environmental conditions towards the vascular biology, immunology and stem cell biology. These studies also provided the future directions for further elucidation or study of these molecules towards exploring their therapeutics properties.

References

BONINI, C., BONDANZA, A., PERNA, S. K., KANEKO, S., TRAVERSARI, C., CICERI, F. & BORDIGNON, C. 2007. The suicide gene therapy challenge: how to improve a successful gene therapy approach. *Molecular Therapy,* 15**,** 1248-1252.

DENHARDT, D. T. & GUO, X. 1993. Osteopontin: a protein with diverse functions. *The FASEB journal,* 7**,** 1475-1482.

FREYTAG, S. O., ROGULSKI, K. R., PAIELLI, D. L., GILBERT, J. D. & KIM, J. H. 1998. A novel three-pronged approach to kill cancer cells selectively: concomitant viral, double suicide gene, and radiotherapy. *Human Gene Therapy,* 9**,** 1323-1333.

HOLTKAMP, A. D., KELLY, S., ULBER, R. & LANG, S. 2009. Fucoidans and fucoidanases—focus on techniques for molecular structure elucidation and modification of marine polysaccharides. *Applied microbiology and biotechnology,* 82**,** 1-11.

JONO, S., PEINADO, C. & GIACHELLI, C. M. 2000. Phosphorylation of osteopontin is required for inhibition of vascular smooth muscle cell calcification. *Journal of Biological Chemistry,* 275**,** 20197-20203.

MINAI-TEHRANI, A., CHANG, S.-H., KWON, J.-T., HWANG, S.-K., KIM, J.-E., SHIN, J.-Y., YU, K.-N., PARK, S.-J., JIANG, H.-L. & KIM, J.-H. 2013. Aerosol delivery of lentivirus-mediated O-glycosylation mutant osteopontin suppresses lung tumorigenesis in K-ras LA1 mice. *Cellular Oncology,* 36**,** 15-26.

PETTY, R. D., SUTHERLAND, L. A., HUNTER, E. M. & CREE, I. A. 1995. Comparison of MTT and ATP‐based assays for the measurement of viable cell number. *Journal of bioluminescence and chemiluminescence,* 10**,** 29-34.

TZIANABOS, A. O. 2000. Polysaccharide immunomodulators as therapeutic agents: structural aspects and biologic function. *Clinical microbiology reviews,* 13**,** 523-533.

VOGT, L. M., MEYER, D., PULLENS, G., FAAS, M. M., VENEMA, K., RAMASAMY, U., SCHOLS, H. A. & DE VOS, P. 2014. Toll-like receptor 2 activation by β2→1-fructans protects barrier function of T84 human intestinal epithelial cells in a chain length-dependent manner. *The Journal of nutrition***,** jn. 114.191643.

WANG, P., HENNING, S. M. & HEBER, D. 2010. Limitations of MTT and MTS-based assays for measurement of antiproliferative activity of green tea polyphenols. *PloS one,* 5**,** e10202.

YOSHINOBU, K., MAYUMI, K., KANA, M.-M., MIDORI, K., YOSHIKI, Y. & YASUHIRO, H. 2014. Osteopontin O-glycosylation contributes to its phosphorylation and cell-adhesion properties. *Biochemical Journal,* 463**,** 93-102.

APPENDIX 1

RECOMBINANT EXPRESSION OF OSTEOPONTIN IN *E. coli*

A1.1 Background

Expression and purification of human OPN in bacteria was carried out as a part of Chapter 2. However, this expressed OPN molecule was not used for the biological assays.

As an expression host, *E. coli* has no machinery to add PTMs in a similar fashion to mammals. Cloning, expression and purification of OPN in a bacterial system were undertaken in-house. For the in-house cloning of OPN, RNA was extracted from EPCs from donor human blood and primers were designed for the full-length OPN nucleotide sequences for isoform 1. OPN was successfully expressed and purified.

A1.2. Material and Methods

A1.2.1. Materials

Ficoll® Paque PLUS was bought from GE Healthcare Bio-Sciences (Piscataway, N.J., U.S.A.), red lysis buffer, human fibronectin, bovine serum albumin (BSA), FITC-labelled UEA-I lectin, isopropyl-α-D-thiogalactopyranoside (IPTG), anti-osteopontin (OPN) antibody produced in goat (catalogue number O7635) and monoclonal anti-HIS-HRP-labelled antibody against 6X histidine tag were bought from Sigma-Aldrich Co. (Wicklow, Ireland). Rabbit anti-chicken IgY-HRP polyclonal antibody was from Promega (Southampton, UK). Fibronectin coated six well plates were bought from BD Biosciences (Oxford, UK), endothelial growth media-2 (EGM-2) was from Lonza (Basel, Switzerland). 1,1,1'-dioctadecyl-3,3,3',3'-tetramethylindocarbocyanine-labelled Ac-LDL (DiI-Ac-LDL) and TRIzol® reagent and first strand cDNA synthesis was performed using SuperScript® III First-Strand Synthesis System (catalogue number 18080-051), nickel-nitrotriacetic acid (Ni-NTA) resin and SYBR® Safe DNA Gel Stain were from Life Technologies (Carlsbad, CA, U.S.A). RNA purification was done using RNeasy® Plus Mini Kit (catalogue number 74204) and gel extraction and purification was done using QIAquick® (catalogue number 28704) bought from QIAGEN. The restriction enzyme Sac1 was from Roche Molecular Biochemicals (Mannheim, Germany) while BamH1 enzyme and ligation kit were bought from Fermentas GmbH (Leon-Rot, Germany). pQE30 vector was from bought from QIAGEN. *E. coli* TOP10 F' (F'[lacIq Tn10(tetR)] mcrA Δ(mrr-hsdRMS-mcrBC) φ80lacZΔM15 ΔlacX74 deoR

nupG recA1 araD139 Δ(ara-leu)7697 galU galK rpsL(StrR) endA1 λ-) were bought from Life Technologies (UK). Ethylenediaminetetraacetic acid (EDTA) coated tubes were from BD Bioscience. All other reagents were from Sigma-Aldrich Co. and were of the highest grade available unless otherwise noted. All oligonucleotide primers were synthesized, and construct sequences were confirmed using the Eurofins MWG facility (Munich, Germany).

A1.2.2. Extraction of EPCs

Peripheral human venous blood was collected from a healthy donor into EDTA coated tubes following signed informed consent under a protocol approved by the National University of Ireland Galway Research Ethics Committee. The collected blood was processed immediately and the tube was kept at room temperature with continuous rocking on a compact digital rocker (Thermo Scientific) at 25 rpm. 20 mL of blood was added to each 50 μL conical tube and diluted (1:1) by adding 20 mL of Hank's balanced salt solution (HBSS). Peripheral blood mononuclear cells (PBMNCs) were isolated by Ficoll Paque density centrifugation at 345 x *g* for 30 min followed by deceleration without any braking applied (deceleration set to 0). The buffy coat layer containing mononuclear cells after centrifuge was carefully collected in a new 50 mL conical tube and centrifuged at 270 x *g* for 10 min at room temperature. After centrifugation, the pellet that was collected from the buffy layer and the RBC were lysed using RBC lysis buffer (155 mM NH_4Cl, 12 mM $NaHCO_3$ and 1 mM EDTA) (Figure A1.1). The progenitor cells were unaffected by the lysis buffer in the extraction procedure This was followed by another round of centrifugation at 270 x *g* for 10 min after which the supernatant was discarded. After three washes with PBS (pH 7.2), 1x 10^7 cells from buffy coat were plated on fibronectin coated 6-well plates in EGM-2 media. Cells were incubated for four days at 5% CO_2 at 37 ^{o}C and allowed to adhere to the fibronectin. Fresh EGM-2 was added and changed daily until day 7 when EPCs were used.

A1.2.3. Confirmation of EPCs

Cells were incubated with 5 μg/mL DiI-acLDL for 4 h at 5% CO_2 at 37 ^{o}C. The cells were washed in PBS twice and then fixed in 4% paraformaldehyde (PFA) for 15 min. The cells were washed for 10 min with gentle agitation in PBS containing 3%

BSA to remove the non-adherent cells. The cells were then incubated in 10 μg/mL of fluorescently labelled lectin UEA-I in 3% BSA for 1 h at room temperature. Once the cells were confirmed as dual positive for staining with UEA-I-FITC and Dil-acLDL, they were considered for RNA extraction.

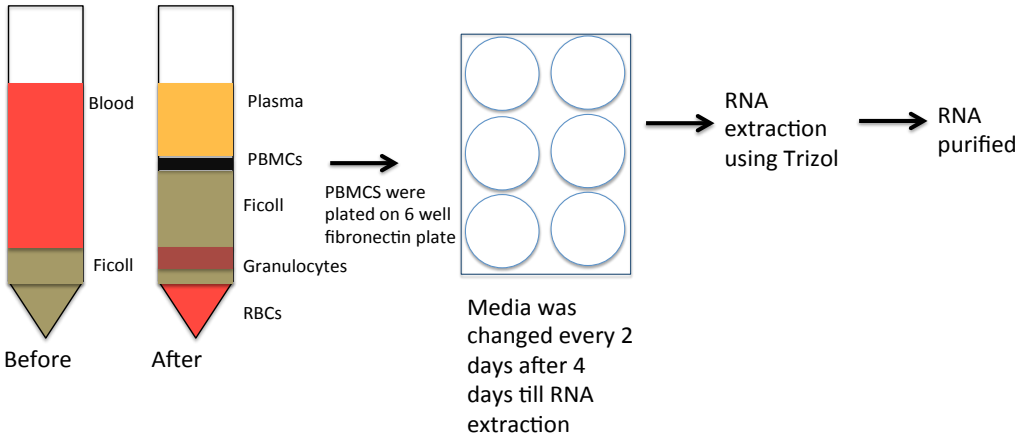

Figure A1.1. Schematic representation of the extraction of PBMCs from blood using Ficoll method followed by the identification of EPCs. RNA was extracted and purified from EPCs.

A1.2.4. Extraction of RNA and purification from monolayer of cells

The cell monolayer was rinsed with ice cold PBS once and the cells were lysed directly in the culture dish by adding 1 mL of TRIzol® reagent per 3.5 cm diameter dish and scraping with a cell scraper under the chemical extraction hood. The cell lysate was passed several times through a pipette and vortexed thoroughly. RNA was stored at -80 ^{o} C until further use.

RNA was thawed and gently warmed to 37 ^{o}C and was aliquoted 1 mL into RNase-free 1.5 mL microtubes. RNA purification was done using the RNeasy Plus Mini Kit (QIAGEN) following the manufacturer's instructions. Briefly, 0.2 mL chloroform was added per 1 mL extract and left for 3 min at room temperature. The tube was centrifuged at 4^{o} C at 11,000 x *g* for 15 min. After the centrifugation, the upper aqueous layer was carefully removed and added to a new 1.5 mL tube. To this new tube, 1 volume of 70% ethanol was added. The total volume was then transferred to an RNeasy MinElute spin column placed in a 2 mL collection tube and centrifuged for 15 s at 10,621 x *g*. The flow-through was discarded. The RNeasy MinElute spin

column was placed in a new 2 mL collection tube to which 500 mL Buffer RPE was added centrifuged for 15 s at 10,621 x *g* to wash the spin column membrane. The flow-through was discarded. The RNeasy MinElute spin column was then placed in a new 1.5 mL collection tube. 10 mL RNase-free water was directly added to the centre of the spin column membrane and it was repeated twice. The tube was centrifuged for 1 min at 14,100 x *g* to elute the purified RNA and stored at -80 ^{o}C.

A1.2.5. First-strand cDNA synthesis

Purified RNA was converted into cDNA using the SuperScript® III First-Strand Synthesis System following the manufacturer's instructions. Briefly, 1 μL of oligo $(dT)_{20}$ (50 μM) was added to 1 μg of total RNA and 1 μL of 10 μM dNTP mix (10 mM each dATP, dGTP, dCTP, dTTP at neutral pH) to make up a volume of 13 μL in RNAase-free water. The mixture was heated to 65 ^{o}C for 5 min and incubated on ice for at least 1 min. The contents were collected by brief centrifugation. 4 μL of the proprietary 5x First Strand buffer, 1 μL of 0.1 M DTT, 1 μL of RNaseOUT Recombinant RNase inhibitor was added to the same tube. The tube was incubated at 50 ^{o}C for 30 min and the reaction was stopped by heating at 70 ^{o}C for 15 min. To remove the RNA complementary to the cDNA, 2 U of *E. coli* RNase H was added to the mix and incubated at 37 ^{o}C for 20 min. This synthesized cDNA was used for amplification of the OPN gene transcript, SPP1.

A1.2.6. Gradient PCR and DNA purification

In order to optimise the PCR conditions, gradient PCR was performed using the SPP1 primers at temperatures 53, 55, 57, 59 and 61 ^{o}C where 2 μl of $MgCl_2$, 5 μL of 5x reaction buffer, 1 μL of primers (each 10 μM), 1 μL of 10 mM dNTPs, 0.5 Taq polymerase, (GMP grade) and 1 μL of cDNA were added in each PCR tube and 30 cycles of amplification were performed. Gradient PCR was also performed with primers with restriction enzyme sites (RE) for using the conditions from the first gradient PCR.

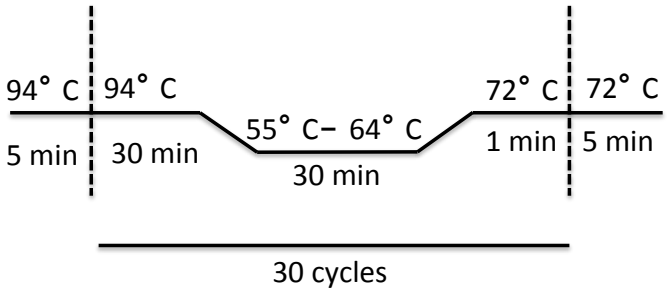

Figure A1.2. Conditions for gradient PCR. The optimized temperature was used for the further amplification steps.

DNA-agarose gel was used to separate the PCR products for analytical and preparative purposes. The matrix composition used for separation was 1% or 2% w/v agarose depending on the size of the PCR product. For visualisation, SYBR® safe at a dilution of 1:10,000 in agarose gel buffer was used. It was left to solidify completely before running the samples. Samples were prepared by addition of 6x loading dye and electrophoresed at 80 V for 1 h (approximately the time required for the loading dye to run off the gel (at least 1 cm). Gels were visualised using a UV transilluminator and recorded using a ChemiDoc® imaging system (Bio-Rad, Hercules, CA, USA).

To recover high quality of DNA and PCR products from the agarose gels, Qiagen QIAquick Gel Extraction kit and QIAquick PCR Purification kit were used, respectively. Purified DNA samples were prepared or electrophoresis by addition of 6x loading dye and again electrophoresed at 80 V for 1 h. Gels were visualised on a UV transilluminator briefly and the bands of interest were excised using a clean, sharp scalpel.

A1.2.7. Restriction digestion of vector and plasmid

The pQE30 vector was used for the transformations and cloning of the SPPI gene. The vector was digested with both restriction enzymes BamH1 and Sac1 at 37 ^{o}C together or one after one for the optimisation of the buffer conditions. The compatibility between buffers and restriction enzymes, Sac1 and BamH1, was tested. All the buffers and enzymes were stored in -20 ^{o} C.

Table A1.1. Buffer conditions used for the digestion of vector using restriction enzymes BamH1 and Sac1. All quantities expressed in μL.

	NEB Buffer 4	Fermentas Buffer	BamH 1	Sac1
Vector	2.5	2.5	2.5	2.5
BamH1	1.0	1.0	0.5	-
Sac1	1.0	1.0	-	0.5
Buffer	1.0	1.0	1.5	1.5
dd H20	4.5	4.5	0.5	0.5
Total	10.0	10.0	5.0	5.0

The uncut vector and the above mixes were run at 100 V on 1% agarose gel to find the optimal conditions and buffers. Thereafter, double digestion was made for the vector using both restriction enzymes with 2 μL each for 8 μL of vector with 5 μL Fermentas buffer making a total volume of 20 μL with 4.5 μL ddH_2O. The new digested product was run on 1% agarose gel and again gel purified using QIAquick Gel Extraction kit.

A1.2.8. DNA ligation

Sticky end ligation was made for the SPP1 DNA insert amplified with SPPI enzymes with RE sites into the pQE30 vector DNA. pQE30 is a 3.4 Kb vector while the 800 bp SPPI PCR product is 0.8 Kb. The ligation ratios for vector and inset were 1:1, 3:1 and 5:1. For using 10 ng of the vector, the corresponding amount of the PCR insert (for 1:1 ratio) was 10/3.4 = N/0.8 (i.e. 2.35 ng was made). Similarly, the other two ratios were calculated for DNA ligation. A total reaction volume of 20 μL was made for the ligation ratios and the positive and negative controls.

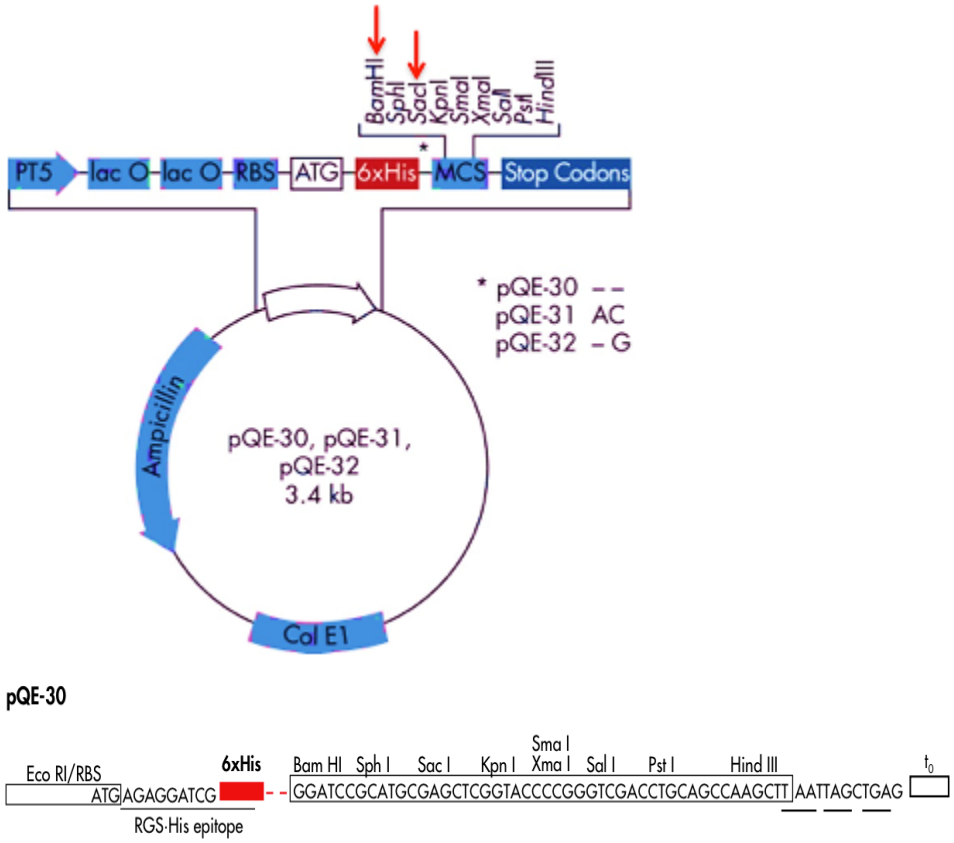

Figure A1.3. pQE 30 vector for N-terminal 6xHis tag constructs. PT5: T5 promoter, lac O: lac operator, RBS: ribosome-binding site, ATG: start codon, 6xHis: 6xHis tag sequence, MCS: multiple cloning site with restriction sites indicated, Stop Codons: stop codons in all three reading frames, Col E1: Col E1 origin of replication, Ampicillin: ampicillin resistance gene, lacIq, lacIq repressor gene. The restriction sites BamH1 and Sac1 chosen for the ligation are shown with red arrows.

For the band intensity method, the product of length and intensity of the band on the agarose gel was used to calculate PCR insert (Chandra and Wikel, 2005). PCR insert = 6 x 250, Purified vector = 6 x 800, Purified gel vector = 7 x 2000. For calculation purposes, molar ratios were considered.

Table A1.2. DNA ligation conditions using different ligation ratios of vector to PCR insert.

	Ratio 1:1 (μL)	Ratio 1:3 (μL)	Ratio 1:5 (μL)
dH_2O	2.4	0.10	1.01
Vector	0.5	0.25	0.25
Insert	1.1	1.65	2.74
T4 buffer	0.5	0.25	0.50
T4 ligase	0.5	0.25	0.50
Total	5.0	2.50	5.0

Different ratios (Table A1.2) were incubated for 30 min at 25 °C and each ligated product were used for transformation of competent cells.

A1.2.9. Transformation of *E. coli* by heat shock

Bacterial transformation was carried out with the ligation products by heat shock method (Froger and Hall, 2007). Five μL of the ligation mixes were added to thawed vials of competent cells (20 μL). The tubes were incubated on ice for 30 min, heat shocked at 42 °C for 30 s and incubated on ice for 2 min. Following this, 250 μL of super optimal broth with catabolite repression (SOC media) (2% tryptone, 0.5% yeast extract, 10 mM NaCl, 2.5 mM KCl, 10 mM $MgCl_2$, 10 mM $MgSO_4$, and 20 mM glucose) with antibiotics (ampicillin and tetracycline) was added to the heat shocked cells and was shaken at 37 °C for 1 h. After an hour, the suspension was plated on LB plates and incubated at 37 °C overnight. The following day, glycerol stocks of the positive clones were prepared and stored in -80 °C.

A1.2.10. Transformation of *E. coli* strain by electroporation

Competent cells were thawed on ice. A 1.5 μL centrifuge tube and a 0.2 cm electroporation cuvette were also placed on ice to pre-cool. To the ice-cold 1.5 μL tube, 100 μL of the competent cells and 2 μL of DNA were added. The mixture was incubated for 1 min on ice and transferred to ice cold electroporation cuvette. The cuvette was brought to the chamber slide of the electroporator (MicroPulser® E2). Cells were pulsed at 3kV/cm for 2-3 s 3 times. After pulsing, the cells were quickly

placed on ice and 1 mL of SOC media with antibiotics was added. The cells in SOC were then transferred to a 20 mL tube. The tube was shaken gently at 37 ^{o}C for 1 h to help increase cell survival after transformation and improve the efficiency of the transformation. For the positive selection, the media and the plates were supplemented with the same antibiotics, as were in the SOC media. For longer storage, glycerol stocks of the clones were prepared and stored in -80 ° C.

A1.2.11. Colony PCR

E. coli cells transformed with vector containing the desired PCR insert were grown in SOC for 1 h and later were spread on agar plates at three different dilutions; 1:1, 1:2 and 1:5. The plates were incubated at 37 ^{o}C for at least 16 h (overnight) to form colonies. The following morning, positive single colonies from different plates were picked, streaked onto new agar plates and used to perform colony PCR (Clackson, 1989) using the SPP1 primers. Four such positive clones from the colony PCR streaked on the agar was regrown overnight and LB media (10 g tryptone, 5 g yeast extract, and 10 g NaCl in 950 mL deionized water) overnight with antibiotics for the plasmid extraction.

A1.2.12. Plasmid DNA purification

Plasmid DNA purification was performed for four selected positive clones (clones 6, 12, 15 and 21) using manufacturer's instructions. The protocol was performed for 10 mL of overnight cultures of *E. coli* in Luria-Bertani (LB) media. Three different buffers provided with the kit were used mixed step by step, added to the cell pellet and poured over the spin columns. These steps were performed to wash DNA before its elution. In the final step, pure DNA is eluted using 50 uL of elution buffer provided in the kit. Clone 21 was sent for sequencing at Eurofins MWG facility to confirm the right insert was present in the plasmid.

A1.2.13. Expression and purification of protein

100 mL of pre-warmed liquid LB medium (including antibiotics) was inoculated with 1 mL of the overnight cultures of transformed cells and grown at 37 °C for 30 min with vigorous shaking, until the absorbance reached 0.5–0.7 at 600 nm. An aliquot (1 mL) from this culture was saved as the non-induced control while the rest

of the media was induced by adding IPTG to a final concentration of 1 mM for the protein expression as shown in Figure A1.4. The cultures were grown overnight and then transferred to 50 mL tubes. The cells were harvested by centrifugation at 5,000 x *g* for 1 min and the supernatants were discarded. Cell pellets obtained in this step were then lysed.

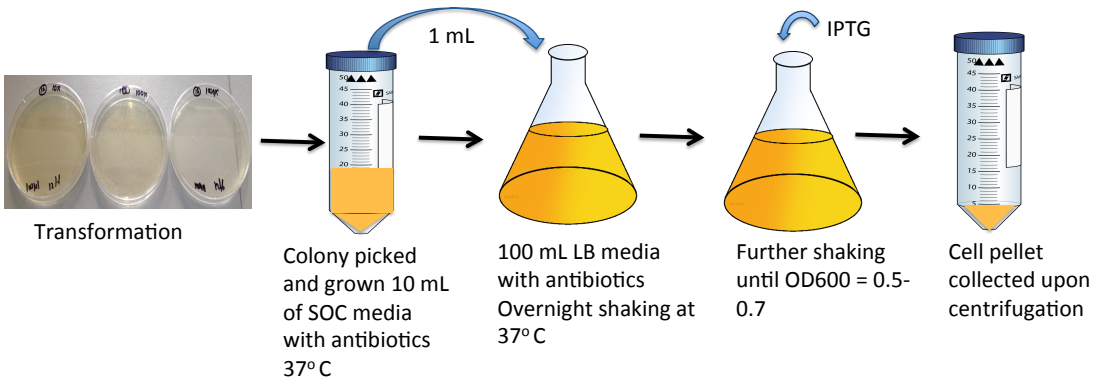

Figure A1.4. Schematic representation of steps of transformation, cell growth, protein induction and pellet collection.

A1.2.14. Cell lysis and preparation of clear lysate for protein purification

The cell pellet was re-suspended in 10 mL of equilibration buffer (50 mM Na_2HPO_4, 250 mM NaCl, 250 mM imidazole, adjusted to pH 7.4 with phosphoric acid). The cells were incubated with 1 mg/mL of lysozyme and 10 μg/mL DNase for 30 min on ice. The cells were further disrupted by a sonication step using six 6 s bursts at 40 kHz on ice to completely lyse the cells. The cells were disrupted with a 3 mm micro-tip sonicator (Sonics & Materials Inc., Newtown, CT). These completely lysed cells were centrifuged at 1700 x *g* for 30 min at 4 ^{o}C to pellet any insoluble material. The cleared cell lysate was transferred to fresh 50 mL conical tubes and passed through 0.2 μM cellulose acetate filter to remove cell debris and stored 4 ^{o}C until use.

For the purification steps, Ni-NTA beads were washed intensively in elution buffer and equilibration buffer. Following washes, the supernatants were mixed with 1 mL of the Ni-NTA beads for 30 min at room temperature with tubes in continuous circular motion. The columns with dimensions (0.7 x 10 cm) were packed with Ni-NTA beads with samples and allowed to settle. Upon settling of the beads, flow through was collected. 2 mL of the equilibration buffer was added to the bed of

beads in the column and collected. It was followed by five washes with equilibration buffer and 40 mM imidazole buffer. Sample was eluted with 2 mL elution buffer and four fractions were collected. The used beads were stored in elution buffer for regeneration.

A1.2.15. Protein quantification, SDS-PAGE and Western blot analysis

The purified protein was quantified in a microtitre plate using the Pierce™ Coomassie Plus (Bradford) Protein Assay Kit. Bovine serum albumin (BSA) was used as the reference protein and protein concentration of individual samples was determined from this standard curve The purified protein fractions were separated on NuPAGE 4–12% Bis-Tris gels using MOPS running buffer at 150 V constant for approximately 1 h. Gels were stained with 0.05% (w/v) Coomassie G-250 in a fixative solution containing 30% ethanol and 10% acetic acid for an hour. Stained gels were then partially de-stained with distilled de-ionized water (ddH_2O) until the protein bands became clear. Gels were imaged using a ChemiDoc® imaging system (Bio-Rad).

In parallel, protein samples separated in 4-12% gels were electro-transferred to 0.22 μm PVDF membrane using the semi-dry method (Froger and Hall, 2007). Before the transfer, PVDF membranes were washed in methanol and rinsed in transfer buffer. Cathode (0.3M aminocaproic acid, 0.03M Tris, 0.0375% SDS) and anode (0.3M Tris, 0.1M glycine, 0.0375% SDS) buffers facilitated the transfer of the proteins from the gel to the PVDF membrane. Semi-dry transfer was performed at 1.5 mA/cm2 for 30 min. Membranes were blocked directly after transfer with 1.5% BSA in TBST (20 mM Tris-HCL, 180 mM NaCl and 0.05% Tween® 20) for 1 h at room temperature. Following washing, membranes were incubated with 1:1000 dilution of anti-OPN and anti-HIS antibodies prepared in TBST. The blots were incubated with the primary overnight at 4 °C and washed in TBST for 10 min for three times. Blots were incubated with secondary antibodies against mouse or rabbit conjugated to HRP diluted 1:5,000 in TBST for 1 h at room temperature. Detection was performed by enhanced chemiluminescence (ECL) using WesternBright™ ECL substrate. The blots were imaged using a ChemiDoc® imaging system (Bio-Rad).

A1.3. Results

EPCs were purified from human blood and total RNA was extracted and used for further cDNA synthesis, cloning, expression and purification of OPN.

A1.3.1. Sequence of human OPN

Human OPN genomic sequence information (accession number J04765) was obtained from the National Centre for Biotechnology Information (NCBI, www.ncbi.nlm.nih.gov). The NCBI database revealed that 5 isoforms have been reported for human OPN to date (Figure A1.5). Although OPN is encoded by a single gene copy, different isoforms that arise both from alternative translation and alternative splicing (Gimba and Tilli, 2013).

Figure A1.5. Multiple sequence alignment for OPN protein isoforms.

To design the primers for the isoform 1, nucleotide sequence of OPN isoform 1 retrieved from NCBI (accession number J04765) was translated to protein and aligned to protein sequence from Uniprot.

```
tr              ----------------IPVKQADSGSSEEKQLYNKYPDAVATWLNPDPSQKQNLLAPQTL 44
NCBI            MRIAVICFCLLGITCAIPVKQADSGSSEEKQLYNKYPDAVATWLNPDPSQKQNLLAPQTL 60
                                 ****************************************

tr              PSKSNESHDHMDDMDDEDDDDHVDSQDSIDSNDSDDVDDTDDSHQSDESHHSDESDELVT 104
NCBI            PSKSNESHDHMDDMDDEDDDDHVDSQDSIDSNDSDDVDDTDDSHQSDESHHSDESDELVT 120
                ************************************************************

tr              DFPTDLPATEVFTPVVPTVDTYDGRGDSVVYGLRSKSKKFRRPDIQYPDATDEDITSHME 164
NCBI            DFPTDLPATEVFTPVVPTVDTYDGRGDSVVYGLRSKSKKFRRPDIQYPDATDEDITSHME 180
               ************************************************************

tr              SEELNGAYKAIPVAQDLNAPSDWDSRGKDSYETSQLDDQSAETHSHKQSRLYKRKANDES 224
NCBI            SEELNGAYKAIPVAQDLNAPSDWDSRGKDSYETSQLDDQSAETHSHKQSRLYKRKANDES 240
                ************************************************************

tr              NEHSDVIDSQELSKVSREFHSHEFHSHEDMLVVDPKSKEEDKHLKFRISHELDSASSEVN 284
NCBI            NEHSDVIDSQELSKVSREFHSHEFHSHEDMLVVDPKSKEEDKHLKFRISHELDSASSEVN 300
                ************************************************************
```

Figure A1.6. Alignment of translated OPN sequences to OPN sequence retrieved from NCBI.

A1.3.2. Sequences of primers for OPN with and without restriction sites

The SPP1 gene isoform 1 primers with and without restriction sites for restriction enzymes Sac1 and BamH1 were designed using the Primer 3 online design tool (Whitehead Institute for Biomedical Research, http://primer3.ut.ee/) (Table A1.3). The primers with RE were selected to be compatible with the restriction sites on the pQE30 vector.

Table A1.3. Primers without or with RE sites for the amplification of the SPPI gene

Primers	**Sequences**	**Tm (°C)**	**Mr (g/mol)**	**GC (%)**
SPP1 FP	5’ ATACCAGTTAAACAGGCTG 3’	52.4	5820	42.1
SPP1 RP	5’ ATTGACCTCAGAAGATGCAC 3’	55.3	6110	45
SPP1 FP + RE	5’ GGATCCATACCAGTTAAACAG 3’	59.3	7329	41.7
SPP1 RP +RE	5’GATGAGCTCATTGACCTCAGAAGATG 3’	63.2	8019	46.2

A1.3.3. Quantification of purified RNA and cDNA synthesis

The concentration of isolated total RNA extracted from primary EPCs was 9.2 ng/µL. One µg of RNA was transcribed into cDNA. The cDNA template was used

for testing SPP1 primers and selecting the best conditions for the further amplifications.

A1.3.4. Optimised gradient PCR for SPPI primers with and without RE site

A gradient PCR was performed from 55 to 61 ^{o}C alongside the full-length gene that was considered as positive control (Figure A1.3). 53 °C and 61 ^{o}C were selected and subjected to PCR again with total reaction volume of 100 μL and selected, purified upon excision from agarose gel and sequenced which confirmed the right sequence insert for the amplification performed at 61 ^{o}C (Table A1.4). The gradient PCR provided the optimal conditions for the downstream steps.

Table A1.4. Concentrations of the purified PCR products

Samples	Concentration (ng/μL)	260/280	260/230
53^{o} C	107	1.85	2.29
61^{o} C	11.2	1.74	1.7

Gradient PCR was performed for 61 °C purified samples with new primers. The amplified product at 58 °C using 61 °C samples was a selected further round. PCR was performed for 58 °C sample to obtain increased yield (Figure A1.8).

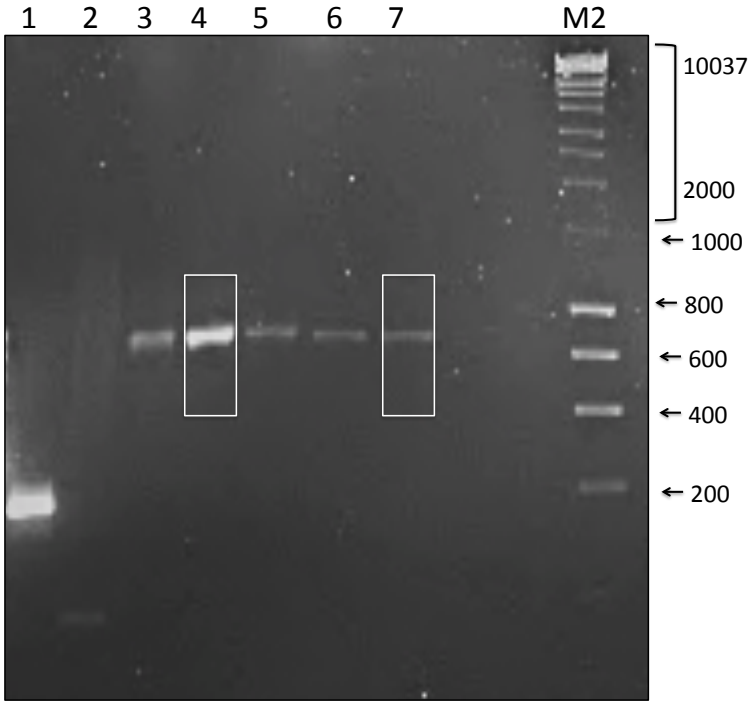

Figure A1.7. Gel electrophoresis of PCR products using SPP1 primers for EPC extracted RNA. Two ladders 100 bp and 1000 bp were run along the samples. Lane 1 is the positive control (HeLa cell RNA and β actin primers), lane 2 is another positive control (HUVECs RNA and SPP1 primers), lane 3, 4, 5, 6 and 7; EPC RNA amplified using SPP1 primers at 55, 53, 57, 59 and 61 °C temperatures, respectively.

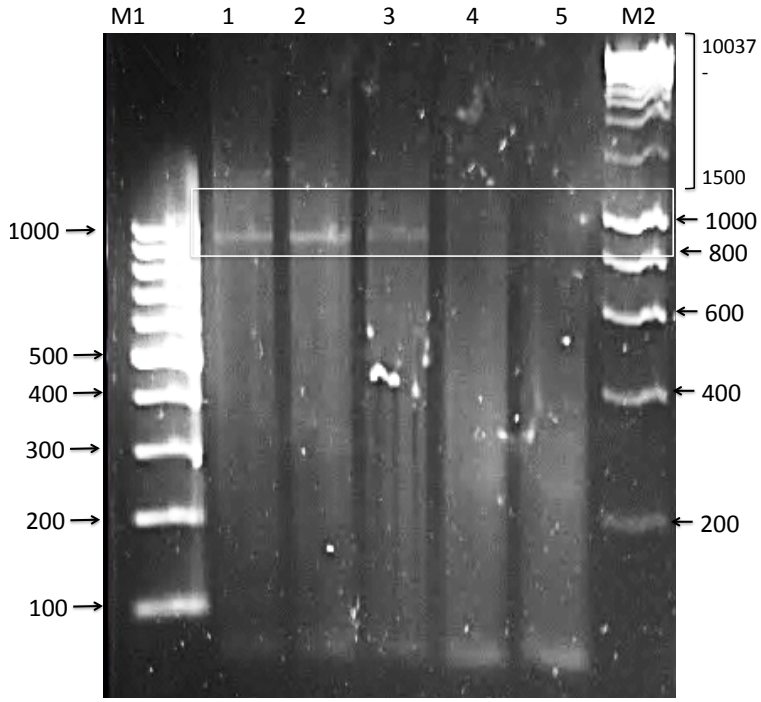

Figure A1.8. Gel electrophoresis of gel purified template of 61 °C samples using gradient PCR products using SPP1 primers with RE sites. EPC RNA (61 °C samples) amplified using SPP1 primers with RE sites at 56, 58, 61, 64 and 66 °C temperatures.

A1.3.5. Ligation, transformation and cloning

Before the ligation of the amplified PCR insert with primers including RE sites into the pQE30 vector, the restriction enzymes were tested with different buffer conditions to ensure efficiency and compatibility with the buffer. The stock concentration of pQE30 vector was 110 ng/μL. Upon the digestion of the vector with the restriction enzymes, the vector and the digested products were separated on 1% agarose gel (Figure A1.9). Figure A1.9 lane 1 shows the uncut vector while lanes 2-5 were used to run the digested vector with restriction enzymes sequentially. The Fermentas buffer was found to be optimal for the double digestion (lane 3 and lane 5) as the NEB 4 (lane 2 and 4) because digestion with Sac 1 in NEB buffer in lane 2 led to multiple bands on agarose gel.

Prior to the ligation step, double digestion of the vector was performed with the vector using restriction enzymes in Fermentas buffer. This digested vector was

ligated to the PCR insert. The vector with PCR insert was transformed into the *E. coli* cells either via electroporation or heat-shock method. The transformed cells were grown on the agar plates with the appropriate antibiotics overnight. The positive colonies were picked and colony PCR was performed using the SPP1 primers (Figure A1.10). All of the selected clones were re amplified and separated on agarose gel (Figure A1.11). Clone 21 had a concentration of 34.2 ng/mL.

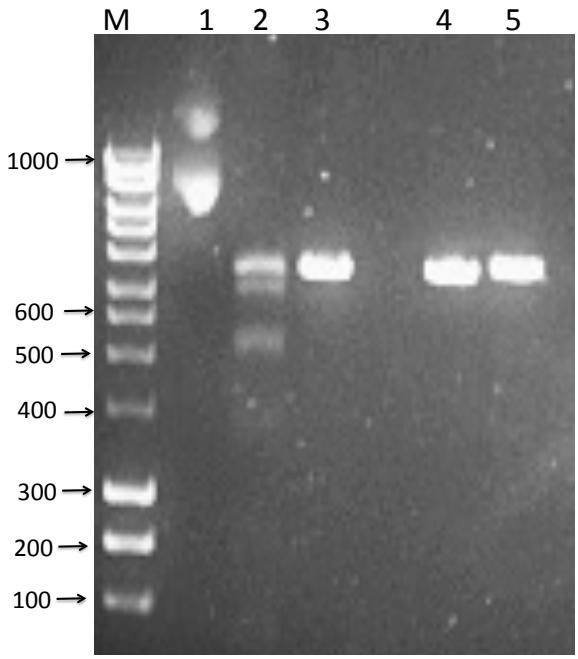

Figure A1.9. Gel electrophoresis of pQE30 vector (lane 1) and the digestion products after cutting it with Sac1 in NEB buffer 4 alone (lane 2), BamH1 in Fermentas buffer (lane 3), Sac1 and BamH1in NEB buffer 4 (lane 4) and Fermentas buffer (lane 5).

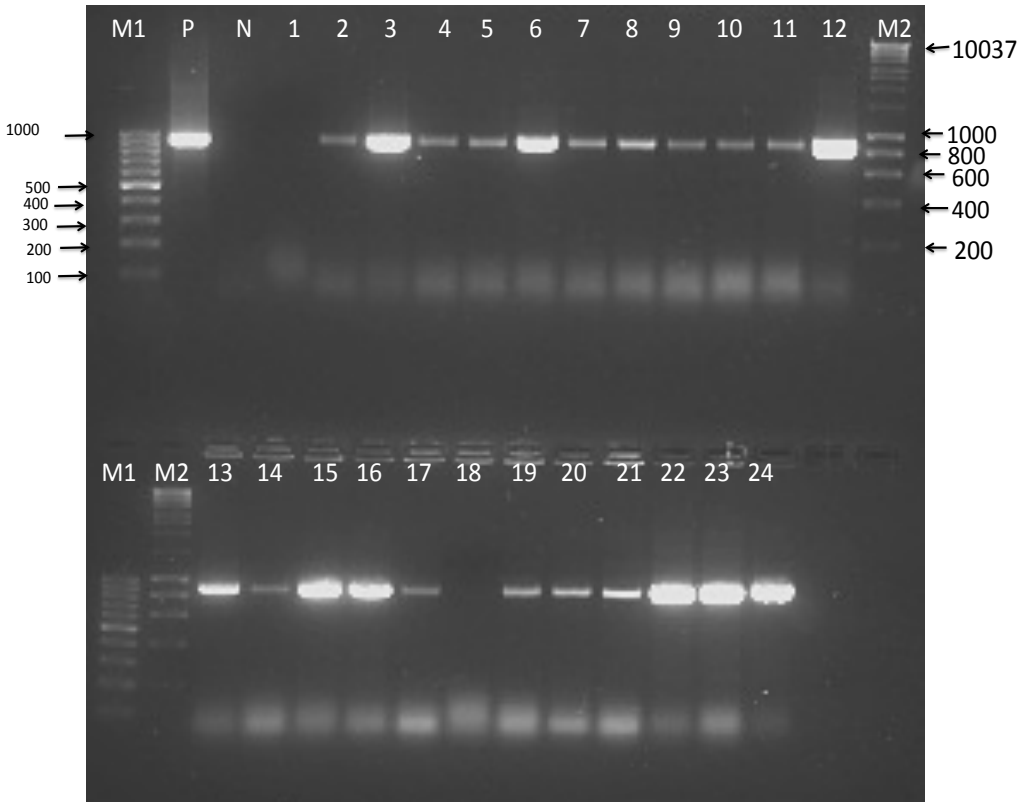

Figure A1.10. Gel electrophoresis of colony PCR products using SPP1 primers. 100 bp marker (M1) and 1000 bp marker (M2) ladders, positive control (P), negative control (N) and clones from (1-24) were separated on 1% agarose gel.

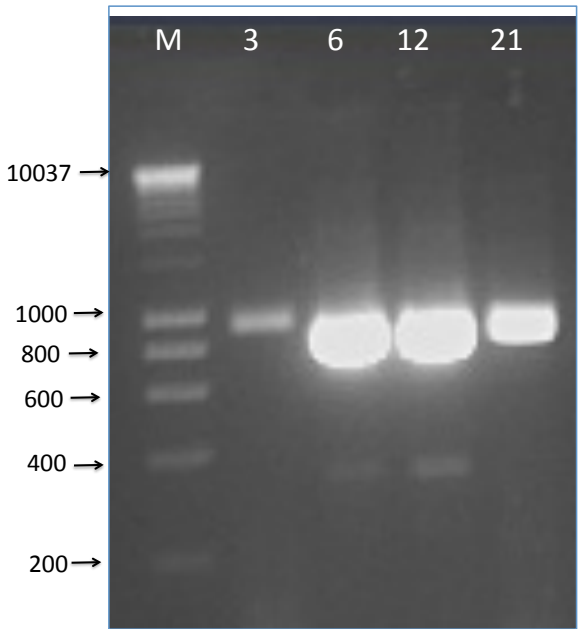

Figure A1.11. (A) Gel electrophoresis of colony PCR products using SPP1 primers. 100 bp (M1) ladder and four selected clones were separated on 1% agarose gel.

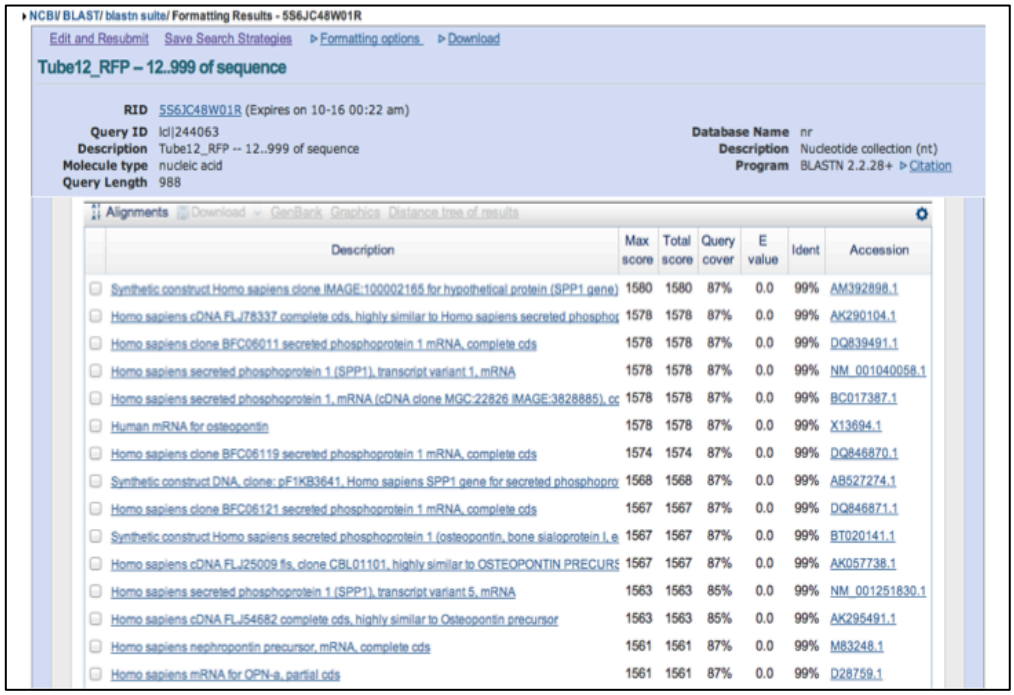

Figure A1.12. Sequencing results used for the BLAST analysis of clone 21.

A1.3.6. Protein purification and confirmation of protein

Clones (3, 6, 12 and 21) were induced for protein expression. The gene product was purified on a Ni-NTA and then quantified by Bradford assay was carried out. Ni-NTA provides an efficient and fast tool for the affinity purification of recombinant proteins. It is based on the high affinity binding of six consecutive histidine residues to the immobilised nickel ions.

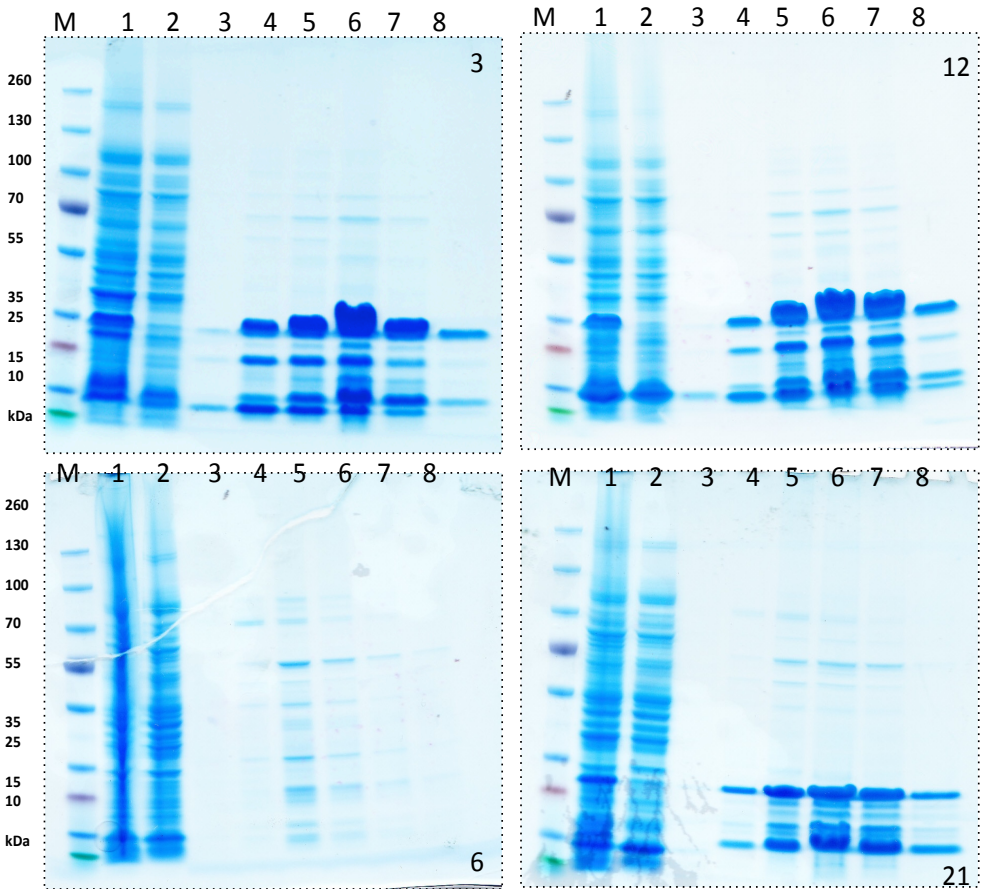

Figure A1.13. SDS-PAGE was carried out for all the clones containing the correct insert (3, 6, 12 and 21). Gels show whole cell lysate after sonication (lane 1), flow through (lane 2), wash 1 (lane 3), wash 2 (lane 4), and elutions 1- 4 (lane 4- 8).

The purified products of all selected positive clones and their respective un- purified lysates were electrophoresed on 4-12% Bis-Tris gels along the positive controls for HIS tag protein and OPN. Anti-HIS antibody was used for the detection of purified protein with HIS tag. A single-chain variable fragment (scFv) is a fusion protein, a non-covalent heterodimer made of the variable regions of the heavy (V_H) and light chains (V_L). A His-tagged scFv was used as the positive control for the HIS tag antibody (Figure 1.14, A). Anti-OPN antibody Western blotting confirmed that the purified protein was OPN (Figure 1.14, B).

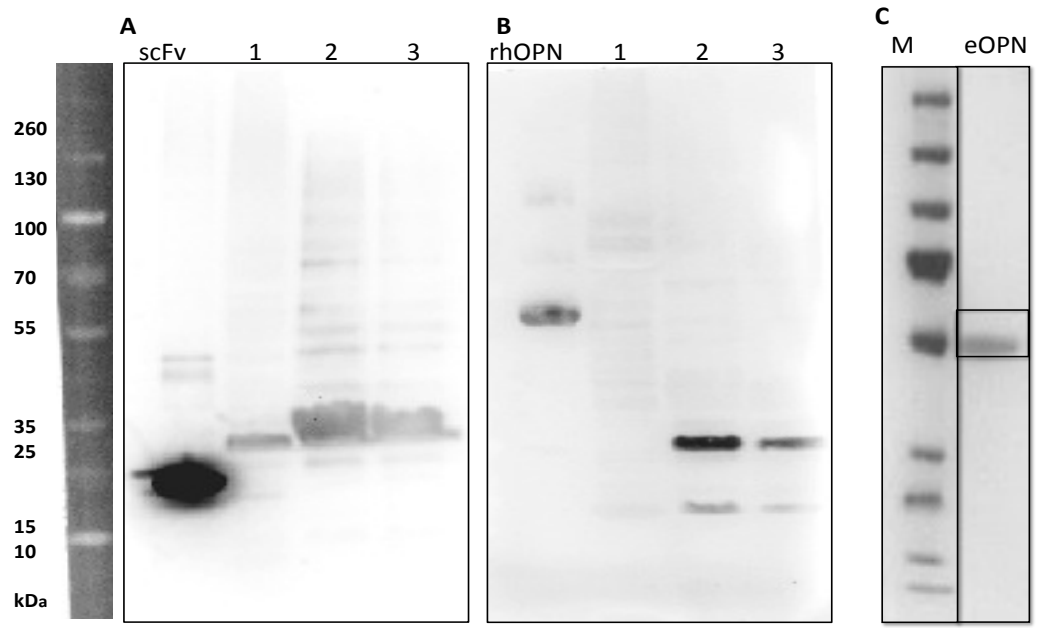

Figure A1.14. Western blot was performed using an anti-His antibody (A), where scFv with HIS tag was used as the positive clone, elution fraction 2 (lane 1) and elution fraction 3 (lane 2) and rhOPN was detected using anti OPN antibody and used as positive control (B) and commercial eOPN (C).

A1.4. Discussion

Despite successful extraction and purification of in house bacterially expressed OPN (eOPN1), it was not used in biological assays, as there is no definitive platform to test the biological activity of eOPN. Both eOPN and eOPN1 when separated on 4-12% SDS-PAGE gels resolved at different apparent molecular masses (Figures 2.4, 2.5 and A1.14 (C) and Figure A1.14B and C, respectively). The differences in eOPN Mr may be due to the source of OPN RNA and/or variation of protein translation and PTM events such as splicing, sulfation, glycosylation and proteolytic processing. The OPN gene has alternative translation start site and thus there occurs variants of OPN.

A1.5. References

CHANDRA, P. K. & WIKEL, S. K. 2005. Analyzing ligation mixtures using a PCR based method. *Biological Procedures Online,* 7**,** 93-100.

CLACKSON, T. 1989. Direct clone characterization from plaques and colonies by the polymerase chain reaction. *Nucleic Acids Research,* 17**,** 4000-4000.

FROGER, A. & HALL, J. E. 2007. Transformation of plasmid DNA into E. coli using the heat shock method. *Journal of Visualized Experiments: JoVE*.

GIMBA, E. & TILLI, T. 2013. Human osteopontin splicing isoforms: known roles, potential clinical applications and activated signaling pathways. *Cancer Letters,* 331**,** 11-17.

APPENDIX 2

ANTI-ANGIOGENIC PROPERTIES OF OLIGO- AND POLY-SACHRIDES

A2.1. Introduction

Endothelial cells are the building blocks for angiogenesis and vasculogenesis. They form the inner lining of a blood vessel and provide an anticoagulant barrier between the vessel wall and blood. Angiogenesis occurs in a highly regulated fashion during normal physiological events while aberrant angiogenesis can occur in a number of pathological states. In both conditions, angiogenesis requires endothelial cell proliferation, migration and tube formation. The acquisition of an angiogenic phenotype is believed to be a critical event in the progression of tumours. HUVECs are a model system for the study of the regulation of endothelial cell function and the role of the endothelium in the response of the blood vessel wall to stretch, shear forces and angiogenesis (Bouïs et al., 2001, Fajardo, 1989).

Polysaccharides from different sources are known to possess broad-spectrum therapeutics properties (Section 3.1). They are also been currently explored for their anti-angiogenic properties (Sagar and Yance, 2006). Six oligo- and polysaccharides that were assessed for their potential immunomodulatory effects in Chapter 3 have been tested for their effects on endothelial cells their angiogenic properties.

A2.2. Material and methods

A2.2.1. Materials

Materials were as per section 2.1.1. In addition, saputin-1,3-methyladenine (3-MA) and crystal violet solution was bought from Sigma-Aldrich Co. (Wicklow, Ireland) and necrostatin-1 (Nec-1) was from Cayman Chemical Company (MI, U.S.A.). Anti-caspase-3 antibody (#9662) was from Cell signalling (Danvers, MA, U.S.A) and acetyl Asp-Glu-Val-Asp 7-amido-4-methylcoumarin (DEVD-AM) was from Peptide Institute Inc. (Japan). Transwell chambers (pore size 8.0 μm) were from Costar, Corning Inc., (NY, U.S.A).

A2.2.2. Cell culture

HUVECs were grown in the EGM-2 media supplemented with the provided Singlequot cocktail. Cells were passaged with 0.25% trypsin and 1 mM EDTA every 3-4 days and culture and were replaced with fresh EGM-2 media. Confluent, serum-

deprived HUVECs cells in *passages* 5 to 10 were used in the studies described below.

A2.2.3. Proliferation assay

HUVECs with a density of 1 x 10^4 cells per well in 200 μL of EGM-2 media were plated for overnight to adhere. Next day, SRM was then changed carefully without disturbing the cells and replaced with different concentrations of oligo and poly-saccharide in SFM (10, 100 and 500 μg/mL). The cells were incubated for 24 and 48 h. MTT at concentration of 5 μg/mL (1:10 of the cell suspension media) was added to the media. The plate was incubated for 5 h. The plate was observed under microscope to see formed purple formazan. The formed formazon was dissolved by adding 200 μL of isopropanol. The plate was shaken for 5 min and the absorbance was read at 570 nm. Data was analysed for the percentage inhibition of cell proliferation. The inhibition ratio (*I*%) was calculated by the equation, $I\% = (1 - (A_{treated} - A_{blank})/(A_{control} - OD_{blank})) \times 100\%$, and expressed as the average of five experiments. The cells were also imaged under light microscope (10X).

A2.2.4. Matrigel® assay

Matrigel®, thawed at 4 °C overnight (50 μL), was aliquoted into a 96-well plate and allowed to stand at room temperature for 60 min. HUVECs (5 x 10^4/well) after trypsinization were plated onto polymerized Matrigel® in triplicate wells with optimised concentration of 10 μg/mL of polysaccharides were plated. The plate was incubated at 37 °C at 5% CO_2 for 24 h and tubule formation in the Matrigel® was observed under the light microscope.

A2.2.5. Transwell migration assay

A sub-confluent T-75 cm^2 flask of HUVECs was serum-starved for 24 h prior to use in migration assay. The cells were harvested using trypsin, centrifuged at 500 *g* for 5 minutes to create a pellet. The cell pellet was re-suspended in serum-free media. 100 μL of 30 x 10^4 cells/mL was added to the upper chamber of the transwell (Figure A2.1). 600 μL of serum free EGM-2 to lower chamber was added with migratory stimulus (e.g. 10 μg/mL of polysaccharides along the positive and negative

controls) was added on the lower chamber. The plate was incubated at 37 °C at 5 % CO_2 for 24 h. The supernatants were discarded and the membranes were fixed with 4% formaldehyde for 20 min. The cells from upper well were swabbed using cotton buds. The wells were washed with PBS and 100 µL of methanol was added to permeabilize the cells. The transwells were washed with PBS to remove excess methanol. This was followed by addition of 500 µL of 25 % crystal violet to new 24 well plates and the transwells were immersed into it for 15 min for staining. The transwells were washed with PBS until no stain came off. The transwells were air-dried and imaged for migratory cells across the transwell membrane. The stained cells on the transwell were then solubilized in 10 % acetic acid and absorbance was measured at 595 nm.

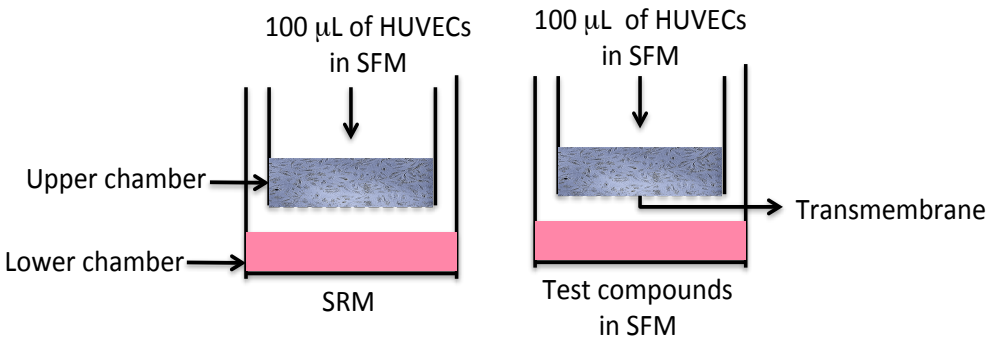

Figure A2.1. Schematic illustration of experimental setup for transwell migration assay.

A2.2.6. Caspase 3 assay

HUVECs were seeded at a density of 10^5 in T-25 cm^2 flasks. SRM was replaced with SFM different concentrations polysaccharides (10 and 100 µg/mL) and incubated for 24 and 48 h. Cells were imaged using light microscopy before harvesting and were transferred t into 15 mL tubes. The cell pellet was collected by centrifuging the tube at 1500 rpm for 5 min. After carefully removing the supernatant, the pellet was resuspended in 1 mL ice-cold PBS. Cells were collected by centrifugation at 10,000 *g* for 3 min with slow acceleration and the medium was removed. The cell pellet was resuspended in 50 µL of PBS and frozen rapidly by transferring them directly into microtitre plate, which was already frozen at -80 °C. The cells were stored at -80 °C until required.

50 μL of buffer (100 mM HEPES (pH 7.25), 10% sucrose, 0.1% CHAPS, 1 mM dithiothreitol (DTT), 0.1% NP-40) containing 50 μM DEVD-AMC was added to each well. Substrate cleavage leading to the release of free AMC (excitation 355 nm, emission 460 nm) was monitored over 3 h at 37 °C. Fluorescence units were converted to nmoles of AMC released using a standard curve generated with free AMC. Bradford assay was performed to determine protein concentration of every sample.

A2.2.7. Cell death inhibition assay

The cells were plated as per section A2.2.2 for cell death inhibition assay. Different cell death inhibitors such as Nec-1, 3 MA and spautin were incubated with cells prior the addition of oligo- and polysaccharides.

A2.2.8. ELISA for cytokine release

ELISA was performed as described in section 3.2.5 (Chapter 3) to quantify IL-6 and TNF-α concentrations in the supernatants collected from HUEVCs upon incubation with 10 μg/mL of oligo- and polysaccharides.

A2.2.9. Pathway analysis

HUEVCs were pre-treated with different (10, 100 and 500 μg/mL) concentrations of oligo- and poly- saccharides for 24 h. After 24 h, cells were lysed using RIPA buffer and quantified. The HUVEC lysates (50 μg) were separated on 4-12% gradient SDS-PAGE gels and transferred to PVDF membranes as per details (Section 2.2.9). The membrane was probed with primary antibodies caspase 3 and Bcl-xL. β-actin was used as the loading control. The appropriate goat secondary antibodies conjugated to horseradish peroxidase were obtained from Pierce. Protein bands were visualized by using the ECL Western Blot chemiluminescence's reagents Supersignal (Pierce).

A2.3. Results

A2.3.1. Inhibition of HUVECs

A concentration range of oligo- and polysaccharides (10, 100 and 500 μg/mL) were incubated with HUVECs for 24 h and 48 h to assess their effects on the HUVEC proliferation. The results showed a significant difference in cell proliferation between the oligo- and polysaccharides treatments and time points. It was observed that test compounds treatments at higher concentration at 48 h had inhibitory effects on cell proliferation. MAN had the maximum inhibitory effects on the cell proliferation at 100 μg/mL of 26.4 % and 86.5 % at 24 h while at 500 μg/mL concentration led to 58.9 % and 93.4 % cell inhibition at 48 h. FUC at 100 μg/mL led to cell inhibition to 44.35 % and 74.1 % at 24 h and 48 h while FUC at 500 μg/mL led to 74.1 % and 78.8 % cell inhibition at 24 h and 48 h respectively. While xGLU and HGL led to increased cell proliferation at 10 μg/mL by 15 % and 8.3 % at 24 h and FUC and HGL, inhibited the cell proliferation (Figure A2.A1).

Before the addition of MTT, the cells were carefully imaged under light microscope and disrupted cell morphology was observed (Figure A2.1B). FUC at 500 μg/mL concentration, formed mesh-like structures that extended and lost contact with neighbouring cells. MAN at both 100 and 500 μg/mL led to clumping of cells and may be cell death. For HGL and xGLU, the cells were dispersed in the well losing the contact among cells.

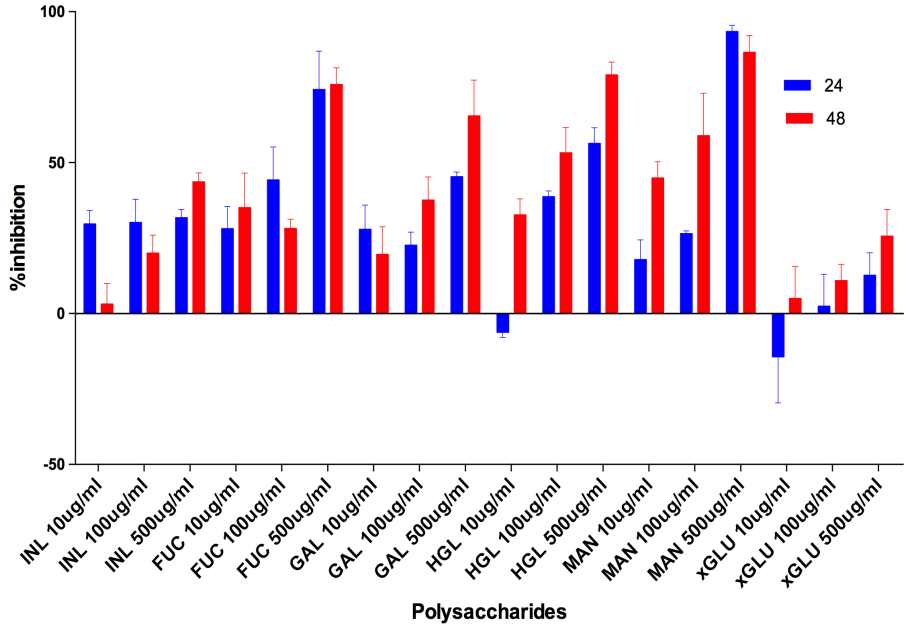

Figure A2.2A. Percentage inhibition of cell proliferation upon incubation with oligo- and polysaccharides at 10, 100 and 500 μg/mL.

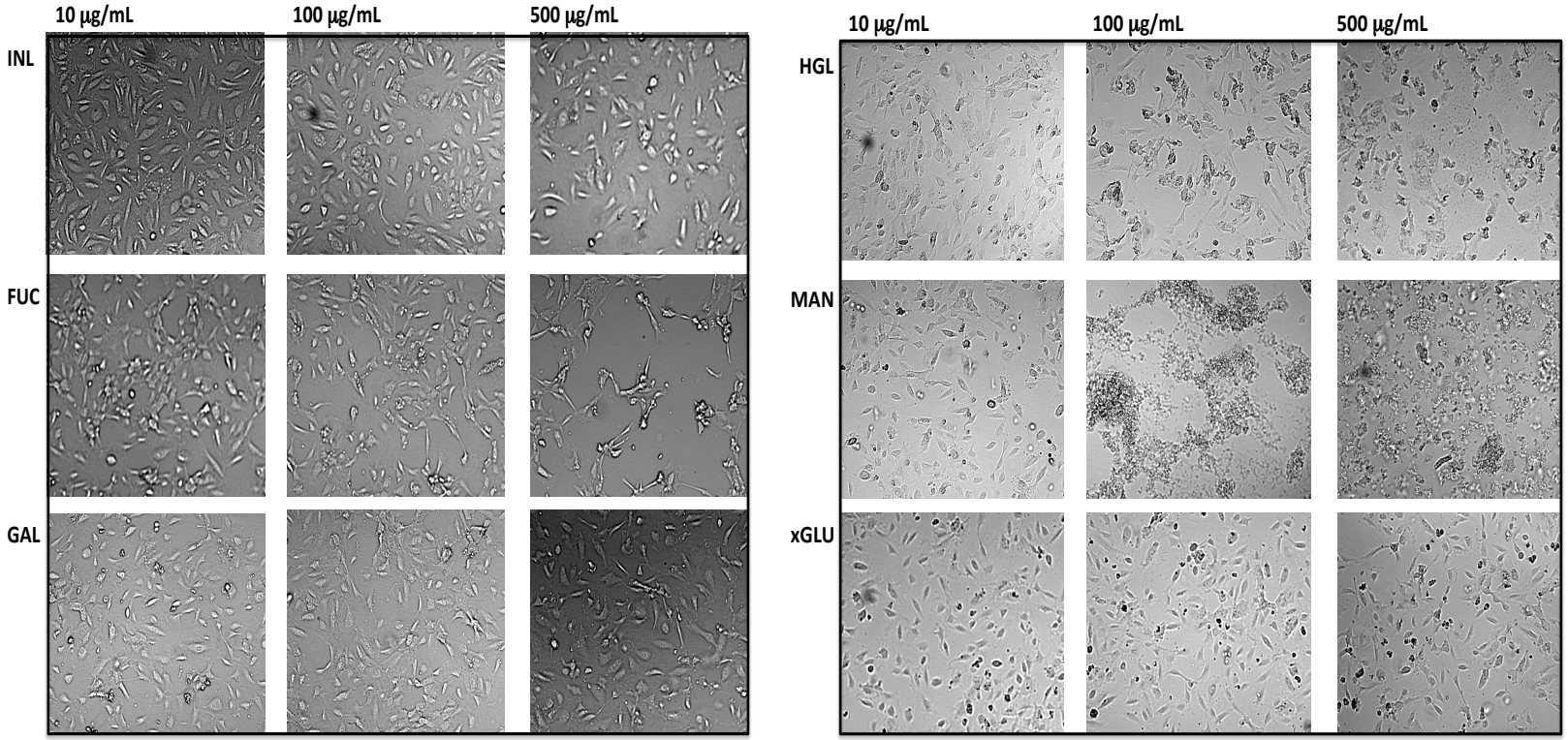

Figure A2.2B. Micrographs of HUVECs upon incubation with different oligo- and polysaccharides under light microscope (10x) at 48 h.

A2.3.2. Tubule formation

The tubule formation is *in vitro* model for the *in vivo* tubule generation in the multistep process of angiogenesis. All the test compounds at concentrations,10, 100 and 500 µg/mL did not lead to the formation of tubules on the angiogenic factor rich matrigel (Figure A2. This suggested that oligo- and polysaccharides at concentrations tested do not support the tubule formation.

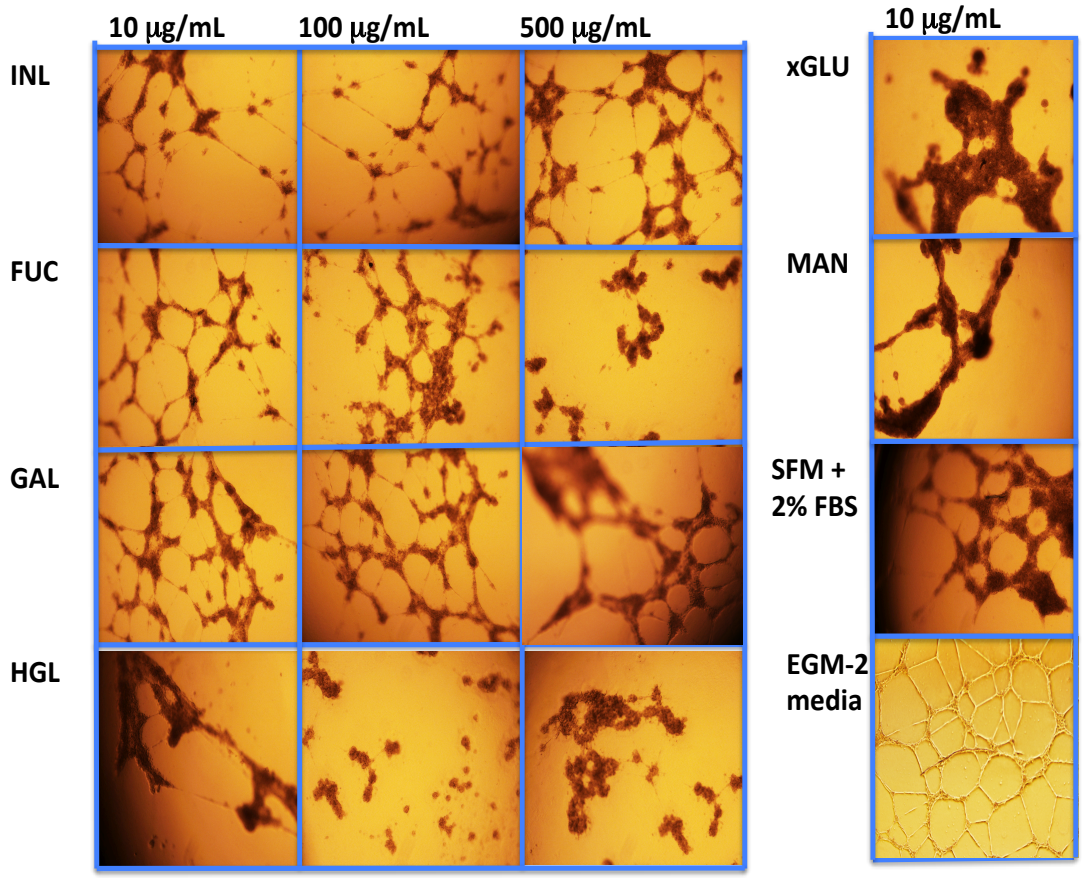

Figure A2.3. Effect of oligo- and polysaccharides on the tubule formation assay.

A2.3.3. Inhibitory effects on migration of endothelial cells

The transwell migration assay is a method of measuring cell chemotaxis towards a stimulus. Migration is a key property of live cells and critical for normal development, immune response, and disease processes such as cancer metastasis and inflammation. In the transwell migration setup, HUVECs migrated towards all the oligo- and polysaccharides along with a control well i.e SRM. INL and GAL at 10 µg/mL led to movement of cells from the upper well to the lower chamber in the transwell (Figure A2.4, A). The migrated cells were stained with crystal violet and

the trapped cells in the trans-membrane were imaged (Figure A2.2, B). HGL at 100 µg/mL and MAN at 100 and 500 µg/mL did not lead to cell migration cell across the membrane. Taken together, these data implied that HGL and MAN lack chemotaxis capabilities and may even exhibit inhibitory properties.

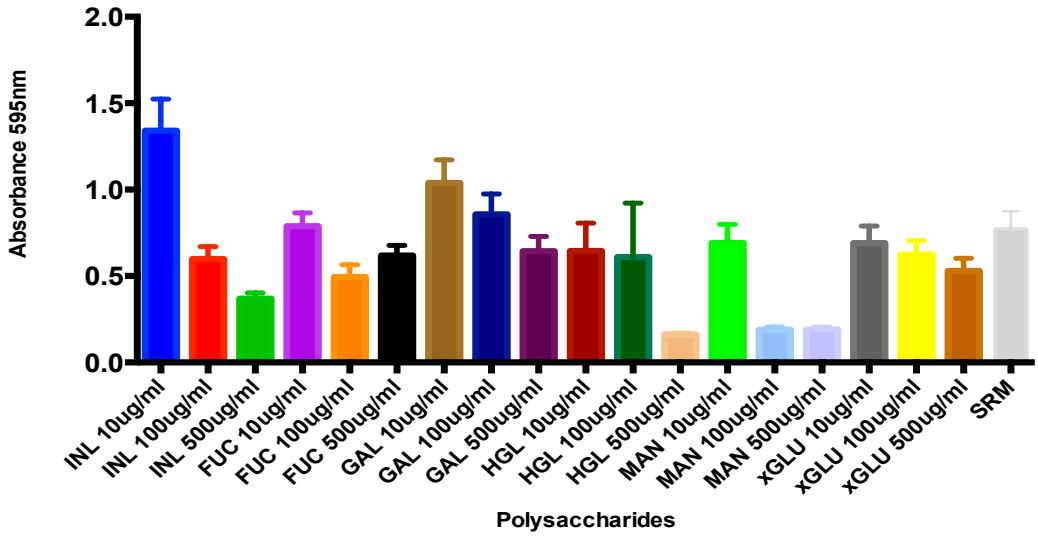

Figure A2.4 (A). Absorbance of the migrated cells that were stained with crystal violet.

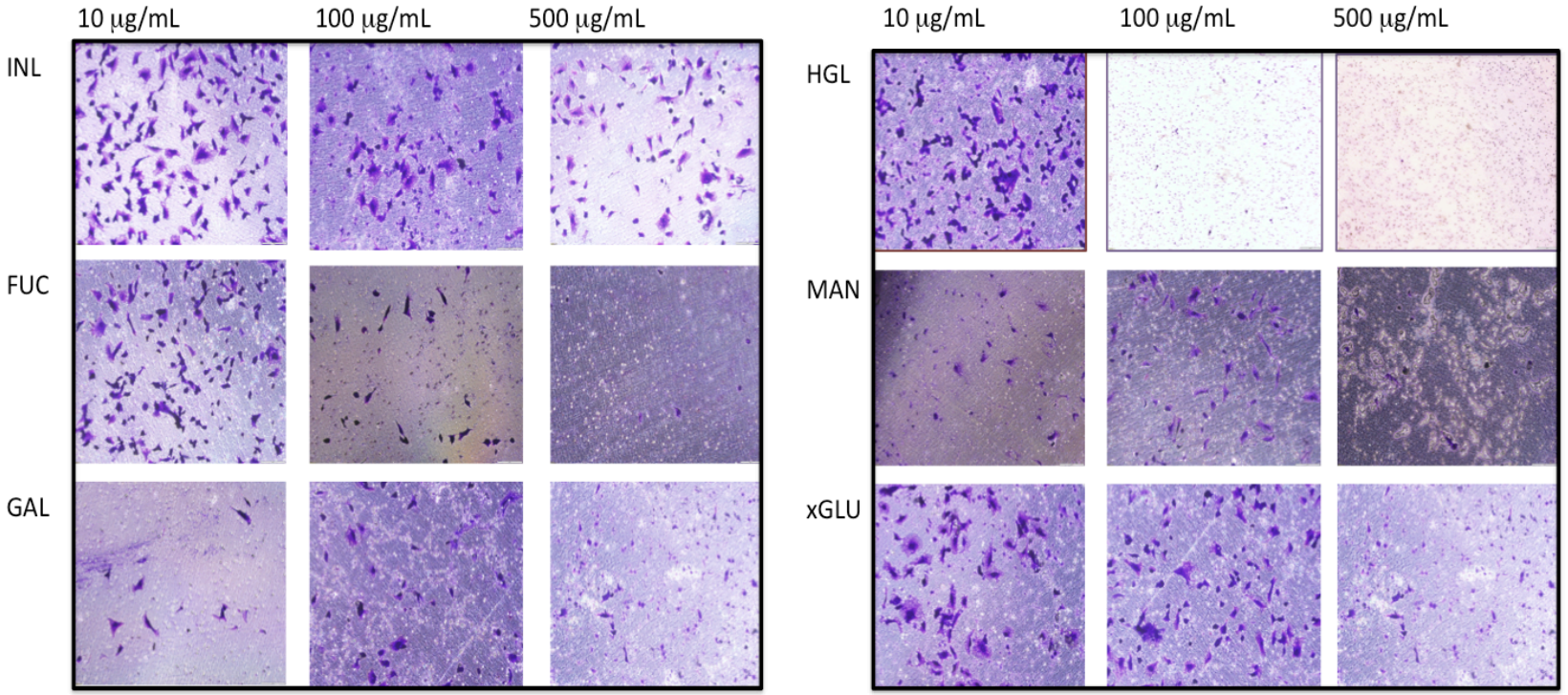

Figure A2.4 (B). Migration of HUVECs to the lower well of transwells in response to the oligo- and poly- saccharide stained with crystal violet.

A2.3.4. Cytokine release in response to test compounds

Four of the test compounds (FUC, GAL, HGL and INL) were assessed for their effect on the secretion of cytokines such as IL-6 and TNF-α. These four oligo- and polysaccharides were selected from the study in chapter 3, where they were found to be most immunomodulatory properties exhibiting their ability to secret higher concentration of cytokines and chemokines in THP-1 cells and HWBC. None of these four compounds lead to the secretion of TNF-α while there was significant release of IL-6 (Table A2.1).

Table A2.1. Quantification of released IL-6 was done using the supernatant from HUVECS after incubation with 10 μg/mL of polysaccharides.

Test compounds (10 μg/mL)	**IL-6 concentration (ng/mL)**
FUC	243.4
GAL	407.3
HGL	425
INL	281.5

A2.3.5. Pathway analysis

All oligo- and polysaccharides were tested for their ability to activate the capase-3 pathway (Figure A2.5, A). We reported the expression of caspase-3 of different isoforms when performed Western blots for total protein lysate of HUVECs upon incubation with test compounds. All the oligo- and polysaccharides led to capase-3 expression except MAN at 500 μg/mL.

The cells were stressed and dead cell debris was imaged when incubated with MAN at 500 μg/mL (Figure A2.5). Therefore, there was no signal observed on the blot due limited live cells after incubation with MAN at 500 μg/mL.

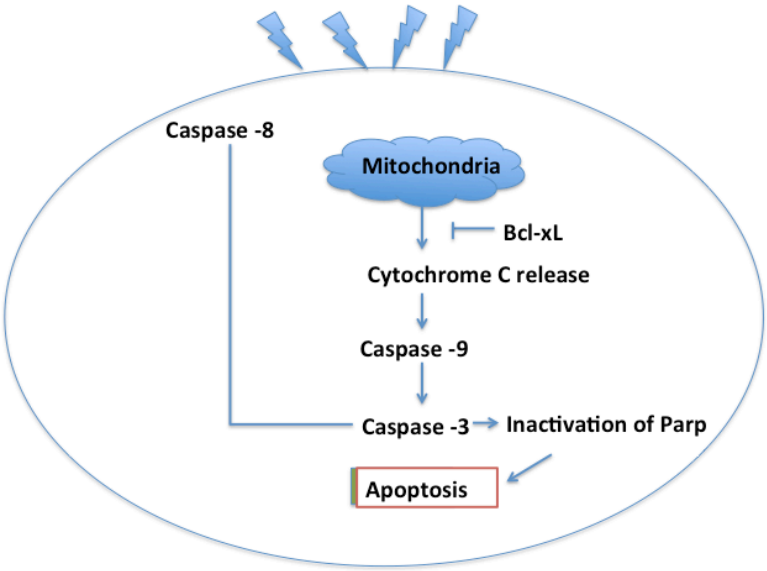

Figure A2.5 (A). Activation of Bcl-xL and caspase-3 pathway when cells undergo apoptosis.

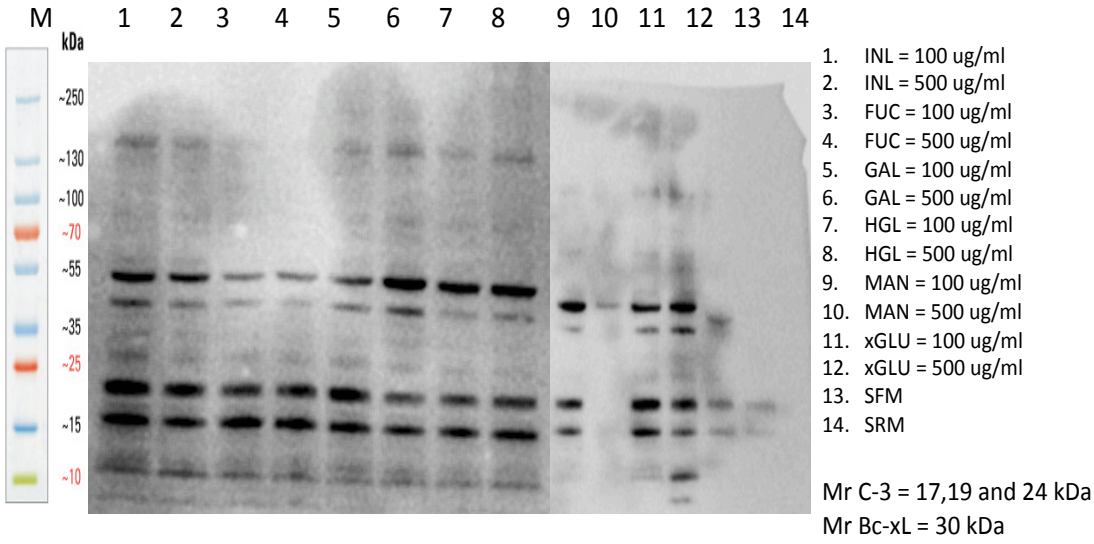

Figure A2.5 (B). Western blot performed for expression of caspase 3 and Bc-xL expression for total protein lysate upon incubation with oligo- and polysaccharides.

A2.3.6. Cell death pathway inhibition

Cell proliferation inhibition and inhibitory effects on the cell migration and activation of apoptotic pathway led to further exploration of the cell death pathways. Cells were co-incubated with different drugs to inhibit different cell death pathways. Nec-1 is used for necroptosis, i.e. is a regulated caspase-independent cell death mechanism that results in morphological features resembling necrosis (Wang et al.,

2014). Saputin (*S*pecific and *p*otent *aut*ophagy *in*hibitor-*1*) is a specific and potent autophagy inhibitor (Shao et al., 2014) while 3-MA is used to inhibit and study the mechanism of autophagy (lysosomal self-degradation) and apoptosis under various conditions (Takatsuka et al., 2004).

The oligo- and polysaccharides were added after the incubation of HUVECs with cell death inhibitors so the mode of cell death can be administrated. The trend of increased cell proliferation overcoming cell inhibition was indicated by the absorbance values when incubated with 3-MA and compared to cells that were not incubated with the drugs. These results suggest that the oligo- and polysaccharides led to the cell death by the mechanism of autophagy indicated by cell death inhibition data upon saputin and 3-MA.

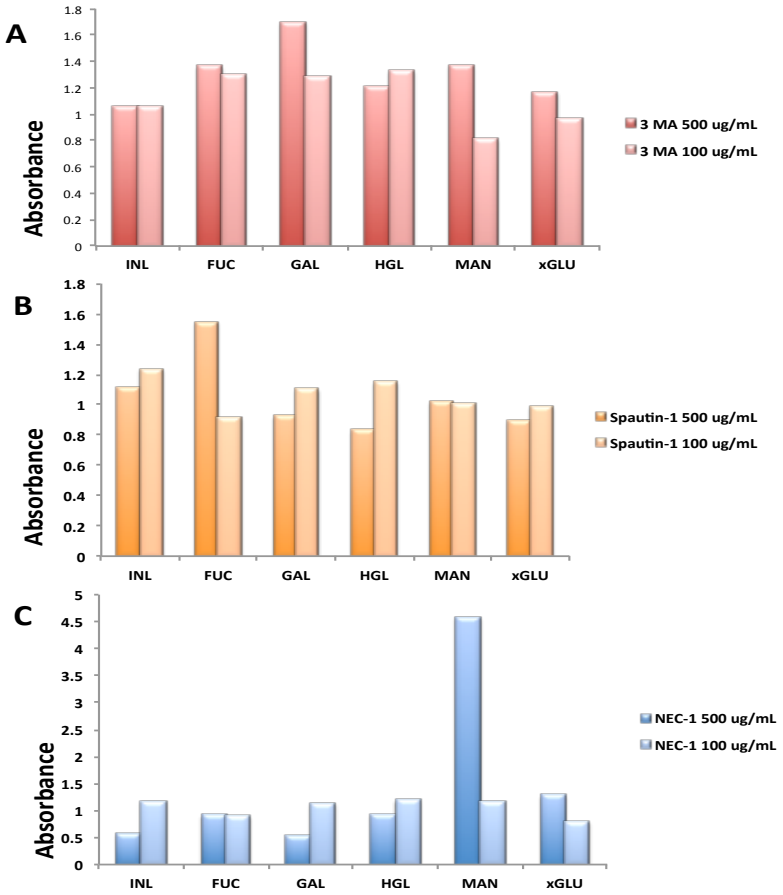

Figure A2.6. Effect of different cell death inhibition drugs (A) 3 MA (B) Spautin and (C) NEC-1 on proliferation of HUVECs where absorbance of untreated control was subtracted.

A2.4. Discussion

Polysaccharides have been studied for their therapeutic and immunomodulatory effects (Section 3.4). They have been also explored for their angiogenic or anti-angiogenic properties in ischemia and tumour conditions respectively. With an increase in the types and severity of cancers, anti-angiogenic therapy has attracted attention. Inhibition of tumour vasculature was first proposed by Judah Folkman and his colleagues (Folkman, 2003). Natural compounds are routinely explore for their anti-angiogenic properties (Sagar and Yance, 2006). Understanding the roles of these natural compounds, they can act as modifiers of biologic response enhancing the efficacy of available therapies such as chemotherapy and radiation.

In order to understand the potential therapeutic effects of oligo- and polysaccharides in vascular biology, functional assays were carried out. These oligo- and polysaccharides were tested for their angiogenic properties by cell proliferation, tubule formation and migration assays. They were also tested for the abilities to secrete angiogenic factors. However, it was observed that the compounds demonstrated anti-angiogenic properties. All the compounds exhibited inhibition of cell proliferation except xGLU at 10 μg/mL at 24 h and FUC, HGL and MAN at 500 μg/mL at the maximum inhibitory effect on the cell proliferation. Also FUC, HGL and MAN altered the cell morphology either by forming extended mesh-like structures or clumps. All test compounds when incubated with HUVECS did not lead to the formation any tubules on Matrigel or migration of cell towards the stimulus, which suggested their anti-angiogenic roles. Expression of the angiogenic factors IL-6 and TNF-α supernatants collected upon incubation of HUVECs with test compounds was measured. IL-6 expression was observed for four polysaccharides (FUC, GAL, HGL and INL) but no TNF-α expression was noted.

With the indication of anti-angiogenic properties of oligo- and polysaccharides, they were studied for the expression of caspase-3 and Bc-xL in downstream pathways that may lead to the apoptosis of cells. In parallel, cell death inhibition drugs were incubated with cells prior the addition to oligo- and polysaccharides to predict possible pathway or mode of action of test compounds leading to the development of new drugs (Kepp et al., 2011). All the angiogenic assays such as matrigel, migration, secretion of cytokines identified FUC, MAN and HGL with the anti-angiogenic properties. Their mode of cell inhibition and death that were administrated by

incubation with cell death inhibitors suggested autophagy as one of the possible reasons of cell death. This data highlights the potential of FUC, MAN and HGL as promising new-apoptotic and anti-angiogenic treatments in killing cells in uncontrolled cell growth such as tumours.

A2.5. References

BOUÏS, D., HOSPERS, G. A. P., MEIJER, C., MOLEMA, G. & MULDER, N. H. 2001. Endothelium in vitro: a review of human vascular endothelial cell lines for blood vessel-related research. *Angiogenesis,* 4**,** 91-102.

FAJARDO, L. F. 1989. Special Report The Complexity of Endothelial Cells: A Review. *American journal of clinical pathology,* 92**,** 241-250.

FOLKMAN, J. 2003. Angiogenesis Inhibitors: A New Class of Drugs. *Cancer Biology & Therapy,* 2**,** 126-132.

KEPP, O., GALLUZZI, L., LIPINSKI, M., YUAN, J. & KROEMER, G. 2011. Cell death assays for drug discovery. *Nature Reviews Drug Discovery,* 10**,** 221-237.

SAGAR, S. M. & YANCE, D. 2006. Natural Health Products that Inhibit Angiogenesis: Part 1. *Current Oncology,* 13.

SHAO, S., LI, S., QIN, Y., WANG, X., YANG, Y., BAI, H., ZHOU, L., ZHAO, C. & WANG, C. 2014. Spautin-1, a novel autophagy inhibitor, enhances imatinib-induced apoptosis in chronic myeloid leukemia. *International Journal of Oncology,* 44**,** 1661-1668.

TAKATSUKA, C., INOUE, Y., MATSUOKA, K. & MORIYASU, Y. 2004. 3-Methyladenine inhibits autophagy in tobacco culture cells under sucrose starvation conditions. *Plant and Cell Physiology,* 45**,** 265-274.

WANG, Y., WANG, H., TAO, Y., ZHANG, S., WANG, J. & FENG, X. 2014. Necroptosis inhibitor necrostatin-1 promotes cell protection and physiological function in traumatic spinal cord injury. *Neuroscience,* 266**,** 91-101.

APPENDIX 3

STATISTICAL ANALYSIS OF LECTIN MICROARRAY DATA*

*This appendix is presented as the pubished article;
Ross, Sarah A., Jared Q. Gerlach, Satbir K. Gill, Jonathan A. Lane, Michelle Kilcoyne, Rita M. Hickey, and Lokesh Joshi. "Temporal alterations in the bovine buttermilk glycome from parturition to milk maturation." *Food Chemistry* 211 (2016): 329-338.

Food Chemistry 211 (2016) 329–338

Contents lists available at ScienceDirect

Food Chemistry

journal homepage: www.elsevier.com/locate/foodchem

Temporal alterations in the bovine buttermilk glycome from parturition to milk maturation

Sarah A. Ross [a,b], Jared Q. Gerlach [b], Satbir K. Gill [b], Jonathan A. Lane [a], Michelle Kilcoyne [b,c], Rita M. Hickey [a], Lokesh Joshi [b,*]

[a] Teagasc Food Research Centre, Moorepark, Fermoy, Co. Cork, Ireland
[b] Glycoscience Group, National Centre for Biomedical Engineering Science, National University of Ireland Galway, Galway, Ireland
[c] Carbohydrate Signalling Group, Microbiology, School of Natural Sciences, National University of Ireland Galway, Galway, Ireland

ARTICLE INFO

Article history:
Received 11 February 2016
Received in revised form 3 May 2016
Accepted 5 May 2016
Available online 6 May 2016

Keywords:
Milk fat globule membrane
Glycosylation
Glycoconjugates
Lectin microarray
Buttermilk

ABSTRACT

The bovine milk fat globule membrane (MFGM) has many associated biological activities, many of which are linked with specific carbohydrate structures of MFGM glycoconjugates. Bovine buttermilk is a commercially viable source of MFGM and is an under-valued by-product of butter making. However, the changes in buttermilk glycosylation over the course of lactation have not been extensively investigated. In this study, buttermilk was generated from three individual multiparous cows at 13 time points over the first three months of lactation. Buttermilk glycosylation was profiled using lectin microarrays and lectin blotting. Suggested differences in glycosylation, including N-glycosylation, sialylation and fucosylation, were observed between early and late time points and between individual animals. Overall, these data suggest temporal changes in the glycosylation of buttermilk proteins which may have an important impact on commercial isolation of glycosylated ingredients.

1. Introduction

The milk fat globule membrane (MFGM) is a heterogeneous membrane which surrounds and stabilises milk fat droplets (Evers et al., 2008) and is a rich source of proteins and lipids, many of which are glycosylated. The glycoconjugates of MFGM include glycoproteins such as mucins (Muc), butyrophilin (BTN), and Pas6/7, and glycolipids such as monosialogangliosides (GM), disialogangliosides (GD) and trisialogangliosides (GT) (Berglund, Petersen, & Rasmussen, 1996; Hvarregaard, Andersen, Berglund, Rasmussen, & Petersen, 1996; Pallesen et al., 2001; Ross, Lane, Kilcoyne, Joshi, & Hickey, 2015; Seok, Shimoda, Azuma, & Kanno, 2001).

Many potential health benefits imparted by MFGM glycoconjugates have been demonstrated *in vitro* and *in vivo*. For example, MFGM can inhibit pathogenic colonisation and subsequent infection in the gut and MFGM glycoconjugates are likely to contribute to this anti-infectivity (Ross, Lane, Kilcoyne, Joshi, & Hickey, 2016). Muc1 from human MFGM demonstrated prevention of *Escherichia coli* adhesion to buccal epithelial cells *in vitro* (Schroten et al., 1992) and Muc1 from bovine MFGM demonstrated inhibition of neuraminidase-sensitive rotavirus infection in MA104 cells (Kvistgaard et al., 2004). Specific carbohydrate structures on MFGM glycoconjugates have been demonstrated to play a role in the inhibition of microbial attachment. For example, sialylation of bovine Muc1 was suggested to reduce binding of *E. coli* and *Salmonella enterica* serovar Typhimurium to Caco-2 cells *in vitro* (Parker et al., 2010). In addition, deglycosylation of a complex of human milk mucin led to a reduction in rotavirus inhibitory activity which indicated the potential importance of glycosylation in imparting the anti-rotaviral activity (Yolken et al., 1992).

Changes in milk glycosylation and protein abundance occur as lactation progresses, with concentrations and specific structures differing between colostrum and mature milks (Takimori et al., 2011; Wilson et al., 2008). For instance, Muc1, Muc15, adipophilin and BTN are upregulated in bovine MFGM 7 days post-partum compared to colostrum (Reinhardt & Lippolis, 2008) while the abundance of immunoglobulin G (IgG) and lactoferrin are higher in whole milk colostrum than in samples taken later in lactation. Additionally, concentrations of sialylated and highly fucosylated glycoproteins in bovine whole milk are highest in colostrum compared to milk sampled at later time points and the ratio of *N*-glycolylneuraminic acid (Neu5Gc) to *N*-acetylneuraminic acid (Neu5Ac) is significantly higher in colostrum, and decreases gradually thereafter (Takimori et al., 2011). Glycosylation profiles of

* Corresponding author.
E-mail address: lokesh.joshi@nuigalway.ie (L. Joshi).

http://dx.doi.org/10.1016/j.foodchem.2016.05.027
0308-8146/

individual bovine milk glycoproteins have also demonstrated changes in glycosylation over the course of lactation (O'Riordan et al., 2014; Ujita et al., 1993) as have MFGM glycoprotein components. For example, MFGM glycoproteins from one Holstein cow's milk at days 0, 1, 3 and 5 post-parturition was analysed for glycosylation changes by soybean agglutinin (SBA) blotting which revealed that binding to a glycoprotein, believed to be CD36, increased over the six day period assessed (Ujita et al., 1993).

While changes in MFGM glycosylation over the course of lactation are expected, few investigations have been undertaken to date. Previous studies have focused on MFGM from milk sampled at just a few time points (Reinhardt & Lippolis, 2008) or from a single animal using a small number of lectins (Ujita et al., 1993). Other studies have compared bovine milk from early time points and late time points but did not monitor the potentially critical changes in between (Wilson et al., 2008). Since glycosylation of bovine MFGM components is an important factor contributing to their health-promoting activities, further knowledge on how lactation affects this glycosylation may be of commercial importance. Identification of lactation time points associated with the most glycosylated components may aid in generation of bovine milk fractions best suited for use as functional ingredients. For instance, since glycoproteins such as BTN are known to be conserved across MFGM from human and bovine milk (Lu et al., 2016), it may be of benefit to utilise highly glycosylated bovine milk ingredients to enrich infant formula since infant formula often has less free oligosaccharide and glycoconjugate content than human milk. This may help to narrow the gap between formula composition and breast milk. Buttermilk is a viable commercial source of MFGM and its associated functional glycoconjugates which have the potential to further benefit human health if used as nutritional food additives. To the best of our knowledge, changes in bovine buttermilk glycosylation over an extended lactation period in multiple animals have not been investigated.

In this study, buttermilk was generated from milk sampled from three animals at 13 time points (days 1–10 (D1–D10) and days 30, 70 and 90 (D30, D70 and D90) post-partum) from colostrum to mature milk. The glycosylation of the individual buttermilk samples was profiled using lectin microarrays featuring a panel of 43 lectins, electrophoretic analysis and lectin blotting.

2. Materials and methods

2.1. Materials

The bicinchoninic acid (BCA) Protein Assay Kit and the SuperSignal Pico kit were from Pierce Biotechnology (Thermo Fisher Scientific Inc., Dublin, Ireland). NuPAGE 4–12% Bis-Tris gels, MOPS buffer, and carboxylic acid succinimidyl ester Alexa Fluor® 647 (AF647) were purchased from Life Technologies (Carlsbad, CA). Molecular mass ladder (Mark12 Unstained Standard), LDS sample buffer, antioxidant and Coomassie Brilliant Blue (SimplyBlue SafeStain) were from Thermo Fisher Scientific (Carlsbad, CA). Pure, unlabelled lectins were acquired from EY Laboratories, Inc. (San Mateo, CA) or Vector Laboratories, Ltd. (Orton Southgate, UK) (Table S1). Biotinylated lectins (RCA-I, MPA, LTA, WGA, WFA, LEL and AIA) were from EY Laboratories, Inc. Avidin-D horseradish peroxidase (HRP) conjugate was from Vector Laboratories, Ltd. Nexterion® Slide H microarray slides were from Schott AG (Mainz, Germany). Glycoprotein Detection Kit, streptavidin horseradish peroxidase conjugate, bovine serum albumin (BSA), bovine asialofetuin (ASF), bromochloroindophosphate nitroblue tetrazolium (BCIP/NBT) were from Sigma-Aldrich Co. (Dublin, Ireland). Neu5Ac monosaccharide was obtained from Dextra Ltd. (Reading, U.K.). Polyvinylidene fluoride (PVDF) membranes (0.2 μm) were from Merck-Millipore Corp., (Dublin, Ireland). Unless otherwise noted, all other reagents were from Sigma-Aldrich Co. and were of the highest grade available.

2.2. Sample collection

Morning milk was collected daily from three multiparous Holstein-Friesian cows (animals 1, 2 and 3) at Teagasc Research Centre, Moorepark, Fermoy, Co. Cork. Samples were collected from D1 to D10 and at D30, D70, and D90 post-parturition per animal. Milk from D9 for animal 1 and D2 for animal 3 was not collected due to scheduling conflicts.

2.3. Buttermilk generation

Buttermilk generation was adapted from Morin, Britten, Jiménez-Flores, and Pouliot (2007). Briefly, samples were incubated at 45 °C for 1 h immediately after collection, followed by cream separation from whole milk using an FT15 disc bowl centrifuge (Armfield Ltd., Ringwood, England). The fat content was adjusted to 40% using Milkoscan FT120 (FOSS, Denmark) and cream was stored at 4 °C for 24 h. Buttermilk and butter were generated by agitating the cream using a food mixer. The buttermilk was passed through glass wool twice to remove butter granules. Samples were frozen at −20 °C, freeze-dried and stored in a desiccator at room temperature (RT) until further use.

2.4. Characterisation of buttermilk samples

Protein concentration was determined using the BCA Protein Assay Kit (Smith et al., 1985), with BSA as the standard. Carbohydrate content was assayed by the Monsigny method (Monsigny, Petit, & Roche, 1988) using glucose (Glc) as the standard. Total sialic acid content was determined using the periodate-resorcinol assay (Jourdian, Dean, & Roseman, 1971), using Neu5Ac as the standard. Assays for all samples were carried out in triplicate and the mean value is reported.

2.5. Sodium dodecyl sulphate-polyacrylamide gel electrophoresis (SDS-PAGE) analysis

Dithiothreitol-reduced buttermilk samples were electrophoresed in 4–12% Bis-Tris gels. Briefly, 65 μg protein was loaded for each sample with a molecular mass ladder in a single lane and all samples were diluted 1:10 with LDS sample buffer. The gel was resolved at 200 V for 50 min using NuPAGE MOPS buffer. NuPAGE MOPS buffer containing 0.25% NuPAGE antioxidant was used in the upper chamber. Protein bands were visualised on the gels using Coomassie Brilliant Blue following the manufacturer's procedure. Glycoprotein bands were visualised using a Glycoprotein Detection Kit. ImageJ software (http://rsb.info.nih.gov/ij/index.html) was used for relative quantitation of gel bands by densitometric analysis.

2.6. Fluorescent labeling of MFGM and glycoproteins

The bovine MFGM samples and the ASF standard for lectin microarrays were labelled with AF647 (λ_{ex} 650 nm, λ_{em} 665 nm) in 100 mM sodium bicarbonate, pH 8.3. Briefly, 10 μL of AF647, dissolved in DMSO, was added to 500 μL of sample (2 mg/mL) and incubated for 1 h in the dark at RT. Samples were kept in the dark after this point. Excess dye was removed from the labelled bovine buttermilk samples on a Bio-Gel P-6 column (1 × 12 cm) (Bio-Rad Laboratories, Ltd., Hertfordshire, U.K.) eluted with phosphate buffered saline (PBS), pH 7.4. Absorbance at 647 and 280 nm for each sample was measured and the protein concentration and degree of

substitution was calculated according to manufacturer's instructions. Extinction coefficients of 100,000 and 19,844 M^{-1} cm^{-1} and molar masses of 100,000 and 48,400 g/mol were used for the calculations for the samples and ASF (based on fetuin) (Spiro, 1960), respectively.

2.7. Construction of lectin microarrays and MFGM profiling

Microarrays consisting of 43 lectins with reported carbohydrate binding specificities (Table S1) were constructed as previously described (Gerlach, Kilcoyne, & Joshi, 2014; O'Riordan et al., 2014). Each feature was printed on Nexterion® Slide H microarray slides in replicates of six and eight replicate subarrays were printed per slide. Lectin performance after printing was tested by incubation with fluorescently-labelled glycoprotein standards (Gerlach et al., 2014). The lectin microarrays were stored at 4 °C with desiccant until use.

Microarray slides were incubated in the dark using an eight-well gasket slide and incubation cassette system (Agilent Technologies, Cork, Ireland) as previously described (Gerlach et al., 2014; O'Riordan et al., 2014). Initially, four randomly selected fluorescently labelled MFGM samples were titrated (5–20 μg/mL) on the lectin microarrays for optimal signal to noise ratio and a concentration of 10 μg/mL in Tris-buffered saline (TBS; 20 mM Tris-HCl, 100 mM NaCl, 1 mM $CaCl_2$, 1 mM $MgCl_2$, pH 7.2) with 0.05% Tween® 20 (TBS-T) was selected for all fluorescently labelled MFGM samples. Three replicate slides were incubated per experiment with appropriate haptenic carbohydrates (100 mM) co-incubated in parallel for a subset of samples to verify carbohydrate-mediated binding (Gerlach, Kilcoyne, Eaton, Bhavanandan, & Joshi, 2011). ASF labelled with AF647 (0.5 μg/mL TBS-T) was included in one subarray per experiment to verify the presence and retained function of the printed lectins. Dried microarrays were scanned immediately in an Agilent G2505B microarray scanner using the Cy5 channel (633 nm excitation, 80% PMT, 5 μm resolution) (Fig. S1).

2.8. Data extraction, hierarchical clustering and statistical analysis

Data extraction was performed essentially as previously described (Gerlach et al., 2014; O'Riordan et al., 2014). For graphical representation, data were normalized to the mean total intensity value of three replicate microarray slides and binding data was presented in histogram form of average intensity with one standard deviation of experimental replicates (n = 3; 18 total data points per probe). Heat mapping and unsupervised hierarchical clustering of normalized data was performed with Hierarchical Clustering Explorer v3.0 (http://www.cs.umd.edu/hcil/hce/hce3.html) using the following parameters: no pre-filtering, complete linkage, Euclidean distance.

The normalized, unfiltered lectin microarray data also was subjected to multi-scale bootstrap re-sampling prior to hierarchical clustering analysis in the R 'pvclust' environment (http://cran.r-project.org/web/packages/pvclust/index.html). Estimation of certainty for each of the *p*-value calculations for clusters was obtained from the bootstrapped data. The matrix was generated using the method.dist = 'euclidean', cluster method using hclust function = 'average' and 10,000 bootstraps where with relative sample size was fixed from 0.5 to 1.4, incrementing in steps of 0.1. Using this matrix, approximately unbiased p-values were calculated for every node.

To further refine the hierarchical clustering, a threshold cut-off filter was also used to identify the most critical subsets of lectin data for clustering and statistical analysis similar to that previously reported (Gerlach et al., 2014). For these, a minimum deviation value (1000 relative fluorescence units (RFU)) was applied resulting in the selection of 12 lectins (AIA, SNA-II, WFA, GSL-II, LEL, GNA, HHA, WGA, PCA, LTA, RCA-I, MPA) which most strongly supported the hierarchy. These data were again statistically evaluated within the R environment using the same parameters listed above.

2.9. Lectin blotting analysis

After SDS-PAGE, proteins were transferred to 0.2 μm PVDF membranes using semi-dry transfer for 120 min at 15 V. Membranes were blocked overnight in 1% BSA in TBS-T at 4 °C and all following procedures were carried out at RT. The membranes were washed three times in TBS-T for 5 min per wash. All subsequent washes were 5 min per wash. All biotinylated lectins were diluted in TBS-T with 0.05% BSA (final concentrations were 2.5 μg/mL for RCA-I and 2 μg/mL for MPA, LTA, WFA, AIA, LEL and WGA). Each membrane was incubated in 10 mL biotinylated lectin with gentle shaking for 90 min. Membranes were washed three times in TBS-T. For RCA-I, MPA, LTA and WFA, the streptavidin alkaline phosphatase conjugate (1 mg/mL stock concentration) was incubated with the membrane at a dilution of 1:15,000 with gentle shaking for 1 h. The membrane was washed three times in TBS-T and once in TBS. BCIP/NBT solution (1 tablet in 10 mL water) was added to the membrane and incubated until colour enhancement was adequate for visualisation (approximately 2 min). Colour development was halted by rinsing in distilled H_2O. Membranes were allowed to fully dry prior to imaging.

For AIA, LEL and WGA, previously probed membranes were stripped by incubating membranes twice for 5 min in 100 mM glycine supplemented with 1% (v/v) Tween® 20 and 3.5 mM SDS, pH 2.2. Membranes were then washed three times in TBS before blocking again in 1% BSA in TBS-T for 1 h. Each membrane was washed and probed again with one biotinylated lectin as described above. Membranes were washed as above before incubation in 1:20,000 Avidin-D HRP conjugate in TBS-T for 1 h. Lectin-binding glycoprotein bands on the membranes were visualised by chemiluminescence using ECL substrates diluted in a 1:1 ratio. All membranes were imaged using an Image Station 4000 MM imaging system (Carestream Health, USA). ImageJ software (http://rsb.info.nih.gov/ij/index.html) was used for lectin blot band quantitative densitometric analysis.

3. Results and discussion

3.1. Characterisation of bovine buttermilk over 3 month lactation

The total protein content of all buttermilk samples from three animals from D1 to D90 post-parturition was estimated by the BCA method (Fig. 1A) and the distribution of protein was analysed by SDS PAGE (Figs. 1B and S2A). For all three animals, protein content was highest at D1 post-partum (760–893 μg/mL) but decreased by approximately 46% by D2, and steadily decreased further until D10. Similarly, Ujita et al. (1993) previously reported a bovine MFGM protein concentration decrease over the first 5 days of lactation. After D10, protein concentration was fairly constant (approximately 310 μg/mg) until the end of the sampling period (D90) (Fig. 1A).

Coomassie Brilliant Blue staining of the SDS-PAGE gels revealed approximately 16 protein bands in the buttermilk samples (Figs. 1B and S2A). High intensity bands were visible at approximately 34, 31, 26, 19 kDa. Protein bands demonstrating lower intensity were observed at 10, 45, 50, 54, 60 and 130 kDa. Low intensity bands were detected at approximately 40, 50, 64, 66 80 and 150 kDa. Rombaut, Dejonckheere, and Dewettinck (2007) demonstrated a similar variety of protein bands by Coomassie-stained SDS-PAGE analysis of acidified buttermilk. Interestingly,

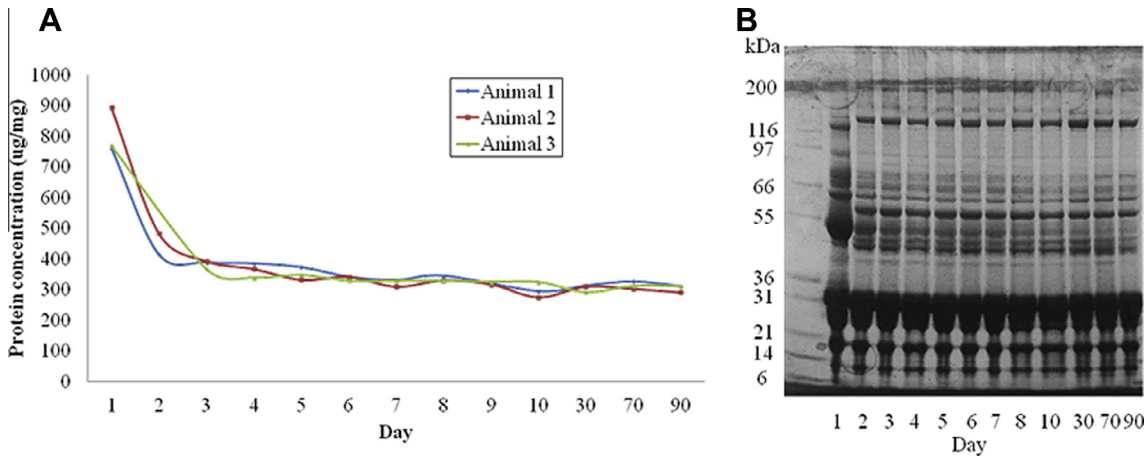

Fig. 1. Protein characterisation of buttermilk samples over the course of lactation. Protein concentration determined using bicinchoninic acid (BCA) protein assay for all buttermilk samples from all animals (A). Buttermilk samples from animal 1 from D1 to D90 post-partum separated on a NuPAGE 4–12% SDS PAGE gel and Coomassie-stained for total protein (B).

the relative band intensity changed as lactation progressed highlighting differences in the buttermilk composition as lactation progressed. For example, the relative abundance of the 130 kDa band increased over time (Figs. 1B and S2A). Changes in relative abundance of bovine milk proteins over lactation have been previously demonstrated. For example, bovine milk xanthine dehydrogenase concentrations were higher in milk taken 7 days post-parturition compared to colostrum (Reinhardt & Lippolis, 2008).

Densitometric analysis of the Coomassie-stained gel from animal 1 suggested that the relative abundances of the proteins at 45 and 50 kDa in the buttermilk samples remained relatively unchanged over the post-parturition timeline (Fig. S3), with the exception of D8 and D90 where relative protein abundances were highest and lowest, respectively. Interestingly, differences in relative band intensities were evident between individual animals (Fig. S2A). For example, the increase in intensity of the 60 kDa protein band at D7 and D9 for animal 3 was not observed for animal 1. However, overall relative protein band intensities for animal 1 were most similar to those of animal 3. In contrast, animal 2 had a greater number of band intensities which differed from the other two animals. For instance, band intensities for 130 kDa protein band increased over the course of lactation for animals 1 and 3. However the relative intensity of the 130 kDa band for animal 2 decreased at D3 and D4, increased from D6 to D8 and decreased again at D9. Thus the relative compositions of the buttermilk samples varied from animal to animal over the course of lactation. Studies by Ye, Singh, Taylor, and Anema (2002) also observed differences in bovine MFGM protein abundance throughout the course of lactation through the use of Coomassie-stained gels. The authors noted differences in the abundance of proteins including BTN, Pas 7 and xanthine oxidase in milk sourced from early, mid and late season milks.

PAS staining of SDS-PAGE gels (Figs. 2A and S2B) demonstrated the presence of numerous glycoproteins in buttermilk throughout lactation. Similar to the Coomassie-stained gels, the relative band intensity changed throughout the progression of lactation, highlighting changes in glycoprotein abundance may have occurred as milk matured. The presence of glycoproteins in buttermilk was not surprising as it has been documented previously (Hvarregaard et al., 1996; Pallesen, Pedersen, Petersen, & Rasmussen, 2007; Ross et al., 2016; Takamizawa, Iwamori, Mutai, & Nagai, 1986), however it was interesting to note the change in intensity as lactation progressed.

Furthermore, comparison of the PAS-stained gels suggested the relative abundances of individual glycoproteins in the buttermilk samples varied between individual animals as lactation progressed (Fig. S2B). Similar findings have been shown for human milk oligosaccharides which incorporate fucose and sialic acid (Miller, Bull, Miller, & McVeagh, 1994). In addition, the acidic and neutral sugar content of buttermilk was assayed based on mg of lyophilised buttermilk. The sialic acid concentration in buttermilk was highest for all three animals on D1 at 192–237 nmoles/mg and decreased gradually until D10 when it levelled off between 119 and 151 nmoles/mg and maintained this concentration into milk maturity. Overall the data suggested a time-dependent fluctuation of sialic acid in the buttermilk samples.

A rapid increase in neutral sugar concentration was observed from D1 to D2 (1857 and 1880 nmoles/mg for animals) in animals 1 and 2, respectively, over the first 10 days and then increased more gradually up to D10 for all three animals. Neutral sugar concentration plateaued by D30 and remained constant through milk maturation (2166–2533 nmoles/mg) (Fig. 2C). It should be noted that the increase in neutral sugar concentration observed could have resulted due to the known increase in lactose which occurs throughout milk maturation (Ontsouka, Bruckmaier, & Blum, 2003). The decline in sialic acid concentration over the course of lactation may reflect the role that sialylation plays in protection of the early postnatal gut from pathogen adhesion (Kelly & Coutts, 2000). The rise in concentration of neutral sugars after parturition may reflect a role for nutrition rather than protection and may also contribute to the growth of beneficial bacteria such as Bifidobacteria and Lactobacilli in the gut (Lönnerdal, 2003).

3.2. MFGM glycoprofiling on lectin microarray

To establish the optimum concentration for lectin microarray profiling, four randomly selected, labelled buttermilk samples were titrated on the lectin microarray consisting of a panel of 43 immobilised lectins of established binding specificities (Table S1). A sample concentration was chosen such that the response of the majority of the lectins was within the dynamic range of the microarray scanner (0–65,000 RFU, approximately). Subsequently, all 37 fluorescently labelled samples were profiled on lectin microarrays at the optimal concentration in triplicate (Fig. 4).

Lectin microarray data was examined for similarities between animals and time points. Unsupervised hierarchical analysis of the complete lectin microarray data set was performed without (Fig. 3A) and with (Fig. 3B) bootstrapping to obtain *p*-values for the different cluster relationships calculated in the R environment using the pvclust package. Animals 1 and 3 displayed the greatest

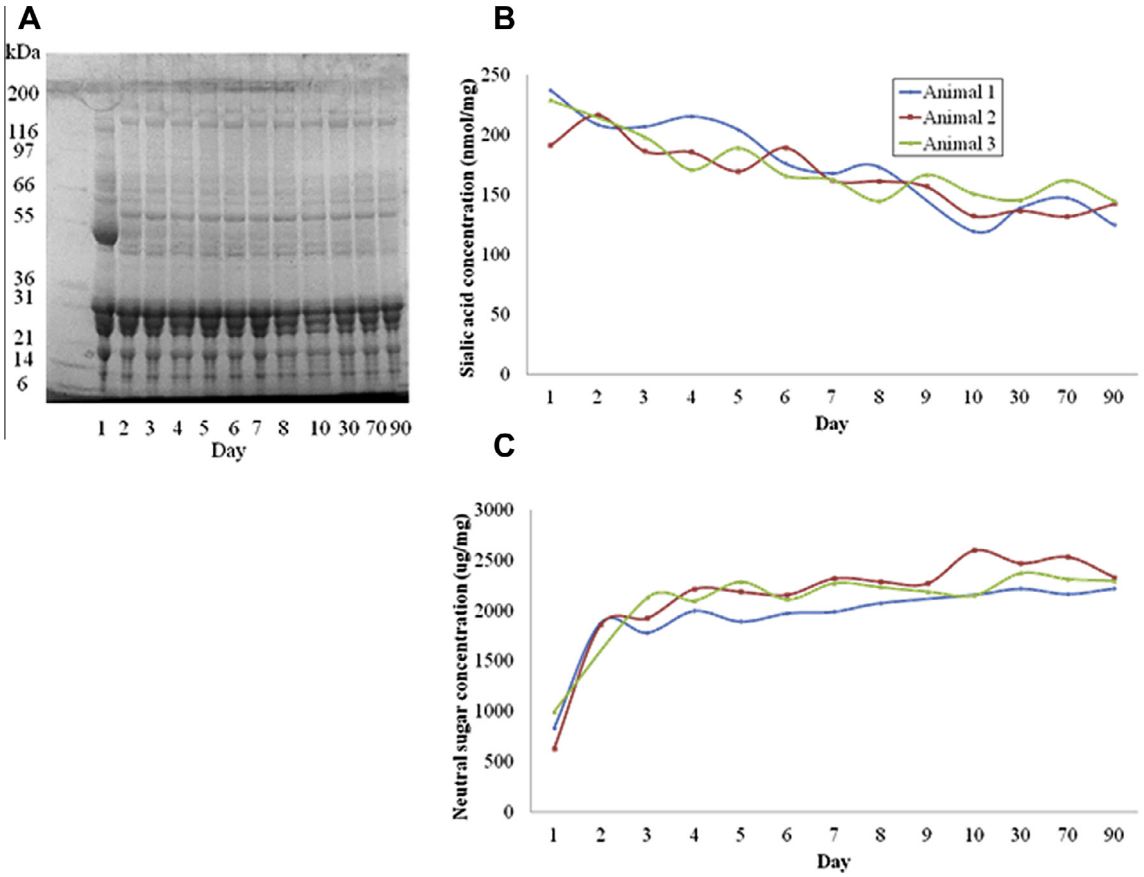

Fig. 2. Acidic and neutral sugar characterisation of buttermilk samples over the course of lactation. Buttermilk samples from animal 1 from D1 to D90 post-partum separated on a NuPAGE 4–12% SDS PAGE gel and PAS-stained (A). Sialic acid concentration (B) for all buttermilk samples from all animals determined using Monsigny method and carbohydrate content (C) determined using periodate-resorcinol assay.

similarity to one another at the greatest number of time points and animal 2 was indicated to be less similar to the others (Fig. 3B). After the initial hierarchical clustering, filtering was applied to select only data from lectins that significantly contributed towards the hierarchical relationship. Increasing the minimum intensity cut-off to exclude all lectins demonstrating <1000 RFU deviation resulted in the selection of just 12 lectins (AIA, SNA-II, WFA, GSL-II, LEL, GNA, HHA, WGA, PCA, RCA-I, LTA, MPA). Including only data from these in the clustering calculations greatly strengthened the certainty of the dendrogram (Fig. 3C). The D1 data for all animals clustered together on one branch and were distant from the remaining data, which suggested that these profile differences were most significant compared to profiles of buttermilk MFGM derived from the following days' samples. Profiles generated for samples later in lactation did not cluster with any strict pattern, thus demonstrating the heterogeneity of the profiles at later time points. As well as more firmly positioning D1 MFGM as being quite different than later samples, filtering the lectin profile data also tightened the overall relationship between the animals, which resulted in them appearing to be more similar overall than the unfiltered data suggested (Fig. 3C).

On the lectin microarrays, buttermilk samples bound to mannose (Man)-binding lectins Con A, GNA and HHA (Table S1) (Fig. 4). Man residues are attached to the chitobiose (GlcNAc-β-(1,4)-GlcNAc) core of all N-linked glycans and Man residues are more abundant in hybrid and high-Man type N-linked structures. Goat MFGM proteins including BTN, Pas6/7 and mucins have also been demonstrated to bind ConA lectin (Cebo, Caillat, Bouvier, & Martin, 2010). Colostrum (D1–3) buttermilk samples had relatively higher binding to GNA and HHA compared to mature (D30–90) buttermilk samples. The data suggested that animal 2 may have a greater proportion of high Man type N-linked structures in its colostrum buttermilk than animals 1 and 3.

PCA lectin predominantly binds to biantennary N-linked glycans (Table S1). Based on PCA binding, the proportion of biantennary structures was much greater in colostrum than in transitional and mature buttermilk samples for all three animals (Fig. 4). The binding intensities of buttermilk samples with PCA did not differ much between the later time points with the exception of samples from animal 2, which increased in binding intensity at D5 and D6 of lactation (Fig. S5B). No binding was observed for PHA-E and PHA-L lectins which have an affinity for extended biantennary and bisecting GlcNAc motifs, and tri- and tetraantennary N-linked complex structures, respectively (Table S1).

The lectins GSL-II and STA have an affinity for GlcNAc residues and GlcNAc oligomers, respectively while LEL has been reported to have greatest affinity for the chitobiose core of N-linked structures (Table S1). LEL bound to all buttermilk samples with low to intermediate intensity (Fig. 4). The binding intensity of GSL-II for all samples from all animals was reduced in mature buttermilk compared to colostrum (Figs. 4 and S4), which suggested a lower prevalence of terminating GlcNAc structures as lactation progressed. The binding intensities of LEL with buttermilk samples from animals 1 and 3 changed very little over lactation. However the D1 sample from animal 2 bound intensely to LEL and samples from later timepoints had decreased binding intensity (Figs. 4 and S4). The binding intensities of samples with the lectins PCA and

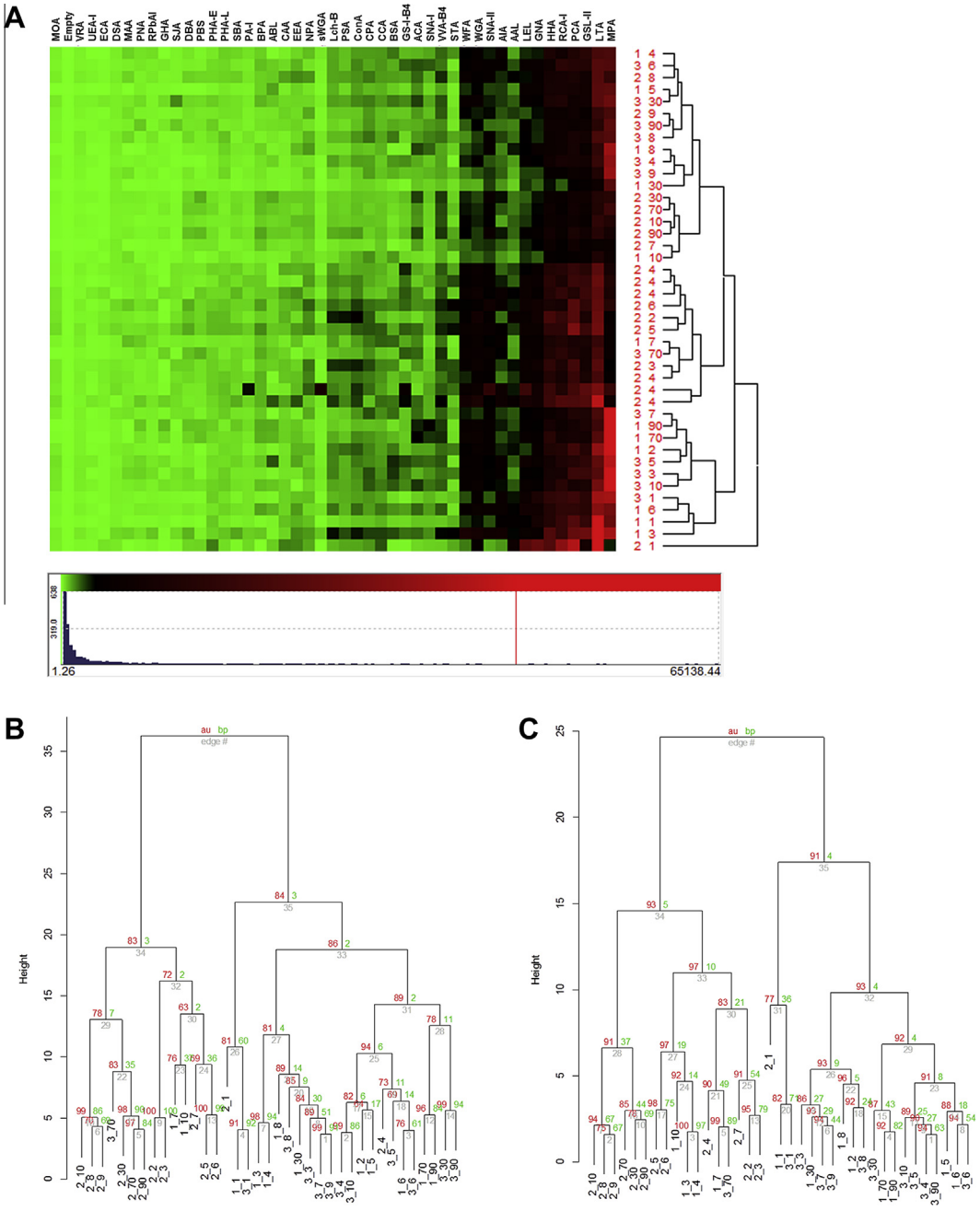

Fig. 3. Heatmap and hierarchical clustering results for lectin microarray profiles generated for labelled buttermilk samples. (A) Total intensity mean normalized data subjected to unsupervised, Euclidean distance, complete linkage clustering without bootstrapping. (B) Bootstrapped clustering of Euclidean distance by Ward method using the entire lectin microarray data set. (C) Bootstrapped clustering of Euclidean distance by Ward method using only data which qualified after 1000 RFU minimum deviation filtering (AIA, SNA-II, WFA, GSL-II, LEL, GNA, HHA, WGA, PCA, LTA, RCA-I, MPA). Approximately Unbiased (AU) *p*-value and Bootstrap Probability (BP) value.

RCA-I (both with affinity to Type II LacNAc (Table S1)) were also highest for the D1 sample from animal 2 compared to animals 1 and 3 (Figs. 4 and S4). Binding of bovine MFGM glycoproteins to lectins such as RCA-I has been reported previously (Ujita et al., 1993), and thus it was not surprising to see binding in this study also.

WGA binding indicated the presence of GlcNAc and/or sialic acid (Neu5Ac and/or Neu5Gc) (Table S1) and all samples exhibited binding intensity with WGA. In this study, a sinusoidal binding pattern, i.e. the binding intensity successively increased and decreased repetitively, was observed for all samples with WGA lectin as lactation progressed (Figs. S4 and S5A). Relatively low binding intensities for all samples with SNA-I indicated the presence of α-(2,6)-linked sialic acid (Table S1 and Fig. 4). SNA binding to MFGM components has been observed previously for goat MFGM glycoproteins (Cebo et al., 2010). It has previously been demonstrated that bovine whole milk sialylation decreased during the transition from colostrum to mature milk (Takimori et al., 2011) and bovine MFGM sialylation decreased over the first 5 days of lactation (Ujita et al., 1993).

Binding of samples to Lch-B and PSA lectins (Table S1) indicated the presence of fucosylated high Man structures in the buttermilk (Fig. 4). Very intense LTA binding by all samples for all animals and lower intensity AAL binding (Fig. 4) indicated the presence of Fuc in α-(1,3)- and α-(1,6)-linkages, respectively (Table S1). Although only low binding was observed for all samples with Lch-B and

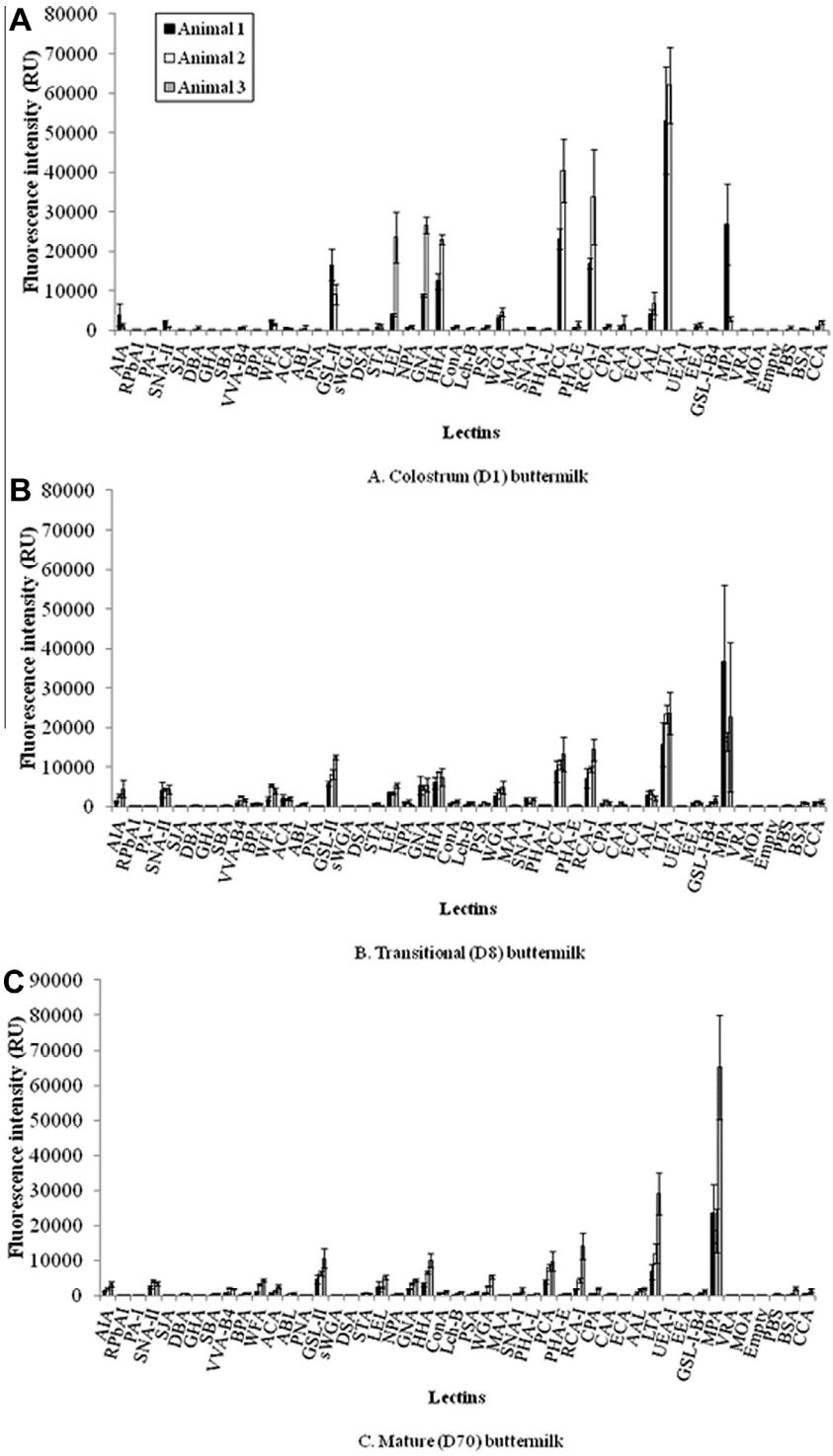

Fig. 4. Lectin microarray profiles of bovine buttermilk generated for three animals over the course of lactation. Each histogram represents the differences in recognition of lectins by fluorescently labelled buttermilk. Data represents the average of three replicate experiments and error bars represent standard deviation. Colostrum (A – D1), transitional (B – D8), mature (C – D70).

PSA, binding intensities were highest for samples from early lactation and decreased thereafter. Binding intensities of samples with both LTA (Fig. S5C) and AAL also decreased as lactation progressed (Figs. 4 and S4) which indicated a lower proportion of Fuc in mature buttermilk compared to colostrum buttermilk. Similarly, concentrations of fucosylated N-linked glycans were reported to be most abundant in bovine colostrum and decreased thereafter (Takimori et al., 2011). This may indicate a possible requirement of Fuc residues in specific linkages for prevention from pathogenic infection in early infancy (Morrow et al., 2004).

The presence of non-sialylated, O-linked mucin core type 1 glycans is often indicated by binding of PNA, which has highest affinity for T-antigen (Gal-β-(1,3)-GalNAc), and by the lectins ABL and ACA, which also have an affinity for mucin core-type structures (Table S1). The presence of O-linked glycosylation may also be indicated by the presence of Gal, as observed by low binding by

the lectin AIA (Fig. 4 and Table S1). For the buttermilk samples, no binding was observed for PNA and ABL. However, very low binding with ACA was observed, with lowest binding in colostrum samples for all three animals (Fig. 4). Since ACA lectin binding was evident coupled with no binding by PNA and ABL, this indicated the presence of sialylated T-antigen as PNA and ABL do not bind to the T-antigen when it is sialylated. AIA binding intensities were lower in mature samples compared to colostrum for animals 1 and 3 (Fig. S5D). Animal 2 differed as binding intensities did not change much over the course of lactation, with the exception of buttermilk from D6 which bound to AIA with the greatest intensity for all sample time points for animal 2 (Fig. S5D). This binding intensity pattern over the course of lactation indicated an overall lower abundance of terminal Gal residues in the buttermilk samples of animal 2 compared to animals 1 and 3, particularly in colostrum buttermilk.

Low intensity binding was observed for all samples with the lectins VVA-B4 and WFA (Fig. 4), which suggested the presence of GalNAc (Table S1), with lowest binding for D1 samples for all animals (Fig. S4). WFA binding intensity increased in D2 to D3 samples and binding intensities followed a sinusoidal trend in the days thereafter with a slight increase in the mature milk samples of animals 1 (D70 and D90) and 3 (D30 and D70), but not of animal 2 (Fig. S5F). Additionally, low binding of the samples with SNA-II (Fig. 4), which also binds to GalNAc residues (Table S1), likely indicated the presence of LacNAc and N,N′-diacetyllactosamine (GalNAc-β-(1–4)-GlcNAc, LacdiNAc). RCA-I binding to the samples was observed with buttermilk at early time points (e.g. D1) with lower binding observed for samples from later time points (e.g. D90) (Figs. 4 and S5E). RCA-I typically binds to type II LacNAc (Gal-β-(1,4)-GlcNAc) (Table S1). Interestingly no binding was observed for the samples with ECA (Fig. 4), which binds to type II LacNAc oligomers (Table S1). SNA-II binding displayed a sinusoidal binding trend for samples over the course of lactation for all animals (Fig. S4). Interestingly, relative binding intensities of the samples with SBA, which has an affinity for GalNAc (Table S1), increased from D1 to D3 for animal 1 and increased from D1 to D5 for animals 2 and 3. This trend was broadly in agreement with Ujita et al. (1993) who reported an increase in SBA binding intensities over the first 6 days of lactation (Fig. S6).

Very high binding by MPA lectin to all samples (Fig. 4) indicated the presence of terminal α-linked Gal (Table S1) and the binding intensity varied sinusoidally over time. Overall, MPA binding intensities were among the highest lectin binding intensities for samples for animals 1 and 3. Most prominently, the relative binding intensity for MPA with MFGM from animal 2 was markedly lower compared to animals 1 and 3 for much of the early portion (D1–D10) of the lactation time course (Fig. S5G). For animal 2, binding to MPA lectin was lowest in colostrum (D1–D3) and highest in late transitional buttermilk (D9) while MPA binding decreased slightly in mature buttermilk (D30–D90). For animals 1 and 3, MPA binding intensity varied sinusoidally over time. These results may suggest that Gal residues play a larger role in nutrition throughout the course of lactation rather than in the protection of the infant gut from infection. For instance, the presence of Gal throughout lactation may be beneficial for establishing a Bifidobacteria-rich flora, given that bacteria such as *B. bifidum* are known to utilise Gal as a carbon source, in the infant gut (Asakuma et al., 2011).

The global changes observed for bovine buttermilk throughout lactation were diverse and expected since buttermilk is a source of many glycosylated components (Ross et al., 2015). For example, N-linked glycosylation has been reported on many MFGM components including mucins (Pallesen et al., 2001), BTN (Sato, Takio, Kobata, Greenwalt, & Furukawa, 1995), Pas6/7 (Hvarregaard et al., 1996) and CD36 (Nakata, Furukawa, Greenwalt, Sato, & Kobata, 1993). Bovine MFGM is also known to contain predominantly mucin core type 1 O-linked structures with core type 2 structures present up to three days post-parturition (Wilson et al., 2008). Furthermore, BTN (Sato et al., 1995) and α-lactalbumin (Takimori et al., 2011) contain LacdiNAc while PP3 contains LacNAc and LacdiNAc (Inagaki et al., 2010). GM2 and GD2 also contain terminating GalNAc residues (Jensen & Newburg, 1995; Smilowitz, Lebrilla, Mills, German, & Freeman, 2014). Additionally, sialylated buttermilk glycoproteins include Pas6/7 (Seok et al., 2001), Muc1 (Pallesen et al., 2001), Muc15 (α-(2,6)-linked sialylation) (Pallesen et al., 2007), IgG (α-(2,6)-linked sialylation) (Takimori et al., 2011) and the gangliosides, including GM (α-(2,3)-linked sialic acid), and GD (α-(2,3)- and α-(2,8)-linked sialic acid) (Lee, German, Kjelden, Lebrilla, & Barile, 2013; Smilowitz et al., 2014). Fucosylation has also been documented for bovine buttermilk with Pas7 containing α-(1,6)-linked Fuc (Seok et al., 2001). Additionally, CD36 (Berglund et al., 1996), PP3 fraction (Inagaki et al., 2010) and mucins (Pallesen et al., 2007) were reported as potentially modified with Fuc.

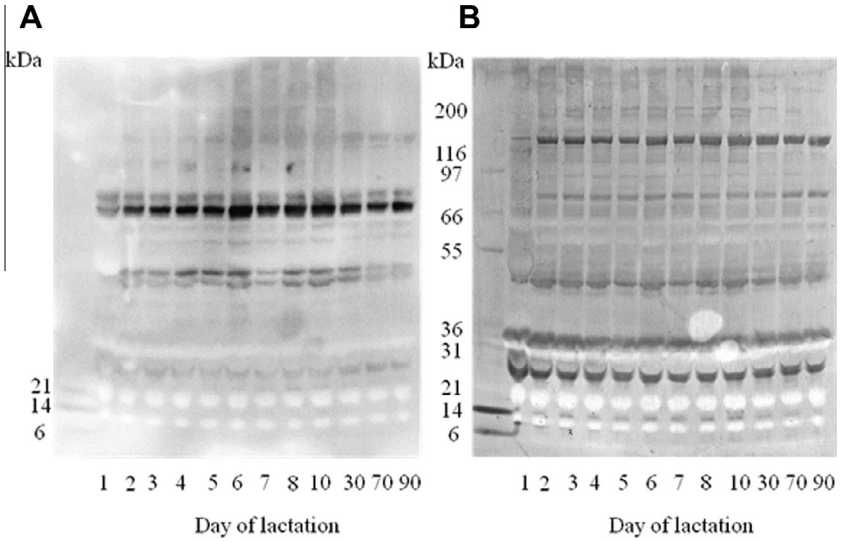

Fig. 5. Lectin blot profiles of bovine buttermilk generated for animal 1 over the course of lactation for lectins LEL (A) and LTA (B).

3.3. Lectin blotting analysis of bovine buttermilk samples

Proteins from buttermilk samples generated from animal 1 were transferred to PVDF membrane and incubated with seven (RCA-I, MPA, LTA, WFA, AIA, LEL and WGA) of the 12 lectins identified by threshold filtering of the lectin microarray data (Figs. 5 and S7). Day by day, relative binding patterns for the lectins RCA-I, WFA and LEL with the samples were similar to those for the lectin microarrays. RCA-I demonstrated high binding to bands from early day samples (D1–D6), with particularly high binding on D1 for most bands. Binding dropped again and increased slightly in later time points (D10–D90). No binding was evident to the band at approximately 30 kDa (Fig. S7A). WFA showed a similar pattern to that of RCA-I but with less binding overall to bands below approximately 40 kDa (Fig. S7B). LEL lectin bound more intensely to proteins of transitional milk (D4–D10) than those from other time points, with high binding intensity at D6 (Fig. 5A), in agreement with lectin microarray data. Densitometric quantification of LEL lectin blot supported these observations (Fig. S8A) and the relative densities were highest for band 2 and band 3 (approximately 66 and 46 kDa, respectively).

The relative binding intensities for lectins MPA, LTA, AIA and WGA differed over time to those of the lectin microarrays. This is likely due, in part, to the absence of glycolipids in the blots which would be included in samples profiled on the microarray. Binding by MPA increased at the later time points for certain bands, such as at approximately 130 kDa, while binding decreased in later time points for other bands, such as those at approximately 31 and 66 kDa (Fig. S7C). To our knowledge, terminal α-linked Gal is not found on bovine milk glycolipids (Ito et al., 2012; Jensen and Newburg, 1995; Martín, Martín-Sosa, & Hueso, 2001; Takamizawa et al., 1986). Thus, the differences seen between the MPA blots and arrays could be simply a result of differences in the intact MFGM glycosylation accessibility with the lectin microarray approach.

High intensity bands in samples from later time points in the LTA lectin blot, such as those at approximately 80 and 130 kDa, were in contrast to lectin microarray data which showed high LTA binding in colostrum which declined as lactation progressed (Fig. 5B). AIA lectin binding indicated no binding at bands below approximately 55 kDa (Fig. S7D). High intensity binding was evident at some bands for colostrum, for example D1 at approximately 55 and 116 kDa, and high intensity binding was evident for other bands later in lactation, for example at approximately 97 kDa (Fig. S7D). Similarly, densitometric analysis of AIA blot revealed highest binding of AIA at D1 for 2 bands – band 2 and 5 which correspond to the bands at approximately 116 and 55 kDa, respectively (Fig. S8B). For all other bands, the analysis demonstrated binding was highest in transitional and mature time points. However these data did not correlate strongly with the lectin microarray data. For instance, the relative binding at D8 and D10 was low in the lectin microarray data but was higher in the lectin blot. WGA in general had increased binding to bands as lactation progressed (Fig. S7E). Bands at approximately 45, 50 and 64 kDa displayed the most intense binding overall. For the band at 64 kDa highest binding was evident at the late transitional and mature time points while for the bands at 45 and 50 kDa binding was highest at D10 and 30.

4. Conclusions

Lectin analysis demonstrated that temporal changes of bovine buttermilk glycosylation occurred during milk maturation which may vary between individuals. Future investigations would benefit from including a greater number of animals in order to fully investigate the potential for variation among individuals. Also examining different breeds of animals and varying feeding systems should provide additional insights into factors affecting glycosylation of buttermilk proteins. In this study, glycosylation differed to such a remarkable extent that exploitation of buttermilk at different stages of lactation could provide functional ingredients which could be tailored to target health promotion in a variety of areas, such as to narrow the gap between infant formula and human breast milk.

Conflict of interest

The authors declare that there are no conflicts of interest.

Acknowledgements

The authors thank Mr. John Glavin for technical assistance. Sarah Ross is in receipt of a Teagasc Walsh Fellowship and is funded by the Department of Agriculture and Food, Ireland, under the Food Institutional Research Measure (FIRM), project reference number 10 RD TMFRC 708. Funding was provided by the following agencies and institutions: Science Foundation Ireland (SFI) (grant no. 08/SRC/B1393) in support of the Alimentary Glycoscience Research Cluster (AGRC) and the European Union FP7 programme (grant no. 260600) in support of the GlycoHIT project.

Appendix A. Supplementary data

Supplementary data associated with this article can be found, in the online version, at http://dx.doi.org/10.1016/j.foodchem.2016.05.027.

References

Asakuma, S., Hatakeyama, E., Urashima, T., Yoshida, E., Katayama, T., Yamamoto, K., & Kitaoka, M. (2011). Physiology of consumption of human milk oligosaccharides by infant gut-associated bifidobacteria. *Journal of Biological Chemistry, 286*(40), 34583–34592.

Berglund, L., Petersen, T. E., & Rasmussen, J. T. (1996). Structural characterization of bovine CD36 from the milk fat globule membrane. *Biochimica et Biophysica Acta (BBA) – Gene Structure and Expression, 1309*(1–2), 63–68.

Cebo, C., Caillat, H., Bouvier, F., & Martin, P. (2010). Major proteins of the goat milk fat globule membrane. *Journal of Dairy Science, 93*(3), 868–876.

Evers, J. M., Haverkamp, R. G., Holroyd, S. E., Jameson, G. B., Mackenzie, D. D., & McCarthy, O. J. (2008). Heterogeneity of milk fat globule membrane structure and composition as observed using fluorescence microscopy techniques. *International Dairy Journal, 18*(12), 1081–1089.

Gerlach, J. Q., Kilcoyne, M., Eaton, S., Bhavanandan, V., & Joshi, L. (2011). Non-carbohydrate-mediated interaction of lectins with plant proteins. In A. M. Wu (Ed.), *The molecular immunology of complex carbohydrates-3* (pp. 257–269). New York: Springer.

Gerlach, J. Q., Kilcoyne, M., & Joshi, L. (2014). Microarray evaluation of the effects of lectin and glycoprotein orientation and data filtering on glycoform discrimination. *Analytical Methods, 6*(2), 440–449.

Hvarregaard, J., Andersen, M. H., Berglund, L., Rasmussen, J. T., & Petersen, T. E. (1996). Characterization of glycoprotein PAS-6/7 from membranes of bovine milk fat globules. *European Journal of Biochemistry, 240*(3), 628–636.

Inagaki, M., Nakaya, S., Nohara, D., Yabe, T., Kanamaru, Y., & Suzuki, T. (2010). The multiplicity of N-glycan structures of bovine milk 18 kDa lactophorin (Milk GlyCAM-1). *Bioscience Biotechnology and Biochemistry, 74*(2), 447–450.

Ito, E., Tominaga, A., Waki, H., Miseki, K., Tomioka, A., Nakajima, K., ... Suzuki, A. (2012). Structural characterization of monosialo-, disialo- and trisialo-gangliosides by negative ion AP-MALDI-QIT-TOF mass spectrometry with MSn switching. *Neurochemical Research, 37*(6), 1315–1324.

Jensen, R., & Newburg, D. (1995). Bovine milk lipids. In R. G. Jensen (Ed.). *Handbook of milk composition* (pp. 543–575). Academic Press Inc.

Jourdian, G. W., Dean, L., & Roseman, S. (1971). The sialic acids XI. A periodate-resorcinol method for the quantitative estimation of free sialic acids and their glycosides. *Journal of Biological Chemistry, 246*(2), 430–435.

Kelly, D., & Coutts, A. (2000). Early nutrition and the development of immune function in the neonate. *Proceedings of the Nutrition Society, 59*(02), 177–185.

Kvistgaard, A. S., Pallesen, L. T., Arias, C. F., López, S., Petersen, T. E., Heegaard, C. W., & Rasmussen, J. T. (2004). Inhibitory effects of human and bovine milk constituents on rotavirus infections. *Journal of Dairy Science, 87*(12), 4088–4096.

Lee, H., German, J. B., Kjelden, R., Lebrilla, C. B., & Barile, D. (2013). Quantitative analysis of gangliosides in bovine milk and colostrum-based dairy products by ultra-high performance liquid chromatography-tandem mass spectrometry. *Journal of Agricultural and Food Chemistry, 61*(40), 9689–9696.

Lönnerdal, B. (2003). Nutritional and physiologic significance of human milk proteins. *The American Journal of Clinical Nutrition, 77*(6), 1537S–1543S.

Lu, J., Wang, X., Zhang, W., Liu, L., Pang, X., Zhang, S., & Lv, J. (2016). Comparative proteomics of milk fat globule membrane in different species reveals variations in lactation and nutrition. *Food chemistry, 196*, 665–672.

Martín, M.-J., Martín-Sosa, S., & Hueso, P. (2001). Bovine milk gangliosides: Changes in ceramide moiety with stage of lactation. *Lipids, 36*(3), 291–298.

Miller, J. B., Bull, S., Miller, J., & McVeagh, P. (1994). The oligosaccharide composition of human milk: Temporal and individual variations in monosaccharide components. *Journal of pediatric gastroenterology and nutrition, 19*(4), 371–376.

Monsigny, M., Petit, C., & Roche, A.-C. (1988). Colorimetric determination of neutral sugars by a resorcinol sulfuric acid micromethod. *Analytical Biochemistry, 175*(2), 525–530.

Morin, P., Britten, M., Jiménez-Flores, R., & Pouliot, Y. (2007). Microfiltration of buttermilk and washed cream buttermilk for concentration of milk fat globule membrane components. *Journal of Dairy Science, 90*(5), 2132–2140.

Morrow, A. L., Ruiz-Palacios, G. M., Altaye, M., Jiang, X., Lourdes Guerrero, M., Meinzen-Derr, J. K., ... Newburg, D. S. (2004). Human milk oligosaccharides are associated with protection against diarrhea in breast-fed infants. *The Journal of Pediatrics, 145*(3), 297–303.

Nakata, N., Furukawa, K., Greenwalt, D. E., Sato, T., & Kobata, A. (1993). Structural study of the sugar chains of CD36 purified from bovine mammary epithelial cells. Occurrence of novel hybrid-type sugar chains containing the Neu5Ac-α-2-6GalNAc-β-1-4GlcNAc and the Man-α-1-2Man-α-1-3Man-α-1-6Man groups. *Biochemistry, 32*(16), 4369–4383.

Ontsouka, C. E., Bruckmaier, R. M., & Blum, J. W. (2003). Fractionized milk composition during removal of colostrum and mature milk. *Journal of Dairy Science, 86*(6), 2005–2011.

O'Riordan, N., Gerlach, J. Q., Kilcoyne, M., O'Callaghan, J., Kane, M., Hickey, R. M., & Joshi, L. (2014). Profiling temporal changes in bovine milk lactoferrin glycosylation using lectin microarrays. *Food Chemistry, 165*, 388–396.

Pallesen, L. T., Andersen, M. H., Nielsen, R. L., Berglund, L., Petersen, T. E., Rasmussen, L. K., & Rasmussen, J. T. (2001). Purification of MUC1 from bovine milk fat globules and characterization of a corresponding full-length cDNA clone. *Journal of Dairy Science, 84*(12), 2591–2598.

Pallesen, L. T., Pedersen, L. R. L., Petersen, T. E., & Rasmussen, J. T. (2007). Characterization of carbohydrate structures of bovine MUC15 and distribution of the mucin in bovine milk. *Journal of Dairy Science, 90*(7), 3143–3152.

Parker, P., Sando, L., Pearson, R., Kongsuwan, K., Tellam, R. L., & Smith, S. (2010). Bovine Muc1 inhibits binding of enteric bacteria to Caco-2 cells. *Glycoconjugate Journal, 27*(1), 89–97.

Reinhardt, T. A., & Lippolis, J. D. (2008). Developmental changes in the milk fat globule membrane proteome during the transition from colostrum to milk. *Journal of Dairy Science, 91*(6), 2307–2318.

Rombaut, R., Dejonckheere, V., & Dewettinck, K. (2007). Filtration of milk fat globule membrane fragments from acid buttermilk cheese whey. *Journal of Dairy Science, 90*(4), 1662–1673.

Ross, S. A., Lane, J. A., Kilcoyne, M., Joshi, L., & Hickey, R. M. (2016). Defatted bovine milk fat globule membrane inhibits association of enterohaemorrhagic *Escherichia coli* O157:H7 with human HT-29 cells. *International Dairy Journal, 59*, 36–43.

Ross, S. A., Lane, J. A., Kilcoyne, M., Joshi, L., & Hickey, R. M. (2015). The milk fat globule membrane: A potential source of health promoting glycans. In V. K. Gupta & M. G. Tuohy (Eds.), *Biotechnology of bioactive compounds: Sources and applications* (pp. 631–668). UK: Wiley Blackwell.

Sato, T., Takio, K., Kobata, A., Greenwalt, D. E., & Furukawa, K. (1995). Site-specific glycoyslation of bovine butyrophilin. *Journal of Biochemistry, 117*(1), 147–157.

Schroten, H., Hanisch, F. G., Plogmann, R., Hacker, J., Uhlenbruck, G., Nobis-Bosch, R., & Wahn, V. (1992). Inhibition of adhesion of S-fimbriated *Escherichia coli* to buccal epithelial cells by human milk fat globule membrane components: A novel aspect of the protective function of mucins in the nonimmunoglobulin fraction. *Infection and Immunity, 60*(7), 2893–2899.

Seok, J. S., Shimoda, M., Azuma, N., & Kanno, C. (2001). Structures of the N-linked sugar chains in PAS-7 glycoprotein sharing the same protein core with PAS-6 glycoprotein from the bovine milk fat globule membrane. *Bioscience Biotechnology and Biochemistry, 65*(4), 901–912.

Smilowitz, J. T., Lebrilla, C. B., Mills, D. A., German, J. B., & Freeman, S. L. (2014). Breast milk oligosaccharides: Structure-function relationships in the neonate. *Annual Review of Nutrition, 34*, 143–169.

Smith, P. K., Krohn, R. I., Hermanson, G. T., Mallia, A. K., Gartner, F. H., Provenzano, M. D., ... Klenk, D. C. (1985). Measurement of protein using bicinchoninic acid. *Analytical Biochemistry, 150*(1), 76–85.

Spiro, R. G. (1960). Studies on fetuin, a glycoprotein of fetal serum. *Journal of Biological Chemistry, 235*, 2860–2869.

Takamizawa, K., Iwamori, M., Mutai, M., & Nagai, Y. (1986). Gangliosides of bovine buttermilk. Isolation and characterization of a novel monosialoganglioside with a new branching structure. *Journal of Biological Chemistry, 261*(12), 5625–5630.

Takimori, S., Shimaoka, H., Furukawa, J. I., Yamashita, T., Amano, M., Fujitani, N., ... Nishimura, S. I. (2011). Alteration of the N-glycome of bovine milk glycoproteins during early lactation. *FEBS Journal, 278*(19), 3769–3781.

Ujita, M., Furukawa, K., Aoki, N., Sato, T., Noda, A., Nakamura, R., ... Matsuda, T. (1993). A change in soybean agglutinin binding patterns of bovine milk fat globule membrane glycoproteins during early lactation. *FEBS Letters, 332*(1–2), 119–122.

Wilson, N. L., Robinson, L. J., Donnet, A., Bovetto, L., Packer, N. H., & Karlsson, N. G. (2008). Glycoproteomics of milk: Differences in sugar epitopes on human and bovine milk fat globule membranes. *Journal of Proteome Research, 7*(9), 3687–3696.

Ye, A., Singh, H., Taylor, M. W., & Anema, S. (2002). Characterization of protein components of natural and heat-treated milk fat globule membranes. *International Dairy Journal, 12*(4), 393–402.

Yolken, R. H., Peterson, J. A., Vonderfecht, S. L., Fouts, E. T., Midthun, K., & Newburg, D. S. (1992). Human milk mucin inhibits rotavirus replication and prevents experimental gastroenteritis. *Journal of Clinical Investigation, 90*(5), 1984–1991.

APPENDIX 4

OUTPUTS

Output from PhD work

Published peer reviewed research articles

Gill, Satbir Kaur, Nahidul Islam, Iain Shaw, Andreia Ribeiro, Benjamin Bradley, Michelle Kilcoyne, Rhodri Ceredig, and Lokesh Joshi. "Immunomodulatory effects of natural polysaccharides assessed in human whole blood culture and THP-1 cells show greater sensitivity of whole blood culture." *International immunopharmacology* 36 (2016): 315-323.

Ross, Sarah A., Jared Q. Gerlach, Satbir K. Gill, Jonathan A. Lane, Michelle Kilcoyne, Rita M. Hickey, and Lokesh Joshi. "Temporal alterations in the bovine buttermilk glycome from parturition to milk maturation." *Food Chemistry* 211 (2016): 329-338.

Manuscripts in preparation

- Role of post-translational modifications on osteopontin in endothelial cell biology
  Satbir Kaur Gill, Jared Q. Gerlach, Timothy O' Brien, Michelle Kilcoyne, Rhodri Ceredig, and Lokesh Joshi
  (Manuscript in preparation)

- Proteomic and glycomic analysis of extracellular matrix produced by murine stromal cells under hypoxic and normoxic conditions
  Satbir Kaur Gill, Andreia Riberio, Timothy O' Brien, Michelle Kilcoyne, Rhodri Ceredig, and Lokesh Joshi
  (Manuscript in process, 2)

- Differential glycosylation expression in injured rat spinal cord treated with immunosuppressive Cyclosporin A
- Michelle Kilcoyne, Dearbhaile Dooley, Ciara Bradley, Kerry Thompson, Catherine Liptrot, Timothy O'Brien, Frank Barry, Lokesh Joshi, and Siobhan S. McMahon

- *In vitro* selection and characterisation of DNA aptamer as an analytical tool against non-human sialic acid: Neu5Gc
  Shashank Sharma, Satbir Kaur Gill, Marian Kane, and Lokesh Joshi
  (Manuscript in process)

Oral Presentations

- 23rd International Symposium on Glycoconjugates, Split, Croatia, (15-20 September, 2015).
  Title: Proteomic and glycomic analysis of extracellular matrix produced by murine stromal cells under hypoxic and normoxic conditions

- Microscopy Society Ireland Symposium, Limerick, Ireland (26-28 August 2015), **Title:** Differential staining of ECM produced by the murine stromal cells

- Matrix Biology Ireland, Galway (19-21 November 2014),

Title: Immunomodulatory effects of natural polysaccharides on human whole blood culture and human monocytic THP-1 cell line

- Glycoscience Ireland, Westport, Ireland (8 November, 2013).

Title: Effect of OPN in endothelial cell biology

Poster Presentations

- Annual Meeting of the Irish Cytometry Society 2014, Dublin, Ireland (February 25, 2014).
    - Investigation of the immunomodulatory effect of polysaccharides on intracellular TNF-α by monocytes in human whole culture.
    - Satbir Kaur Gill, Nahidul Islam, Iain Shaw, Shirley Hanley, Benjamin Bradley, Rhodri Ceredig and Lokesh Joshi

- BSRT PhD Symposium "Regeneration is Communication: Fireside Chats between Cells Matrices" in Berlin, Germany (3-5 December, 2013).
    - Osteopontin promotes angiogenesis of Human Umbilical Vein Endothelial cells and Endothelial Progenitor Cells
    - Satbir Kaur Gill, Jared Q Gerlach, Lokesh Joshi and Timothy O' Brien

- Research day Ireland, National University of Ireland, Galway, Ireland. (25 September 2013).
    - Assessing the immunomodulatory properties of natural polysaccharides on human whole blood culture and human monocytic cell line.
    - Satbir Kaur Gill, Nahidul Islam, Iain Shaw, Shirley Hanley, Benjamin Bradley, Rhodri Ceredig and Lokesh Joshi
    - Role of glycosylation in OPN mediated angiogenesis in endothelial cells
    - Satbir Kaur Gill, Jared Q Gerlach, Lokesh Joshi and Timothy O' Brien.

- VIII Annual Meeting of the Irish Cytometry Society at National University of Ireland, Galway, (November 6-7, 2012).

- GlycoScience Ireland- 5th Annual Meeting, Salthill, Galway, Ireland (October 19, 2012).

- Symposium on "Vascular Progenitors in Biology and Medicine Symposium", Switzerland (13-15 September, 2012).
    - Osteopontin enhances angiogenic potential of endothelial cells
    - Satbir Kaur Gill, Jared Q Gerlach, Hsien-Yu, Lokesh Joshi[1] and Timothy O' Brien

- RAMI 2012, Royal Academy of Medicine Ireland (June, 2012).
    - Glycomic studies of osteopontin and endothelial progenitor cells in angiogenesis
    - Satbir Kaur Gill, Timothy O'Brien and Lokesh Joshi

- Summer Course Glycosciences in Groningen, Netherlands (12th edition, 3-7 June 2012).

- GlycoScience Ireland - 4th Annual Meeting, Teagasc Food Research Centre - Cork , Ireland (October 21, 2011) .

Modules under taken during the course of PhD

- GS501 Seminar Programme
- GS502 Participation in Journal Club Program
- GS509: Participation in Workshops/Courses
- GS526: Oral/poster communication
- MD536: Advanced and applied immunology
- CH441: Biopharmaceutical Chemistry
- Advanced course in Biostatistics 11-15 June, 2012

International Immunopharmacology 36 (2016) 315–323

Contents lists available at ScienceDirect

International Immunopharmacology

journal homepage: www.elsevier.com/locate/intimp

Immunomodulatory effects of natural polysaccharides assessed in human whole blood culture and THP-1 cells show greater sensitivity of whole blood culture

Satbir Kaur Gill [a,c,1], Nahidul Islam [b,1], Iain Shaw [a], Andreia Ribeiro [b], Benjamin Bradley [b], Timothy O'. Brien [c], Michelle Kilcoyne [a,d], Rhodri Ceredig [b,*,1], Lokesh Joshi [a,*,1]

[a] Glycoscience Group, National Centre for Biomedical Engineering Science, National University of Ireland Galway, Galway, Ireland
[b] Immunology and Transplant Biology, Regenerative Medicine Institute, National University of Ireland Galway, Galway, Ireland
[c] Regenerative Medicine Institute, National University of Ireland Galway, Galway, Ireland
[d] Microbiology, School of Natural Sciences, National University of Ireland Galway, Galway, Ireland

ARTICLE INFO

Article history:
Received 7 January 2016
Received in revised form 19 April 2016
Accepted 11 May 2016
Available online 21 May 2016

Keywords:
Immunomodulation
Polysaccharides
Cytokines
Chemokines
Whole blood culture
THP-1 cell line

ABSTRACT

Immunomodulatory drugs are available to maintain immune homeostasis but some have undesirable side effects. Six oligo- and poly-saccharides were assessed for their pro- and anti-inflammatory responses in two in vitro model systems, the monocytic THP-1 cell line and human whole blood cultures (HWBC). The compounds were first characterised for their molecular mass and physical properties. Following incubation with lipopolysaccharide (LPS) or the compounds, cytokine and chemokine secretion was assayed in both models and intracellular TNF-α was measured by flow cytometry in HWBC cell sub-populations. LPS, inulin, galacturonan, heteroglycan and fucoidan demonstrated pro-inflammatory properties and intracellular TNF-α expression was increased in the monocytes of HWBC. Mannan and xyloglucan did not elicit any significant responses. Inulin induced maximum cytokine secretion and heteroglycan induced maximum chemokine secretion in HWBC. This study emphasises the potential of inulin and heteroglycan as potential immunomodulatory therapeutics and that HWBC had a greater and more varied response in comparison to THP-1 cells.

1. Introduction

Infections and physical traumas affect the immune status of the organism, inducing an initial inflammatory cascade followed by a transient anti-inflammatory response [1]. Activated monocytes and macrophages produce inflammatory mediators including cytokines and chemokines to overcome the trauma or biological insult. Immunomodulators are potential therapeutics to maintain immunological balance in patients with infectious and non-infectious traumas, and diseases such as autoimmune disease or cancer. Several immunomodulatory drugs are available but some have known side effects [2]. Immunomodulatory drugs with less side effects and more targeted functions are needed.

Polysaccharides are one of the most abundant renewable natural resources and are widely used in the food industry [3], in tissue engineering, for drug delivery and in therapeutic applications [4]. Polysaccharides have diverse biological effects including anti-tumour, anti-viral, anti-complementary, anti-coagulant, anti-oxidant and immunomodulatory properties [5–9]. The biological properties of polysaccharides are governed by their chemical structures which includes the identity of the residues, specific linkages, length of the polysaccharide backbone, degree of branching, substituents and their positions, and overall charge of the molecule [10]. By virtue of their wide range of biological activities, relatively low toxicity, negligible side effects and ease of accessibility, naturally occurring carbohydrates are attractive potential immunomodulators [7].

The human-derived myeloid leukaemia THP-1 cell line is widely used to investigate the potential effects of drugs on monocytes and macrophages. THP-1 cells are often selected over other human monocytic cell lines such as U937 and Mono Mac-6 cells due to their more homogenous genetic background [11]. Human whole blood culture (HWBC) is a heterogeneous population of cells normally present in whole blood [12]. HWBC contains all the essential components for the stimulation of both innate and T-cell mediated immunity, hence mimicking in vivo condition. HWBC and THP-1 cells were previously used to investigate cytokine and chemokine production in response to bacterial lipopolysaccharide (LPS), allergens and drugs [12,13] and these systems were previously compared to human peripheral blood mononuclear cell (PBMCs) [14]. However, the responses of cell sub-populations of HWBC have not previously been investigated to the best of our knowledge.

* Corresponding authors.
E-mail addresses: rhodri.ceredig@nuigalway.ie (R. Ceredig), lokesh.joshi@nuigalway.ie (L. Joshi).
[1] Authors contributed equally.

http://dx.doi.org/10.1016/j.intimp.2016.05.009
1567-5769/

In the present study, six poly- and oligo-saccharides, inulin (INL), galacturonan (GAL), mannan (MAN), heteroglycan (HGL), fucoidon (FUC) and xyloglucan (xGLU) (Table S1), were screened for their immunomodulatory effects in two cell model systems, THP-1 cells and HWBC from three healthy individuals, by comparing secreted pro- and anti-inflammatory cytokines and chemokines. In addition, the intracellular expression of TNF-α in cell sub-populations of HWBC was quantified in response to treatments using flow cytometry. Four compounds (FUC, INL, HGL, GAL) had pro-inflammatory effects that could have potential therapeutic use. HWBC had a greater and more varied response to the compounds in comparison to THP-1 cells which may indicate that HWBC is closer to an in vivo model than a homogenous cell line.

2. Material and methods

2.1. Materials

Lyophilized oligo- and poly-saccharides (Table S1) were purchased from Elicityl (Crolles, France). All except MAN were reconstituted to 1 mg/mL in phosphate buffered saline (PBS, pH 7.2). MAN (2 mg) was first dissolved in 500 μL of 5% aqueous sodium hydroxide and then diluted to 1 mg/mL in PBS. RPMI-1640 media, foetal bovine serum (FBS), *L*-glutamine, periodic acid, Alcian Blue 8GX (AB), Schiff's reagent for aldehydes (catalogue number 84655) and bovine serum albumin (BSA, molecular biology grade) were from Sigma-Aldrich Co. (Wicklow, Ireland). Penicillin-streptomycin (10,000 U/mL penicillin and 10 mg/mL streptomycin), NuPAGE® Tris-acetate (3–8%) gels and NuPAGE® LDS sample buffer were from Life Technologies (Carlsbad, CA, U.S.A.). Ultrapure LPS from *Escherichia coli* 0111:B4 was from Invivogen (San Diego, CA, USA). Sterile pyrogen-free 96-well flat-bottom microplates from Nunc Maxisorp (Roskilde, Denmark) were used for the enzyme-linked immunosorbent assays (ELISA). Cytokine (IL-1β, IL-6, TNF-α, IL-10 and IL-13) and chemokine (IL-8, MCP-1 and macrophage inflammatory protein-1α (MIP-1α)) ELISA DuoSet® kits were purchased from R&D Systems (Abingdon, U.K.). Vacutainer® cell preparation tube (CPT™) heparin-coated tubes were obtained from Becton Dickinson Bioscience (San Jose, CA, U.S.A.). Brefeldin A (BFA) solution (3 mg/mL in methanol) and the fluorescently labelled mouse anti-human antibodies anti-CD45 conjugated to peridinin-chlorophyll protein-Cyanine5.5 (CD45-PerCP-Cy5.5) (catalogue number 45-0459-42, clone 2D1), anti-CD14 conjugated to allophycocyanin (CD14-APC) (catalogue number 17-0149-42, clone 61D3) and anti-cytoplasmic TNF-α conjugated to phycoerythrin (Cy-TNF-α-PE) (catalogue number 12-7349-41), were from eBioscience (San Diego, CA, U.S.A.). IntraPrep™ kit (catalogue number A07802) was from Beckman Coulter (High Wycombe, U.K.). The THP-1 cell line was from the American Type Culture Collection (Rockville, MD). All other reagents were from Sigma-Aldrich Co. and were of the highest grade available unless otherwise noted.

2.2. Poly- and oligo-saccharide characterisation

The poly- and oligo-saccharides were prepared in NuPAGE® LDS sample buffer with 25 mM dithiothreitol and heated at 95 °C for 5 min. Ten μg of each compound was loaded on a 3–8% Tris-acetate polyacrylamide gel and then electrophoresed with MES buffer (150 V, 1 h). The gels were stained with Coomassie Brilliant Blue R-250 (CBB) and destained in 40% methanol, 10% acetic acid solution [15]. Separate electrophoresed gels were stained with periodic acid Schiff's reagent (PAS) [16] with minor modifications. After electrophoresis, the gels were rinsed in deionised water, fixed with 30% ethanol and 5% acetic acid solution for 1 h, then rinsed twice in 10% ethanol for 5 min each rinse followed for two further rinses in deionised water for 15 min each. The gels were then oxidised separately by incubation in 25 mL of 1% periodic acid for 1 h in three different buffers, 7% acetic acid buffer (pH 2.5), 50 mM sodium acetate (pH 4) or 50 mM sodium phosphate (pH 7). The gels were washed three times in 3% acetic acid for 5 min per wash, incubated in 20 mL Schiff's reagent for aldehydes for 1 h and washed three times in deionised water for 5 min each. AB staining was also performed on separate electrophoresed gels as previously described [17]. All gels were imaged on a document scanner and were saved digitally as tif files.

2.3. Human whole blood culture (HWBC)

Peripheral human venous blood was collected into CPT™ heparin-coated tubes with signed informed consent from three healthy donors under a protocol approved by the National University of Ireland Galway Research Ethics Committee. Human blood culture was performed as previously described with minor modifications [18]. Briefly, heparinized blood samples were diluted in a 1:10 ratio in RPMI-1640 and were cultured with a final concentration of 10 and 100 ng/mL of LPS. Diluted blood cultures were also incubated with various concentrations (1, 5, and 10 μg/mL) of the six compounds and assayed for cytokine and chemokine response for incubation periods of 6, 12 and 24 h at 37 °C in 5% CO_2 and 10 μg/mL was selected as the optimal concentration for use in both model systems. Following centrifugation for 5 min at 2151 ×*g*, the supernatants were collected and stored at −80 °C until further use.

2.4. THP-1 cell culture

Aliquots of 1 mL with 1×10^6 cryopreserved THP-1 cells were thawed in a 37 °C water bath, diluted with culture medium (RPMI-1640 supplemented with 10% heat inactivated FBS, 1 mM *L*-glutamine, 100 ng/mL streptomycin and 100 U/mL penicillin) and cultured in 175 cm^2 flasks in a humidified atmosphere at 5% CO_2 at 37 °C. Cells were passaged at 80% confluency. After 6 to 8 passages, the cells were suspended in fresh culture medium and adjusted to 1×10^6 viable cells/mL. Cells were then incubated for 6, 12, 24 and 48 h at 37 °C and 5% CO_2 in a humidified incubator with LPS at 10 and 100 ng/mL, test compounds at 10 μg/mL and unstimulated control cells. Following centrifugation as above, supernatants were collected and stored at −80 °C until further use.

2.5. Cytokine and chemokine quantification

ELISA was performed to assay the concentrations of IL-1β, IL-6, IL-8, IL-10, IL-13, TNF-α, MCP-1 and MIP-1α in the collected supernatants from both THP-1 cells and HWBC using ELISA DuoSet® kits following the manufacturer's instructions with minor modification. The supernatants were incubated overnight at 4 °C on the coated ELISA plates. The concentrations of each analyte were quantified by comparison with standard curves of known concentrations. Cytokine and chemokine quantifications were performed using three biological replicates of the HWBC culture and analysing in duplicate (for three patients separately). The average of each sample was then calculated and mean and standard deviation (SD) of the averages of three donors was obtained from these data sets.

2.6. Intracellular TNF-α (iTNF-α) quantification

Fluorescence-activated cell sorting (FACS) buffer was prepared with 2% FBS and 0.05% sodium azide in PBS. Heparinised blood (4 mL) collected from two healthy donors was diluted 10 times in RPMI-1640 medium supplemented with BFA (final concentration 2 nM). HWBC samples were cultured for 6 h at 37 °C and 5% CO_2 and monocytes were labelled in the dark at room temperature for 15 min with 17.5 ng each of anti-CD14-APC and anti-CD45-PerCPCy5.5 antibodies using the IntraPrep™ kit following manufacturer's instructions with minor modifications. Following staining, cells were fixed with 60 μL of Reagent 1 from the Intraprep™ kit for each sample, mixed thoroughly and incubated for 10 min at room temperature in the dark. Following this, 200 μL of FACS buffer was added in each tube, mixed well and

centrifuged at 250 *g* for 5 min and supernatant was decanted. White blood cells were permeabilized and red blood cells were lysed using 50 μL of Reagent 2 from the IntraPrep™ kit per sample by vigorous mixing at room temperature. Anti-human-CyTNF-α-PE was then added to the sample (17.5 ng/sample), incubated for 15 min at room temperature in the dark, cells were washed twice in PBS and resuspended in 60 μL of FACS buffer. FACS analysis was performed for labelled monocytes from HWBC on a BD Accuri™ C6 flow cytometer (Becton Dickinson Bioscience, San Jose, CA, U.S.A.). Data was collected for 10,000 events for each sample using C-Flow software.

The monocytes were defined by sequential gating on all CD45 + CD14 + cells in HWBC by triggering FL3 and FL4 emission detectors, respectively, and cytoplasmic TNF-α expressing monocytes were enumerated within the CD14 + population. The number and percentage of TNF-α expressing CD14 + cells and the mean fluorescence intensity (MFI) were recorded for each sample.

2.7. Statistical analysis

Statistical analysis was performed using Prism (version 5.0.1, GraphPad Software Inc., La Jolla, CA, USA). Two-way ANOVA was performed to assess the time-dependent statistical variations. Paired *t*-tests were performed on percentage TNF-α expression by monocytes in HWBC to assess variations between oligo- and poly-saccharide treatment by comparing each with the no treatment values. Matrices of concentrations of the secreted cytokines and chemokines values for both THP-1 (Table S1) and HWBC (Table S2) cell models in response to treatment with poly- and oligo-saccharides were used to generate heat map using R programming language (http://www.r-project.org/). The concentration values below the detection limit were considered null (0) for calculation purposes and dendrograms were placed along the heat map for ordering of the data.

3. Results

Six poly- and oligo-saccharides, INL, GAL, MAN, HGL, FUC and xGLU (Table S1), which encompassed a range of structures, were assessed for their pro- and anti-inflammatory effects in two cell model systems, THP-1 cell culture and HWBC from three healthy donors. The concentrations of pro-inflammatory cytokines (IL-1β, IL-6 and TNF-α), anti-inflammatory cytokines (IL-10 and IL-13) and chemokines (IL-8, MCP-1 and MIP-1α) were measured at different time points in response to treatment of the cell models with the test panel.

3.1. Characterisation of oligo- and poly-saccharides

As poly- and oligo-saccharides from varying sources can influence the molecular mass (Mr), degree of substitution and physical properties of the purified carbohydrates and the Mr range given by the manufacturer was quite wide (Table 1), the test compounds (Table S1) were initially characterised for their apparent molecular mass and physical properties.

A lack of CBB staining of the electrophoresed gels confirmed the absence of protein as expected (Fig. S1 and Table 1). AB staining detects charged polysaccharides, which included FUC, GAL and HGL. In this work, AB stained FUC and HGL but not INL, MAN or xGLU as expected, but unexpectedly, GAL did not evolve any colour (Fig. S1 and Table 1). However, AB binds to molecules due to their polyanionic nature [19] so very low molecular mass (Mr) compounds are not detected. In support of the assumption of the low Mr (<3 kDa) of GAL used here, PAS staining also did not allow visualisation at any pH tested despite GAL having the vicinal hydroxy groups required for PAS reactivity [16].

On the other hand, both FUC and HGL were readily detected by PAS staining at an apparent Mr of >205 kDa (Table 1). Varying the pH of periodate oxidation leads to different oxidation rates for some carbohydrate structures [16]. FUC was detected by PAS staining at all pHs, while HGL was observed at pH 4 and 7, but not at pH 2.2 (Fig. S1 and Table 1). INL, MAN and xGLU did not stain with PAS under any condition despite the presence of the required vicinal hydroxyl groups which was likely due to very low Mr ranges (<3 kDa) [20].

3.2. Effect of LPS on secreted cytokine and chemokine production in the cell models

LPS and the test compounds did not have any morphological changes or cell death effects on THP-1 cells as verified by light microscopy before and after incubations compared to controls. HWBC was opaque and could not be imaged.

Stimulating HWBC with LPS significantly increased production of all measured pro-inflammatory cytokines, IL-1β, IL-6 and TNF-α, and chemokines, IL-8, MCP-1 and MIP-1α, at 6 h post-stimulation (Fig. 1, Tables S2 and S3) (p-value <0.02 to <0.0001) for cytokine and chemokines except for IL-6 which had high error bars. The concentrations of all secreted cytokines and chemokines continued to increase slightly up to 24 h for both concentrations of LPS, except for IL-6.

In contrast, THP-1 cells secreted lower overall concentrations of cytokines and chemokines upon LPS stimulation in comparison to HWBC, except for TNF-α and MIP-1α, which showed similar response magnitudes in both cell models. However, the overall concentration trend increased over time in the THP-1 cells (Fig. 1). All measured pro-inflammatory cytokine concentrations increased at the 6 h time point and only increased marginally at all later time points for THP-1 cells, except for IL-6 which was undetectable at all time points (Fig. 1, Table S2). On the other hand, IL-8 and MIP-1α concentrations stayed unchanged after their initial increase at 6 h until 48 h for 100 ng/mL LPS stimulation for THP-1 cells and dropped slightly by 48 h for the 10 ng/mL LPS stimulation. For MCP-1 upon incubation with 10 ng/mL LPS, the concentrations rose from 36.3 ± 4.2 to 190.0 pg/mL from 6 h to 12 h, reduced again by 24 h to 84.5 ± 64.7 pg/mL and remained approximately constant until the final time point (Fig. 1).

The anti- inflammatory cytokines IL-10 and IL-13 did not have measurable response to any LPS stimulation and their concentrations were below the lower limit of detection (LLOD) of the assays (31 pg/mL and 93 pg/mL, respectively) and so were not evaluated for the test compounds.

Table 1
Compound characterisation using various stains.

Compounds	Reported Mr	Apparent Mr	CBB	AB	PAS		
					pH 2.2	pH 4.0	pH 7.0
INL	164 Da–164 kDa	ND (<3 kDa)	−	−	−	−	−
FUC	3–320 kDa	>205 kDa	−	+	+	+	+
GAL	<250 kDa	ND (<3 kDa)	−	−	−	−	−
HGL	NA	>205 kDa	−	+	−	+	+
MAN	342 Da–<1 kDa	ND (<3 kDa)	−	−	−	−	−
xGLU	312 Da–50 kDa	ND (<3 kDa)	−	−	−	−	−

CBB, Coomassie Brilliant Blue; AB, Alcian Blue; PAS, periodic acid-Schiff's reagent; (+), staining; (−), absence of staining, ND, not detected, NA, information not available. Reported Mr is as reported by the manufacturer.

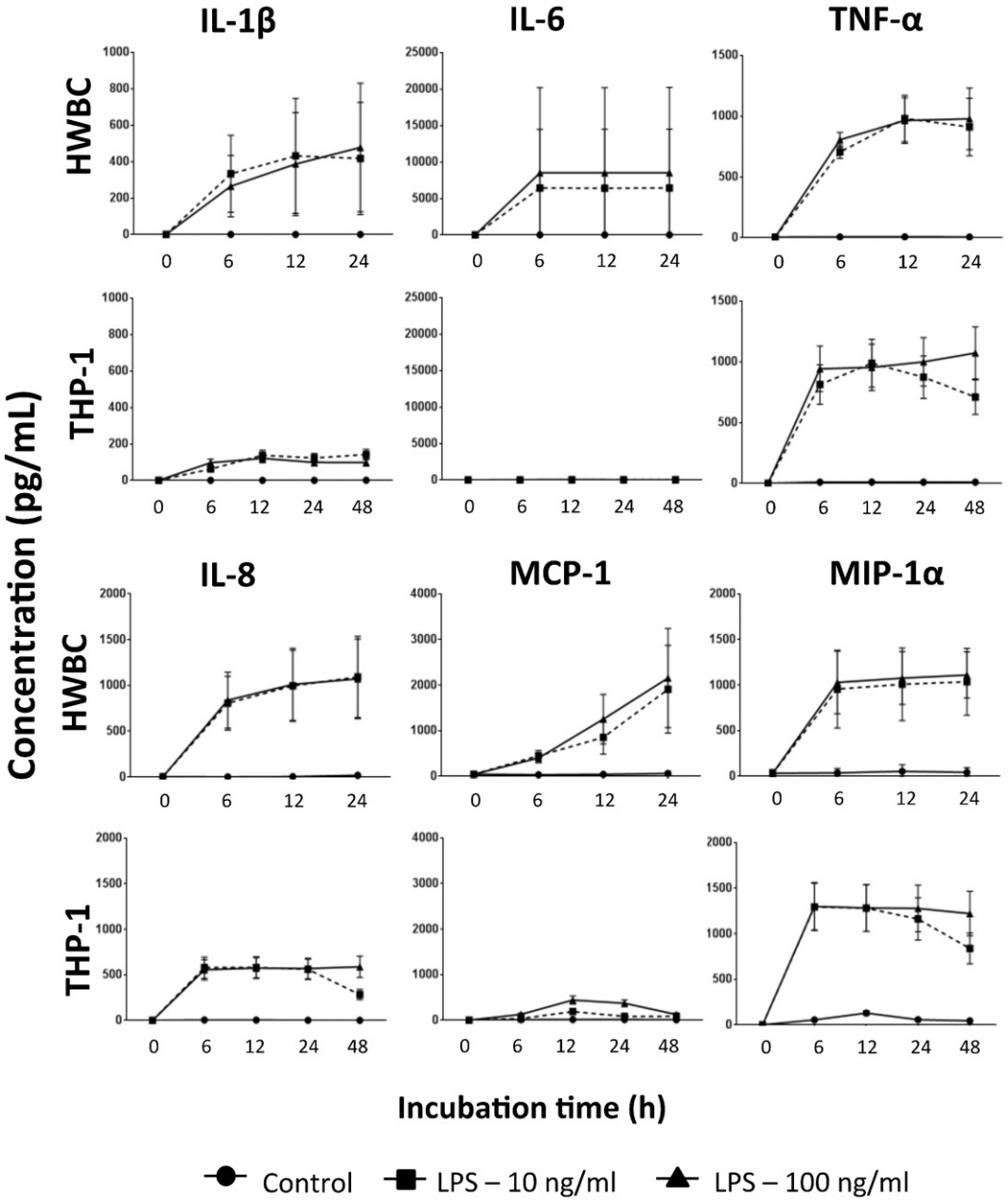

Fig. 1. Cytokine (IL-1β, IL-6 and TNF-α) and chemokine (IL-8, MCP-1 and MIP-1-α) production by HWBC (top and third row) and THP-1 cells (second and fourth) rows in response to incubation with LPS at 10 ng/mL and 100 ng/mL. HWBC were incubated for 6, 12 and 24 h and THP-1 cells for 6, 12, 14 and 48 h.

3.3. Effect of poly- and oligo-saccharides on secreted cytokine production in HWBC and THP-1 culture

Compared with the unstimulated cells in the HWBC cell model, FUC, INL HGL and GAL showed significant increases in production of all assessed pro-inflammatory cytokines (IL-1β ($p = <0.0001$), IL-6 ($p = 0.02$) and TNF-α ($p \leq 0.0001$)) over time (Fig. 2 and Table S2). The cytokine secretion profiles for all three blood donors followed a similar trend upon incubation with the compounds (Fig. S2). INL stimulated the greatest production of cytokines (e.g. IL-6 at 12 h with 3445.89 ± 3848.81 ng/mL) whereas GAL stimulated the lowest concentration of cytokine secretion (e.g. IL-1β at 6 h with 16.5 ± 3.3 ng/mL).

For THP-1 cells, production of the cytokines was very limited in response to treatment with the compounds and concentrations of IL-1β and IL-6 were below the LLOD (3.6 pg/mL and 9 pg/mL, respectively) at all incubation times tested (Table S2). However, upon treatment with HGL, the TNF-α concentration was 36.3 ± 3.3 pg/mL at 6 h, which remained approximately constant.

3.4. Effect of poly- and oligo-saccharides on secreted chemokine production in HWBC and THP-1 culture

The concentration of secreted chemokines significantly increased over time in HWBC upon treatment with FUC, INL HGL and GAL with individual variation, although the pattern of the onset of chemokine secretion was the same across all volunteers (Figs. 3 and S3). HGL induced the greatest chemokine production in HWBC for MCP-1 (686.7 ± 378.7 pg/mL at 24 h) whereas GAL had the least effect on any chemokine except for MIP-1α (Fig. 5A). The concentration of MIP-1α increased significantly at 6 h ($p = 0.04$) in response to FUC, INL and HGL, and remained high while GAL treatment slightly decreased

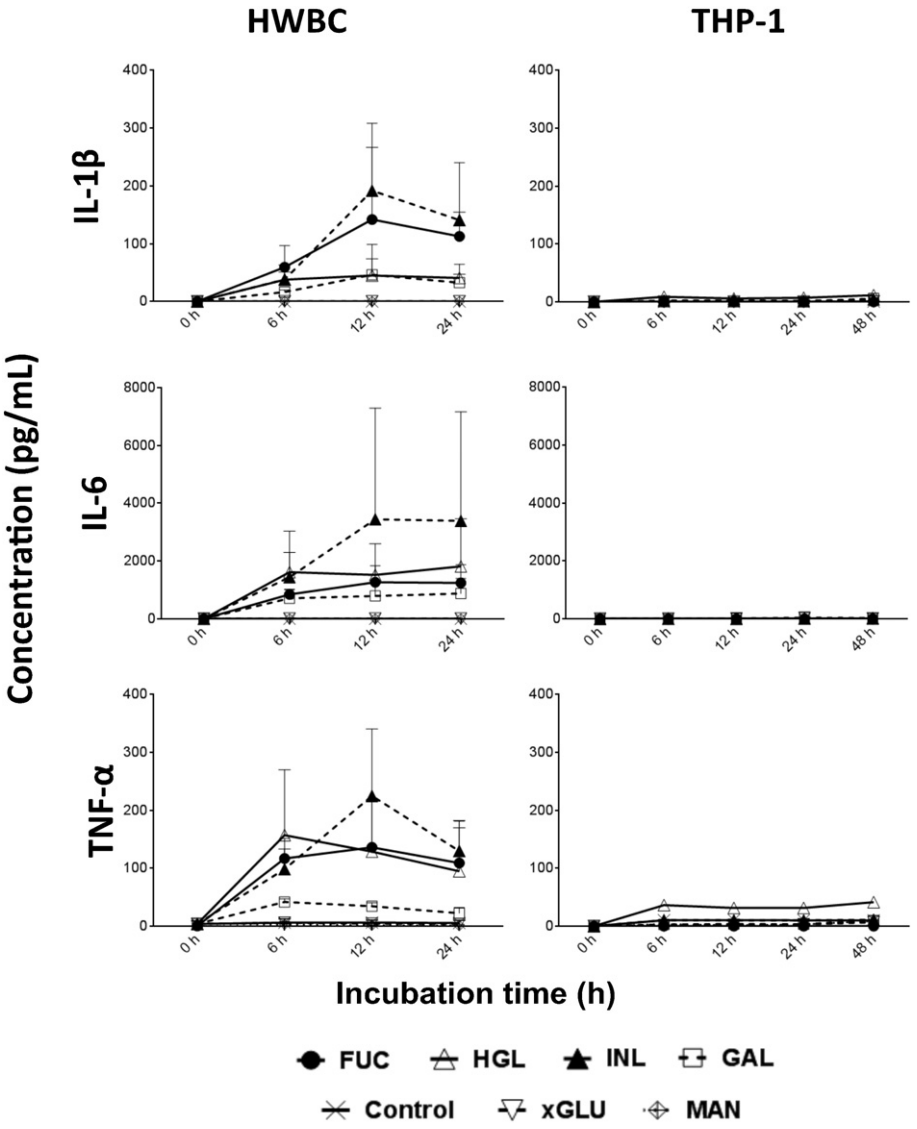

Fig. 2. Cytokine (IL-1β, IL-6 and TNF-α) production by HWBC (left) and THP-1 cells (right) in response to co-incubation with 10 μg/mL of oligo- and poly-saccharides. THP-1 cells were incubated up to 48 h while HWBC were incubated up to 24 h.

MIP-1α concentration after 6 h. Time-dependent elevations in IL-8 concentrations were observed.

In THP-1 cells, the general concentration responses of IL-8, MCP-1 and MIP-1α to poly- and oligo-saccharide treatments were very low to undetectable compared to HWBC. Both IL-8 and MIP-1α concentrations increased at 6 h when treated with HGL to 86.5 ± 3.6 and 624.5 ± 54.6 pg/mL, respectively. Interestingly, MIP-1α concentration was significantly elevated at 6 h compared to control when treated with either HGL or INL, decreased at 24 h to 148.6 ± 3.6 pg/mL and increased again by 48 h to 416.6 ± 8.1 pg/mL. However, production of IL-8 and MCP-1 by THP-1 cells was inconsistent between the incubation times and treatments, with undetectable ranges. HGL led to low detectable concentrations of TNF-α. Again, xGLU and MAN did not have any effect on the production of secreted chemokines in either model system (Fig. 3).

3.5. Effect of poly- and oligo-saccharides on intracellular TNF-α (iTNF-α) expression

Detection of iTNF-α expression avoids the influence of the extracellular environment and can quantify the contribution of the different cell types [21,22]. In order to determine which sub-population of HWBC contributed most to TNF-α production, the expression of iTNF-α was tested in several HWBC sub-populations, including the CD3+ T-cells (both CD4+ and CD8+, together and separately), CD19+ B-cells and natural killer cells, after LPS stimulation for 6 h. None of these cell types showed any significant iTNF-α expression compared to control (data not shown). However, a significant increase in percentage of iTNF-α expressing HWBC monocytes after 6 h of incubation was found upon treatment with GAL, HGL, INL and FUC (Table S3, Fig. 4 and S4) with a mean increase of 8.5-, 15.8-, 14.5-, and 13-fold, respectively, compared to untreated control. xGLU and MAN had no effect on iTNF-α expression, with mean change of 4.8% (1.2 fold) and 4.3% (no fold change) compared with untreated control, respectively. In three volunteers, the monocyte concentration varied <10% and in these, 1 mL of blood contained on average 1.8×10^5 $CD45^+/CD14^+$ monocytes as determined by flow cytometry analysis. Therefore, when diluted tenfold, the number of monocytes present in the HWBC iTNF-α assays, as well as the assay for secreted cytokines and chemokines was 1.8×10^4.

As THP-1 cells secreted only very low concentrations of TNF-α and furthermore are comprised of a single homogenous population, iTNF-α expression was not determined for THP-1 cells.

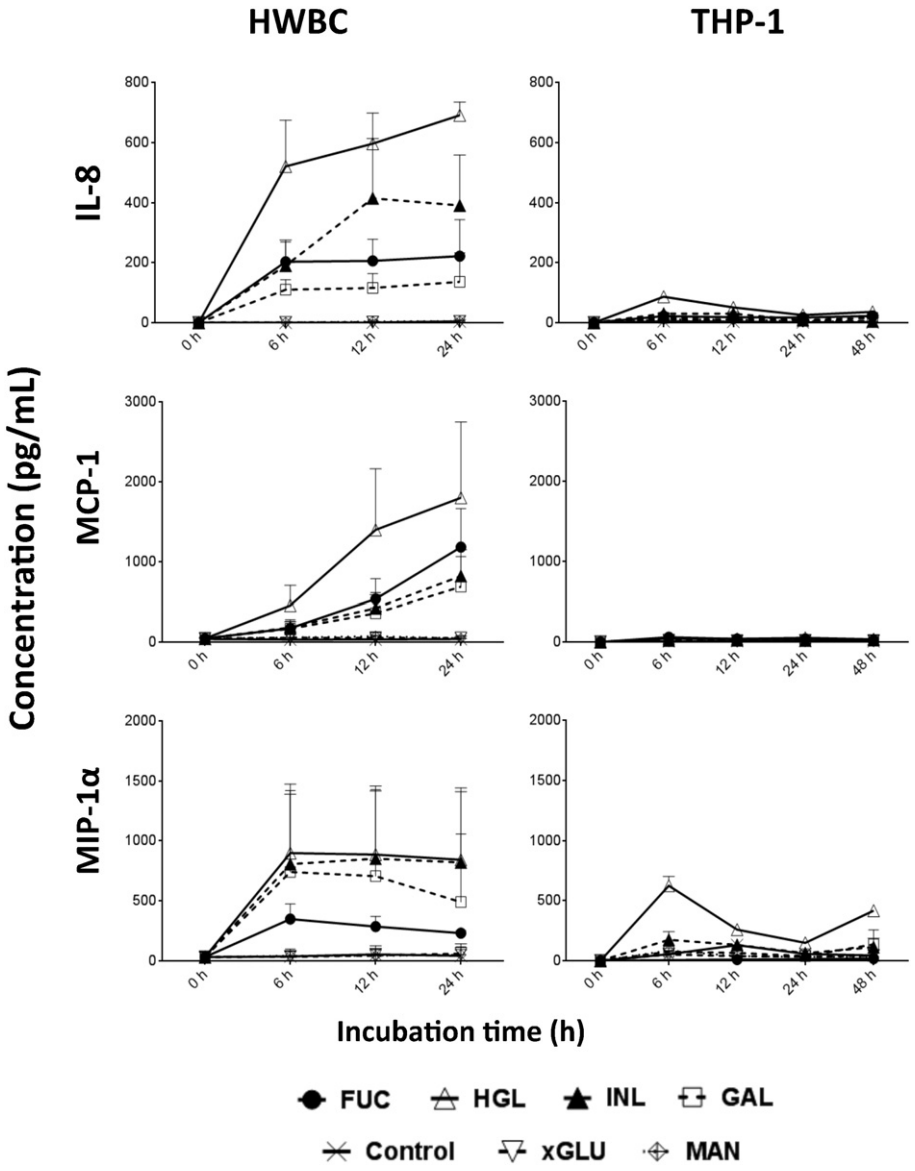

Fig. 3. Chemokine (IL-8, MCP-1 and MIP-1α) production by HWBC (left) and THP-1 cells (right) in response to co-incubation with 10 μg/mL of various oligo- or poly-saccharides. THP-1 cells were incubated up to 48 h and HWBC up to 24 h.

3.6. Overall effect of poly- and oligo-saccharides on secreted chemokines and cytokines

All cytokine and chemokine responses upon incubation with oligo- and poly-saccharides in the HWBC and THP-1 cell models were represented by heat maps (Fig. 5). For HWBC, INL and HGL had the greatest effect on the secretion of cytokines and chemokines, respectively, followed by FUC and GAL while MAN and xGLU had no effect on the secretion of either cytokines or chemokines when compared to control (Fig. 5A). Low concentrations of secreted cytokines and chemokines were induced by incubation of the compounds for THP-1 cells, except for HGL, which induced detectable chemokine secretion (Fig. 5B). Similar heat maps were generated for LPS responses and 0 h time point for both HWBC and THP-1 cells (Fig. S5), where LPS lies on a different branch of the dendrogram due to significantly higher responses induced in the two model systems compared to the oligo- and poly-saccharides.

4. Discussion

As structural variations influence biological activity, the characterisation of the test panel for apparent Mr and biochemical properties revealed more specific details about the poly- and oligo-saccharides employed in this study which can facilitate better comparison with future studies and better correlation of biological activity with defined chemical properties and structures, e.g. charge and Mr.

Upon incubation with LPS and the poly- and oligo-saccharides, HWBC secreted higher concentrations of pro-inflammatory cytokines and chemokines compared to THP-1 cells. For HWBC, INL and HGL had the greatest effect on the secretion of cytokines and chemokines, respectively, followed by FUC and GAL while MAN and xGLU had no effect on the secretion of either cytokines or chemokines when compared to control (Fig. 5A). Individual variations between three healthy donors for HWBC were observed, but the concentration trends of cytokines and chemokines over time were similar. Low concentrations of secreted cytokines and chemokines were induced by incubation of the compounds for THP-1 cells, except for HGL, which induced detectable chemokine secretion (Fig. 5B).

The greatest cytokine and chemokine expression in the HWBC model elicited by INL, a type of fructan, and HGL, a sulfated arabinogalactan, respectively, may indicate that these compounds have potential roles in the recruitment of immune cells to the site of inflammation. Despite the different structures of INL and HGL, their

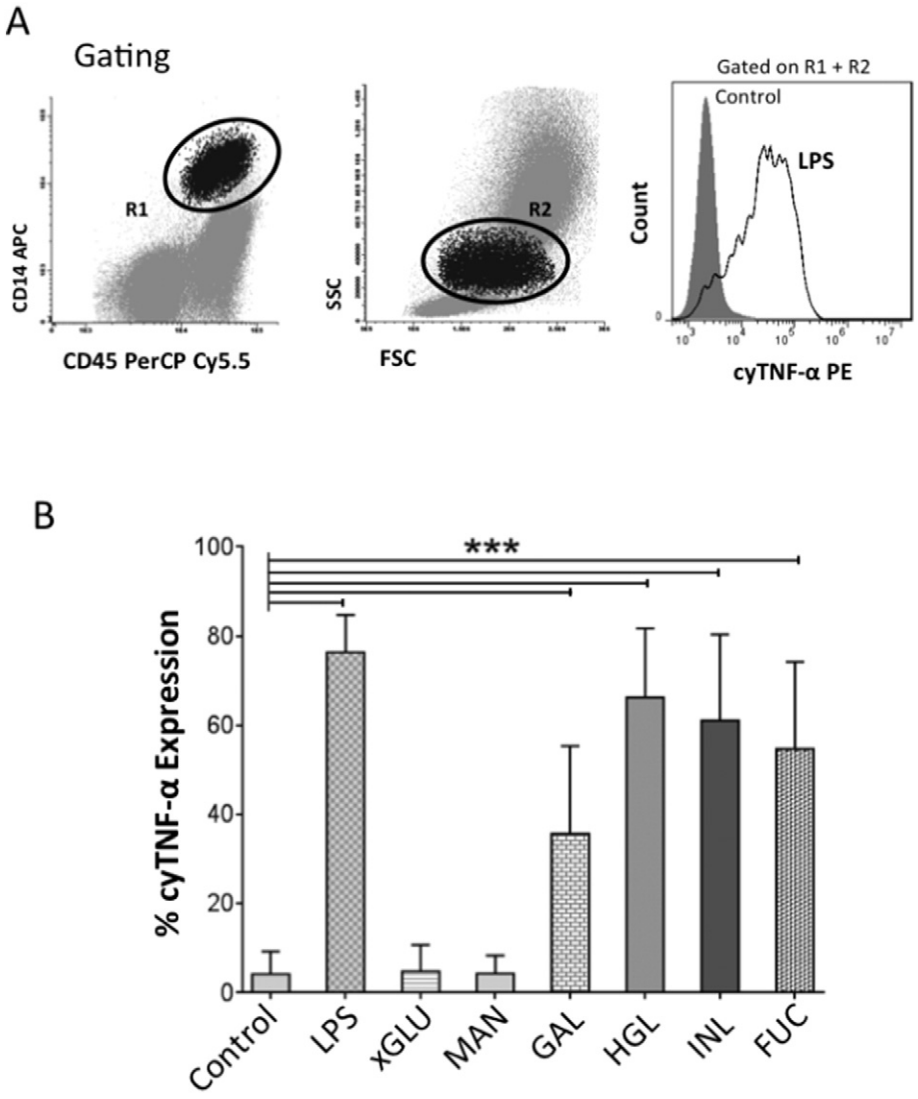

Fig. 4. Intracellular TNF-α production in monocytes of HWBC (A) after labelling with human anti-CD45 and anti-CD14 antibodies in response to co-incubation with 10 μg/mL oligo- and poly-saccharides. The histogram represents the percentage of cytoplasmic TNF-α expressed by monocytes following 6 h incubation where *** indicates the p value <0.001 (B).

similar effects may indicate a common mode of action by the heterogeneous cell population in HWBC. Fructans, irrespective of chain lengths, activate the inflammatory cascades and initiate signalling cascades in Toll like receptor dependent manner [23]. FUC extracted from *Ascophyllum nodosum* is a highly sulfated fucoidan which is known for its anti-inflammatory effects [8]. However, the present study demonstrated the pro-inflammatory effects of FUC on HWBC. The contrary immunomodulatory properties of FUC compared to previous reports may be attributed to FUC structural differences depending on the source and method of extraction and also different model systems [24]. Varying the sulfation on FUC has altered its anti-tumour and anti-angiogenic properties [5]. Both FUC and HGL have varying degrees of sulfation that may be responsible for their ability to induce cytokine production.

GAL is a major constituent of pectins and the immunomodulatory properties of pectins depend on the GalA content [25]. The GAL used in the present study had 62% GalA which presumably induced the secretion of pro-inflammatory cytokines and chemokines. INL, HGL, FUC and GAL also had significant effects on iTNF-α expression in HWBC monocytes and the results were comparable to the secreted TNF-α profiles at 6 h of HWBC, which was not surprising considering that monocytes were the main cell sub-population which expressed TNF-α in HWBC. HGL was the most stimulatory compound for the secretion of both iTNF-α and secreted TNF-α followed by INL. Interestingly, there were high SD values between donors for the HWBC assays, notwithstanding the similar number of monocytes present between donors, but this may be due to the variability of monocyte activation state between individuals. HGL also had little effect on the concentration of the secreted TNF-α in the THP-1 cells, despite the approximately 55 times less monocytes assayed in HWBC compared to THP-1 cells (1.8×10^4 compared to 1×10^6 cells per mL, respectively).

Different genetics and immune status between animal models and humans have led to the failure of many drugs in human trials [26]. Side effects and unforeseen complications such as the Tegenero disaster have also been reported, where immunomodulatory anti-CD28 monoclonal antibody (mAb) (TGN1412) triggered an immediate systemic inflammatory response and a serious adverse event referred to as a "cytokine storm" during phase I clinical trials [27]. While cell lines can elucidate mechanisms and can be a good choice to identify specific molecular pathways, they cannot completely predict clinical efficacy due to the lack of coherent complex and multi-functional cells. In contrast, HWBC is a heterogeneous population of blood cells and other soluble mediators in the plasma. HWBC cannot confirm any specific triggered pathway due to the involvement of various cell types but can account for individual donor variations and mimic human in vivo conditions.

The relative insensitivity of the THP-1 cells compared to HWBC in response to both LPS and the test panel, despite the dramatically lower

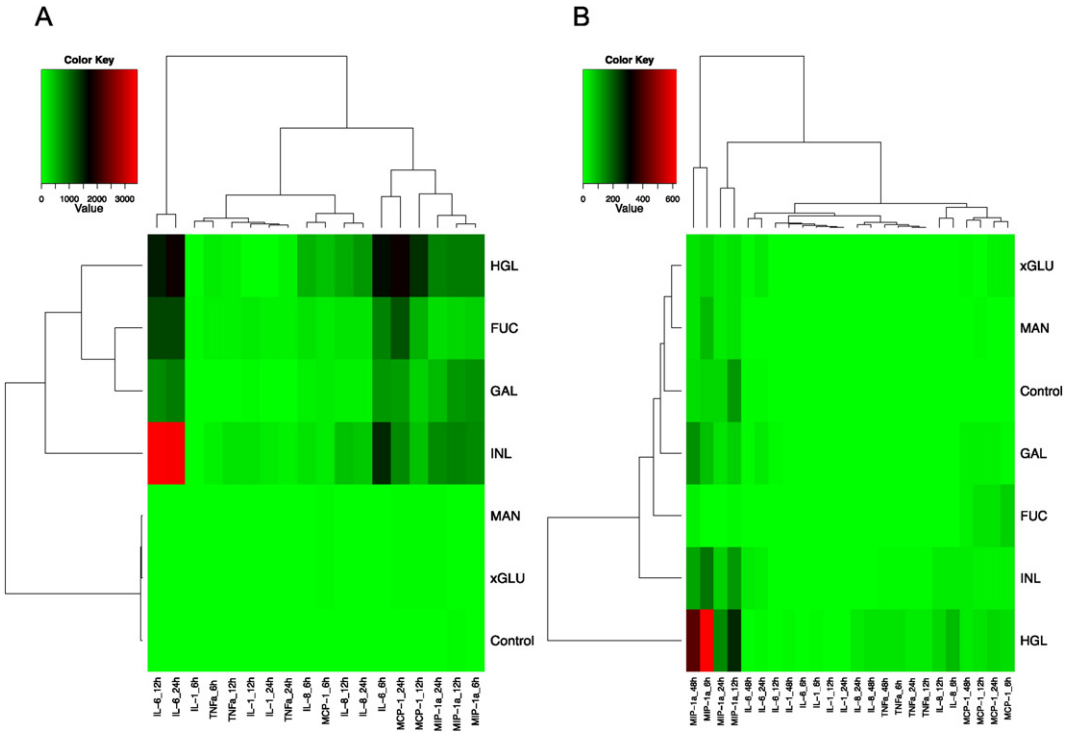

Fig. 5. Hierarchical clustering correlating relative expression of the cytokines and chemokines upon incubation with test compounds in HWBC (A) and THP-1 cells (B). Colours represent the chemokine and cytokine concentrations indicated by the legend.

number of monocytes assayed in HWBC compared to THP-1 cells, indicated that HWBC could be a model that is more predictive of the in vivo situation. One possibility that could account for the insensitivity of THP-1 cells is that they have been in culture for decades and could have lost some of the components involved in intracellular signalling. Another possibility is that THP-1 cells do not represent genuine resting monocytes. Monocytes are produced in the bone marrow and migrate into tissues where they rapidly differentiate. Therefore, blood monocytes are primed to differentiate and produce cytokines. THP-1 cells are an established myelomonocytic cell line and perhaps do not represent the equivalent blood monocyte. That THP-1 cells are less sensitive than monocytes clearly has important implications for testing potential drugs for their immunomodulatory ability, in that false negative results would be obtained using THP-1 cells.

In conclusion, we suggest that HWBC is a better model than THP-1 cells to test compounds for their immunomodulatory ability. We also present INL and HGL as potentially effective immunomodulatory therapeutics.

Acknowledgements

The authors thank the following agencies for financial support; the Irish Research Council for a PhD scholarship EMBARK Award (RS/2011/223) to NI, Science Foundation Ireland Strategic Research Cluster (SRC) programme (grant no. SFI09/SRC/B1794) and a Science Foundation Ireland Stokes Professorship (SFI07/SK/B1233b) (RC) and the Alimentary Glycoscience Research Cluster (grant no. 08/SRC/B1393) (LJ, IS), the Simulation Science Programme for a PhD scholarship for SKG funded by the Higher Education Authority (HEA) through the Programme for Research at Third Level Institutions, Cycle 5 (PRTLI-5), which is 50% co-funded by the European Regional Development Fund (ERDF) and the European Union FP7 programme in support of the GlycoHIT project (grant no. 260600) (LJ, MK) and People Programme (Marie Curie Actions) of the EU FP7 programme Research Executive Agency grant agreement No. 315902 (AR). The authors thank Dr. Shirley Hanley for assistance with FACS analysis.

Appendix A. Supplementary data

Supplementary data to this article can be found online at http://dx.doi.org/10.1016/j.intimp.2016.05.009.

References

[1] S. Hirsiger, H.P. Simmen, C.m.M. Werner, G.A. Wanner, D. Rittirsch, Danger signals activating the immune response after trauma, Mediat. Inflamm. 2012 (2012).
[2] A. Bascones Martinez, R. Mattila, R. Gomez-Font, J.H. Meurman, Immunomodulatory drugs: oral and systemic adverse effects, Med. Oral Patol. Oral Cir. Bucal 19 (2014) e24.
[3] F. Paul, A. Morin, P. Monsan, Microbial polysaccharides with actual potential industrial applications, Biotechnol. Adv. 4 (1986) 245–259.
[4] P. Tiwari, P. Panthari, D.P. Katare, H. Kharkwal, Nat. Polym. Drug Deliv. (2014).
[5] S. Koyanagi, N. Tanigawa, H. Nakagawa, S. Soeda, H. Shimeno, Oversulfation of fucoidan enhances its anti-angiogenic and antitumor activities, Biochem. Pharmacol. 65 (2003) 173–179.
[6] S.N. Fedorov, S.P. Ermakova, T.N. Zvyagintseva, V.A. Stonik, Anticancer and cancer preventive properties of marine polysaccharides: some results and prospects, Mar. Drugs 11 (2013) 4876–4901.
[7] I.A. Schepetkin, M.T. Quinn, Botanical polysaccharides: macrophage immunomodulation and therapeutic potential, Int. Immunopharmacol. 6 (2006) 317–333.
[8] S.H. Lee, C.-I. Ko, G. Ahn, S. You, J.S. Kim, M.S. Heu, et al., Molecular characteristics and anti-inflammatory activity of the fucoidan extracted from Ecklonia cava, Carbohydr. Polym. 89 (2012) 599–606.
[9] C.M.P.G. Dore, M.G.d.C.F. Alves, L.S.E.P.r. Will, T.G. Costa, D.A. Sabry, L.A.R. de Souza Rêgo, et al., A sulfated polysaccharide, fucans, isolated from brown algae *Sargassum vulgare* with anticoagulant, antithrombotic, antioxidant and anti-inflammatory effects, Carbohydr. Polym. 91 (2013) 467–475.
[10] I. Wijesekara, R. Pangestuti, S.K. Kim, Biological activities and potential health benefits of sulfated polysaccharides derived from marine algae, Carbohydr. Polym. 84 (2011) 14–21.
[11] W. Chanput, J.J. Mes, H.J. Wichers, THP-1 cell line: an in vitro cell model for immune modulation approach, Int. Immunopharmacol. 23 (2014) 37–45.
[12] R.H. Brookes, J. Hakimi, Y. Ha, S. Aboutorabian, S.F. Ausar, M. Hasija, et al., Screening vaccine formulations for biological activity using fresh human whole blood, Hum. Vaccines Immunother. 10 (2014) 1129–1135.
[13] W. Chanput, J. Mes, R.A. Vreeburg, H.F. Savelkoul, H.J. Wichers, Transcription profiles of LPS-stimulated THP-1 monocytes and macrophages: a tool to study inflammation modulating effects of food-derived compounds, Food Funct. 1 (2010) 254–261.
[14] A. Schildberger, E. Rossmanith, T. Eichhorn, K. Strassl, V. Weber, Monocytes, peripheral blood mononuclear cells, and THP-1 cells exhibit different cytokine expression patterns following stimulation with lipopolysaccharide, Mediat. Inflamm. 2013 (2013).

[15] M. Kilcoyne, M. Shah, J.Q. Gerlach, V. Bhavanandan, V. Nagaraj, A.D. Smith, et al., O-glycosylation of protein subpopulations in alcohol-extracted rice proteins, J. Plant Physiol. 166 (2009) 219–232.
[16] M. Kilcoyne, J.Q. Gerlach, M.P. Farrell, V.P. Bhavanandan, L. Joshi, Periodic acid-Schiff's reagent assay for carbohydrates in a microtitre plate format, Anal. Biochem. 416 (2011) 18–26.
[17] A.H. Wardi, G.A. Michos, Alcian blue staining of glycoproteins in acrylamide disc electrophoresis, Anal. Biochem. 49 (1972) 607–609.
[18] P. Yaqoob, E.A. Newsholme, P.C. Calder, Comparison of cytokine production in cultures of whole human blood and purified mononuclear cells, Cytokine 11 (1999) 600–605.
[19] P. Whiteman, The quantitative determination of glycosaminoglycans in urine with Alcian Blue 8GX, Biochem. J. 131 (1973) 351–357.
[20] B. Azis, B. Chin, M. Deacon, S. Harding, G. Pavlov, Size and shape of inulin in dimethyl sulphoxide solution, Carbohydr. Polym. 38 (1999) 231–234.
[21] W.C. Sewell, M.E. North, A.D.B. Webster, J. Farrant, Determination of intracellular cytokines by flow-cytometry following whole-blood culture, J. Immunol. Methods 209 (1997) 67–74.
[22] C. Prussin, Cytokine flow cytometry: assessing cytokine production at the single cell level, Clin. Immunol. Newsl. 16 (1996) 85–91.
[23] L. Vogt, U. Ramasamy, D. Meyer, G. Pullens, K. Venema, M.M. Faas, et al., Immune modulation by different types of beta 2 → 1-fructans is toll-like receptor dependent, PLoS One 8 (2013) e68367.
[24] J.Y. Jang, S.Y. Moon, H.G. Joo, Differential effects of fucoidans with low and high molecular weight on the viability and function of spleen cells, Food Chem. Toxicol. 68 (2014) 234–238.
[25] S. Popov, Y.S. Ovodov, Polypotency of the immunomodulatory effect of pectins, Biochem. Mosc. 78 (2013) 823–835.
[26] J. Mestas, C.C. Hughes, Of mice and not men: differences between mouse and human immunology, J. Immunol. 172 (2004) 2731–2738.
[27] G. Suntharalingam, M.R. Perry, S. Ward, S.J. Brett, A. Castello-Cortes, M.D. Brunner, et al., Cytokine storm in a phase 1 trial of the anti-CD28 monoclonal antibody TGN1412, N. Engl. J. Med. 355 (2006) 1018–1028.